University of Alberta

Mitochondrial Protein Import in *Neurospora crassa*

by

Suzanne C. Hoppins ©

A thesis submitted to the Faculty of Graduate Studies and Research in partial
fulfillment of the requirements for the degree of Doctor of Philosophy

in

Molecular Biology and Genetics

Department of Biological Sciences

Edmonton, Alberta

Fall 2005

Library and
Archives Canada

Published Heritage
Branch

395 Wellington Street
Ottawa ON K1A 0N4
Canada

Bibliothèque et
Archives Canada

Direction du
Patrimoine de l'édition

395, rue Wellington
Ottawa ON K1A 0N4
Canada

0-494-08657-2

Your file Votre référence
ISBN:
Our file Notre reference
ISBN:

NOTICE:
The author has granted a non-exclusive license allowing Library and Archives Canada to reproduce, publish, archive, preserve, conserve, communicate to the public by telecommunication or on the Internet, loan, distribute and sell theses worldwide, for commercial or non-commercial purposes, in microform, paper, electronic and/or any other formats.

The author retains copyright ownership and moral rights in this thesis. Neither the thesis nor substantial extracts from it may be printed or otherwise reproduced without the author's permission.

AVIS:
L'auteur a accordé une licence non exclusive permettant à la Bibliothèque et Archives Canada de reproduire, publier, archiver, sauvegarder, conserver, transmettre au public par télécommunication ou par l'Internet, prêter, distribuer et vendre des thèses partout dans le monde, à des fins commerciales ou autres, sur support microforme, papier, électronique et/ou autres formats.

L'auteur conserve la propriété du droit d'auteur et des droits moraux qui protège cette thèse. Ni la thèse ni des extraits substantiels de celle-ci ne doivent être imprimés ou autrement reproduits sans son autorisation.

In compliance with the Canadian Privacy Act some supporting forms may have been removed from this thesis.

While these forms may be included in the document page count, their removal does not represent any loss of content from the thesis.

Conformément à la loi canadienne sur la protection de la vie privée, quelques formulaires secondaires ont été enlevés de cette thèse.

Bien que ces formulaires aient inclus dans la pagination, il n'y aura aucun contenu manquant.

Canada

Dedicated to Robert

ABSTRACT

Mitochondria are the primary sites of energy production in most eukaryotic cells. A vast majority of the proteins that function in mitochondria are encoded by nuclear genes. Multisubunit protein translocase complexes in the mitochondrial outer (MOM) and inner membranes (MIM) mediate the import and sorting of these proteins. All proteins utilize the TOM complex (translocase of the outer membrane) to cross the MOM or insert into it. Outer membrane β-barrel proteins are assembled by the TOB (topogenesis of outer membrane β-barrel proteins) complex. The TIM23 complex (translocase of the inner membrane) is primarily responsible for import of proteins to the matrix. Multitopic proteins are inserted into the MIM by the TIM22 complex. Tim9-10 and Tim8-13 are small, soluble complexes in the intermembrane space (IMS) that act as chaperones to shield hydrophobic regions from the hydrophilic environment.

The mutation responsible for the mitochondrial disorder, Mohr-Tranebjaerg Syndrome is DDP1, the human homologue of Tim8. To investigate the function of the Tim8-13 complex in *Neurospora crassa*, strains with null alleles of each gene were generated. Investigation of the import of mitochondrial precursors into mitochondria lacking these proteins showed that the Tim8-13 complex is involved in import of Tim23 to the MIM and in import and assembly of the β-barrel proteins porin and Tom40 to the MOM.

Tim23 is a component of the TIM23 complex in the MIM. Yeast Tim23 contains an N-terminal domain that crosses the MOM, tethering the TIM23 complex to the MOM. Investigation of the N-terminal domain of *N. crassa* Tim23 did not support the existence of a region that crosses the MOM in this protein. However, loss of the first fifty residues

results in decreased growth rate, diminished import capacity of mitochondrial proteins and aberrant mitochondrial morphology.

Tob55 is the primary component of the TOB complex. Tob55 is an essential protein and decreased expression results in slow growth of *N. crassa* cells and decreased import and assembly of outer membrane β-barrel proteins.

ACKNOWLEDGEMENTS

I would like to thank the following people who have provided me with technical support, plasmids and *N. crassa* strains. W. Neupert for supplying *N. crassa* Tim8 and Tim23 antibodies, Simmone Kerswell and the staff at Biological Sciences Animal Services for care of rabbits used for generation of antibodies, Troy Locke for running the Sephacryl columns, H. Prokish for providing the plasmid pTIM23, R. Metzenberg for supplying the strain Helper 5, G. Eitzen for providing me with technical advice as well as aliquots of Affi-Gel 10 and Affi-Gel 15.

Frank Nargang and members of the lab provided discussion, advice and support that were invaluable to me during the course of my program.

I am grateful to my examination committee members, Dr. Glerum, Dr. Adames, Dr. Bell and Dr. Court, for their time and guidance.

I have received funding from the Department of Biological Sciences, Alberta Ingenuity Fund and NSERC.

Finally, I thank my friends and family for their encouragement and support, in particular my husband, Robert.

TABLE OF CONTENTS

page

1. INTRODUCTION 1

1.1 Mitochondrial Functions 1

1.2 Origin of Mitochondria 3

1.3 Mitochondrial Genome 5

1.4 Mitochondrial Dynamics 5

1.5 Mitochondrial Protein Import 6

1.5.1 Mitochondrial Protein Import is Usually a Post-Translational Event 7

1.5.2 Protein Targeting and Chaperones 8

1.5.3 Energy Dependence of Import 11

1.6 The TOM Complex 12

1.6.1 Components of the TOM complex 12

1.6.2 Structure of the TOM complex 16

1.6.3 Biogenesis of the TOM complex 17

1.7 The TOB Complex and MIM1 19

1.8 Import Components of the IMS 21

1.8.1 Structure of the Tiny Tim Complexes 24

1.8.2 Import of the Tiny Tim Proteins to the IMS 25

1.9 The TIM Complexes 27

1.9.1 Components of the TIM23 Complex 27

1.9.2 Components of the PAM Machinery 29

1.9.4 Structure of the TIM23 Complex and Import Motor 32

1.9.5 Precursor Processing and Folding in the Matrix 33

1.9.6 Components of the TIM22 Complex 34

1.9.7 Structure of the TIM22 Complex 35

1.10 Protein Insertion to the Inner Membrane from the Matrix 36

1.11 Objectives of this study 37

2 MATERIALS AND METHODS 44

2.1 Growth of *N. crassa* 44

2.2 Oligonucleotides and Plasmids 44
2.3 Creation of RIP Mutants of *tim8* and *tim13* 44
2.4 Creation of Sheltered RIP Mutant of *tim23* 45
2.5 Nucleus Swapping of T23R4-12 47
2.6 Creation of *tob55* Knockout Strain 47
2.7 Transformation of Yeast 48
2.8 Purification of PCR Fragments from Agarose Gels 49
2.9 Transformation of *N. crassa* 50
2.10 Purification of Transformant Strains 51
2.11 Purification of Su9-DHFR for in vitro Import 51
2.12 In vitro Import of Radiolabeled Proteins into Isolated Mitochondria 52
2.13 Crosslinking of Radiolabeled Proteins During in vitro Import 52
2.14 Alkaline Extraction of Membranes 53
2.15 TCA precipitation of proteins 53
2.16 Immunoprecipitation 54
2.17 Creation of Strains Expressing Mutant Versions of Tim23 55
2.18 Size Determination of the Native Tim8-13 Complex by Sephacryl Chromatography 55
2.19 Mitochondrial Subfractionation 56
2.20 BNGE 56
2.21 Antibody Supershift and BNGE 56
2.22 Antibody Production 57
2.23 Antibody Affinity Purification 57
2.24 Preparation of *N. crassa* for Electron Micrographs 58
2.25 Substituted Cysteine Accessibility Mapping 59
2.26 Other Techniques 59
3 RESULTS 79
3.1 Investigation of the Function of the *N. crassa* Tim8-13 complex 79
3.1.1 Identification and Cloning of the Genes 79
3.1.2 Characterization of Tim8 and Tim13 in *N. crassa* 80

3.1.3 Creation of RIP (repeat induced point mutation) Mutant Strains 81
3.1.4 Characterization of the Mutant Strains 82
3.1.4.1 Growth Phenotypes 82
3.1.4.2 Mitochondrial Protein Levels 82
3.1.4.3 Mitochondrial Protein Import 82
3.1.4.4 Assembly of Tom40 and Porin 84
3.1.4.5 Crosslinking of Tim8-13 to Precursor Proteins 84
3.2 Investigation of the Structure and Function of Tim23 in *N. crassa* 86
3.2.1 Identification of the Gene 87
3.2.2 Construction of Fusion Proteins for *in vitro* Import 87
3.2.3 Generation of a Sheltered RIP Mutant Strain 88
3.2.3.1 Nutritional Testing of T23R4-12 89
3.2.4 Creation of Strains Expressing N-terminal Deletions of Tim23 90
3.2.5 Characterization of Truncated Tim23 Strains 91
3.2.5.1 Growth Rates 91
3.2.5.2 Mitochondrial Protein Import 91
3.2.5.3 Mitochondrial Morphology in T23Δ50 Mitochondria 92
3.2.6 Treatment of Mitochondria with Proteinase K 93
3.2.7 Mapping the Topology of the Tim23 N-terminus 93
3.2.7.1 Creation of Single Substituted Cysteine Tim23 Variants 94
3.2.7.2 Substituted Cysteine Accessibility Mapping 95
3.3 Investigation of the Structure and Function of *tob55* in *N. crassa* 95
3.3.1 Identification and Cloning of the Gene 96
3.3.2 Creation of a *tob55* Knockout Strain 96
3.3.3 Characterization of Tob55KO-3 97
3.3.3.1 Growth Rate 97
3.3.3.2 Nutritional Testing 97

3.3.3.3 Mitochondrial Protein Levels 98

3.3.3.4 Mitochondrial Protein Import 98

3.3.3.5 Tob55 is Involved in Tom40 and Porin Assembly 99

3.3.4 Creation of Strains Expressing Tagged Versions of Tob55 99

4 DISCUSSION 185

4.1 *N. crassa* Tim8-13 Complex 185

4.2 *N. crassa* Tim23 187

4.3 *N. crassa* Tob55 191

5 REFERENCES 194

LIST OF TABLES

page

Table 1 Strains used in this study. 65

Table 2 Oligonucleotides used in this study. 69

Table 3 Plasmids used in this study. 77

LIST OF FIGURES

Page

Figure 1 Import and Sorting of Mitochondrial Proteins. 41
Figure 2 Tom40 assembly intermediates as observed by BNGE. 43
Figure 3 Generation of a *tim23* sheltered RIP strain. 62
Figure 4 *Neurospora crassa* gene knockout strategy. 64
Figure 5 Alignment of the Tim8 and Tim13 proteins. 102
Figure 6 Determination of the size of the Tim8-13 complex in *N. crassa.* 104
Figure 7 Association of Tim8 and Tim13. 106
Figure 8 Localization of Tim8-13 in mitochondria. 108
Figure 9 Southern blots of candidate *tim8* duplication containing isolates. 110
Figure 10 Steady state levels of mitochondrial proteins in the *tim8*^{RIP} and *tim13*^{RIP} strains. 112
Figure 11 Sequence analysis of the *tim8*^{RIP} allele. 114
Figure 12 Southern blots of candidate *tim13* duplication containing isolates. 116
Figure 13 Tim8-13 deficient mitochondria are defective in import of Tim23 when $\Delta\Psi$ is reduced. 118
Figure 14 Tim8-13 deficient mitochondria are defective in import of porin and Tom40. 120
Figure 15 Tim8-13 deficient mitochondria are not defective in import of all mitochondrial proteins. 122
Figure 16 Import and assembly of porin and Tom40 into Tim8-13 deficient mitochondria. 124
Figure 17 Tom40 precursor contacts the Tim8-13 complex. 126
Figure 18 A Tom40 mutant precursor stalls at a position where contact with the Tim8-13 complex occurs. 128
Figure 19 Crosslinked adducts of Tom40 are not accessible to externally added protease. 130
Figure 20 Tom40 precursor contacts Tim9. 132
Figure 21 Tim8-13 and Tim9-10 contact the Tim23 precursor during import. 134
Figure 22 Sequence alignment of Tim23 protein. 136

Figure 23 Import of Tim23(1-67) fusion protein. 138

Figure 24 Import of Tim23(1-83)-IgG fusion protein. 140

Figure 25 Southern blots of candidate *tim23* duplication containing isolates. 142

Figure 26 Sequence analysis of the *tim23*^{RIP} allele. 144

Figure 27 Southern blots of *tim23*^{RIP} strain to determine copy number. 146

Figure 28 Nucleus swap for *tim23*^{RIP} strain genetic testing. 148

Figure 29 Growth phenotype of the T23Δ10 and T23Δ50 strains. 150

Figure 30 Rescue of the *tim23*^{RIP} allele with truncated versions of *tim23*. 152

Figure 31 Truncation of Tim23 does not result in severe deficiency in import of mitochondrial proteins. 154

Figure 32 Deletion of the first 50 amino acids of Tim23 affects the rate of import of mitochondrial matrix proteins. 156

Figure 33 Appearance of T23Δ50 mitochondria. 158

Figure 34 Treatment of mitochondria with Proteinase K. 160

Figure 35 Tim23 residues to be mapped by SCAM. 162

Figure 36 SCAM analysis of eight positions in the N-terminus of *N. crassa* Tim23. 164

Figure 37 Sequence alignment of Tob55 protein. 166

Figure 38 Parent Heterokaryon. 168

Figure 39 Southern analysis of *tob55* knockout isolates. 170

Figure 40 Growth of *tob55* knockout isolates. 172

Figure 41 Steady state levels of mitochondrial proteins in the *tob55* knockout strain. 174

Figure 42 Tob55 deficient mitochondria are defective in import of outer membrane β-barrel proteins. 176

Figure 43 Tob55 deficient mitochondria are not defective in import of non β-barrel mitochondrial proteins. 178

Figure 44 Assembly of Tom40 and Porin in Tob55↓ mitochondria. 180

Figure 45 Antibody supershift of Tom40 and porin assembly intermediates. 182

Figure 46 Generation of Tob55 protein tag strains. 184

List of Abbreviations

3D	three dimensional
A	adenine
AAC	ATP/ADP carrier
AAO	Antimycin A & oligomycin
Å	Angstroms
ABC transporter	ATP-binding cassette
ADP	adenosine diphosphate
ALDH	aldehyde dehydrogenase
AMS	4-acetamido-4'-maleimidylstilbene-2,2-disulfonic acid
ATP	adenosine triphosphate
Ben	benomyl
Biotin maleimide	N^{α}-(3-maleimydylpropionyl) biocytin
BLAST	basic local alignment search tool
BNGE	blue native gel electrophoresis
bp	base pair
BSA	bovine serum albumin
C	cytosine
°C	degree Celcius
CCHL	cytochrome *c* heme lyase
cDNA	complimentary deoxyribonucleic acid
CH2-CH3 domains	domains from the Fc fragment of IgG
CORR	co-localization for redox regulation
Cox	cytochrome oxidase
cys	cysteine
Δ	deletion
Da	dalton
DDM	dodecylmaltoside
DIG	digitonin
DMSO	dimethylsulfoxide

DFDNB	1,5-difluoro-2,4-dinitrobenzene
DMP	dimethylpimelimidate
DNA	deoxyribonucleic acid
DPP	human deafness dystonia protein
DSG	disuccinimidylglutarate
ECL	enzyme catalyzed light generation
E. coli	*Escherichia coli*
EM	electron microscopy
EST	expressed sequence tag
ETC	electron transport chain
$F_1\beta$	F_1beta subunit of the ATP synthase
$FADH_2$	flavin adenine dinucleotide, reduced form
FCCP	carbonyl cyanide *p*-trifluoromethoxyphenylhydrazone
Fe-S	iron sulfur
fpa	fluorophenylalanine
G	guanine
g	gravity
gDNA	genomic DNA
GFP	green fluorescent protein
GIP	general import pore
GTP	guanosine triphosphate
HeLa cells	Henrietta Lack's cells
his	histidine
Hot	helper of tim
hr	hour
HRP	horse radish peroxidase
H. sapiens	*Homo sapiens*
Hsp	heat shock protein
hyg	hygromycin
IgG	immunoglobulin G
IMS	intermembrane space

IP	immunoprecipitate
IPTG	isopropyl-beta-D-thiogalactopyranoside
kbp	kilo base pair
kDa	kilo Dalton
kV	kilo volts
L	litre
LB	Luria-Bertani
LG	linkage group
μg	microgram
μl	microlitre
μm	micrometer
M	molar
MM	minimal medium
Mas	mitochondrial assembly protein
MCC	mitochondrial inner membrane conductance channel
Mg	milligrams
MIM	mitochondrial inner membrane
ml	milliliter
mM	millimolar
min	minute
Mia	mitochondrial intermembrane space import and assembly
MIP	mitochondrial intermediate peptidase
MOM	mitochondrial outer membrane
MOPS	4-morpholinepropanesulfonic acid
MPP	matrix processing peptidase
mRNA	messenger ribonucleic acid
ms	millisecond
MSF	mitochondrial import stimulation factor
MTS	Mohr Tranebjaerg Syndrome
mtDNA	mitochondrial DNA
NADH	nicotinamide adenine dinucleotide, reduced form

NAC	nascent associated polypeptide complex
N. crassa	*Neurospora crassa*
NiNTA	nickel-nitrilotriacetic acid
NMR	nuclear magnetic resonance imaging
OD	optical density
Ω	ohms
Oxa1	oxidase assembly protein 1
PAGE	polyacrylamide gel electrophoresis
PAM	presequence translocase-associated protein import motor
PBS	phosphate buffered saline
PBSS	phosphate buffered saline, sucrose
PBSSP	phosphate buffered saline, sucrose, PMSF
PCR	polymerase chain reaction
PiC	phosphate carrier
PK	proteinase K
PMSF	phenylmethylsulfonyl fluoride
pN	pico Newton
polyG/E	glycine/glutamic acid repeats
PVDF	polyvinylidene fluoride
RIP	repeat induced point mutation
RNA	ribonucleic acid
rRNA	ribosomal RNA
rpm	revolutions per minute
SAM	sorting and assembly machinery
SAXS	small angle x-ray scattering
S. cerevisiae	*Saccharomyces cerevisiae*
SCAM	substituted cysteine accessibility mapping
sec	second
SDS-PAGE	sodium dodecyl sulfate polyacrylamide gel electrophoresis
S. pombe	*Schizosaccharomyces pombe*

STAM	signal transduction adaptor molecule
Su9DHFR	subunit 9 of the ATPase (residues 1-69) & dihydrofolate reductase
T	thymine
TCA	tricarboxylic acid cycle
TEV	Tobacco Etch Virus
TIM	translocase of the mitochondrial inner membrane
Tris	tris (hydroxymethyl) aminomethane
TOB	topogenesis of mitochondrial outer membrane β-barrel proteins
TOM	translocase of the mitochondrial outer membrane
TPR	tetratricopeptide repeat
UTR	untranslated region
WD repeat	tryptophan-aspartate repeat
zf-CHY	zinc finger cysteine-histidine-tyrosine motif

1 INTRODUCTION

1.1 *Mitochondrial Functions*

Mitochondria are dynamic organelles that grow by the incorporation of newly synthesized proteins into pre-existing structures which eventually divide. Mitochondria are bounded by two phospholipid membranes, dividing the organelle into four compartments: the outer membrane (MOM), the inner membrane (MIM), the intermembrane space (IMS), and the matrix. These organelles are involved in several cellular processes, the most well known being production of adenosine triphosphate (ATP) by oxidative phosphorylation. Other functions performed in the mitochondria include iron-sulfur (Fe-S) metabolism, amino acid metabolism, the Krebs cycle, the urea cycle and ketone body synthesis. Mitochondria are also involved in other cellular functions such as apoptosis and calcium signaling.

Oxidative phosphorylation harnesses the energy from the oxidation of the reduced electron carriers NADH + H^+ and $FADH_2$ to generate ATP (Joseph-Horne *et al.*, 2001). NADH + H^+ and $FADH_2$ are produced by metabolic processes such as glycolysis, the Kreb's cycle and through β-oxidation of fatty acids. The latter results in the production of reduced electron carriers as well as acetyl-coA which is fed into the Kreb's cycle (Bartlett and Eaton, 2004). These agents donate electrons to the electron transport chain (ETC) which consists of a series of electron transport complexes and smaller carriers housed in the MIM. Three of the four complexes of the ETC are also proton pumps which couple electron transfer with the movement of protons from the matrix to the IMS creating an energy-rich gradient across the MIM. The F_1F_0 ATP synthase in the MIM allows the movement of protons back into the matrix and harnesses the energy stored in this gradient to generate ATP (Saraste, 1999; Capaldi, 2000).

Fe-S cluster proteins are ancient proteins that are involved in a variety of processes including electron transport and regulation of gene expression (Lill and Kispal, 2000; Muhlenhoff and Lill, 2000; Mansy and Cowan, 2004). In eukaryotes, the proteins for Fe-S cluster biogenesis are localized to the mitochondria (Schilke *et al.*, 1999). It is believed that there are at least ten components with homology to their bacterial ancestors that act as scaffolds or chaperones in the mitochondrial matrix for assembly of Fe-S centers. Demonstration of the involvement of a mitochondrial ABC transporter, Atm1, in the pathway suggests that the Fe-S clusters can be exported from the matrix to the cytosol to assemble with Fe-S proteins found in that compartment (Kispal *et al.*, 1999). Interestingly, the neurodegenerative disease Friedreich's Ataxia is caused by a mutation in the gene encoding Frataxin, a protein involved in Fe-S cluster synthesis (Knight *et al.*, 1999; Stehling *et al.*, 2004).

Many human diseases are the result of mitochondrial dysfunction (Simon and Johns, 1999; Wallace, 1999). Mitochondrial dysfunction causes a diverse array of clinical phenotypes. The neurological system is often affected which can result in hearing and vision loss, seizures, dementia, developmental delay, ataxia, peripheral neuropathy and myopathy. In addition, cardiomyopathy and cardiac conduction defects are a common phenotype and skeletal muscles are often affected resulting in weakness, pain, hypotonia or cramping. The mutations causing these disorders can be divided into two general classes. In the most common class, the disease causing mutation is in the mitochondrial DNA (mtDNA) (Lightowlers *et al.*, 1997; DiMauro, 2001). These diseases differ in inheritance patterns from any nuclear mutation as mtDNA is primarily maternally inherited. Characterization of these diseases is complicated by the fact that there are multiple mtDNA molecules present in a mitochondrion and usually only a proportion of those carry the disease-causing mutation. This condition, known as heteroplasmy, often results in one mutation causing several different phenotypes, depending on what proportion of the mtDNAs carry the mutation. The second class is caused by mutations in nuclear genes encoding mitochondrial proteins (Shoubridge, 2001; Zeviani, 2001).

Mitochondrial dysfunction has also been implicated in several other disorders such as Alzheimer's disease, Parkinson's disease, diabetes, Huntington's disease, and cancer (Enns, 2003). Direct evidence has recently been reported implicating accumulation of mtDNA mutations in the aging process (Trifunovic *et al.*, 2004). Mice were generated that expressed an allele of mitochondrial DNA polymerase lacking proofreading activity. It was found that mtDNA mutations accumulated in somatic cells. This correlated with decreased life span and development of phenotypes in young mice that were typical of aged mice (Trifunovic *et al.*, 2004).

1.2 *Origin of Mitochondria*

The idea that mitochondria were once free living cells is the basis of the endosymbiotic theory. In its simplest terms, the theory proposes that an ancestral eukaryotic cell engulfed an ancient relative of bacteria and this relationship evolved so that the bacteria became integrated into the function of the host cell (Gray *et al.*, 2001; Martin *et al.*, 2001). The presence of a circular DNA molecule in mitochondria supports the endosymbiotic theory. When compared to modern organisms, the sequence of mtDNAs have been shown to be most closely related to the obligate parasites of α-proteobacteria such as *Rickettsia* (Yang *et al.*, 1985).

The exact nature of the symbiotic event is not clear. One theory suggests that an archezoon with a nucleus and cytoskeleton endocytosed a eubacterium. This theory suggests that the relationship was symbiotic because the eubacterium provided ATP for the archezoon and the archezoon provided a favorable living environment for the eubacterium (Andersson and Kurland, 1999; Karlberg *et al.*, 2000). However this theory has been disputed since it is unlikely that the eubacterium would actively export ATP. A hypothesis was recently put forward that considers the metabolic needs of both the host and symbiont called the "Hydrogen Hypothesis". This theory suggests that mitochondria and hydrogenosomes have a common ancestor (Martin and Muller, 1998). The authors propose that a methanogenic archaebacterium was the host to a hydrogen and carbon dioxide producing eubacterium. The relationship is thought to have been founded by the host's dependence on the hydrogen produced by the eubacterium as an energy source after being removed to an environment where geological hydrogen was no longer abundant. This would generate selective pressure for the archaebacterium to develop a large surface area to associate with the eubacterium, eventually leading to engulfment. Through specialization for different habitats, hydrogenosomes and mitochondria evolved different forms of energy production.

The question of whether or not the host cell of the endosymbiotic event was a eukaryote or not has also been a matter of much discussion. The existence of amitochondriate eukaryotes was once interpreted to mean that these organisms diverged from the main eukaryotic lineage before mitochondria were acquired. However, the identification of genes within the genome of these organisms encoding proteins related to those found in mitochondria suggests that this is not necessarily the case (Gray *et al.*, 2001). There are two kinds of amitochondriate eukaryotic cells: those that contain hydrogenosomes or those containing mitosomes. Hydrogenosomes are double membrane bound organelles found in some amitochondriate protists that function in the anaerobic conversion of organic carbon to energy. In most organisms, these organelles do not contain their own genome, but there have been proteins identified that are common to mitochondria and hydrogenosomes (Martin *et al.*, 2001). Mitosomes are a double membrane bound organelle that do not make ATP or contain a genome (Embley *et al.*, 2003; Leon-Avila and Tovar, 2004). Mitosomes were first identified in *Entamoeba histolytica*, a pathogen of the human intestine (Tovar *et al.*, 1999). This study demonstrated that the Hsp60 related chaperone protein CPN60 was imported into the mitosome using an N-terminal extension that could be replaced by a mitochondrial targeting sequence (Tovar *et al.*, 1999). Hydrogenosomes also import proteins using similar pathways as those used by mitochondrial proteins destined to either the matrix, using an N-terminal extension, or to the MIM, using internal targeting information (Bradley *et al.*, 1997; Dyall *et al.*, 2000). Compelling evidence of a common ancestry for both mitochondriate and amitochondriate eukaryotes is the observation that proteins involved in FeS cluster biosynthesis are conserved in mitochondria, hydrogenosomes and mitosomes. A key enzyme involved in this process, cysteine desulfurase, is proposed to have originated from the endosymbiont (Tachezy *et al.*, 2001). More recently, hydrogenosomes in *Trichomonas* have been shown to be responsible for Fe-S cluster synthesis using a homologous system to that found in mitochondria of other eukaryotes (Sutak *et al.*, 2004). Components of an Fe-S biosynthesis pathway have also been identified in the mitosome of *Entamoeba histolytica* that were most likely derived from horizontal transfer of genes from an ancestor of α-proteobacteria (Ali *et al.*, 2004). Together, these observations suggest that hydrogenosomes, mitosomes and mitochondria are all related leading to the hypothesis that the evolution of eukaryotic cells and mitochondria may have occurred simultaneously (Embley *et al.*, 2003).

1.3 *Mitochondrial Genome*

The mitochondrial genome varies in size depending on the organism. For example, the mitochondrial genome of *N. crassa* is approximately 65 kbp while the most complex mitochondrial genomes, found in plants, can be larger than 2000 kbp. Mitochondrial genomes in general encode only a few proteins that are components of the ETC. The *N. crassa* mitochondrial genome encodes 14 components of the respiratory chain complexes and ATP synthase, mitochondrial tRNAs, rRNAs, the 5S protein of the small ribosomal subunit and maturases (Kennell, 2004). Most of the original eubacterial genome has either been lost or the genes have transferred to the nucleus. A plasmid introduced into yeast mitochondria was observed to spontaneously move to the nucleus (Thorsness and Fox, 1990). This provides direct evidence that the relocation of genetic material is possible. It is not completely clear why certain genes are maintained as mitochondrial genes rather than moving to the nucleus. The CORR (co-localization for redox regulation) hypothesis suggests that genes that remain in the organelle do so to facilitate direct gene regulation in response to redox changes which would be more rapid and specific than a signal between the organelle and the nucleus (Allen, 2003). The selective pressure described as Muller's ratchet may have also driven the transfer of genes to the nucleus (Blanchard and Lynch, 2000). This theory suggests that asexually inherited genomes are more likely to accumulate mutations because they are not repaired as efficiently as those in the nucleus.

1.4 *Mitochondrial Dynamics*

Mitochondria are highly dynamic organelles that are found as large reticular networks in most organisms and are maintained by a balanced occurrence of fission and fusion events (Yaffe, 1999; Shaw and Nunnari, 2002; Westermann, 2002). Different protein complexes are responsible for fission and fusion events at each mitochondrial membrane. Disruption of fusion leads to fragmentation of mitochondria while loss of fission leads to a highly branched and interconnected net-like structure. The mechanism underlying the fission and fusion of four mitochondrial membranes is not well understood but several players have been identified, including members of a family of dynamin-related GTPases.

Electron microscopic tomography is providing new insights into the internal structure of mitochondria (Frey and Mannella, 2000). There appears to be an unexpected diversity in the structure of cristae when different types of cells are examined. Some are shown to have a tubular shape while others are flat, lamellar structures. All types of cristae appear to attach to the MIM through tubular cristae junctions.

As mitochondria cannot be formed *de novo*, it is important that their inheritance is ensured by an active sorting mechanism. This requires the directed movement of the organelles during cell division events. Movement of mitochondria is mediated by interaction of MOM proteins with actin in yeast and tubulin in *N. crassa* (Westermann and Prokisch, 2002). To ensure inheritance of mitochondria in *S. cerevisiae*, mitochondrial tubules extend into the bud along polarized actin cables and are immobilized at the bud tip (Catlett and Weisman, 2000). This active inheritance of the organelle is also coupled to the inheritance of mitochondrial genomes (Scott *et al.*, 2003). In most cell types, mtDNA is present in multiple copies and is packaged into DNA-protein structures called nucleoids that appear to be tethered to regions of the MIM. Genetic screens for mutants unable to maintain the mitochondrial genome have identified two classes of mutants: those that affect nucleoids directly and those that affect organelle morphology which then results in defective nucleoid inheritance (Scott *et al.*, 2003).

1.5 *Mitochondrial Protein Import*

The vast majority of proteins that function in mitochondria are encoded by nuclear genes and translated on cytosolic ribosomes as precursor proteins. The majority of these proteins are targeted to mitochondria post-translationally where they are translocated across the membranes and sorted into their functional compartments. This process is mediated by protein translocase complexes located in the MOM and MIM (Figure 1). All proteins targeted to mitochondria utilize the TOM complex (translocase of the outer membrane) which can insert proteins into the MOM, move proteins into the IMS or pass proteins on to further assembly machinery in the MOM or one of two translocase complexes in the MIM. The TOB (topogenesis of β-barrel proteins) complex, also known as the SAM (sorting and assembly machinery) complex, is involved in assembly of β-barrel proteins into the MOM. The TIM23 complex (translocase of the inner membrane) recognizes mitochondrial preproteins with amino-terminal targeting sequences. Most of these proteins are destined for the matrix but a few that contain additional sorting signals are inserted into the MIM through a stop-transfer pathway. Some of the latter class may then be further processed, resulting in their release into the IMS. The PAM (presequence translocase associated motor) import motor is associated with the TIM23 complex and is necessary to import proteins into the matrix. The TIM22 complex facilitates the insertion of multitopic membrane proteins with internal targeting information into the MIM. In addition, an export complex, OXA, is located in the MIM to insert proteins into the membrane from the matrix.

1.5.1. *Mitochondrial Protein Import is Usually a Post-Translational Event*

Evidence of translocation of a mitochondrial precursor following completion of translation was first observed in live cells and a cell homogenate of *N. crassa* (Hallermayer *et al.*, 1977; Harmey *et al.*, 1977). Both works observed a lag between protein synthesis and protein import into mitochondria. As well, it was observed that inhibition of protein synthesis with cycloheximide did not interfere with import of proteins into mitochondria. Similar results were then observed with *S. cerevisiae* suggesting that post-translational import was a common mechanism (Maccecchini *et al.*, 1979). There is evidence that some proteins are targeted to mitochondria co-translationally. One group found that mitochondrial protein import was dependent on translation and the presence of ribosomes, supporting a purely co-translational model of import (Fujiki and Verner, 1991, 1993). In a somewhat unique case, it was the rapid folding kinetics of the protein fumarase that established its requirement for co-translational import into mitochondria (Knox *et al.*, 1998). Further evidence that some proteins are translocated co-translationally comes from *in vivo* import studies in HeLa cells (Ni *et al.*, 1999; Mukhopadhyay *et al.*, 2004). This work showed that a protein with a mitochondrial targeting signal at the N-terminus in addition to an ER targeting signal or a peroxisomal targeting signal on the C-terminus, was always localized to the mitochondria. This lends support to a co-translational model of import for the proteins tested in this study.

While ribosomes have been found in association with mitochondrial membranes (Kellems *et al.*, 1975; Crowley and Payne, 1998) there is no direct evidence that this is the result of co-translational import. The association seems to be regulated by GTP and is dependent on an unidentified protein associated with the MOM (Crowley and Payne, 1998; MacKenzie and Payne, 2004). In analyzing the mRNA extracted from both free cytosolic and mitochondrially bound polysomes, it was found that certain mRNAs are exclusively found in mitochondrially-bound polysomes and that the 3'UTR or 5' targeting signal was sufficient for this specificity (Egea *et al.*, 1997; Corral-Debrinski *et al.*, 2000; Marc *et al.*, 2002). This is not true for all mRNAs encoding mitochondrial proteins as some show distribution throughout the cytoplasm (Egea *et al.*, 1997). These observations suggest that mRNA localization may play a role in targeting certain proteins to the mitochondria.

1.5.2. *Protein Targeting and Chaperones*

Mitochondrial precursor proteins contain targeting information that ensures the correct localization of the protein within the cell. The most common type of targeting signal is called a presequence, a leader sequence, a leader peptide or an N-terminal targeting signal and is located at the amino terminus of the mitochondrial precursor protein. Most proteins with this kind of signal sequence are sorted to the mitochondrial matrix (see below). The presequence is removed from the protein in the matrix by the mitochondrial processing peptidase (MPP) so it is not a part of the mature protein. Presequences show no overall conservation at the amino acid sequence level but do share a number of physical characteristics. Typically they are 20 to 60 amino acid residues in length and contain hydrophobic, hydroxylated and basic residues while lacking acidic residues (Hammen and Weiner, 1998). The positively charged residues are spaced such that an amphipathic helix is formed. Both the secondary structure and the charge are thought to facilitate interactions with components of the translocase complexes and are thus significant for import competence of the precursor protein (see Section 1.6.1) (von Heijne, 1986; Roise *et al.*, 1988). The relative importance of each has been debated. Using aldehyde dehydrogenase (ALDH), Hammen *et al.*, performed mutagenesis of the leader peptide and determined that the overall positive charge of the sequence was less important for import competence than the helical structure for that precursor protein (Hammen and Weiner, 1998). On the other hand, Horwich *et al*., mutagenized the leader peptide of ornithine transcarbamylase and suggested that the net positive charge was more important than the amphipathic helix for efficient import of the precursor peptide (Horwich *et al.*, 1987). Although most presequences lack acidic residues, this is not an absolute requisite as some mitochondrial protein leader sequences contain negatively charged amino acids without affecting the targeting or import of the precursor (Mukhopadhyay *et al.*, 2003). An exception to the location of the presequence at the N-terminus was recently reported as a cleavable presequence was identified at the carboxy terminus of the mtDNA helicase, Hmi1p (Lee *et al.*, 1999). The targeting signal contains several positively charged residues and is capable of forming an amphipathic helix making the only significant difference from classical presequences its location.

Some proteins that are sorted to the MIM contain sorting information in addition to the leader peptide signal. Referred to as a bipartite pre-sequence, the presence of a hydrophobic stretch of amino acid residues immediately following the typical presequence will initiate this sorting pathway, often referred to as the stop-transfer pathway (Beasley *et al.*, 1993). The hydrophobic residues stop the preprotein as it crosses the TIM23 complex whereupon it is moved directly from the pore into the membrane. Further sorting of bipartite signal-containing proteins can occur through proteolysis of another recognition sequence. For example, cytochrome b_2 is inserted into the MIM by the stop-transfer mechanism and is further processed by the Imp1 protease of the MIM resulting in its release into the IMS (Schneider *et al.*, 1991; Esaki *et al.*, 1999).

Other mitochondrial proteins contain targeting information within the coding sequence of the mature protein. The most common example of this type of targeting is the large class of metabolite carrier proteins that are found in the MIM. The best characterized of these is the ADP-ATP carrier protein (AAC). All members of the carrier family have similar structure with three modules, each containing two transmembrane domains connected by a hydrophilic loop. The import and sorting signal is not found in a single domain of the protein but is composed of several different signals in different regions of the protein. Deletion analysis revealed that the carboxy two thirds of AAC was sufficient for targeting and insertion to the MIM suggesting that all targeting information was contained within this part of the protein (Pfanner *et al.*, 1987; Smagula and Douglas, 1988). However, information sufficient for targeting to the TOM complex has been shown to reside in the N-terminus of the protein although it could not target the protein for insertion into the MIM (Smagula and Douglas, 1988). While the regions are capable of functioning individually under experimental conditions, it is most likely that they function cooperatively *in vivo* (Wiedemann *et al.*, 2001).

Four structural classes of proteins exist in the MOM including N-terminally anchored, C-terminally anchored, β-barrel proteins and those with two membrane spanning domains (Rapaport, 2003). There is no sequence conservation in the targeting signals of these proteins. The N-terminally anchored proteins require the transmembrane domain and a few flanking amino acids with positive charges for targeting and insertion into the MOM (McBride *et al.*, 1992; Kanaji *et al.*, 2000; Suzuki *et al.*, 2002; Waizenegger *et al.*, 2003). Given the dual role of this region, these proteins are also known as signal-anchor proteins. The targeting information in C-terminally anchored or tail anchored proteins has similar properties to the signal-anchor proteins. These transmembrane domains are relatively short and hydrophobic with flanking positive charges, all contributing to targeting and insertion into the MOM (Kuroda *et al.*, 1998; Kaufmann *et al.*, 2003). Some of the components of the TOM complex are included in this class and it has been shown that a proline residue within the membrane spanning domain of these proteins is important for targeting (Allen *et al.*, 2002). The targeting signals of β-barrel proteins have not been well characterized. Deletion analysis suggests that the import signal is not restricted to one region, but is dispersed throughout the protein (Hamajima *et al.*, 1988; Court *et al.*, 1996; Rapaport and Neupert, 1999).

Most mitochondrial preproteins are imported in an unfolded state (Eilers and Schatz, 1986; Schwartz *et al.*, 1999). Cytosolic molecular chaperones maintain the mitochondrial precursor proteins in this state to facilitate import (reviewed in (Beddoe and Lithgow, 2002)). MSF (mitochondrial import stimulating factor) and Hsp70 were identified as proteins that stimulated the import of mitochondrial precursor proteins in an ATP-dependent manner (Murakami *et al.*, 1988; Hachiya *et al.*, 1993). MSF is the only chaperone identified that is capable of restoration of import competence of an aggregated precursor protein using ATP suggesting that its chaperone activity is specifically involved in mitochondrial precursor protein targeting and import (Hachiya *et al.*, 1994; Komiya *et al.*, 1994; Hachiya *et al.*, 1995; Komiya *et al.*, 1996). Hsp70 seems to play a more general chaperone role, and is involved in stabilizing proteins targeted to various cellular compartments (reviewed in (Rassow *et al.*, 1995)). In mammalian cells, the chaperones have been shown to work cooperatively as the mitochondrial protein phosphate carrier (PiC) binds to both mammalian Hsp70 and Hsp90 in a multichaperone complex for targeting as a precursor protein (Young *et al.*, 2003). In yeast, there are seven isoforms of Hsp70 in the cytosol. Two of these isoforms have been implicated in the import efficiency of mitochondrial precursor proteins (Deshaies *et al.*, 1988; Gautschi *et al.*, 2001). Loss of the yeast Hsp40 homologue Ydj1p, results in reduced import of mitochondrial precursors suggesting that this chaperone cooperates with Hsp70 to facilitate import into mitochondria (Atencio and Yaffe, 1992). Yeast NAC (nascent associated polypeptide complex), which is composed of two non-essential subunits, is also involved in stimulating import of nascent polypeptides into mitochondria (George *et al.*, 1998; Funfschilling and Rospert, 1999).

1.5.3. *Energy Dependence of Import*

The import of proteins into mitochondria generally requires two sources of energy: ATP hydrolysis and membrane potential across the MIM ($\Delta\Psi$). The membrane potential creates a negatively charged environment in the matrix. High $\Delta\Psi$ is required for import of proteins to both the matrix and the MIM. It is thought that this energy may trap, or perhaps exert a physical force referred to as the "electrophoretic force", on the positively charged presequences. High membrane potential is also essential for the activity of the TIM22 complex which imports non-presequence containing precursors (see section 1.9.4 and 1.9.7). ATP hydrolysis both in the cytosol and the matrix appears to be important for import of various precursor proteins. Matrix ATP is used by mtHsp70, an essential component of the PAM complex (see section 1.9.2). In the cytosol, it has been shown that while AAC is transferred from MSF to Tom70 without ATP hydrolysis, the release of MSF from Tom70 does require ATP (Komiya *et al.*, 1996; Komiya *et al.*, 1997). In mammalian cells, it has been demonstrated that the precursor protein AAC must be presented to Tom70 by the ATP-dependent chaperones for import of the precursor to occur (Young *et al.*, 2003). In contrast, the transfer of a presequence-containing protein to Tom20 does not require ATP (Asai *et al.*, 2004). The latter class of precursors are kept in an import competent state with cycles of precursor binding and release by cytosolic Hsp70 in an ATP-dependent manner, but do not require external ATP upon or after binding to mitochondria (Asai *et al.*, 2004).

1.6 *The TOM Complex*

The TOM complex is responsible for recognition of mitochondrial preproteins and their passage into or through the MOM (reviewed in (Pfanner and Neupert, 1990; Paschen and Neupert, 2001; Prokisch *et al.*, 2002; Endo *et al.*, 2003; Rehling *et al.*, 2003; Hoppins, 2004; Koehler, 2004)). The components of the TOM complex can be divided into two functional categories: those that are important in formation of the general import pore and those that act as receptors responsible for recognition of mitochondrial preproteins.

1.6.1 *Components of the TOM complex*

The TOM complex contains the three receptor proteins Tom70, Tom22 and Tom20. Tom70 is an amino-terminally anchored protein with a large cytosolic domain containing seven TPR (tetratrico peptide repeat) repeats (Steger *et al.*, 1990). TPR repeats are thought to be important in mediating protein-protein interactions (Blatch and Lassle, 1999). Tom70 is primarily responsible for recognition of proteins with internal targeting sequences. Loss of this receptor is not lethal in yeast or *N. crassa* (Hines *et al.*, 1990; Ramage *et al.*, 1993; Grad *et al.*, 1999). The protein was identified by showing that loss of Tom70 function resulted in decreased import of AAC (Sollner *et al.*, 1990; Steger *et al.*, 1990). Initial attempts to reconstitute the interaction between Tom70 and precursor proteins *in vitro* suggested that an additional cytosolic factor was necessary for efficient interaction of some precursors and the receptor (Schlossmann *et al.*, 1994). One such factor was later identified when it was found that the interaction between the cytosolic domain of Tom70 and precursors is enhanced by the presence of MSF *in vitro* (Komiya *et al.*, 1997). The TPR repeats of Tom70 likely perform two separate functions. First, a ‘core domain’ was identified containing the four C-terminal repeats that were sufficient for precursor binding *in vitro* (Brix *et al.*, 2000). Second, prompted by the knowledge that some Hsp70 and Hsp90 cofactors contain TPR repeats, Young *et al.* found that the three N-terminal TPR repeats of Tom70 form a dicarboxylate clamp domain that facilitates interactions with Hsp70 in yeast and Hsp70 and Hsp90 in mammals (Young *et al.*, 2003).

Tom20 is also an N-terminally anchored MOM protein with a large cytosolic domain containing a single TPR repeat. This was the first receptor protein to be identified and was found using specific antibodies to inhibit the function of the protein *in vitro* (Sollner *et al.*, 1989). This receptor is predominantly responsible for recognition of preproteins with N-terminal presequences. Loss of Tom20 causes severe growth phenotypes, reduction in the levels of Tom22 and inhibition of precursor import (Harkness *et al.*, 1994; Harkness *et al.*, 1994; Moczko *et al.*, 1994). There is some functional redundancy between Tom20 and Tom70 *in vivo* as loss of both is lethal (Ramage *et al.*, 1993; Lithgow *et al.*, 1994). Tom20 contains a region of negatively charged residues which led to the suggestion that ionic interactions would exist between the receptor and precursor proteins. In contrast to this prediction, it was determined that interaction with the leader peptide of the precursor protein is strengthened at high salt concentrations. Thus, it seems more likely that Tom20 interacts with precursor proteins via hydrophobic interactions (Brix *et al.*, 1997). This is supported by the NMR structure of rat Tom20 bound to a leader peptide. The helical structure of the peptide is accommodated by a hydrophobic groove in the cytosolic domain of Tom20, facilitating an interaction between the hydrophobic face of the amphipathic helix of the presequence and Tom20 (Abe *et al.*, 2000). Closer examination of the interaction of Tom20 with a variety of presequences suggests that a relatively small portion of the presequence interacts with Tom20 (Muto *et al.*, 2001).

Tom22 is a tail-anchored MOM protein that contains several negatively charged amino acids within both the N-terminal cytosolic and C-terminal IMS domains (Kiebler *et al.*, 1993). Tom22 was identified in *N. crassa* through its interaction with Tom20 and Tom70 (Kiebler *et al.*, 1990). Initial characterization of the yeast homologue suggested that Tom22 was essential for growth, as ascospores lacking the gene were inviable (Lithgow *et al.*, 1994; Honlinger *et al.*, 1995; Nakai and Endo, 1995). However, it was found that a haploid *tom22Δ* strain expressing wild type Tom22 on a plasmid would continue to grow on a fermentable carbon source even when the plasmid was lost (van Wilpe *et al.*, 1999). Analysis of this strain demonstrated that the loss of Tom22 results in a very slow growth rate, loss of mtDNA and severely reduced import of precursor proteins. In contrast to yeast, Tom22 is essential for viability in *N. crassa* (Nargang *et al.*, 1995). This difference is likely explained by the fact that *N. crassa* is an obligate aerobe and therefore cannot live without mtDNA. In yeast and *N. crassa* Tom22 is involved in import of most preproteins, with the exception of a few MOM proteins (Kiebler *et al.*, 1993; Lithgow *et al.*, 1994; Nargang *et al.*, 1995). Negative charges found in both the cytosolic and IMS domains of Tom22 were initially thought to interact with positive charges in leader sequences of precursor proteins. It was determined that the C-terminal domain is not essential for Tom22 function (Court *et al.*, 1996; Moczko *et al.*, 1997). The absence of this IMS domain resulted in decreased import efficiency of presequence containing proteins suggesting that this domain is a component of the trans binding site (see section 1.6.2) (Moczko *et al.*, 1997). While the cytosolic domain is essential, mutational analysis of this region suggests that the negative charges in the region are not critical for function of Tom22 (Nargang *et al.*, 1998).

Tom40 is an essential integral membrane protein that was identified as a component of the general import pore (GIP) in the MOM (Vestweber *et al.*, 1989; Baker *et al.*, 1990; Kiebler *et al.*, 1990). It was later predicted that Tom40 was a β-barrel protein, structurally similar to bacterial porin proteins (Mannella, 1996). Tom40 is essential in yeast and *N. crassa* (Baker *et al.*, 1990; Taylor *et al.*, 2003). Precursor proteins were found to crosslink with Tom40 implicating the protein directly in mitochondrial protein import (Sollner *et al.*, 1992; Rapaport *et al.*, 1997). A variety of analyses including electron microscopy and electrophysiology suggest that Tom40 forms a pore through the MOM (Hill *et al.*, 1998; Kunkele *et al.*, 1998; Ahting *et al.*, 1999). Reduction of Tom40 protein levels results in very slow growth and diminished import efficiency of all precursors tested (Taylor *et al.*, 2003). In the TOM complex, Tom40 exists as an oligomer with dimers as the basic structural unit (Rapaport *et al.*, 1998). Removal of the negatively charged region of the cytosolic domain of Tom22 causes the protease sensitivity of Tom40 to change suggesting that this region influences the structure of Tom40 (Rapaport *et al.*, 1998). Tom40 dynamics, as observed by dimerization of Tom40 and interaction with Tom6, also changed in response to a translocating precursor protein (Rapaport *et al.*, 1998). This may reflect opening of the pore to allow translocation. Unexpectedly, the reported topology of the protein differs in yeast and *N. crassa*. In *N. crassa*, both the N- and C-termini are found in the IMS (Kunkele *et al.*, 1998) while in yeast the N-terminus is exposed on the cytosolic side of the MOM (Hill *et al.*, 1998). Rat Tom40 has a topology that is similar to yeast as suggested by accessibility of N- and C-terminal epitope tags (Suzuki *et al.*, 2004). Structural analysis of yeast Tom40 expressed as a recombinant protein in *E. coli*, purified, refolded and inserted into liposomes revealed a structure with more than 60% β-sheets (Hill *et al.*, 1998). In contrast, purification of *N. crassa* Tom40 suggested that the β-sheet content was only around 30% (Kunkele *et al.*, 1998).

The TOM complex also contains three small tail-anchored proteins, Tom5, Tom6 and Tom7. Tom6 and Tom7 were identified when they were found to co-purify with other components of the TOM complex in immunoprecipitaion experiments (Moczko *et al.*, 1992; Sollner *et al.*, 1992) and Tom6 was also identified as a high copy suppressor of a Tom40 temperature sensitive allele (Kassenbrock *et al.*, 1993). Tom5 was later identified as a protein that also co-immunoprecipitated with Tom40 (Dietmeier *et al.*, 1997). All three of the small Tom proteins have been characterized in yeast and none are essential for viability. Tom7 is the only one that has been shown to have a human homologue (Johnston *et al.*, 2002). In yeast, Tom6 and Tom7 are functionally antagonistic toward each other. Deletion of Tom6 results in the destabilization of the interaction between Tom40, Tom20 and Tom22 suggesting that it plays a role in maintaining the structure of the complex (Alconada *et al.*, 1995; Dekker *et al.*, 1998). Loss of Tom6 also caused a decrease in import efficiency of precursor proteins. Conversely, deletion of Tom7 caused the interaction between Tom40, Tom20 and Tom22 to become more resistant to dissociation (Honlinger *et al.*, 1996; Dekker *et al.*, 1998). Honlinger *et al.* found that loss of Tom7 significantly decreased the efficiency of import of porin, an abundant MOM β-barrel protein. Loss of Tom5 in yeast is lethal at 37°C and caused a decrease in growth rate at 30°C. Tom5 has a cytosolic domain that has a net negative charge that was thought to be important for function (Dietmeier *et al.*, 1997), but deletion of the domain did not alter growth (Horie *et al.*, 2003). Loss of yeast Tom5 caused the import efficiency of all proteins tested to decrease suggesting a central role in the import process. This is also supported by crosslinks identified between the incoming precursor protein and Tom5 (Dietmeier *et al.*, 1997). However, in *N. crassa* deletion of *tom5* did not affect growth or import of any precursors tested (Schmitt *et al.*, 2005; Sherman, 2005). Interestingly, even though the phenotypes of mutants lacking Tom5 in the two organisms are quite different, the *N. crassa* protein is able to rescue the growth defects of the yeast *tom5Δ* mutant, suggesting that function in the TOM complex is conserved (Schmitt *et al.*, 2005). Further study of single and double mutants lacking the small Tom proteins of *N. crassa* demonstrated that all three are involved in maintaining TOM complex stability and have different effects on the import of various precursors than was observed in the corresponding yeast mutants (Sherman, 2005).

1.6.2 *Structure of the TOM complex*

Purification of the TOM complex has provided information about the stoichiometry of the components and the mode of function of the pore. When purified from a strain of *N. crassa* expressing a hexahistidinyl tagged version of Tom22 and solubilized in digitonin, the TOM complex was estimated to be 550-600 kDa in size and was referred to as the holo complex (Kunkele *et al.*, 1998). The components included Tom70, Tom40, Tom22, and Tom20 estimated to be in a 1.5:8:3.1:2 ratio. The small Toms were also present but their stoichiometry was not determined. When the TOM complex is examined following solubilization in the stronger detergents *n*-dodecylmaltoside or Triton-X-100, Tom70 and Tom20 dissociate leaving a core complex of 400 kDa (Dekker *et al.*, 1998; Ahting *et al.*, 1999; Meisinger *et al.*, 2001). The stoichiometry of the components of the TOM core complex were estimated at 8:4:2:2 for Tom40:Tom20:Tom6 and Tom7 (Ahting *et al.*, 1999). Resistance to proteolysis by the matrix processing peptidase (MPP) suggests that a presequence containing protein inserts into the pore of the purified TOM complex in the absence of chaperones and a lipid bilayer (Stan *et al.*, 2000).

The purified TOM complex has also been analyzed by electrophysiology, electron microscopy, and size exclusion studies. The pore was found to be cation selective and had electrophysiological properties consistent with a homodimeric pore with a large conductance (Hill *et al.*, 1998; Kunkele *et al.*, 1998a; Kunkele *et al.*, 1998b). Depending on the isolation procedures used, electron microscopy suggested that the TOM complex could contain either two or three pores (Kunkele *et al.*, 1998a; Ahting *et al.*, 1999). This was explained when Model *et al.*, found that the complex has three pores when purified with Tom20 and only two when purified in the absence of Tom20 (Model *et al.*, 2002). The pore is suggested to be between 20 and 30Å in diameter (Kunkele *et al.*, 1998b; Ahting *et al.*, 1999; Schwartz and Matouschek, 1999; Model *et al.*, 2002).

The TOM complex has several binding sites for incoming precursor proteins. Two well defined binding sites are called the cis and trans binding sites, found on the cytosolic and IMS faces, respectively. The cis site requires the presence of the cytosolic domains of Tom20 and Tom22 as demonstrated by the protease sensitivity of binding at this site (Mayer *et al.*, 1995). The binding is also sensitive to salt suggesting that the interaction involves electrostatic forces (Mayer *et al.*, 1995; Rapaport *et al.*, 1997). There is also evidence that Tom40 contributes to precursor binding at the cis site. A precursor imported under conditions that result in binding primarily at the cis site can be crosslinked to Tom40 and the conformation of Tom40 is altered upon binding of a preprotein (Rapaport *et al.*, 1998). This binding site likely represents a later stage than the binding of the presequence to Tom20, which was found to be based on hydrophobic interactions (Abe *et al.*, 2000). Binding at the trans site corresponds to the unfolding of the incoming precursor protein (Mayer *et al.*, 1995). The precursor protein could also be crosslinked to Tom40 when bound to this site (Rapaport *et al.*, 1997). Binding of the precursor protein at the trans site was stable in high salt (Rapaport *et al.*, 1998) and is important in keeping the precursor protein from sliding out of the pore (Mayer *et al.*, 1995). The IMS C-terminal domain of Tom22 and of Tom7 have both been shown to crosslink to preproteins bound at the trans site and deletion of both domains results in growth defects in yeast (Esaki *et al.*, 2004).

1.6.3 *Biogenesis of the TOM complex*

The individual components of the TOM complex have different requirements for import and insertion into the MOM and assembly into the TOM complex. The TOM complex seems to be dynamic, with subunits being exchanged over time (Rapaport *et al.*, 2001). Tom40, Tom6 and Tom7 all require Tom20 and Tom22 for efficient import into the MOM and Tom40 also requires the presence of Tom70 (Keil *et al.*, 1993; DEMBOwski *et al.*, 2001; Model *et al.*, 2001). Tom20, Tom70 and Tom5 seem to interact directly with Tom40, having no requirement for receptor domains in the cytosol for efficient import (Schneider *et al.*, 1991; Schlossmann *et al.*, 1994; Suzuki *et al.*, 2000; Horie *et al.*, 2003; Ahting *et al.*, 2005). Conceivably, this could happen with or without insertion into the pore. A model whereby the insertion of these proteins is facilitated by an interaction with Tom40 at its interface with the lipid bilayer is favored over a model that calls for the pore to open so the protein can diffuse laterally (Ahting *et al.*, 2005).

Tom22, Tom5 and Tom7 all appear to assemble directly into the 400 kDa GIP in yeast mitochondria (Model *et al.*, 2001). Tom6 assembles into the complex via a 100 kDa intermediate (Model *et al.*, 2001). Unlike the observations in yeast, human Tom7 assembly to the TOM complex involves a 120 kDa intermediate (Johnston *et al.*, 2002). The assembly of Tom40 into the GIP is more complex. It has been studied by following the progress of a newly imported subunit into the final assembled TOM complex by BNGE and was found to involve at least two assembly intermediates (Figure 2). As discussed above, the Tom40 precursor initially interacts with the receptor proteins on the surface of the MOM. As it crosses the membrane through the GIP and emerges on the IMS side, the precursor interacts with one of two soluble complexes, Tim8-13 or Tim9-10 (Hoppins and Nargang, 2004; Wiedemann *et al.*, 2004). At this point the precursor is protected from externally added protease. The precursor then interacts with the TOB/SAM assembly machinery giving an assembly intermediate about 250 kDa in size (Wiedemann *et al.*, 2003). For Tom40 to assemble into the 250 kDa intermediate, Tom20, Tom22 and Tom5 are needed (Model *et al.*, 2001; Wiedemann *et al.*, 2003). When the precursor dissociates from the large TOB/SAM complex it forms a 100 kDa intermediate with some of the characteristics of assembled Tom40 suggesting that it is folded and integrated into the MOM. The final step in assembly for an incoming Tom40 subunit involves the association of Tom6 and Tom22 which is mediated by MDM10 and MIM1/Tom13 (Ishikawa *et al.*, 2004; Meisinger *et al.*, 2004; Waizenegger *et al.*, 2005).

The formation of the 400 kDa complex is inhibited in the absence of Tom6 (Model *et al.*, 2001).

Mutations in different regions of Tom40 have variable affects on the assembly of the protein. Deletions at either the C-terminus or the N-terminus in *N. crassa* Tom40 reveal that residues in these regions are required for Tom40 assembly but not targeting (Rapaport *et al.*, 2001; Taylor *et al.*, 2003). In another study, four classes of defective assembly mutants were identified (Sherman, 2005). In Class I, Tom40 variants accumulated at the 250 kDa intermediate and did not assemble into the 400 kDa complex. The variants included in Class II also accumulated at the 250 kDa intermediate but did assemble into the 400 kDa complex after extended time. The third phenotypic class accumulated precursor at the 100 kDa intermediate with little 250 kDa or 400 kDa forms observed. In the final group, mutant variants of Tom40 assembled into the 400 kDa complex normally.

The biogenesis of human Tom40 was recently examined and some differences with the fungal assembly pathway were revealed. The import of human Tom40 is dependent on ATP as the cytosolic chaperone Hsp90 delivers the precursor protein to the TOM complex (Humphries *et al.*, 2005). The initial association of Tom40 precursor with the TOM complex was seen by blue native gel electrophoresis (BNGE) in a complex of about 500 kDa. The precursor progresses to the human TOB/SAM complex, although this interaction appears to be more transient than the interaction in fungal assembly and a 250 kDa intermediate is not observed unless mutant Tom40 precursors are imported. The precursor then progresses to the 100 kDa stage and assembles into the 400 kDa TOM complex (Humphries *et al.*, 2005).

1.7 *The TOB Complex and MIM1*

The MOM contains machinery responsible for the insertion of proteins that span the membrane multiple times to form a β-barrel structure (Figure 1) (reviewed in (Pfanner *et al.*, 2004)). The first component of this machinery identified was a protein that had previously been characterized as a component of the TOM complex due to genetic interactions with Tom70 (Gratzer *et al.*, 1995). Subsequent investigation revealed that this protein, originally called Tom37 and renamed first to Mas37 and subsequently to Sam37, was a component of the TOB/SAM complex (Wiedemann *et al.*, 2003). Sam37 is not essential for viability in yeast and is a component of a protein complex of about 210 kDa. Wiedemann *et al.*, demonstrated that the assembly of both Tom40 and porin was defective in mitochondria lacking Sam37, suggesting that the TOB complex is needed for biogenesis of different β-barrel proteins of the MOM (Wiedemann *et al.*, 2003). The human homologue of Sam37, metaxin1, was identified as a gene essential for the survival of mouse embryos (Armstrong *et al.*, 1997). The primary component of the SAM complex, Tob55/Sam50/Omp85, was identified by three different experimental approaches in fungi (Kozjak *et al.*, 2003; Paschen *et al.*, 2003; Gentle *et al.*, 2004). The human homologue has also recently been characterized (Humphries *et al.*, 2005). Tob55 (Sam50/Omp85) is essential for viability and encodes an integral MOM protein with a predicted β-barrel structure (Kozjak *et al.*, 2003; Paschen *et al.*, 2003; Gentle *et al.*, 2004). All four groups also found Tob55 to be important for the biogenesis of Tom40 and porin. Electron microscopy of purified Tob55 suggests that it may form a pore (Paschen *et al.*, 2003). A third component of the TOB complex is Sam35/Tob38/Tom38 (Ishikawa *et al.*, 2004; Milenkovic *et al.*, 2004; Waizenegger *et al.*, 2004). These three studies illustrate that Tob38 is a peripheral MOM protein that is essential for viability in yeast. When the level of Tob38 is reduced, the assembly of Tom40 and porin is compromised. A yeast 2-hybrid screen using Metaxin1 as bait identified the human homologue of Tob38, Metaxin2 (Armstrong *et al.*, 1999). The function of the individual components within the TOB complex is still unclear.

MDM10 has also been characterized as a protein that interacts with the TOB complex (Meisinger *et al.*, 2004). MDM10 was previously characterized as a protein required for mtDNA maintenance (Sogo and Yaffe, 1994). Meisinger *et al.* identified an association of MDM10 with the TOB/SAM complex under high salt conditions revealing a 350 kDa complex(Meisinger *et al.*, 2004). Loss of Mdm10 results in impaired assembly of Tom40 from the 100 kDa intermediate to the fully assembled 400 kDa complex. There was no defect observed in the assembly of porin. Thus it appears that Mdm10 functions specifically in the biogenesis of the TOM complex rather than in the biogenesis of all MOM β-barrel proteins.

MIM1/Tom13 is essential for the viability of yeast and is involved specifically in the assembly of a newly imported subunit of Tom40 into the TOM complex (Ishikawa *et al.*, 2004; Waizenegger *et al.*, 2005). Though reports differ in the estimation of the size of the MIM1/Tom13 complex, there is agreement that it is not a component of the TOB/SAM complex (Ishikawa *et al.*, 2004; Waizenegger *et al.*, 2005). Depletion of MIM1/Tom13 results in diminished assembly of Tom40 from the 100 kDa intermediate to the TOM complex but has no effect on the assembly of other MOM β-barrel proteins. Therefore, like MDM10, MIM1/Tom13 is specifically involved in the assembly of Tom40 to the TOM complex.

1.8 *Import Components of the IMS*

Two soluble complexes have been identified in the IMS that play a role in mitochondrial protein import. These complexes are believed to act as chaperones to shield hydrophobic domains of precursor proteins from the hydrophilic environment of the IMS. While they appear to be somewhat redundant in function, the Tim9-10 complex is essential while the Tim8-13 complex is not. The 'tiny Tim' proteins include Tim8, Tim9, Tim10, Tim12 and Tim13 and are about 25% identical and 50% similar to each other (Bauer *et al.*, 2000). A common feature of this family is the presence of a twin CX_3C motif: two separate motifs of two cysteine residues separated by three amino acids, with the motifs separated by 16-18 amino acids (Bauer *et al.*, 2000).

S. cerevisiae Tim12 and Tim10 were the first members of the tiny Tim family characterized (Jarosch *et al.*, 1996; Jarosch *et al.*, 1997). Tim10 is an essential protein that is soluble in the IMS (Jarosch *et al.*, 1997). Tim12 is also essential but is associated with the TIM22 complex on the IMS side of the MIM (Jarosch *et al.*, 1996; Adam *et al.*, 1999). Depletion of Tim10 or Tim12 resulted in import deficiencies of multitopic carrier proteins (Jarosch *et al.*, 1996; Jarosch *et al.*, 1997; Koehler *et al.*, 1998; Sirrenberg *et al.*, 1998). Tim9 is also essential and was identified through its interaction with Tim10 (Koehler *et al.*, 1998; Adam *et al.*, 1999). Tim9 and Tim10 associate to form a soluble 70 kDa complex in the IMS that can associate with the TIM22 complex through an interaction with Tim12 resulting in the formation of a Tim9-10-12 complex (Koehler *et al.*, 1998; Adam *et al.*, 1999).

The Tim9-10 complex is required and sufficient for release of the AAC precursor from the TOM complex (Truscott *et al.*, 2002; Vasiljev *et al.*, 2004). Peptide scanning analysis using purified Tim9-10 complex suggests that it interacts most strongly with the hydrophobic domains of AAC, consistent with its proposed role as a chaperone (Curran *et al.*, 2002; Vasiljev *et al.*, 2004). AAC is thought to cross the TOM complex in a loop structure whereby two hydrophobic stretches are in the pore at the same time with the intervening hydrophilic stretch emerging at the IMS side first (Wiedemann *et al.*, 2001). A model has been proposed suggesting that the Tim9-10 complex begins binding to the incoming AAC molecule in the hydrophilic region so that the hydrophobic domains can be transferred to the Tim9-10 complex directly from the TOM complex, avoiding exposure to the hydrophilic IMS (Vasiljev *et al.*, 2004). Interestingly, the Tim9-10 complex does not need to be soluble in yeast in order to function. A mutation in Tim9 that causes the complex to be strongly associated with the TIM22 complex as the Tim9-10-12 complex rather than in the soluble Tim9-10 form is not lethal (Murphy *et al.*, 2001). Recently, the Tim9-10 complex has also been shown to be involved in import of β-barrel proteins of the MOM (Wiedemann *et al.*, 2004).

In humans, there are two *tim10* genes and no homologue of Tim12. However, similar to the observations in yeast, there are two complexes containing tiny Tim proteins in humans. The first is a 70 kDa complex composed of Tim9 and Tim10a while the second is composed of Tim9, Tim10a and Tim10b and is 450 kDa due to its association with the TIM22 complex (Muhlenbein *et al.*, 2004). Both complexes are associated with the MIM (Muhlenbein *et al.*, 2004).

Tim8 and Tim13 were identified in a search for homologues of the other tiny Tim proteins in the yeast genome database (Koehler *et al.*, 1999). The proteins also form a soluble complex in the IMS of 70 kDa in yeast and 80 kDa in *N. crassa* (Koehler *et al.*, 1999; Hoppins and Nargang, 2004). Neither Tim8 nor Tim13 is essential for viability under normal growth conditions. However, a strain of yeast lacking the *tim8* gene was found to be inviable when grown at 15°C with glucose as a carbon source (Paschen *et al.*, 2000). Growth of yeast under these conditions would result in reduced levels of oxidative phosphorylation, which could result in a reduction of membrane potential. Therefore, it was proposed that Tim8-13 may be important for import of its substrates when membrane potential is reduced. *In vitro* import experiments using mitochondria that have been treated to artificially lower the membrane potential, have shown that the Tim8-13 complex is important for efficient import of Tim23 under such conditions (Davis *et al.*, 2000; Paschen *et al.*, 2000; Hoppins and Nargang, 2004). Conversely, other groups have demonstrated that Tim8-13 is involved in the import of Tim23, even when the membrane potential is high in yeast (Leuenberger *et al.*, 1999; Curran *et al.*, 2002) and humans (Rothbauer *et al.*, 2001). Peptide scanning analysis suggests that there is a specific interaction between Tim8-13 and Tim23 in yeast (Curran *et al.*, 2002). Recently another substrate of Tim8-13 has been identified. Loss of the Tim8-13 complex has been shown to decrease the efficiency of import of β-barrel proteins such as Tom40 and porin to the MOM (Hoppins and Nargang, 2004; Wiedemann *et al.*, 2004).

Tim8 is the fungal homologue of the human protein DDP1 (deafness dystonia peptide). Mutations in the gene encoding DDP1 result in Mohr-Tranebjaerg Syndrome (MTS), the first human disease found to be caused by a mutation in a component of the import machinery (Mohr and Mageroy, 1960; Tranebjaerg *et al.*, 1995; Koehler *et al.*, 1999). The disease is characterized by early onset progressive sensorineural hearing loss and dystonia that can also be accompanied by vision loss, psychiatric symptoms and cognitive impairment (Tranebjaerg *et al.*, 1995; Binder *et al.*, 2003; Hofmann, 2004). In contrast to most mitochondrial diseases, MTS is not associated with a defect in energy generation (Binder *et al.*, 2003; Hofmann, 2004). All patients identified to date have no functional Tim8-13 complex due to either premature stop codons in the *tim8* gene or point mutations converting one of the conserved cysteine residues to tryptophan which results in defective assembly of the complex (Hofmann *et al.*, 2002; Roesch *et al.*, 2002; Binder *et al.*, 2003; Hofmann, 2004). An interaction of DDP1 with a signal transduction adaptor molecule called STAM1 was detected by yeast two-hybrid and confirmed by co-immunoprecipitation (Blackstone *et al.*, 2003). Since STAM1 is a cytoplasmic protein, the authors suggest that the interaction occurs before Tim8 is imported to mitochondria (Blackstone *et al.*, 2003). The function of this interaction is not clear. A lymphoblast cell line from a MTS patient was found to have a general decrease in NADH levels suggesting that Tim8-13 could be important for import of a protein involved in movement of reducing equivalents from the cytosol to the mitochondrial matrix (Roesch *et al.*, 2004). In support of this idea, the human-specific calcium binding aspartate/glutamate carriers (AGCs) and the yeast counterpart, Agc1p, were recently identified as substrates of the Tim8-13 complex (Roesch *et al.*, 2004). These carriers function to catalyze the exchange of aspartate for glutamate resulting in NADH shuttling (Palmieri *et al.*, 2001; Cavero *et al.*, 2003).

1.8.1 *Structure of the Tiny Tim Complexes*

Both 70 kDa complexes are thought to contain three molecules of each component protein. Low resolution 3D structure of recombinant purified Tim9-10 complex suggests that the complex has a unique structure, unlike other chaperone proteins, that is highly flexible and exposes a large hydrophobic surface (Lu *et al.*, 2004). It is agreed that the CX_3C motif is important in assembly of both Tim9-10 and Tim8-13, but there is debate as to whether this motif co-ordinates zinc or is involved in the formation of disulfide bonds (reviewed in (Koehler, 2004)). It has been shown that the tiny Tim monomers bind zinc when expressed and purified from *E. coli* (Sirrenberg *et al.*, 1998; Rothbauer *et al.*, 2001; Hofmann *et al.*, 2002; Lutz *et al.*, 2003). When a divalent cation chelator is present during import of Tim23 and AAC, efficiency of import is reduced and crosslinking adducts with Tim9-10 are lost (Sirrenberg *et al.*, 1998; Paschen *et al.*, 2000). This also supports a role for zinc in Tim9-10 function *in vivo*. However, when similar experiments were performed by a different group, addition of chelators did not affect import of Tim23 or its crosslinking with Tim8 (Curran *et al.*, 2002b). Another argument in favor of the co-ordination of zinc is the observation that the interaction between DPP1 and STAM1 was dependent on zinc (Blackstone *et al.*, 2003).

Thiol trapping analysis of the purified Tim9-10 complex and Tim8-13 complex was performed (Curran *et al.*, 2002a; Curran *et al.*, 2002b). The authors suggest that the purified Tim9-10 and Tim8-13 complexes were functional as interaction with their substrates was observed in peptide scanning analysis (Curran *et al.*, 2002a; Curran *et al.*, 2002b). Thiol trapping measures alkylation of free thiol groups by AMS (4-acetamido-4'-maleimidylstilbene-2,2'-disulfonic acid). Results from the analysis of the purified complex suggest that the cysteine residues are occupied by disulfide bonds and therefore do not co-ordinate zinc. However, when the thiol trapping method was used under conditions that prevent exposure to oxygen during isolation and treatment of whole mitochondria, results suggested that Tim13 does not contain disulfide bonds (Lutz *et al.*, 2003).

Limited trypsin digestion of Tim10 and mass spectrometry analysis of the resulting fragments suggest that the disulfide bonds observed by this group are intramolecular (Allen *et al.*, 2003). They further propose the involvement of one cysteine residue from each of the twin motifs with cys44 and cys61 forming one bond and cys40 and cys65 forming the second (Allen *et al.*, 2003). Circular dichroism analysis and thiol trapping of the purified complex suggest that the disulfide bonds are highly resistant to reduction by treatment with DTT and therefore may be buried within the assembled protein complex (Lu *et al.*, 2004). NMR, circular dichroism, and small angle x-ray scattering (SAXS) analysis suggested that oxidation of the Tim9 or Tim10 proteins changes their structure to a more defined state (Lu *et al.*, 2004). Similar changes were not observed upon the co-ordination of zinc, leading the authors to suggest that the functional complex contains disulfide bonds (Lu *et al.*, 2004). Binding zinc was found to stabilize the proteins against protease digestion but not to the same degree that oxidation did. Further, when zinc-bound proteins were mixed, they did not appear to assemble into a higher complex as occurred when the oxidized monomers were combined (Lu *et al.*, 2004).

1.8.2 *Import of the Tiny Tim Proteins to the IMS*

Proteins imported into the IMS can be divided into three classes based on their sorting pathway and energy requirements (reviewed in (Herrmann and Hell, 2005)). One class contains N-terminal targeting signals and is sorted to the IMS in a multi-step pathway via the TIM23 complex (see section 1.9.1). The other classes are composed of small proteins that are able to diffuse out of the IMS via the TOM complex. The second class of proteins is trapped in the IMS by adopting a folded conformation. Finally, some proteins are trapped in the IMS due to their association with membrane proteins.

The tiny Tim proteins belong to the second class. In yeast, they do not show any dependence on Tom20, Tom22 or Tom70 but are highly dependent on Tom5 for import (Kurz *et al.*, 1999). The dependence on Tom5 is not observed in *N. crassa* (Schmitt *et* *al.*, 2005; Sherman, 2005). The conversion of any of the four conserved cysteine residues to serine abolished the import of Tim13 (Lutz *et al.*, 2003). Import of Tim13 was decreased if a chelator was present but this effect could be reversed if zinc was added back in excess. These observations imply that the presence of zinc is important for efficient translocation of Tim13 to the IMS or its maintenance in the IMS (Lutz *et al.*, 2003). Import of purified Tim10 suggests that the protein must be reduced and unfolded to cross the TOM complex (Lu *et al.*, 2004). In contrast to the observation made with Tim13, Lu *et al.* show that mutation of Tim10 converting one cysteine residue to serine does not affect its import (Lu *et al.*, 2004). Notably, the import experiments performed by Lu *et al.* omit a proteinase K treatment designed to remove precursor that is not imported.

A protein in the IMS involved in import and/or assembly of the tiny Tim proteins was recently identified by two groups. Tim40/Mia40 (mitochondrial intermembrane space import and assembly) is an essential protein in yeast, localized to the MIM by a bipartite sorting signal, and has a large C-terminal domain exposed to the IMS (Chacinska *et al.*, 2004; Naoe *et al.*, 2004). The IMS domain of the protein contains a cluster of negatively charged residues followed by a highly conserved sequence that contains six cysteine residues, the last four of which form a twin CX_9C motif (Chacinska *et al.*, 2004). Both groups show that strains expressing either low levels of Mia40 or a mutant version of the gene are impaired in the import and assembly of tiny Tim family members. An interaction between Mia40 and Tim9 precursor protein was observed by BNGE as a 140 kDa complex. The function of Mia40 is not restricted to the Tim proteins as a deficiency in import of two other IMS proteins, Cox17 and Cox19, was observed when a mutant version of Tim40 was expressed (Chacinska *et al.*, 2004). This observation makes it unlikely that the role of Tim40/Mia40 is to donate a zinc metal ion or stimulate disulfide bond formation since Cox17 and Cox19 contain neither zinc nor disulfide bonds.

A novel protein involved in the assembly of the tiny Tim proteins to their respective complexes was identified in yeast (Curran *et al.*, 2004). Hot13p is a member of the zf-CHY domain family and is conserved among yeasts and prokaryotes. This protein contacts newly imported tiny Tim proteins and loss of the protein resulted in decreased assembly of the Tim8-13 and Tim9-13 complexes (Curran *et al.*, 2004). The mechanism of Hot13p in assembly of these complexes is not understood, though the authors postulate that it may be a component of an oxidation folding pathway.

1.9 *The TIM Complexes*

As mentioned in section 1.5, the MIM possesses two multi-subunit translocase complexes, the TIM23 complex and the TIM22 complex, that work with the TOM complex to sort mitochondrial precursor proteins to their functional compartment (Figure 1) (reviewed in (Bauer *et al.*, 2000; Neupert and Brunner, 2002; Rehling *et al.*, 2003; Hoppins, 2004; Rehling *et al.*, 2004). The MIM also contains the OXA complex which inserts proteins from the matrix into the inner membrane (reviewed in (Herrmann and Neupert, 2003)).

1.9.1 *Components of the TIM23 Complex*

The TIM23 complex has three different protein components: Tim23, Tim17 and Tim50. Tim23 is an essential MIM protein with four membrane spanning domains (Dekker *et al.*, 1993; Emtage and Jensen, 1993). Tim23 mutants were found to be defective in import of N-terminally targeted precursors and wild type Tim23 could be crosslinked to these precursors while they were in transit (Dekker *et al.*, 1993; Emtage and Jensen, 1993; Kubrich *et al.*, 1994). The protein has two distinct domains. The N-terminus is hydrophilic while the C-terminus is generally hydrophobic and contains the four membrane spanning domains. The hydrophilic domain contains a leucine zipper motif that is believed to be responsible for dimerization (Bauer *et al.*, 1996). This domain is essential for the function of the protein and dimerization is dependent on the presence of high membrane potential. It appears that Tim23 is not dimerized during translocation of a peptide as the dimer is dissociated upon the addition of a precursor protein with an N-terminal presequence (Bauer *et al.*, 1996). The membrane embedded portion of Tim23 is responsible for its interaction with another component of the TIM23 complex, Tim17 (Ryan *et al.*, 1998). It has also been reported that yeast Tim23 contains a domain at its extreme N-terminus that is integrated into the MOM (Donzeau *et al.*, 2000). This topology would ensure that the location of the TIM23 complex was restricted to regions where the MOM and MIM are adjacent to facilitate efficient passage of precursor proteins from the TOM complex to the TIM23 complex. The mechanism necessary to insert the N-terminus of yeast Tim23 into the MOM is not known.

Tim17 is also an integral protein of the MIM (Maarse *et al.*, 1994). There is a high degree of similarity between Tim17 and the C-terminal half of Tim23 (Maarse *et al.*, 1994). Reduction of Tim17 levels impairs import of precursor proteins (Milisav *et al.*, 2001) and precursors in transit can be crosslinked to Tim17 (Kubrich *et al.*, 1994). These data imply that Tim17 is a component of the pore through which precursor proteins pass to enter the matrix. However, electrophysiological studies using purified Tim23 suggest that Tim23 alone forms the pore (Truscott *et al.*, 2001). Tim17 cannot substitute for Tim23 function, suggesting a unique role for Tim17 in protein import. Further studies are needed to elucidate the nature of the function of Tim17 in the TIM23 complex. In contrast to the single *tim17* gene in fungi, two *tim17* genes have been identified in humans and are thought to be responsible for the formation of two different complexes with Tim23, one containing Tim17a and the other Tim17b (Bauer *et al.*, 1999). In plants, Tim17 contains a C-terminal extension that is not found in the fungal counterparts (Murcha *et al.*, 2005). It has recently been demonstrated that the C-terminus of Tim17 in *Arabidopsis* crosses the MOM in a manner that is analogous to the N-terminus of Tim23 in *S. cerevisiae* (Murcha *et al.*, 2005).

Tim50 was discovered more recently as a member of the TIM23 complex in yeast and *N. crassa* (Geissler *et al.*, 2002; Yamamoto *et al.*, 2002; Mokranjac *et al.*, 2003). All three studies showed that Tim50 contains a single transmembrane domain anchoring it to the MIM and a large C-terminal domain in the IMS. Precursor proteins in transit can be crosslinked to Tim50, even when the precursor is bound at the TOM complex trans site, suggesting an early role in precursor recognition by the TIM23 complex (Geissler *et al.*, 2002; Yamamoto *et al.*, 2002; Mokranjac *et al.*, 2003). Interestingly, the Tim50 protein appears to be more important for efficient import of matrix proteins with an N-terminal presequence than for proteins with the additional stop-transfer signal (Geissler *et al.*, 2002; Mokranjac *et al.*, 2003). A yeast 2-hybrid assay showed that Tim50 interacts with the soluble domain of Tim23 (Geissler *et al.*, 2002; Yamamoto *et al.*, 2002). It is possible that Tim50 also plays a role in the topology of Tim23 since over-expression of

Tim50 lead to an increase in the proportion of Tim23 with a domain integrated in the MOM while under-expression resulted in the inverse (Yamamoto *et al.*, 2002).

1.9.2 *Components of the PAM Machinery*

The molecular chaperone DnaK of *E. coli* has several homologues in yeast. The gene with the highest degree of similarity was found to be essential and contained an N-terminal extension for targeting to mitochondria (Craig *et al.*, 1987; Craig *et al.*, 1989). The protein has three domains: an N-terminal ATPase domain, a central peptide binding domain and a short C-terminal segment thought to form a lid over the peptide binding domain (Hartl, 1996; Bukau and Horwich, 1998). The protein was named mtHsp70 and it was found to have a role in import of precursors into the mitochondrial matrix when a temperature sensitive allele was analyzed (Kang *et al.*, 1990). The protein binds incoming precursors in an ATP-dependent fashion (Ungermann *et al.*, 1994).

Tim44 was identified in a screen for yeast mutants defective for mitochondrial protein import (Maarse *et al.*, 1992; Scherer *et al.*, 1992). It is located in the matrix, associated with the MIM, and it essential for viability of yeast (Maarse *et al.*, 1992; Blom *et al.*, 1993; Weiss *et al.*, 1999). Tim44 connects the TIM23 complex to the import motor in the mitochondrial matrix, both of which are essential at different stages for protein import into the matrix (Milisav *et al.*, 2001). An interaction between Tim44 and mtHsp70 was detected genetically and biochemically (Rassow *et al.*, 1994). A region of Tim44 that facilitates mtHsp70 binding and has similarity to J-proteins was found to be essential (Merlin *et al.*, 1999). J-proteins are cochaperone proteins containing characteristic motifs that interact with the ATPase domains of Hsp70s and stimulate ATPase activity (Kelley, 1998). Characterization of a mutant Tim44 revealed that it played a more significant role in import of tightly folded proteins than those that are loosely folded, a role that probably involves its molecular partner mtHsp70 (Bomer *et al.*, 1998).

In a search for a nucleotide exchange factor partner for mtHsp70, the essential mitochondrial matrix protein, Mge1 was identified in yeast and *N. crassa* (Bolliger *et al.*, 1994; Ikeda *et al.*, 1994; Laloraya *et al.*, 1994; Nakai *et al.*, 1994; Voos *et al.*, 1994). This protein was believed to play a key role in import of matrix proteins, aiding in the cycling of mtHsp70 from its Tim44-bound state to its precursor-bound state and then stimulating the release of ADP from mtHsp70 causing it to release the precursor (Schneider *et al.*, 1996).

Recently, additional partners for mtHsp70 have been identified by different approaches. Pam18/Tim14 is an essential MIM protein with its C-terminal domain, which has similarity to a J-domain, facing the matrix (D'Silva *et al.*, 2003; Mokranjac *et al.*, 2003; Truscott *et al.*, 2003). Pam18 stimulates the ATPase activity of mtHsp70 and loss of Pam18 function impairs import of proteins to the matrix. Most J proteins also contain a zinc finger motif in addition to the conserved carboxy-terminal region that bears homology to Pam18. Burri *et al.* reasoned that since Pam18 does not contain a zinc finger, these domains may be fractured in yeast so that the zinc finger might be present in a separate protein (Burri *et al.*, 2004). The essential protein product called Tim15/Zim17 has been shown to fulfill such a role (Burri *et al.*, 2004; Yamamoto *et al.*, 2005). Tim15/Zim17 contains a twin CX_2C motif, is localized to the mitochondrial matrix where it is associated peripherally with the MIM (Burri *et al.*, 2004; Yamamoto *et al.*, 2005). A genetic and physical interaction was observed with mtHsp70 (Yamamoto *et al.*, 2005) and a genetic interaction was found with Pam18/Tim14 leading to the suggestion that this protein works with Pam18 in its role to stimulate the ATPase activity of mtHsp70 (Burri *et al.*, 2004). Another component of the motor, Pam16, was identified as an essential matrix protein that is associated peripherally with the MIM (Frazier *et al.*, 2004; Kozany *et al.*, 2004). This protein functions to mediate the interaction between Pam18 and Tim23 and impaired function of Pam16 results in decreased import efficiency of matrix precursor proteins (Frazier *et al.*, 2004; Kozany *et al.*, 2004).

Working together, these components are involved in a cyclical reaction that results in translocation of a preprotein into the matrix. As the preprotein emerges from the TIM23 complex, it interacts with Tim44 which has recruited mtHsp70 that is bound to ATP and Mge1. The J-domain of Pam18 then stimulates ATP hydrolysis resulting in tight binding of mtHsp70 to the precursor. The ADP-bound mtHsp70 dissociates from Tim44 and Mge1 stimulates the release of ADP from the ATPase domain which is accompanied by release of the precursor. This molecule of mtHsp70 is now free to begin the cycle again. There are currently two models of import motor function that are highly debated in the field. The first favors a Brownian ratchet mechanism where mtHsp70 and its partners bind to the incoming precursor as it moves further into and out of the matrix as portions of the precursor still associated with the TOM complex undergo partial, spontaneous unfolding. The binding would prevent backsliding of the precursor and result in a net forward movement into the matrix. In the power stroke or pulling model, mtHsp70 exerts a force on the incoming peptide through a conformational change in mtHsp70 evoked by ATP hydrolysis. In this model, the forces applied to the presequence stimulate unfolding of the C-terminal region of the precursor which is still associated with the TOM complex.

Evidence for the pulling model centers on data obtained using mutants of mtHsp70 and import of tightly versus loosely folded precursor proteins. For example, *ssc1-2* is a temperature sensitive allele of mtHsp70 that does not show a detectable interaction with Tim44 and results in impaired import of tightly folded precursor proteins only (Voos *et al.*, 1996). Further characterization of the mutant revealed an "enhanced trapping" phenotype meaning that there was a prolonged mtHsp70 interaction with the precursor leading to defective folding of the protein in the matrix (Voisine *et al.*, 1999). Identification of an intragenic suppressor that re-established an interaction between the mutant mtHsp70 and Tim44 correlated with the reestablishment of the ability to unfold incoming precursor proteins, but not with restored folding of imported proteins (Voisine *et al.*, 1999). Given that this mtHsp70 mutant still showed the enhanced trapping phenotype, the authors suggest that the interaction between mtHsp70 and Tim44 is important for unfolding precursors, favoring a pulling model. Other evidence that active unfolding of proteins occurs comes from the finding that the protein barnase unfolds with different properties in solution than when it is being imported to mitochondria by an N-terminal presequence (Huang *et al.*, 1999). This suggests that the unfolding of the protein is being catalyzed by the PAM machinery in the mitochondrial matrix.

The Brownian ratchet model is supported by the finding that the mitochondrial import of the human muscle protein titin occurs despite the fact that studies suggest that unfolding of this protein requires a force of 200-260pN. This is a level of force that a molecular motor like mtHsp70 is not likely to produce, as other motors such as kinesin and myosin are estimated to generate a maximum force of only about 5pN (Okamoto *et* *al.*, 2002). Futhermore, Hsp70 cannot bind to tracts of polyG or polyE repeats with high affinity. Efficient import of synthetic proteins containing large tracts of these residues near the N-terminus makes it unlikely that import requires a pulling mechanism by mtHsp70. Rather, it seems more likely that Brownian movement of the precursor would expose regions C-terminal to the polyG/E tracts in these precursors that Hsp70 could interact with (Okamoto *et al.*, 2002). Working with purified components from yeast including Tim44, mtHsp70 and Mge1, the Craig lab found that release of precursor-bound mtHsp70-Mge1 complex from Tim44 occurs more rapidly than the hydrolysis of ATP (Liu *et al.*, 2003). This rapid release of mtHsp70 suggests that there is not time for a pulling action by mtHsp70 stimulated by hydrolysis of ATP.

There has also been debate regarding which domain of mtHsp70 interacts with Tim44 and whether this interaction would provide the appropriate structure for a lever arm to generate pulling force or not (Moro *et al.*, 2002; Strub *et al.*, 2002). Further work with the purified components determined that although the ATPase domain and peptide binding domain of mtHsp70 are both capable of interaction with Tim44 individually, the full length protein is necessary for the regulated release of mtHsp70 induced by a conformational change when it binds a peptide (D'Silva *et al.*, 2004). The authors propose a model in which the conformational changes of mtHsp70 are coupled such that hydrolysis of ATP and release from Tim44 occur simultaneously. Given the slow off-rate of a peptide-ADP-bound mtHsp70 molecule, this would allow for the precursor to move further into the matrix and for a new mtHsp70 molecule to bind at Tim44 before the previous one had been released from the precursor. Craig and colleagues also suggest that this regulated release is likely to be particularly important when the precursor is tightly folded, accounting for the defects observed in the enhanced trapping allele, *ssc1-2* (D'Silva *et al.*, 2004).

1.9.4 *Structure of the TIM23 Complex and Import Motor*

The TIM23 complex exists as a dimer and, through interaction with dimers of Tim44, also interacts with the protein motor found on the matrix side of the MIM, forming a complex with equimolar amounts of each component (Moro *et al.*, 1999). Only about one third of the total Tim50 protein in mitochondria is found in association with the TIM23 complex and its stoichiometry in the TIM23 complex with Tim23 is estimated to be about 1:2 (Yamamoto *et al.*, 2002).

It was originally proposed that Tim17 and Tim23 together formed a pore in the MIM (Kubrich *et al.*, 1994; Haucke and Schatz, 1997; Milisav *et al.*, 2001). To examine the possibility that Tim23 alone was the pore-forming component of the TIM23 complex, the protein was purified from *E. coli* and reconstituted into lipid bilayers for electrophysiological studies (Truscott *et al.*, 2001). It was found that the protein had characteristics similar to the previously detected MIM conductance channel (MCC) (Lohret *et al.*, 1997). The channel was also sensitive to precursors and $\Delta\Psi$ suggesting that Tim23 alone forms the pore. Using size exclusion analysis, it was estimated that the diameter of the pore was between 13Å and 24Å (Truscott *et al.*, 2001). Based on these results, it is difficult to implicate any potential role for Tim17 in the pore.

When chemical amounts of the matrix destined fusion protein that included the first 167 residues of cytochrome b_2 joined to mouse DHFR were arrested in transit, a supercomplex was formed that spanned both mitochondrial membranes and blocked import of other precursors (Rassow *et al.*, 1989). This supercomplex was found to include components of the TOM complex, the TIM23 complex and the import motor (Berthold *et al.*, 1995; Horst *et al.*, 1995; Schulke *et al.*, 1999). The supercomplex contained the majority of the TIM23 complexes and shifted the molecular weight of the complex from 90 kDa to 600 kDa. Since only about one quarter of the TOM complexes were found in the supercomplex, this suggested that the formation of the supercomplex is limited by the number of TIM23 complexes (Dekker *et al.*, 1997; Sirrenberg *et al.*, 1997). The IMS domain of Tom22 is required to stabilize the supercomplex while the IMS domain of Tim50 is crucial for its formation (Chacinska *et al.*, 2003). Interestingly, the domain of Tim23 that is thought to span the MOM is dispensable in the formation of the supercomplex (Chacinska *et al.*, 2003).

1.9.5 *Precursor Processing and Folding in the Matrix*

The final step in import of a protein with an N-terminal targeting signal is removal of the leader sequence by a processing enzyme in the mitochondrial matrix (reviewed in (Gakh *et al.*, 2002)). MPP is a heterodimer that cleaves the leader peptide from the mature protein in a single event (Hawlitschek *et al.*, 1988; Yang *et al.*, 1988; Arretz *et al.*, 1994). It is believed that MPP recognizes structural elements rather than target sequences (Gakh *et al.*, 2002). When the amphipathic helix of the precursor protein is in an extended confirmation, MPP binding occurs within a large cavity formed between the two subunits of the protein (Taylor *et al.*, 2001). Some proteins are also processed by the mitochondrial intermediate peptidase (MIP) which cleaves proteins that have already been processed by MPP (Isaya *et al.*, 1994).

Proper folding of matrix proteins is ensured by several chaperone proteins in the matrix (reviewed in (Voos and Rottgers, 2002). mtHsp70 functions in this process in addition to its role in import discussed above. When associated with Mdj1, mtHsp70 functions to aid in folding of matrix proteins (Horst *et al.*, 1997). A matrix protein of the Hsp60 family is one of the most important for folding of mitochondrial matrix proteins (Gakh *et al.*, 2002).

1.9.6 *Components of the TIM22 Complex*

Before the identification of Tim22, it was believed that TIM23 was the only translocase of the MIM. Tim22 was identified through its homology to Tim23 and was shown to be an essential protein of the MIM in a complex of about 300 kDa (Sirrenberg *et al.*, 1996). Reduction of the amount of Tim22 protein in cells was accompanied by reduction in levels of AAC and PiC which was correlated to a reduced efficiency of import of these precursors. These data suggested that Tim22 was involved in the biogenesis of carrier proteins (Sirrenberg *et al.*, 1996). Functional distinction from the TIM23 complex was also made when it was observed that import of AAC could still occur if all TIM23 sites were blocked with a matrix precursor in transit (Sirrenberg *et al.*, 1997).

Tim54 was the second component of the TIM22 complex identified (Kerscher *et al.*, 1997). Based on the inviability of ascospores lacking the *tim54* gene it was originally concluded that the protein was essential in yeast (Kerscher *et al.*, 1997). Later, using plasmid shuffling, it was determined that Tim54 is not essential in vegetative cells, but loss of the gene does result in a severe growth defect that could be rescued by overexpression of Tim22 (Kovermann *et al.*, 2002). Impaired function of Tim54 caused a specific decrease in the import efficiency of carrier proteins and an interaction with Tim22 was shown both genetically and by physical crosslinking (Kerscher *et al.*, 1997). There is no known Tim54 homologue in humans.

Tim18 was found through its interaction with Tim54 (Kerscher *et al.*, 2000; Koehler *et al.*, 2000). Tim18 is not an essential component of the TIM22 complex and is localized to the MIM with its C-terminus facing the IMS (Kerscher *et al.*, 2000; Koehler *et al.*, 2000). The function of Tim18 in the TIM22 complex is not well characterized. As with Tim54, there is no known Tim18 homologue in humans.

1.9.7 *Structure of the TIM22 Complex*

It was found that loss of Tim54 resulted in dissociation of the TIM22 complex, suggesting that this protein may play a role in stabilization of the interactions within the 300 kDa complex (Kovermann *et al.*, 2002). Purification of Tim22, Tim54 and Tim18 and electrophysiological analysis of each revealed that only Tim22 had characteristics of a pore, suggesting that this protein forms the channel in the MIM (Kovermann *et al.*, 2002). It was estimated that when the channel is in its most open state it is 18Å in diameter and while in a smaller pore conformation, the opening is closer to 11Å (Kovermann *et al.*, 2002). Purification of the complex from yeast using an affinity-tagged Tim18 provided further insight into the function and structure of the pore (Rehling *et al.*, 2003). This analysis showed characteristics of two coupled pores which are also visible by single particle electron microscopy (Rehling *et al.*, 2003). The steps of import of a carrier protein were studied *in vitro* using purified TIM22 complex generating a model whereby the import occurs in three distinct steps (Rehling *et al.*, 2003). The first step is independent of $\Delta\Psi$ and involves the tethering of the precursor to the complex. This requires Tim9-10 in association with Tim12. Next, the TIM22 complex is partially activated and one loop of the carrier preprotein is inserted into the pore, even if the $\Delta\Psi$ is low. This is facilitated by the electrophoretic force of the positively charged residues located in the hydrophilic loop between two membrane spanning domains of the precursor. The TIM22 complex then recognizes the internal signal and, in the presence of a full membrane potential, the pore is fully activated. The next module of the carrier is then inserted into the second pore of the TIM22 complex. Insertion into the MIM was proposed to occur by lateral opening of the complex.

1.10 *Protein Insertion to the Inner Membrane from the Matrix*

The proteins encoded in the mitochondrial genome include components of the electron transport chain which must be inserted into the MIM following synthesis in the matrix on mitochondrial ribosomes. There are also cases where nuclear encoded proteins that function in the inner membrane are first imported to the matrix by a leader sequence and from there, must insert into the MIM. Oxa1 is a member of a family of proteins that is found in mitochondria, chloroplasts and bacteria. The bacterial counterpart is YidC (Scotti *et al.*, 2000). The Oxa complex (Oxidase assembly mutant) plays a central role in the process of protein export from the matrix to the MIM (Herrmann and Neupert, 2003). Oxa1 was the first protein identified to aid in the assembly of the cytochrome oxidase complex (Bauer *et al.*, 1994; Bonnefoy *et al.*, 1994). Oxa1 is an integral membrane protein with five predicted transmembrane domains that is localized to the MIM (Herrmann *et al.*, 1997). Loss of Oxa1 function in yeast results in respiratory deficiency, defects in cytochrome oxidase activity, and the accumulation of MIM precursors in the matrix (Bauer *et al.*, 1994; Bonnefoy *et al.*, 1994; Altamura *et al.*, 1996; Hell *et al.*, 1997). Oxa1 forms a homo-oligomeric complex probably containing four molecules of Oxa1 that is about 170 or 180 kDa in size in *N. crassa* (Nargang *et al.*, 2002). Oxa1 is essential in *N. crassa* and under conditions that drastically reduce the level the protein, growth is extremely slow and there is a deficiency in Complex I and Complex IV components (Nargang *et al.*, 2002). The C-terminal domain is important for Oxa1 function as it interacts with mitochondrial ribosomes such that nascent polypeptides are inserted directly into the MIM (Jia *et al.*, 2003; Szyrach *et al.*, 2003).

There are additional export proteins which are independent from the Oxa1 complex. Mba1 is functionally related to Oxa1 with some overlapping function (Preuss *et al.*, 2001). Investigation of the mechanism of Cox2p insertion into the MIM in yeast led to the identification of other export proteins, Cox18, Pnt1 and Mss2 (He and Fox, 1999; Broadley *et al.*, 2001; Saracco and Fox, 2002). Oxa2 was identified in *N. crassa* and is functionally related to Cox18 in yeast (Funes *et al.*, 2004).

1.11 *Objectives of this study*

One of the goals of this study was to examine the function of the small, soluble Tim8 and Tim13 proteins that form a complex in the IMS in *N. crassa*. Mutations in the human homologue of *tim8* are implicated in the human disorder MTS (see section 1.8.1). Most of the research completed at the time this study was begun had been performed in yeast and had shown that the complex was involved in the import of Tim23 to the MIM. To study the function in *N. crassa*, null allele mutant strains were created for both *tim8* and *tim13* and the effect of the loss of the proteins was examined. This work revealed that the Tim8-13 complex not only assists in the import of Tim23, but also is important for efficient import of β-barrel proteins of the MOM.

A second study was undertaken to examine the structure and function of the N-terminal domain of *N. crassa* Tim23. At the time this work was started, evidence had recently been presented that revealed a domain in yeast Tim23 that crossed the MOM. This domain was thought to be important for efficient import of mitochondrial precursor proteins (Donzeau *et al.*, 2000). To investigate the mechanism of insertion of such a domain, I created constructs containing a portion of the N-terminal domain of *N. crassa* Tim23 and an inert carrier protein to be used in import assays to elucidate the residues important for targeting and insertion. These studies suggest that this region of Tim23 is not capable of autonomous targeting to the MOM in *N. crassa*. To determine if the extreme N-terminus is important for function, I created strains expressing shortened versions of Tim23. This work illustrates that the first 50 residues of Tim23 are important for function of the *N. crassa* protein and that these residues do not appear to be exposed on the cytosolic face of the MOM. Finally, the accessibility of 15 residues spaced out approximately every four residues over the first 62 residues of *N. crassa* Tim23 to reagents that label cysteine residues in a hydrophilic environment was assessed using substituted cysteine accessibility mapping. Analysis of eight of these positions reveals that all are found in a hydrophilic environment. Together, these data suggest that *N. crassa* Tim23 does not have an N-terminal domain that spans the MOM.

Another project was initiated to identify the components of the TOB complex in *N. crassa*. To facilitate the purification of the complex, strains were generated expressing tagged versions of Tob55. In addition, the function of the protein was assessed using a strain that could be manipulated to contain reduced levels of Tob55. This work confirms that the function of Tob55 is similar in yeast and *N. crassa*.

Figure 1 Import and Sorting of Mitochondrial Proteins. The TOM complex is composed of receptor proteins and pore forming proteins which form a translocase complex through which all mitochondrial proteins pass. Tom40 is the major pore-forming component while Tom5, Tom6 and Tom7 appear to contribute to the stability and dynamics of the TOM complex in *N. crassa*. Tom20 is the primary receptor for proteins containing an amino- terminal cleavable targeting sequence and Tom70 recognizes predominantly proteins with internal targeting sequences, primarily the mitochondrial carrier proteins. The presequence containing precursor moves through the TOM complex in an unfolded state. The presequence is then recognized by Tim50 and Tim23 in the intermembrane space followed by movement through the TIM23 translocase in a membrane potential dependent manner. As the amino-terminus emerges in the matrix space, vectoral movement is facilitated by repeated ATP-dependent binding and release cycles by mtHsp70. There are several factors that co-operate with mtHsp70 to ensure productive interaction with the substrate. Tim44 ensures docking at the TIM23 channel while Pam18 and Tim15 stimulate the ATPase activity of mtHsp70. Pam16 facilitates the interaction of Pam18 with the TIM23 complex. The release of the precursor protein from mtHsp70 is stimulated by Mge1. Once in the matrix, the presequence is removed and the protein is folded into its active conformation. The TIM23 machinery can also facilitate the direct insertion of proteins with a stop-transfer sorting signal into the inner membrane. Carrier proteins cross the TOM complex in loops containing two transmembrane domains. The passage of these loops across the intermembrane space is facilitated primarily by the Tim9-10 complex which docks with Tim12 at the TIM22 complex. Insertion of these proteins into the inner membrane is facilitated by the TIM22 complex in a membrane potential dependent step. Proteins can also be inserted to the inner membrane from the matrix by the OXA complex. Import of β-barrel proteins of the MOM is dependent on the presence of the receptor proteins Tom20 and Tom70. These precursor proteins pass through the TOM complex and interact with the tiny Tim complexes, Tim8-13 or Tim9-10, in the intermembrane space. From the intermembrane space, the precursor is passed to the TOB complex which is thought to mediate insertion of the β-barrel into the membrane. Tob55 appears to form a pore while the function of

the other components is not understood at this time. Tom40 specifically requires an additional protein, Mim1 for its final assembly into the TOM complex.

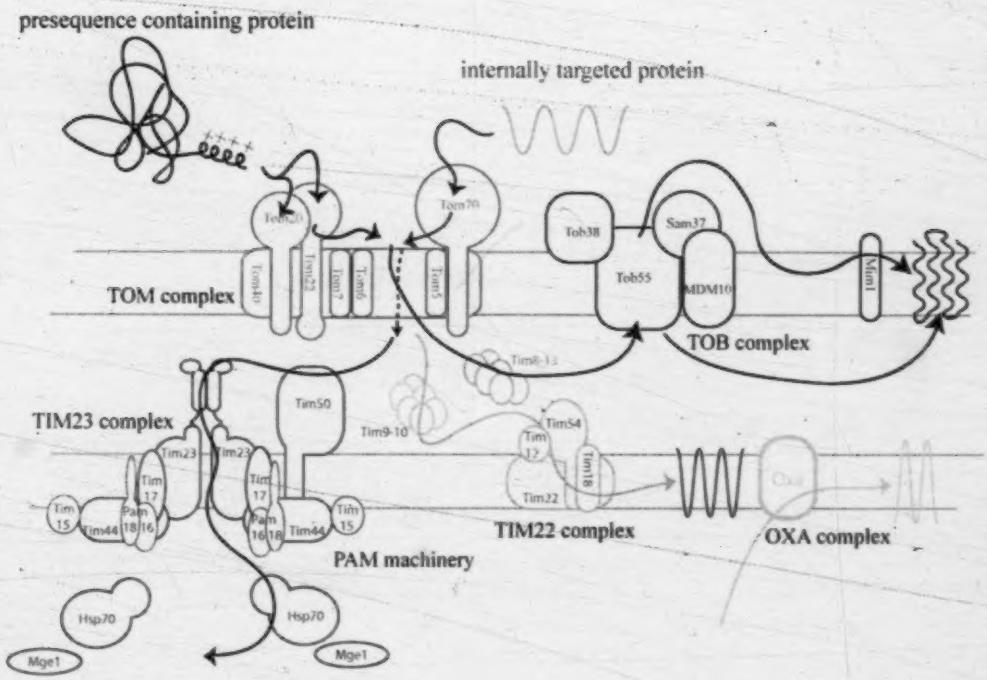
presequence containing protein
internally targeted protein
++++
Tom20
Tom70
Tom40
Tom22
Tom7
Tom6
Tom5
TOM complex
Tob38
Sam37
Tob55
MDM10
Mim1
TOB complex
Tim8-13
Tim50
Tim9-10
TIM23 complex
Tim23
Tim23
Tim17
Tim17
Tim15
Tim15
Tim44
Tim44
Pam18
Pam16
Pam16
Pam18
Tim54
Tim12
Tim18
Tim22
TIM22 complex
Oxa1
OXA complex
PAM machinery
Hsp70
Hsp70
Mge1
Mge1

Figure 2 Tom40 assembly intermediates as observed by BNGE. The first intermediate formed during Tom40 assembly that is visible by BNGE is a 250 kDa complex. This represents a single incoming Tom40 precursor molecule (grey box) along with one or two molecules each of Tom5 and Tom7, associated with the TOB complex. The second intermediate is the 100 kDa complex, most likely representing a dimer of Tom40 formed between the precursor and a pre-existing Tom40 molecule (black box) that is inserted into the membrane and associated with Tom7 and Tom5. The final TOM complex is 400 kDa and requires the association of Tom22 and Tom6 which may be promoted by Mim1.

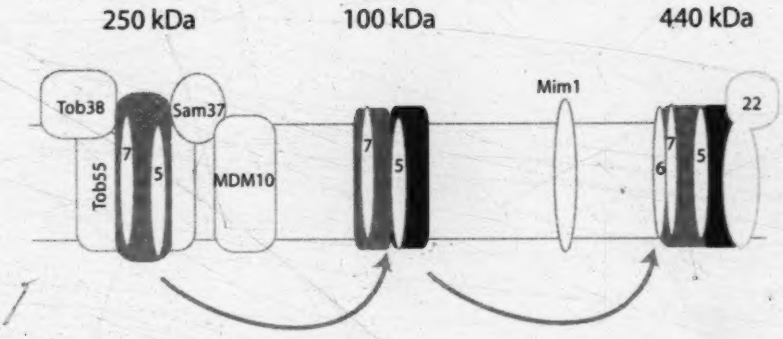
250 kDa
100 kDa
440 kDa
Tob38
Sam37
Tob55
7
5
MDM10
7
5
Mim1
22
6
7
5

2 MATERIALS AND METHODS

2.1 *Growth of N. crassa*

Growth and handling of *N. crassa* was as previously described (Davis, 1970). Measurement of growth rate on race tubes was done in 25 ml pipettes as described (Davis, 1970; White, 1995). Growth rate by colony size was measured by spotting 10 μl of suspensions containing 2×10^7, 2×10^6, 2×10^5, and 2×10^4 conidia/ml onto plates containing standard sorbose media with the appropriate supplements. The plates were incubated at 30°C until growth was seen in the lowest dilution spot of the control strain. Strains used in this study are listed in Table 1.

2.2 *Oligonucleotides and Plasmids*

Oligonucleotides and plasmids used in this study are listed in Table 2 and Table 3, respectively.

2.3 *Creation of RIP Mutants of tim8 and tim13*

Repeat induced point mutation is a phenomenon that occurs during the sexual cycle of *N. crassa* when there is a duplication of sequence in the nuclei of one of the parents in the cross. RIP results in GC to AT transition mutations throughout both copies of the duplicated sequence. This unique property can be exploited to generate null alleles of target genes (Selker, 1990). RIP occurs before karyogamy so only the nucleus containing the duplication is affected. Although RIP does not occur 100% of the time in a given cross, if the duplication is approximately 2 kbp or larger, about half of the meiotic products will contain mutations characteristic of RIP in duplicated sequences.

To generate strains containing a duplication, plasmids with a selectible resistance marker and the cloned target gene are transformed into a standard lab strain of *N. crassa*. For *tim8*, the plasmid pT8HL7 contained 2 kbp of genomic sequence, and a hygromycin resistance gene, and was transformed into *N. crassa* strain 76-26. For *tim13*, the plasmid pCST13 containing 2.2 kbp of genomic DNA and a hygromycin resistance gene was transformed into *N. crassa* strain 76-26. Transformants were selected on hygromycin, taken through one round of purification on hygromycin containing sorbose plates and strains containing a single integration of the gene were identified by Southern analysis. For *tim8*, strain T8HL-7 was chosen as the RIP substrate strain and was the male in a RIP cross with the strain NCN 251. For *tim13*, strain TI13-16 was chosen and was the male in a RIP cross with NCN 251. Ascospores from the crosses were grown on medium containing histidine. Mitochondria preparations were made from several isolates and were screened for loss of the protein by western analysis. T8HL7-7 was chosen as the *tim8*^{RIP} strain and T13R16-45 was chosen as the *tim13*^{RIP} strain.

2.4 *Creation of Sheltered RIP Mutant of tim23*

Sheltered RIP uses the ability of *N. crassa* to form heterokaryons to complement the loss of an essential gene in one nucleus by the presence of the wild type gene in the second nucleus. Tim23 was predicted to be an essential gene product, so sheltered RIP was used to generate mutants in the *tim23* gene (Figure 3). Strains have been developed with the appropriate antibiotic and nutritional markers on each of the seven *N. crassa* chromosomes, which permit the manipulation of the nuclei in the final desired heterokaryon (Metzenberg, 1992). To permit the creation of a strain that has an essential gene inactivated by the process of RIP, the strains used for sheltered RIP also contain a *mei-2* mutation which eliminates meiotic recombination and results in the production of aneuploid spores in a cross. This results in the formation of a variety of meiotic products, many of them inviable because they are lacking entire chromosomes. Some of the progeny will also be disomic for any given linkage group and contain the full complement of the other chromosomes. The desired products of the sheltered RIP cross are disomics that contain an allele of *tim23* on LG III that has been subjected to RIP from the transformed HostIII derivative, and a wild type allele of *tim23* on another copy of the same chromosome from the strain MateIII. This disomic spore will rapidly break down to form a heterokaryon. Fore-knowledge of the linkage group on which the target gene is located is required as this permits the use of strains genetically designed to allow direct selection of the desired heterokaryons from the cross. In addition, the same genetic markers permit the manipulation of the heterokaryon to alter the ratio of the nuclei in the final desired strain, forcing the predominance of the *tim23* RIPed nucleus. This allows the growth of a strain expressing a minimal level of Tim23, making it possible to assess the effects on growth and mitochondrial function.

The *tim23* gene was mapped to chromosome III using RFLP (restriction fragment length polymorphism) analysis (Metzenberg, 1984; Metzenberg *et al.*, 1985). This was done prior to the completion of the *N. crassa* genome project. The cosmid X2D5 was identified from the pCosX *N. crassa* cosmid library using degenerate *tim23* primers as probes by collaborators at the University of Munich. X2D5 was used as the probe for the RFLP mapping. The plasmid pTim23, which contains a hygromycin resistant gene a 2 kbp fragment of *N. crassa* genomic DNA carrying a *tim23* allele with an amino terminal octa-histidine tag, was transformed into the host strain H III to create the duplication containing strain. Hygromycin resistant transformants were isolated and screened by Southern analysis of genomic DNA for a single ectopic integration of the *tim23* fragment. The strain TI23-4 was chosen to act as the male in a sheltered RIP cross with the mate strain M III. Ascospores generated in this cross were grown on minimal medium to select for heterokaryons. The desired sheltered RIP heterokaryon is diagrammed in Figure 3D.

Growth of progeny from the sheltered RIP cross on medium containing acriflavin and tryptophan shifts the ratio of nuclei in the heterokaryon to favor the nuclei carrying the H III version of LG III (*trp*$^-$ *inos*$^-$ *acr*^{R}). These are the progeny that potentially carry RIPed versions of *tim23*. In heterokaryons where the *tim23* gene was affected by RIP, the levels of Tim23 would be reduced and the growth rate of those heterokaryons should be diminished relative to control strains with wild type *tim23* genes in both nuclei. Several progeny of the sheltered RIP cross were tested for reduced growth rate on medium containing tryptophan, inositol and acriflavin. Isolates that grew slowly were then screened for RIP-induced mutations in the *tim23* gene. Genomic DNA was isolated after growth in acriflavin and tryptophan to increase the amount of DNA obtained from the RIP-containing nucleus. The *tim23* gene was amplified by PCR and the products were sequenced. The strain T23R4-12 was chosen for further analysis since mutations characteristic of RIP were present in the *tim23* gene.

2.5 *Nucleus Swapping of T23R4-12*

Attempts to demonstrate that *tim23* was an essential gene in *N. crassa* by performing nutritional testing (see section 2.10) of the sheltered heterokaryon T23R4-12 revealed that the sheltering nucleus was inviable (see section 3.2.3.1). We assumed this to be from a random mutation carried in the M III strain or produced in that nucleus during the sheltered RIP cross. Because of this unexpected inviability of the sheltering nucleus in the sheltered RIP cross, it was necessary to perform nucleus swapping in T23R4-12. To achieve this, the strain Helper 5 (FGSC #96-18, matΔ his-3; hyg^R tk+ Bml^R pan-2) was utilized. This strain harbors a deletion at the *mat* locus making it capable of heterokaryon formation with any strain, regardless of mating type. A trikaryon was made between T23R4-12 and Helper 5 by inoculating the two strains simultaneously on minimal medium. The inositol deficiency of the *tim23^{RIP}* nucleus and MateIII nucleus was complemented by the wild type allele in the Helper 5 nucleus. This trikaryon was then streaked on media containing acriflavin, tryptophan and benomyl for single colonies. The inclusion of tryptophan and acriflavin select for the presence of the *tim23^{RIP}* nucleus while the addition of benomyl simultaneously selects for the inclusion of the Helper 5 nucleus. The resulting *tim23^{RIP}* heterokaryon, Hel23R-1, was used for nutritional testing (section 3.2.3.1).

2.6 *Creation of tob55 Knockout Strain*

In *N. crassa*, homologous recombination occurs at a low frequency and requires large regions of homology making ectopic insertion of transformed DNA the usual event. A technique has recently been developed that reduced the occurrence of ectopic insertions by transforming split marker fragments of a selectable marker into recipient cells (Colot)(Figure 4). Furthermore, the technique avoids difficult cloning of large fragments using recombination in *S. cerevisiae* to construct the knockout plasmid. The components of the knockout plasmid include: 3 kbp of DNA upstream of the target gene, 3 kbp of DNA downstream of the target gene, a resistance cassette and a gapped yeast shuttle vector (pRS416) (Figure 4A). The first three components are generated by PCR and pRS416 is cut with *Xba*I and *Xho*I. For the *tob55* knockout, the *tob55* upstream and downstream regions were amplified using the cosmid X22D7 (identified from *N. crassa* genome project as containing *tob55*) as template and the primer set 55-5F and 55-5R to generate the upstream fragment and primer set 55-3F and 55-3R to generate the downstream fragment. The hygromycin resistance cassette was amplified from the plasmid pCSN44 using the primer set hphF and hphR. The yeast strain FY2 (MATα *ura3-52*) was then transformed (see section 2.7) with about 200 ng of each PCR product and 100 ng of the linearized pRS416 (Figure 4B).

To isolate the knockout plasmid, DNA was isolated from yeast transformants. Colonies were resuspended from the plate into YPAD (1% yeast extract, 2% peptone, 0.27 mM adenine hemisulfate, 0.1% dextrose) and transferred to an eppendorf tube. Cells were pelleted by spinning for 30 sec in a benchtop microcentrifuge. The pellet was resuspended in 200 µl lysis buffer (2% Triton-X-100, 1% SDS, 100 mM NaCl, 10 mM Tris-HCl pH 8, 1 mM EDTA) with 200 µl phenol:chloroform and 0.3 gm of 0.5 mm glass beads. The mixture was vortexed vigorously for 2 min and then spun for 10 min in a microcentrifuge. 100 µl of the aqueous top fraction was removed and DNA was precipitated by addition of 10 µl 3 M sodium acetate and 250 µl 95% ethanol. This DNA was used to transform *E. coli* strain XL2 (see section 2.27) and the knockout plasmid was isolated (see section 2.27).

To generate split marker fragments, the knockout plasmid was used as the template in two separate PCR reactions (Figure 4B, bottom). Reaction one used the primer set U-top and U-bottom while reaction two contained the primers D-top and D-bottom. The resulting PCR fragments were purified from an agarose gel using Qiagen spin columns (Qiagen, Mississauga, ON)(section 2.8). These products were transformed into *N. crassa* (section 2.9) and hygromycin resistant colonies were isolated (Figure 4C).

2.7 *Transformation of Yeast*

1 ml of overnight culture of yeast strain FY2 was used to inoculate 50 ml of YPAD (1% yeast extract, 2% peptone, 0.27 mM adenine hemisulfate, 0.1% dextrose) at an OD_{600} of 0.2 to 0.3. This was grown for about 4 hr at 30°C to an OD_{600} of 1.0. Cells were reisolated by spinning in a 50 ml screw cap tube in a clinical centrifuge for 5 min at 4°C. Cells were rinsed with 25 ml sterile water, reisolated and resuspended in 1 ml 100

mM lithium acetate and transferred to an eppendorf tube. Cells were reisolated by spinning at full speed in a desktop microcentrifuge for 1 min. Cells were resuspended in 400 µl 100 mM lithium acetate by vortexing and 50 µl of the supernatant was transferred to a new tube. Cells were pelleted and the supernatant was discarded. Transformation mix (240 µl 50% PEG-3350; 36 µl 1M LiOAc; 50 µl 10 mg/ml sheared salmon sperm DNA; 200 ng upstream *tob55* PCR fragment [Figure 4A]; 200 ng downstream *tob55* PCR fragment [Figure 4A]; 200 ng hygromycin PCR fragment [Figure 4A]; 100 ng linearized pRS416 [Figure 4A]; and sterile water to 360 µl) was added to the cells and the mixture was vortexed until cells were completely resuspended. The mixture was incubated at 30°C for 30 min. Cells were mixed by inversion several times and then subjected to heat shock at 42°C for 30 min. Cells were reisolated by centrifugation for 1 min in a microcentrifuge, washed with 1 ml of sterile water, reisolated and resuspended in 200 µl sterile water. Cells were plated on two SC-Ura plates (0.16% yeast nitrogen base without amino acids; 0.5% ammonium sulfate; 2% glucose; 0.083% [synthetic complete amino acid mixture] SC-ura mix; pH 5.6) and incubated at 30°C until colonies formed.

2.8 *Purification of PCR Fragments from Agarose Gels*

The desired band of DNA was cut from a 0.8% agarose gel and transferred to a 1.5 ml eppendorf tube. Three volumes of 6 M sodium iodide was added to the agarose fragment and this was heated at 55°C until the agarose was completely dissolved. 750 µl of this mixture was transferred to a mini-prep column containing a DNA binding matrix at the bottom of the column (Qiagen, Mississauga, ON). To bind the DNA to the matrix, the column was spun for 1 min at 5 000 rpm in a microcentrifuge. When the volume of the DNA-containing solution exceeded the capacity of the column, this step was repeated until all DNA was bound to the column. The column was then washed with 500 µl of 6 M sodium iodide by spinning for 1 min at 5 000 rpm in a microcentrifuge. A further wash was done by adding 750 µl of buffer PE (10 mM Tris-HCl pH 8 in 50% ethanol) to the column and spinning for 1 min at 5 000 rpm in a microcentrifuge. All traces of ethanol were removed from the column by spinning for 1 min at 10 000 rpm in a microcentrifuge. 30 to 50 µl of water was added to the column and incubated for 1 min at room temperature. DNA was eluted into a 1.5 ml eppendorf tube by spinning for 1 min at 13 000 rpm in a microcentrifuge.

2.9 *Transformation of N. crassa*

DNA was transformed into *N. crassa* by electroporation of conidia as previously described (Margolin, 1997, 2000) with slight modifications. Conidia that were between three and ten days old were harvested in cold, sterile water and filtered through sterile cheesecloth. The conidia were washed three times with 50 ml of cold, sterile 1 M sorbitol and resuspendeded to a final concentration of 2.0 to 2.5 x 10^9 conidia/ml. 5 μg of linearized plasmid DNA at a concentration of 1 μg/μl was mixed with 40 μl of the conidia and set on ice in electroporation cuvettes (2 mm gap) for 5 min. Electroporation was performed at 2.1kV, 475 Ω, and 25 microfarads on a Gene Pulser (BioRad, Hercules, CA) resulting in a pulse time constant of 11 to 12 ms, or at 1.5kV, 480 Ω on an Electro Cell Manipulator 600 (Harvard Apparatus, Holliston, MA) with time constants between 20 to 21 ms. Immediately following the pulse, 1 ml of cold, sterile 1 M sorbitol was added and the conidia were incubated at 30°C for 45 to 60 min to recover. A modified recovery protocol was used for the *N. crassa* knockout transformation. The transformed conidia in 1 M sorbitol were added to 9 ml of pre-warmed 1X Vogel's medium and shaken at 30°C for 2 hr. For most transformations, aliquots of between 5% and 50% of the total volume of the recovered conidial suspension were added to 50 ml of top agar at 48°C (standard sorbose medium containing 1 M sorbitol (Davis, 1970)) plus the appropriate antibiotics and nutritional requirements for selection of the transformants. For the knockout transformation, the entire conidial suspension (10 ml) was mixed with 40 ml of 1.25X top agar. After gentle but thorough mixing, the top agar containing transformed conidia was spread onto 5 plates of the same media as the top agar, but lacking the 1 M sorbitol, and incubated at 30°C for 3 to 7 days or until transformed colonies were formed.

2.10 *Purification of Transformant Strains*

In an effort to ensure that only pure homokaryotic single colonies were used following transformations, colonies were subjected to a purification procedure. Single transformant colonies were picked using sterile glass pasteur pipettes and transferred to slants with Vogel's medium containing the appropriate nutritional requirements and the selective antibiotic(s) at 0.5X the normal concentration, as the drugs used often inhibit conidiation. The slants were incubated at 30°C until the surface of the agar was covered by the mycelium and then were removed to room temperature to conidiate. Conidia were streaked for single colonies onto plates identical to those used for the electroporation and incubated at 30°C until colonies formed. These were picked to slants without the antibiotic for growth and conidiation.

When heterokaryotic strains were transformed and selected for integration into a single nucleus, the transformed strains were tested for their nutritional requirements following the purification process to ensure that the desired homokaryon was obtained (Nargang *et al.*, 1998).

2.11 *Purification of Su9-DHFR for in vitro Import*

Protein was purified on a NiNTA column (Qiagen, Mississauga, ON) according to manufacturer's instructions with some modifications. *E. coli* B strain BL21 containing a plasmid expressing a fusion protein consisting of the first 68 amino acid residues of mitochondrial subunit 9 of the F_1 ATPase with mouse DHFR was utilized (provided by Doron Rapaport, University of Munich). Expression in a culture with a starting concentration of 0.6 OD_{600} was induced with 1 mM IPTG for 2 hr. Induced cells were pelleted and frozen. Cells were resuspended in lysis buffer (50 mM NaH_2PO_4 pH 8, 300 mM NaCl, 10 mM imidazole, 1 mM PMSF, 10 μl protease inhibitor cocktail per ml of buffer [Sigma Aldrich, Oakville, ON]). Lysozyme was added to 1 mg/ml and the mixture was incubated on ice for 30 min followed by sonication (6 X 10 sec) on ice. The lysate was cleared by centrifugation at 12 000 rpm (SS34 rotor) for 25 min at 4°C and the supernatant was mixed with 1 ml of NiNTA slurry (Qiagen, Mississauga, ON) per gram wet weight of harvested cells for 1 hr at 4°C. The slurry was poured onto an Econo-Pac column (Bio-Rad, Hercules, CA). The column was washed twice with 10 volumes of lysis buffer containing 15 mM imidazole and protein was eluted in 3 fractions of 3 ml each with elution buffer (lysis buffer containing 250 mM imidazole).

2.12 *In vitro Import of Radiolabeled Proteins into Isolated Mitochondria*

For *in vitro* import studies, mitochondria were isolated as described (Mayer *et al.*, 1993) and import of mitochondrial preproteins was basically as described (Harkness *et al.*, 1994). Preproteins were produced by transcription and translation in rabbit reticulocyte lysate (Promega TnT reticulocyte lysate system, Madison WI) in the presence of [^{35}S]-methionine (ICN Biomedicals, Costa Mesa, CA) for the indicated time points, at the indicated temperatures. In some cases, the mitochondria were incubated with 8 μM antimycin A and 20 μM oligomycin prior to import for 2 min at 25°C to reduce the membrane potential. For import with purified Su9-DHFR, 0.1 μg of purified protein was added with the radiolabeled preproteins. Import reactions were analyzed by SDS-polyacrylamide gel electrophoresis (SDS-PAGE) and viewed by autoradiography or a phosphorimager system. Quantification of the image from the latter was done using the Imagequant program (version 5.2, Molecular Dynamics). For *in vitro* assembly studies by blue native gel electrophoresis (BNGE), import of mitochondrial preproteins was as described with minor modifications to times and temperatures (Rapaport *et al.*, 2001). Reactions were analyzed by BNGE and viewed by autoradiography.

2.13 *Crosslinking of Radiolabeled Proteins During in vitro Import*

Radiolabeled precursor protein was imported into wild type mitochondria under two different conditions. For Tom40, import was performed as described (section 2.12). For Tim23, membrane potential was dissipated by pre-incubation of the mitochondria with 1 μM valinomycin and 25 μM carbonyl cyanide 4-(trifluoromethoxy)phenylhydrazone (FCCP) at 25°C for 2 min. Following import, crosslinking was performed with 300 μM 1,5-Difluoro-2,4-dinitrobenzene (DFDNB) or disuccinimidyl glutarate (DSG) for 30 min in an ice bath. The excess crosslinker was quenched with 100 mM Tris-HCl, pH 7.5. For immunoprecipitation, re-isolated mitochondria were lysed in 1% Triton-X-100, 300 mM NaCl, 5 mM EDTA, 10 mM Tris-HCl, pH 7.4, 1mM PMSF.

2.14 *Alkaline Extraction of Membranes*

Mitochondria (20-50 μg) were suspended in 1 ml of cold 0.1 M sodium carbonate (Na_2CO_3), pH 11.5 and incubated on ice for 30 min. Membrane fraction was collected as a pellet after spinning for 15 min in a microcentrifuge. Proteins in the supernatant were precipitated with 11 % trichloroacetic acid precipitation (see section 2.15). Both pellets were solubilized in cracking buffer (0.06 M Tris-HCl pH 6.7, 2.5% SDS, 0.01% β-mercaptoethanol, 5% sucrose). The mixture was shaken for 5 min and boiled for 5 min before being subjected to SDS-PAGE. Separation of soluble and membrane fractions using a sucrose step gradient, was performed as described (D'Agostino *et al.*, 2002). Mitochondria were suspended in 100 μl of cold 0.1 M Na_2CO_3, pH 11.5 and incubated on ice for 30 min. This solution was mixed with 200 μl 2.4 M sucrose, 0.1 M Na_2CO_3, pH 11.5 to generate a final sucrose concentration of 1.6 M. This was transferred to an ultracentrifuge tube and overlaid with 1.4 ml of 1.4 M sucrose, 0.1 M Na_2CO_3, pH 11.5 and then 300 μl of 0.25 M sucrose, 0.1 M Na_2CO_3, pH 11.5. The step gradient was spun at 60 000 rpm in a SW60.1 rotor for 2 hr at 4°C. The step gradient was collected in 2 fractions. The first consisting of the 0.25-1.25 M sucrose interface plus the 1.25 M sucrose layer and containing membrane-integrated proteins and the second, containing soluble proteins in the 1.4 M sucrose layer. The sucrose concentrations of the fractions were reduced to 0.5 M by the addition of water and proteins were precipitated with 15% TCA. Pellets were solubilized in cracking buffer by shaking for 5 min followed by boiling for 5 min. Samples were subjected to SDS-PAGE.

2.15 *TCA precipitation of proteins*

TCA (72% w/v) was added to the protein solution to a final concentration of 11% (15% for Na_2CO_3, pH 11.5 solution) and samples were incubated overnight at 4°C or for 30 min at 0°C. Proteins were pelleted (15 min, 12 000 rpm, microcentrifuge) and washed with 1 ml acetone by shaking for 10 min at room temperature. Pellet was reisolated by spinning 10 min at 12 000 rpm in a microcentrifuge and dried for 30 min at 37°C. Proteins were solubilized by shaking for 5 min in cracking buffer, boiled for 5 min and subjected to SDS-PAGE.

2.16 *Immunoprecipitation*

For Tim8 and Tim13, 40 μl of antisera bound to 4 mg of Protein A Sepharose beads (Amersham Biosciences, Cleveland, OH) was used per 50 μg of mitochondrial protein. For Tim23, immunoprecipitation following biotin maleimide labeling, 50 μl of serum was used per 5 mg of Protein A Sepharose beads.

The serum was bound to the Protein A Sepharose beads by rocking at room temperature for 30 min. The beads were washed 3 times with 10 volumes of PBS (10 mM Na_2HPO_4, 2.7 mM KCl, 137 mM NaCl) and then 3 times with 10 volumes of 0.2 M sodium borate, pH 9. To crosslink the antibodies to the matrix, 10 volumes of 20 mM DMP (dimethylpimelimidate), dissolved in 0.2 M sodium borate, pH 9, was added and this mixture incubated at room temperature with rocking for 30 min. To quench the crosslinker, the beads were washed with 10 volumes of 0.2 M ethanolamine, pH 8 and then incubated in 10 volumes 0.2 M ethanolamine, pH 8.0 for either 2 hr at room temperature or overnight at 4°C. To remove the ethanolamine, beads were washed with 10 volumes of PBS. The beads were either used immediately or stored in PBS containing 0.02% sodium azide at 4°C. If stored, beads were washed with 10 volumes of 0.1 M glycine pH 3 prior to use to remove IgGs that were not crosslinked to the beads.

To prepare mitochondrial samples for immunoprecipitation, samples were lysed at a final concentration ranging from 1 mg/ml to 2 mg/ml in lysis buffer (1% Triton-X-100, 300 mM NaCl, 5 mM EDTA, 10 mM Tris-HCl pH 7.4, 1 mM PMSF) by rocking at 4°C for 30 min. Lysate was cleared by spinning at full speed in a microcentrifuge for 20 min at 4°C. Protein A Sepharose beads crosslinked to the antibody were added to the cleared lysate and rocked at 4°C for 90 min to overnight. Beads were washed 3 times with 10 volumes of lysis buffer and then with once with 10 volumes of 10 mM Tris-HCl, pH 7.4. Bound protein was removed from the beads by addition of 40 μl cracking buffer. The mixture was then shaken for 5 min and boiled for 5 min. The beads were pelleted by spinning at full speed in a microcentrifuge for 2 min and the supernatant was subjected to SDS-PAGE.

2.17 *Creation of Strains Expressing Mutant Versions of Tim23*

Mutant alleles of *tim23* were created by site-directed mutagenesis of single stranded DNA from a plasmid containing the genomic version of *tim23* and a bleomycin resistance gene. The resulting plasmids were linearized and used to transform conidia from T23R4-12, the $tim23^{RIP}$ heterokaryotic strain (section 2.4). Mutant *tim23* alleles that maintained sufficient Tim23 function should have been capable of rescuing the nucleus containing the non-functional $tim23^{RIP}$ allele. Selection for transformation into the $tim23^{RIP}$ nucleus was achieved by plating on medium containing tryptophan, inositol, and acriflavin (25 µg/ml), and bleomycin (1.5 µg/ml). Transformation and purification were performed as described in section 2.9. Nutritional testing (section 2.10) for the tryptophan and inositol requirements was done to confirm the rescue of the RIPed nucleus with the mutant *tim23* gene. Confirmation that the new mutant allele was present in the rescued homokaryon was obtained by sequencing the PCR amplified ectopic *tim23* gene from isolated genomic DNA (section 2.27).

2.18 *Size Determination of the Native Tim8-13 Complex by Sephacryl Chromatography*

Mitochondria (0.5 mg) were solubilized with 1% *n*-dodecylmaltoside in 500 µl column buffer (20 mM HEPES, 50 mM NaCl, 2.5 mM $MgCl_2$, 1 mM EDTA, 10% glycerol, 1 mM Phenylmethylsulfonyl fluoride [PMSF]) for 30 min at 4°C. After centrifugation at 180,000 x g_{max} for 30 min at 4°C in the TLA55 ultracentrifuge rotor, the cleared lysate was subjected to column chromatography through a Sephacryl-S200 column. The column running buffer contained 0.1% DDM. Fractions of 1 ml were collected and proteins were precipitated with 11% TCA. Samples were analyzed by SDS-PAGE, transferred to nitrocellulose and immunoblotted with antibodies against Tim8 or Tim13. For calibration, apoferritin (440 kDa), β-amylase (200 kDa), carbonic anhydrase (29 kDa) and cytochrome *c* (12 kDa) were used as standards. Column chromatography was performed by Troy Locke (University of Alberta).

2.19 *Mitochondrial Subfractionation*

Mitochondria (1 mg) were suspended in swelling buffer (5 mM KPO_4, pH 7.2, 100 mM NaCl, 5 mM EDTA, 1 mM PMSF) and incubated on ice for 1 hr. The sample was subjected to centrifugation at 12 000 rpm for 20 min at 4°C in an SS-34 rotor to pellet the mitoplasts. The supernatant, enriched for intermembrane space proteins, was collected and spun at 28 000 rpm in a TLA-55 rotor for 1hr at 4°C to remove remaining contaminants. Proteins in the intermembrane space fraction were precipitated with 11% TCA and suspended in cracking buffer. Samples (5 µg) from both the pellet and intermembrane space fraction were subjected to SDS-PAGE.

2.20 *BNGE*

Mitochondria (50 µg) were solubilized in 50 µl Buffer N containing detergent (either 1% digitonin (DIG) or 1% DDM in 20 mM Tris-Cl, pH 7.4, 0.1mM EDTA, 50mM NaCl, 1% glycerol [vol/vol], 1mM PMSF). After gentle rocking at 4°C for 15 min and a clarifying spin (30 min, 4°C, 13 000 rpm, microcentrifuge), the supernatant was added to 5 µl of sample buffer (5% Coomassie Brilliant Blue G-250 in 100 mM Bis-Tris, 500 mM 6-aminocaproic acid, pH 7.0) and gently mixed at 4°C. Samples were analyzed on a 6 to 13% gradient blue native gel as previously described (Schagger and von Jagow, 1991; Schagger *et al.*, 1994) except that electrophoresis was performed overnight (about 16 to 20 hrs) at 4°C between 40 and 60 volts before the excess Coomassie Blue was electrophoresed out for 1 to 1 ½ hr at 500 volts.

2.21 *Antibody Supershift and BNGE*

Samples were prepared as above (section 2.20) except that after the lysate was cleared, 25 µl of affinity-purified antibody was added and incubated with rocking at 4°C for 2 hr. Sample buffer was added and samples were subjected to BNGE.

2.22 *Antibody Production*

Antisera were raised against fusion proteins that were purified by NiNTA chromatography (see below). The fusion proteins were comprised of histidine tagged full length mouse DHFR and the C-terminus of Tim8 or Tim13 or the N-terminus of Tob55. For expression of Tim8 and Tim13 fusion proteins in *E. coli* strain M15[pREP4], PCR fragments encoding the sequence of amino acids 35-92 of Tim8 or amino acids 31-86 of Tim13 were cloned into the *Bgl*II and *Hind*III sites of pQE42 and pQE40 respectively (Qiagen, Mississauga, ON) (see Table 3).

For Tob55, the plasmid pGOM55 (see Table 3) was cut with the restriction enzymes *EcoR*I and *Hind*III. This fragment, containing DNA coding for amino acids 1-108 of Tob55, was subcloned into the vector pQE40 resulting in pQET55. This plasmid was transformed into *E. coli* strain BL21 for expression.

Following expression in *E. coli*, the fusion proteins were purified on a NiNTA column (Qiagen, Mississauga, ON) in 8M urea according to the manufacturer's instructions except that the protein was eluted in 0.1% SDS, 10mM Tris Cl, pH7.4. The eluate was injected into rabbits without further processing. The first injection was 1 mg of purified protein at a concentration of 1.33 mg/ml with an equal volume of Freund's Complete Adjuvant (Difco, Kansas, MO). The subsequent injections were 500 μg fusion protein at a concentration of 1mg/ml with an equal volume of Freund's Incomplete Adjuvant (Difco, Kansas, MO). Injections were done once every four weeks. Response of the rabbits was monitored by test bleeds every four weeks. After eight injections for Tim8 and Tim13, rabbits 10-2 and 10-9 respectively, were sacrificed and serum was collected. For Tob55, rabbits 3M1 and 4B3 were sacrificed after 6 injections, and serum was collected.

2.23 *Antibody Affinity Purification*

Following expression in *E. coli* strain BL21, the Tob55 fusion protein was purified on a NiNTA column (Qiagen, Mississauga, ON) in 8 M urea according to the manufacturer's instructions except that protein was eluted in 6 M guanidine, 100 mM NaH_2PO_4, 10 mM Tris-HCl, pH 4.5. A Centriplus centrifugal filter device (Millipore, Bedford, MA) with a molecular weight cut off of 30 kDa was used to exchange the elution buffer to coupling buffer containing 0.1 M $NaHCO_3$, 0.5M NaCl, 6M guanidine. The cycle of concentrating the sample to 1 ml by centrifugation at 5000 rpm for 2 hr followed by addition of 15 ml of coupling buffer was repeated three times. The ligand coupling slurry Affi-Gel 10 or Affi-Gel 15 (Bio-Rad, Hercules, CA) were prepared by washing with 5 volumes of distilled water. About 30 mg of fusion protein in coupling buffer was bound to 1 ml each of Affi-Gel 10 and Affi-Gel 15 by incubation with rocking at 4°C overnight. The next day, the resin was washed with 5 volumes PBS (phosphate buffered saline) and 2 volumes of 100 mM glycine, pH 2.5. To confirm that the antigen was bound to the resin, 10 µl of washed resin was suspended in 1X cracking buffer and subjected to SDS-PAGE and Coomassie staining.

For purification of the antibody, 2 ml of serum was mixed with 100 µl 20X PBS and incubated with 1 ml of the antigen-bound matrix for 4 hr at 4°C with rocking. The resin was washed 3 times with 5 volumes of PBS. Antibody was eluted in 10 fractions of 200 µl with100 mM glycine, pH 2.5. Fractions were neutralized with 20 µl 1 M Tris-HCl, pH 10. The antibody-containing fractions were identified by mixing 2 µl of the eluant with 200 µl Bradford protein assay (Biorad, Hercules, CA) in a microtiter plate. The column was washed with PBS containing 0.05% sodium azide and stored at 4°C.

2.24 *Preparation of N. crassa for Electron Micrographs*

Liquid cultures were inoculated at 1 X 10^6 conidia/ml and grown for 12 to 15 hr at 30°C. An aliquot of 500 µl was removed to a sterile eppendorf tube. Mycelium was pelleted by spinning for 30 sec at 7000 rpm in a microcentrifuge. The pellet was washed with 1 ml of sterile water and pelleted again at 7000 rpm in a microcentrifuge. The pellet was resuspended in 100 µl of sterile water and then incubated for 30 min with rocking at room temperature with 1 ml 1.5% $KMnO_4$. Mycelium was pelleted at 7000 rpm in a microcentrifuge and the supernatent was removed. The stained cells were washed with 1 ml of sterile water 5 times or more (until the water was colorless after centrifugation). The stain was fixed by incubation in 1 ml fixing buffer (0.05 M cacodylate buffer [25 ml 0.2M Na cacodylate, 2.1 ml 0.1% HCl], 15% sucrose, 2% gluteraldehyde) for 30 min on ice. Mycelium was pelleted at 7000 rpm in a microcentrifuge and the supernatent was removed. Cells were resuspended in 1 ml 1% OsO_4, 1.5% $K_2Cr_2O_7$ and incubated on ice for 90 min with occasional mixing. The mycelium was pelleted at 7000 rpm in a microcentrifuge and resuspended in 1% uranyl acetate. The steps of dehydration, embedding and sectioning were performed at the Microscopy Unit, Department of Biological Sciences. Sections were examined by electron microscopy.

2.25 *Substituted Cysteine Accessibility Mapping*

Mitochondria were isolated as previously described (Mayer *et al.*, 1993) and resuspended in PBSSP buffer (137 mM NaCl, 2.7 mM KCl, 10 mM Na_2HPO_4, 2 mM KH_2PO_4, 0.25 M sucrose, 1 mM PMSF) at a final concentration of 5 mg/ml. A solution of biotin maleimide was prepared by dissolving 2 mg Nα-(3-maleimidylpropionyl) biocytin (Molecular Probes, Eugene, OR) in 100 µl of DMSO (dimethyl sulfoxide). A dilution of the mitochondrial sample was prepared by addition of 50 µl of mitochondria at a concentration of 5 µg/µl to 450 µl of PBSSP. To this dilute sample of mitochondria, 5 µl of the biotin maleimide solution was added and incubated at room temperature for 2 hr with gentle rocking. Mitochondria were reisolated by centrifugation and washed with 500 µl of PBSSP. These mitochondria were then subjected to immunoprecipitaion with antibodies to *N. crassa* Tim23 (see section 2.16).

The immunoprecipitate was separated by SDS-PAGE and subjected to western analysis as follows. Following blocking in skim milk TBS-tween buffer (5% skim milk power [w/v]; 20 mM Tris-HCl; 150 mM NaCl; 2.5% Tween 20), the membrane was incubated with a 1:2000 dilution of streptavidin horseradish peroxidase (Amersham Biosciences, Cleveland, OH) in blocking buffer for 4 hr at room temperature. Membranes were then washed twice for 10 min with blocking buffer and once in blocking buffer without milk powder. The membrane was then subjected to ECL (see section 2.27).

2.26 *Other Techniques*

The standard techniques of agarose gel electrophoresis, Southern and Northern blotting of agarose gels, preparation of radioactive probes, transformation of *Escherichia coli*, and PCR using a mixture of *Taq* and *Pfu* polymerase (New England BioLabs, Beverly, MA) to minimize replication errors, were all performed as described (Current Protocols). The following procedures were employed using the supplier's recommendations or previously described procedures: isolation of plasmid DNA (Qiagen, Mississauga, ON), separation of mitochondrial proteins by SDS-PAGE (Laemmli, 1970), western blotting (Good, 1989), western blot ECL detection using LumiGLO chemiluminescent substrate (Kirkegaard and Perry Laboratories, Gaithersburg, MD), genomic DNA extraction (Wendland, 1996), protein determination with the Coomassie dye binding assay (Bio-Rad, Hercules, CA), manual DNA sequencing using thermosequenase (Amersham Biosciences, Cleveland, OH), and automated sequencing using a DyeNamic sequencing kit (Amersham Biosciences) with a Model 373 stretch sequencer separation system (Applied Biosystems, Foster City, CA). Radioactive precursor proteins for import were generated by coupled *in vitro* transcription and translation with the Promega (Madison, WI) TNT reticulocyte lysate system in the presence of [^{35}S]methionine (ICN, Costa Mesa, CA).

Figure 3 Generation of a *tim23* sheltered RIP strain. Genetic markers important for the generation, selection or manipulation of the strains are shown on specific linkage groups (LG) in the host strain H III and mate strain M III. The approximate position of the *tim23* gene is shown on LG III as deduced from RFLP mapping analysis. The host strain H III (FGSC # 72-53) linkage group III (HLG III) is distinguished from the mate strain linkage group III (MLG III) by the presence of the "opposite" genetic markers. Only genetic markers relevant to the generation of the sheltered RIP strain are shown. Rectangles depict cells while rounded rectangles depict nuclei. (A) Generation of a *tim23* duplication containing strain. H III was transformated with a genomic copy of the *tim23* gene encoding an octa-histidine N-terminal tag, carried on a hygromycin resistant plasmid. Transformants were selected on supplemented sorbose medium containing hygromycin. Hygromycin resistant strains were screened by Southern analysis for complete integration of the *tim23* gene. (B) The desired transformant of H III containing a single ectopic copy of *tim23* integrated at a random position in the genome. (C) The MateIII strain (FGSC #72-63) was used as the female in a sheltered RIP cross with the transformant in (B). RIP occured in a percentage of the duplication containing H III nuclei in the cross. Progeny of the cross were grown on sorbose medium lacking tryptophan and adenine to select for disomics of LG III. The disomics rapidly break down into heterokaryons in which one nucleus contains HLG III and the other MLG III. The two possible versions of heterokaryotic strains are shown in (D) and (E). In both cases, the ectopic copy of *tim23* may or may not be present depending on the meiotic segregation of the chromosome on which the ectopic integration occurred.

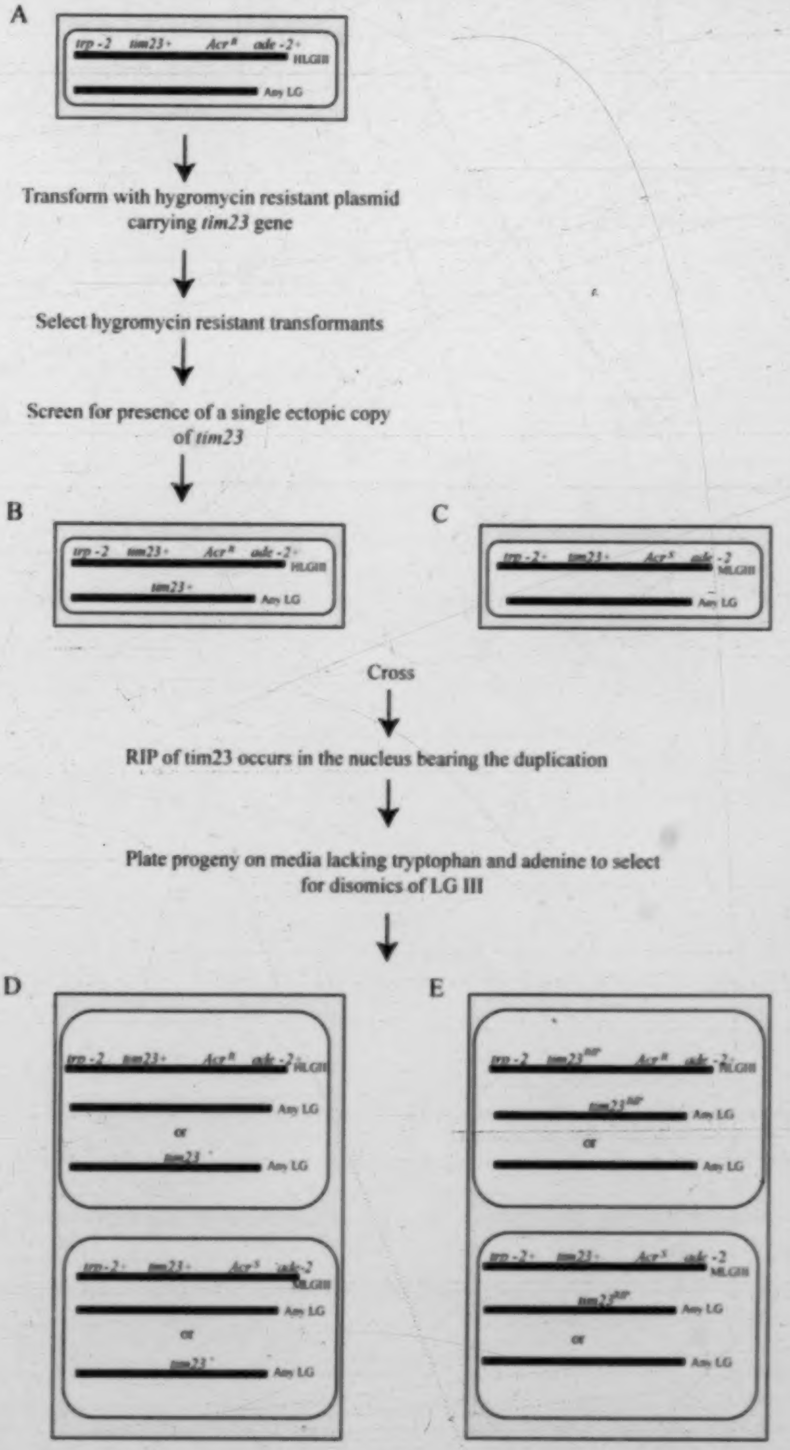
A
trp-2 tim23+ Acr^R ade-2+ HLGIII
Any LG
Transform with hygromycin resistant plasmid carrying tim23 gene
Select hygromycin resistant transformants
Screen for presence of a single ectopic copy of tim23
B
trp-2 tim23+ Acr^R ade-2+ HLGIII
tim23+ Any LG
C
trp-2+ tim23+ Acr^S ade-2 MLGIII
Any LG
Cross
RIP of tim23 occurs in the nucleus bearing the duplication
Plate progeny on media lacking tryptophan and adenine to select for disomics of LG III
D
trp-2 tim23+ Acr^R ade-2+ HLGIII
Any LG
or
tim23+ Any LG
trp-2+ tim23+ Acr^S ade-2 MLGIII
Any LG
or
tim23+ Any LG
E
trp-2 tim23^RIP Acr^R ade-2+ HLGIII
tim23^RIP Any LG
or
Any LG
trp-2+ tim23+ Acr^S ade-2 MLGIII
tim23^RIP Any LG
or
Any LG

tim23$^+$ heterokaryon

Sheltered RIP heterokaryon

Figure 4 *Neurospora crassa* gene knockout strategy. (A) The four DNA components necessary to generate the *tob55* knockout construct including the plasmid pRS416. The three rectangular boxes on the right represent linear fragments that are generated by PCR (also see section 2.6). The two PCR fragments containing the sequence upstream and downstream of *tob55* have regions of homology to both the hygromycin cassette (grey boxes) and the plasmid multiple cloning site (MCS, black boxes) to facilitate assembly in yeast. (B) The four DNAs in panel A are transformed into yeast strain FYα where recombination occurs (top) to generate the knockout construct plasmid (bottom). This plasmid is then used as a PCR template to generate the two pieces of a split hygromycin resistance marker to be transformed into *N. crassa* to create the disruption. Primers U-top and U-bottom produce one portion of the split marker fragment and the primer pair D-top and D-bottom generate the other piece. (C) *N. crassa* genomic DNA is represented by a line and the *tob55* target gene is shown as a white box. The split marker fragments produced by PCR as described in panel B are shown as boxes, with the portions corresponding to the hygromycin resistance gene shown in grey. Three homologous recombination events occur in *N. crassa* at the target gene locus to replace the coding sequence with the hygromycin resistance marker (grey box).

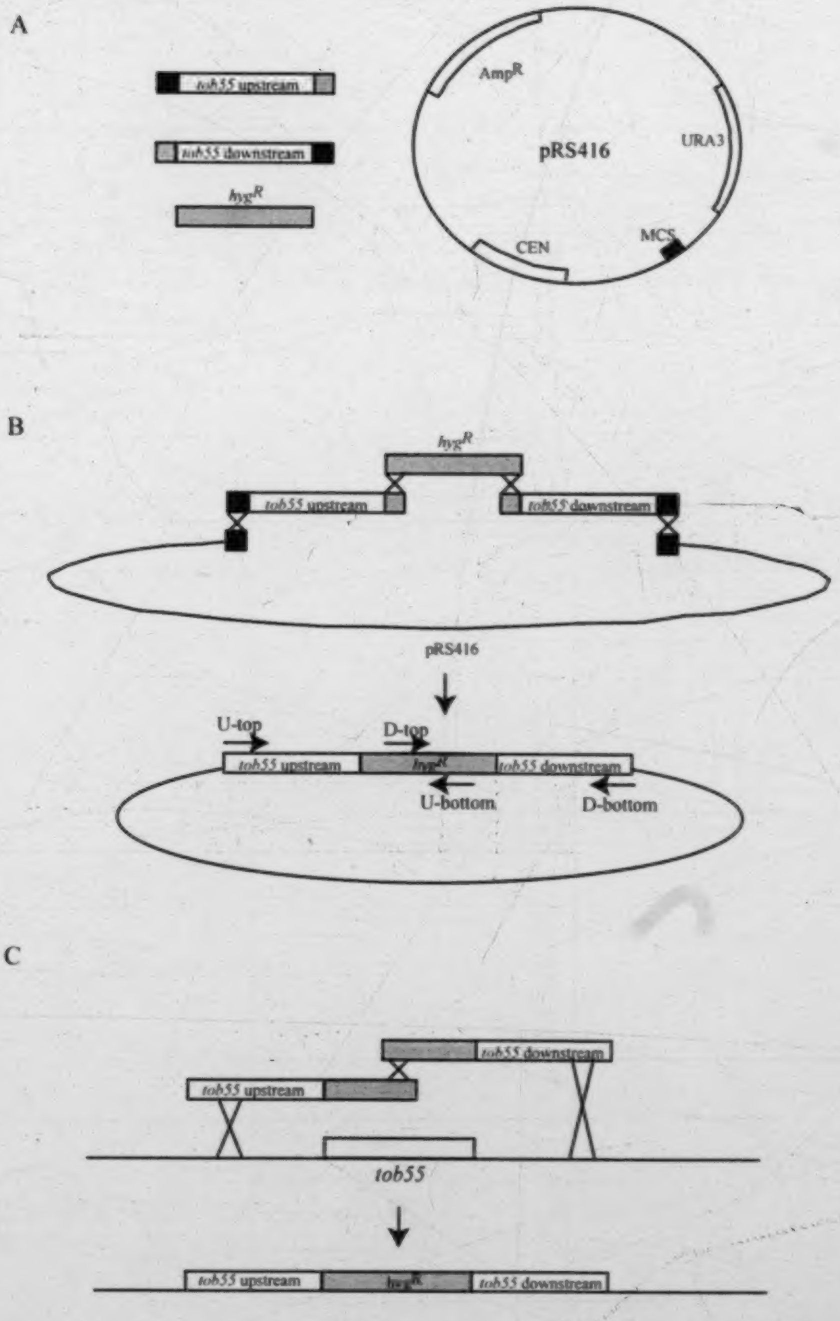
A
tob55 upstream
tob55 downstream
hygR
AmpR
pRS416
URA3
CEN
MCS
B
hygR
tob55 upstream
tob55 downstream
pRS416
U-top
D-top
tob55 upstream
hygR
tob55 downstream
U-bottom
D-bottom
C
tob55 downstream
tob55 upstream
tob55
tob55 upstream
hygR
tob55 downstream

Table 1
Strains Used in This Study.

Stock Strains

Strain	Genotype	Origin or Source
7626	*his-3*	R. L. Metzenberg
NCN 251 (also called 74A)	*A*	Fungal Genetics Stock Center #2489 (74-OR23-1VA)
H III	*acr-2 trp-1; inl inv mei-2*	Fungal Genetics Stock Center #7253
M III	*ad-2; am132 inl inv mei-2 +* *a*^{m1} *ad-3B cyh-1*	Fungal Genetics Stock Center #7263
HP1	*his- FPA*^{R} + *pan-2 Ben*^{R}	heterokaryon of 7626 and Fungal Genetics Stock Center 7118

Tim8 and Tim13 Strains

Strain	Genotype	Origin or Source
T8HL7	As 7626 with an ectopic copy of *tim8*	Transformation of 7626 with the *tim8* plasmid pT8HL
T8HL7-7	As T8HL7 with RIP mutations throughout the *tim8* gene	Cross of NCN251 with T8HL7
T13-16	As 7626 with an ectopic copy of *tim13*	Transformation of 7626 with the *tim13* plasmid pCST13
T13R16-45	As T13-16 with RIP mutations throughout the *tim13* gene(s)	Cross of NCN251 with T13-16

Tim23 Strains

Strain	Genotype	Origin or Source
TI23-4	As H III, but carries an ectopic copy of *tim23*. hyg^R	Transformation of Host III with the *tim23* plasmid pTim23
T23R4-12	Sheltered Heterokaryon *(acr-2 trp-1; inl inv mei-2 tim23*^{RIP} *+ ad-2; am132 inl inv mei-2)*	Cross of MateIII (Fungal Genetics Stock Center #7263) x TI23-4

Strain	Genotype	Origin or Source
Helper 5	*matΔ his-3; hyg*^{R} *tk+ Bml*^{R} *pan-2*	R. Metzenberg (Fungal Genetics Stock Center #9618)
Hel23R-1	Sheltered heterokaryon (*acr-2 trp-1; inl inv mei-2 tim23*^{RIP} *+ matΔ his-3; hyg*^{R} *tk+ Bml*^{R} *pan-2*)	Nucleus swap between T23R4-12 and Helper 5
T23Δ10-14	*acr-2 trp-1; inl inv mei-2 tim23*^{RIP} with an ectopic copy of *tim23* containing a deletion of amino acids 1-10.	Transformation of T23R4-12 with specific *tim23* plasmid (see Table 2)
T23Δ50-50	*acr-2 trp-1; inl inv mei-2 tim23*^{RIP} with an ectopic copy of *tim23* containing a deletion of amino acids *1-50*.	Transformation of T23R4-12 with specific *tim23* plasmid (see Table 2)
T23W5C-11	*acr-2 trp-1; inl inv mei-2 tim23*^{RIP} with an ectopic copy of *tim23* containing an amino acid change of W5 to C5.	Transformation of T23R4-12 with specific *tim23* plasmid (see Table 2)
T23T9C-4	*acr-2 trp-1; inl inv mei-2 tim23*^{RIP} with an ectopic copy of *tim23* containing an amino acid change of T9 to C9.	Transformation of T23R4-12 with specific *tim23* plasmid (see Table 2)
T23K13C-4	*acr-2 trp-1; inl inv mei-2 tim23*^{RIP} with an ectopic copy of *tim23* containing an amino acid change of K13 to C13.	Transformation of T23R4-12 with specific *tim23* plasmid (see Table 2)
T23E17C-6	*acr-2 trp-1; inl inv mei-2 tim23*^{RIP} with an ectopic copy of *tim23* containing an amino acid change of E17 to C17.	Transformation of T23R4-12 with specific *tim23* plasmid (see Table 2)
T23P21C-3	*acr-2 trp-1; inl inv mei-2 tim23*^{RIP} with an ectopic copy of *tim23* containing an amino acid change of P21 to C21.	Transformation of T23R4-12 with specific *tim23* plasmid (see Table 2)
T23A23C-6	*acr-2 trp-1; inl inv mei-2 tim23*^{RIP} with an ectopic copy of *tim23* containing an amino acid change of A23 to C23.	Transformation of T23R4-12 with specific *tim23* plasmid (see Table 2)
T23S27C-2	*acr-2 trp-1; inl inv mei-2 tim23*^{RIP} with an ectopic copy of *tim23* containing an amino acid change of S27 to C27.	Transformation of T23R4-12 with specific *tim23* plasmid (see Table 2)

Strain	Genotype	Origin or Source
T23P29C-10	*acr-2 trp-1; inl inv mei-2 tim23*^{RIP} with an ectopic copy of *tim23* containing an amino acid change of P29 to C29.	Transformation of T23R4-12 with specific *tim23* plasmid (see Table 2)
T23T33C-4	*acr-2 trp-1; inl inv mei-2 tim23*^{RIP} with an ectopic copy of *tim23* containing an amino acid change of T33 to C33.	Transformation of T23R4-12 with specific *tim23* plasmid (see Table 2)
T23S37C	*acr-2 trp-1; inl inv mei-2 tim23*^{RIP} with an ectopic copy of *tim23* containing an amino acid change of S37 to C37.	Transformation of T23R4-12 with specific *tim23* plasmid (see Table 2)
T23Y41C-2	*acr-2 trp-1; inl inv mei-2 tim23*^{RIP} with an ectopic copy of *tim23* containing an amino acid change of Y41 to C41.	Transformation of T23R4-12 with specific *tim23* plasmid (see Table 2)
T23F45C-1	*acr-2 trp-1; inl inv mei-2 tim23*^{RIP} with an ectopic copy of *tim23* containing an amino acid change of F45 to C45.	Transformation of T23R4-12 with specific *tim23* plasmid (see Table 2)
T23Q49C-5	*acr-2 trp-1; inl inv mei-2 tim23*^{RIP} with an ectopic copy of *tim23* containing an amino acid change of Q49 to C49.	Transformation of T23R4-12 with specific *tim23* plasmid (see Table 2)
T23V53C-4	*acr-2 trp-1; inl inv mei-2 tim23*^{RIP} with an ectopic copy of *tim23* containing an amino acid change of V53 to C53.	Transformation of T23R4-12 with specific *tim23* plasmid (see Table 2)
T23L57C-7	*acr-2 trp-1; inl inv mei-2 tim23*^{RIP} with an ectopic copy of *tim23* containing an amino acid change of L57 to C57.	Transformation of T23R4-12 with specific *tim23* plasmid (see Table 2)
T23S61C-1	*acr-2 trp-1; inl inv mei-2 tim23*^{RIP} with an ectopic copy of *tim23* containing an amino acid change of S61 to C61.	Transformation of T23R4-12 with specific *tim23* plasmid (see Table 2)
T23-cys-9	*acr-2 trp-1; inl inv mei-2 tim23*^{RIP} with an ectopic copy of *tim23* containing an amino acid change of C108A and C167A.	Transformation of T23R4-12 with specific *tim23* plasmid (see Table 2)

Tob55 Strains

Strain	Genotype	Origin or Source
Tob55KO-1	Sheltered Heterokaryon. As HP1 with replacement of the *tob55* gene in nucleus 1 with a hygromycin resistance cassette	Transformation of HP1 with split marker fragments generated from knockout construct, pT55KO
Tob55KO-3	Sheltered Heterokaryon. As HP1 with replacement of the *tob55* gene in nucleus 1 with a hygromycin resistance cassette	Transformation of HP1 with split marker fragments generated from knockout construct, pT55KO
T55His6-1	his-3 FPA^R hyg^R bleo^R with an ectopic copy of *tob55* with 6 histidine residues added to the N-terminus	Transformation of Tob55KO-3 with specific *tob55* plasmid (see Table 2)
T55His6-3	his-3 FPA^R hyg^R bleo^R with an ectopic copy of *tob55* with 6 histidine residues added to the N-terminus	Transformation of Tob55KO-3 with specific *tob55* plasmid (see Table 2)
T55HI-2	his-3 FPA^R hyg^R bleo^R with an ectopic copy of *tob55* with the HI affinity tag added to the N-terminus	Transformation of Tob55KO-3 with specific *tob55* plasmid (see Table 2)

Table 2
Oligonucleotides used in this study.

tim8

PRIMER	SEQUENCE (5'-3')	COMMENTS
FNA 272	pCAAGGAAGCTTTCTCCCAAGAA GCCCACCAAGCAGGACC	*tim8* gene; top strand; HindIII site
FNA 273	pGGAACAAGCTTCAATCGCAACA CATAACCCTGCCCAATAC	*tim8* gene; bottom strand; HindIII site
FNA 282	GTTTTTCGGTTGGCTGGTC	*tim8* primer; extension 5' of coding sequence
FNA 283	GTTTTTCGGTTGGCTGGTC	*tim8* primer; extension 3' of coding sequence
FNA 284	TGGACCTTTCCAAGCTTTTGGGC	*tim8* primer; extension 3' of coding sequence
FNA 285	TAGGGAACCTTTGTTGCATCCC	*tim8*primer; extension 5' of coding sequence
SLA 2	TTCATTTCCAACGAGACGCAGC	*tim8* primer; extension 5' of coding sequence
SLA 4	AACCTCAACGATGTTTCCTTCC	*tim8* primer; extension 5' of coding sequence
SLA 5	ATTGCTTGGCAGCCCTTTCCC	*tim8* primer; extension 5' of coding sequence
SLA 6	TCATTTCCATGCCATGGACC	*tim8* primer; extension 3' of coding sequence
Gibco Tim8	TCAAAGGTAGAACTGGAAGGG	*tim8* primer; extension 3' of coding sequence
FNA 286	GTCACTGTGTATTGTTCGATCC	*tim8* sequencing

PRIMER	SEQUENCE (5'-3')	COMMENTS
FNA 287	pGACTGGATTGCGGCCGCGTATACAGGGAAAGGGCTGCCAAGC	*tim8* RIP substrate primer; top strand; *Not*I site
FNA 288	pGTGTCCTTAGCGGCCGCTGTCGCATTGTTATCTGCACTTC	*tim8* RIP substrate primer; bottom strand; *Not*I site
FNA 289	pGTTGACTGCAGCGGCCGCATACCCCTTTGGCGTTTGGTCC	*tim8* RIP substrate primer; bottom strand; *Not*I site
SLA 10	CAAGGAAGCTTGAGACCTACTTGCTGCCACCCCTGG	Tim8 antibody fusion protein cloning primer; top strand; *Hind*III site
SLA 11	GGACAGATGTACCCACGCCCTTACCGATTCCTGCT	Tim8 antibody fusion protein cloning primer; bottom strand; *Bgl*II site

tim13

PRIMER	SEQUENCE (5'-3')	COMMENTS
SLA 28	AGCTAGCGGCCGCAACAAGAGAAGGCTCGACAGG	*tim13* RIP substrate cloning primer; top strand; *Not*I site
SLA 29	AGCTAGGCGGCCGCGATAAGCAAGAAGTTGAGG	*tim13* RIP substrate cloning primer; bottom strand; *Not*I site
SLA 16	TGATCAGATCTAAAATCGGCGAAAACTGCTTCACC	Tim13 antibody fusion protein cloning primer; top strand; *Bgl*II site

PRIMER	SEQUENCE (5'-3')	COMMENTS
SLA 17	TCCATTTCGAATCCTCCCTCTCTACTGGTTGCC	Tim13 antibody fusion protein cloning primer; bottom strand; HindIII site
13 seq down	ACACACGTACACATATGG	*tim13* sequencing primer
13 seq up	TTAAGCGTGATCTTAGCC	*tim13* sequencing primer

tim23

PRIMER	SEQUENCE (5'-3')	COMMENTS
SLA 14	ATACTCGAGGAACAATGTGCGTACGG	*tim23* sequencing primer; bottom strand
SLA 15	TCGCCATGTGCTACAACCTAATCAA	*tim23* sequencing primer; top strand
SLA 30	CCCCTCCACTTCAGTCACAATGAACAAGAAGCAGCAAGAGCA	*tim23* mutagenic primer to remove amino acids 1-10; top strand
SLA 31	TGCTCTTGCTGCTTCTTGTTCATTGTGACTGAAGTGGAGGGG	*tim23* mutagenic primer to remove amino acids 1-10; bottom strand
SLA 34	TCGAAAAGCTTGTGTCAATGGTGCTGC	*tim23* genomic upstream cloning primer; top strand; *Hind*III site
SLA 40	TCAGCTTAGGCGGCCGCGCATTGTGACTGAAGTGG	*tim23* genomic upstream cloning primer; bottom strand; *Not*I site
SLA 41	TGCAATCCAGCGGCCGCGGGGCTGGCTAGCATCGAAGG	*tim23* cloning primer from aa 51; top strand; *Not*I site

PRIMER	SEQUENCE (5'-3')	COMMENTS
SLA 37	TTGCAGAGCTCAGACTAACCCCTTGCGCTATGC	*tim23* genomic downstream cloning primer; bottom strand; *Sst*I site
SLA 42	TGCTTAACGATCCGATAACCC	*tim23* sequencing primer; reads through ATG; top strand
SLA 43	GTCAGAATTCTGCTGGACTTGGGTTGACTCC	*tim23* upstream cloning primer; top strand; *EcoR*I site
SLA 44	GTCAGAATTCTTGCGCTATGCACCACTATGC	*tim23* downstream cloning primer; bottom strand; *EcoR*I site
SLA 49	TCAAGTGGATCCATGGTTCGACCATTGAACTCG	DHFR cloning primer; top strand; *BamH*I site
SLA 50	TACCATAAGCTTCTATTTCTTCTCGTAGACTTCAAAC	DHFR cloning primer; bottom strand; *Hind*III site
SLA 53	TCAGTTGGATCCTCCGGCCTTTGGAACACCC	*tim23* upstream cloning primer; top strand; *BamH*I site
SLA 54	TCAGTTAAGCTTCTATTGTGTGGGGTCGGCGAAGG	Tim23(1-68) cloning primer; bottom strand; *Hind*III site
SLA 59	TCAGTTGGATCCTTCGTCCCCACTTCAGTCAACC	*tim23* cDNA cloning primer; top strand; *Bam*HI site
SLA 60	TCAGTTGGATCCTGAAGGGAACAGAAGATGAC	*tim23* cDNA cloning primer; bottom strand; *Bam*HI site

PRIMER	SEQUENCE (5'-3')	COMMENTS
SLA 68	TCAGTTGGATCCCGAGATGTATTCTAGTGTTTCC	Tim23(1-83) cloning primer; bottom strand; *Bam*HI site
SLA 70	CCTAAGAATCCTCACAGCCACCATGGGACCGTCAGTCTTCCTCTTCCC	CH2CH3 domain cloning primer; top strand; *Eco*RI site; *N. crassa* consensus sequence
SLA 71	TACCATGGATCCCCGGGTACCGCACTCATTTACCC	CH2CH3 domain cloning primer; bottom strand; *Bam*HI site
23C108A	ATACCGGTTCCGTAGGCGAGGTCGTCAGTGAAGCC	*tim23* mutagenic primer; changes amino acid C108 to A108; top strand
23C167A	TTGATTAGGTTGTAGGCGATGGCGACAACACCAGC	*tim23* mutagenic primer; changes amino acid C167 to A167; top strand
T23W5C	TTGTTGCCTCCGGTGAGGGTGTTACAAAGGCCGGACATTGTGACTGAAG	*tim23* mutagenic primer; changes amino acid W5 to C5; top strand
T9C	CTTCTTGTTGCCTCCGCAGAGGGTGTTCCAAAGG	*tim23* mutagenic primer; changes amino acid T9 to C9; top strand
K13C	GCTCTTGCTGCTTGCAGTTGCCTCCGGTG	*tim23* mutagenic primer; changes amino acid K13 to C13; top strand

PRIMER	SEQUENCE (5'-3')	COMMENTS
E17C	CGGGCTCTTGCTGGCATTGCTGCTTCTTGTTGCC	*tim23* mutagenic primer; changes amino acid E17 to C17; top strand
P21C	GGCGGGTGCGGCGCACTCTTGCTGCTC	*tim23* mutagenic primer; changes amino acid P21 to C21; top strand
A23C	GTCTGAGGTGCACAGGGGGCGGGTG	*tim23* mutagenic primer; changes amino acid A23 to C23; top strand
S27C	TGGGGGCGGGACAGGCGGGCTC	*tim23* mutagenic primer; changes amino acid S27 to C27; top strand
P29C	GGTGGTTGTCTGACATGCGCTGGGGGC	*tim23* mutagenic primer; changes amino acid P29 to C29; top strand
T34C	GGAGGTGGTGGTGCAGGTTGTCTGAGG	*tim23* mutagenic primer; changes amino acid T34 to C34; top strand
S38C	ATATGAAGGAGCGCAGGTGGTGGTGGTGG	*tim23* mutagenic primer; changes amino acid S38 to C38; top strand
Y42C	AAGGGCGAGGGACATGAAGGAGCGGAGG	*tim23* mutagenic primer; changes amino acid Y42 to C42; top strand
F46C	GCTGGCTAGCATCGCAGGGCGAGGGATATG	*tim23* mutagenic primer; changes amino acid F46 to C46; top strand

PRIMER	SEQUENCE (5'-3')	COMMENTS
Q50C	GACACCTTGGGGGCAGCTAGCATCGAAGG	*tim23* mutagenic primer; changes amino acid Q50 to C50; top strand
V54C	CGAGAAAGGCCTCGCAACCTTGGGGCTGGC	*tim23* mutagenic primer; changes amino acid V54 to C54; top strand
L58C	AAGGAAGAGCTACCGCAAAAGGCCTCGACACC	*tim23* mutagenic primer; changes amino acid L58 to C58; top strand
S62C	TGGGGTCGGCGAAGCAAGAGCTACCGAGAAAGGC	*tim23* mutagenic primer; changes amino acid S62 to C62; top strand

tob55

PRIMER	SEQUENCE (5'-3')	COMMENTS
N55TOP	CTAGAGCGGCCGCGGTCTGTTCAGTTCTACCTCTAGGATG	*tob55* RIP substrate cloning primer; top strand; *Not*I site
N55BOTT	ATGAAGCGGCCGCGGAGAGGATCAAGCACAAGAAGTAG	*tob55* RIP substrate cloning primer; top strand; *Not*I site
NC55-CDNA-R	GTACCATGGAATTCCACATGCATCGAAACCTTTTACAAG	*tob55* cDNA cloning primer; bottom strand; *Eco*RI site
OM55Asc	AGGCGAGAAGCTGCAATGGGCGCGCCTGCCTCCTCTCCAAGTGC	*tob55* mutagenic primer; insertion of AscI site after ATG; top strand

PRIMER	SEQUENCE (5'-3')	COMMENTS
OM55NH6	AGGCGAGAAGCTGCAATGCATCACCATCACCATCACGCCTCCTCTCCAAGTGC	*tob55* mutagenic primer; insertion of 6 histidine residues after ATG; top strand
55-5F (U-top)	GTAACGCCAGGGTTTTCCCAGTCACGACGATATCAAGAAGGCTCAAGCG	*tob55* knockout construct primer; *tob55* upstream; top strand
55-5R (U-bottom)	ACCGGGATCCACTTAACGTTACTGAAATCTTCCCAATCACAGGTTGGCG	*tob55* knockout construct primer; *tob55* upstream; bottom strand
55-3F (D-top)	CGTTCTATAGTGTCACCTAAATCGTATGTTGCATGTGTAGGAAGTAAAGG	*tob55* knockout construct primer; Tob55 downstream; top strand
55-3R (D-bottom)	GCGGATAACAATTTCACACAGGAAACAGCTCACCAAAAGTGATCGAAGG	*tob55* knockout construct primer; *tob55* downstream; bottom strand
hphF	ACATACGATTTAGGTGACACTATAGAACGCCCGTCGACAGAAGATGATATTGAAGGAGC	hygromycin resistance cassette primer; top strand
hphR	AGCTGACATCGACACCAACG	hygromycin resistance cassette primer; bottom strand
hSM-f	AAAAAGCCTGAACTCACCGCGACG	split marker primer in hygromycin cassette; bottom strand
hSM-r	TCGCCTCGCTCCAGTCAATGACC	split marker primer in hygromycin cassette; top strand

Table 3
Plasmids used in this study.

Plasmid	Source	Description
pT8HL	This Study	Genomic copy of *tim8* with 670 bp upstream and 730 bp downstream cloned into pCSN44
pCST13	This Study	Genomic copy of *tim13* with 594 bp upstream and 1085 bp downstream cloned into pCSN44
pQET8	This Study	Region of *tim8* gene coding for amino acids 35-92 cloned into pQE40
pQET13	This Study	Region of *tim8* gene coding for amino acids 31-86 cloned into pQE40
pTIM23	H. Prokish	Genomic copy of *tim23* with an N-terminal octa-histidine tag cloned into pCB1179
pBRT23	This Study	Genomic copy of *tim23* with 1041 bp upstream and 386 bp downstream, cloned into pBS520
pBRT23Δ10	This Study	As for pBRT23 with nucleotides encoding amino acids 2-10 removed
pBRT23Δ50	This Study	As for pBRT23 with nucleotides encoding amino acids 2-50 removed
pGNcT23N	This Study	Region of *tim23* coding for amino acids 1-67 and mouse DHFR cloned into pGEM4
pGNcT23IgG	This Study	Region of *tim23* coding for amino acids 1-83 and CH2CH3 domain of human IgG cloned into pGEM4
pGDHFR	This Study	Mouse DHFR cloned into pGEM4
pBRT23-cys	This Study	As for pBRT23 with residues encoding C108 changed to A108 and residues encodingC167 changed to A167
pBRT23W5	This Study	As for pBRT23-cys with residues encoding amino acid W5 changed to C5
pBRT23K13	This Study	As for pBRT23-cys with residues encoding amino acid K13 changed to C13
pBRT23E17	This Study	As for pBRT23-cys with residues encoding amino acid E17 changed to C17
pBRT23P21	This Study	As for pBRT23-cys with residues encoding amino acid P21 changed to C21
pBRT23A23	This Study	As for pBRT23-cys with residues encoding amino acid A23 changed to C23
pBRT23S27	This Study	As for pBRT23-cys with residues encoding amino acid S27 changed to C27

Plasmid	Source	Description
pBRT23P29	This Study	As for pBRT23-cys with residues encoding amino acid P29 changed to C29
pBRT23T33	This Study	As for pBRT23-cys with residues encoding amino acid T33 changed to C33
pBRT23S37	This Study	As for pBRT23-cys with residues encoding amino acid S37 changed to C37
pBRT23Y41	This Study	As for pBRT23-cys with residues encoding amino acid Y41 changed to C41
pBRT23F45	This Study	As for pBRT23-cys with residues encoding amino acid F45 changed to C45
pBRT23Q49	This Study	As for pBRT23-cys with residues encoding amino acid Q49 changed to Q49
pBRT23V54	This Study	As for pBRT23-cys with residues encoding amino acid V54 changed to C54
pBRT23L57	This Study	As for pBRT23-cys with residues encoding amino acid L57 changed to C57
pBRT23S61	This Study	As for pBRT23-cys with residues encoding amino acid S61 changed to C61
pRST55KO	This Study	*tob55* knockout plasmid
pBRX22E	This Study	Genomic copy of *tob55* -containing *EcoR* I 4.3 kbp fragment cloned from the cosmid X22D7 into pBS520
pBRXEhis6	This Study	As for pBRX22E with six histidine residues added to the N-terminus
pBRXEhi	This Study	As for pBRX22E with the HI tag added to the N-terminus

3 RESULTS

3.1 *Investigation of the Function of the N. crassa Tim8-13 complex*

At the time this work was begun, most of the characterization of Tim8-13 function had been done in the yeast, *S. cerevisiae*. Two major questions arose out of the yeast work. First, the absence of a clear growth phenotype in yeast cells lacking Tim8 or Tim13 was seemingly at odds with the observation that humans lacking the Tim8 protein suffer from MTS (Tranebjaerg *et al.*, 1995; Koehler *et al.*, 1999). Second, there were conflicting observations from different groups on the role of Tim8-13 in the import of Tim23 (Leuenberger *et al.*, 1999; Davis *et al.*, 2000; Paschen *et al.*, 2000). I decided to create mutants of these genes in *N. crassa* since this organism is an obligate aerobe. It was conceivable that the organism would represent a more reasonable model for the human situation than yeast and that an obvious phenotype might be seen in the mutants. In addition, it was thought that investigation of the import of Tim23 in these mutants might help resolve the debate between groups studying yeast. A final reason for examining Tim8-13 mutants was the observation in our lab that certain mutant strains of *N. crassa*, which are sensitive to damage of the outer mitochondrial membranes during standard isolation procedures, have a decreased ability to import and assemble β-barrel proteins of the MOM. We hypothesized that this could be the result of loss of a soluble intermembrane space component such as the Tim8-13 complex.

3.1.1 *Identification and Cloning of the Genes*

As a summer student in the lab, I was involved in identification of the *tim8* gene in *N. crassa*. An expressed sequenced tag for *tim8* was identified from a database using the *S. cerevisiae* protein sequence as a query and this sequence was used to generate primers to amplify the gene. A technician in the lab, Bryan McHale, identified a cosmid containing *tim8* by probing a *N. crassa* cosmid library. I used this cosmid to sequence the genomic regions both upstream and downstream of the gene to enable development of primers that could be used to clone the gene plus about 1 kbp of surrounding DNA. The gene encodes a 92 amino acid protein containing the twin CX_3C motif characteristic of the tiny Tim proteins (Figure 5).

The identification of *tim13* was done after release 3 of the *N. crassa* genome sequencing project was available. The gene was identified by searching the *N. crassa* genome with the yeast protein sequence and primers were designed from this sequence to clone *tim13* and some surrounding genomic DNA. The *tim13* gene encodes an 86 amino acid protein also with the twin CX_3C motif (Figure 5).

3.1.2 *Characterization of Tim8 and Tim13 in N. crassa*

The native state of Tim8 and Tim13 in mitochondria was examined. Mitochondria solubilized in DDM were analyzed by BNGE and western blotting with Tim8 and Tim13 specific antibodies. Both antibodies detect a complex that is estimated to be 80 kDa in size (Figure 6A). In addition, mitochondrial protein solubilized with DDM were separated by gel filtration on a Sephacryl S200 column with the assistance of Troy Locke. Analysis of the fractions with Tim8 and Tim13 antibodies revealed that both proteins elute in the same fraction that corresponds to 80 kDa (Figure 6B) (see section 2.18).

To further demonstrate a direct interaction between Tim8 and Tim13 *in vivo*, I performed immunoprecipitations from mitochondria solubilized with buffer containing 1% Triton-X-100 with each antibody. The Tim13 antibody precipitates the majority of the Tim13 and Tim8 proteins, as shown by western analysis (Figure 7). The Tim8 antibody immunoprecipitates most of the Tim8 protein, but no detectable amount of the Tim13. Structural analysis in yeast suggests that Tim8 is buried in the complex, making it more protease resistant than Tim13 (Curran *et al.*, 2002). I suggest that the Tim8 antibody does not co-immunoprecipitate Tim13 because binding of the antibody disrupts the stability of the complex. Neither antibody indicates an association of Tim8 or Tim13 with either Tim9 or Tim10 (Figure 7).

To determine the location of the complex, mitochondria were subjected to alkaline extraction and osmotic swelling and the resulting fractions were analyzed by western blotting and immunodecoration. Alkaline extraction results in removal of peripheral membrane proteins from membranes resulting in their localization to the soluble fraction. Integral membrane proteins are found in the pelleted fraction with membranes. Both Tim8 and Tim13 were found with other soluble markers such as mtHsp70 (Figure 8A). No detectable amounts were found with membrane markers such as Tom40 (Figure 8A). When mitochondria are converted to mitoplasts the MOM is broken as the MIM expands due to matrix swelling and the contents of the IMS are released. Following pelleting of mitoplasts, Tim8 and Tim13 were enriched in the supernatant fraction with the IMS marker cytochrome *c* while the matrix marker Hsp60 was enriched in the pellet fraction with membrane proteins Tom40 and AAC (Figure 8B). Thus, Tim8 and Tim13 are soluble proteins localized to the IMS.

3.1.3 *Creation of RIP (repeat induced point mutation) Mutant Strains*

Both the *tim8* and *tim13* genes were inactivated using the process of RIP. This process very effectively detects duplications in the *N. crassa* genome that are larger than 2000 bp and generates mutations throughout both copies of the duplicated sequence. RIP is a phenomenon that may have evolved in *N. crassa* to inactivate transposable elements (Selker, 1990; Galagan and Selker, 2004). The mutations generated are G to A and C to T transition mutations. There is a bias towards mutating CpA dinucleotides, changing the C to a T, thus increasing the likelihood of generating stop codons from CAA and CAG codons. DNA methylation is also associated with RIPed sequences (Irelan and Selker, 1997) which typically results in epigenetic silencing of the gene (Singer *et al.*, 1995). RIP only occurs during the sexual phase of the *N. crassa* life cycle. RIP can be harnessed to specifically inactivate genes of interest resulting in a strain with essentially null alleles of the target gene.

The RIP procedure requires a strain with two copies of the target gene. For *tim8*, I created the duplication containing strain during my Biology 499 Honors project. The lab wild type strain 76-26 was transformed with the cloned *tim8* gene and a hygromycin resistance marker. Hygromycin resistant isolates were chosen to screen for complete integration of *tim8*. Southern analysis confirmed the presence of both the endogenous gene and an exogenous copy of *tim8* in strain T8HL7 (Figure 9). This strain was then crossed with the wild type strain NCN 251. At least some of the progeny from this cross should contain RIP inactivated *tim8* genes. Mitochondria isolated from the progeny were screened by Western analysis using a *N. crassa* Tim8-specific antibody generously provided by W. Neupert (University of Munich) before our own was made. The strain

T8HL7-7 was chosen for further analysis as there was no Tim8 protein detected (Figure 10). The *tim8* gene in T8HL7-7 was amplified by PCR and the product was sequenced directly. RIP mutations were found throughout the gene including three nonsense mutations at amino acids 28, 30 and 33 (Figure 11). The same procedure was used to generate a RIP strain of Tim13. Southern analysis of transformants showed a complete integration event in isolate T13-16 (Figure 12). The progeny from the RIP cross were screened for absence of the Tim13 protein and T13R16-45 was chosen for further analysis based on absence of Tim13 (Figure 10).

3.1.4 *Characterization of the Mutant Strains*

3.1.4.1 *Growth Phenotypes*

Growth rates were tested most thoroughly with the $tim8^{RIP}$ strain as it was obtained first. The growth rate of *N. crassa* can be assessed by growth in race tubes (see section 2.1). There was no significant difference observed between the growth of the $tim8^{RIP}$ strain and wild type controls at 15°C, 22°C or 37°C with either glucose or glycerol as carbon sources (not shown).

3.1.4.2 *Mitochondrial Protein Levels*

The levels of various mitochondrial proteins were examined in both RIP strains (Figure 10). In the $tim8^{RIP}$ strain, there was no detectable Tim8 protein and the level of Tim13 was severely reduced. There was no detectable Tim13 in the $tim13^{RIP}$ strain and Tim8 was only detectable if the blot was overexposed to film. This suggests that neither protein is stable in the cell if it is not a component of the Tim8-13 complex. The levels of all other mitochondrial proteins examined were unchanged in the mutant strains compared to the control samples.

3.1.4.3 *Mitochondrial Protein Import*

The effect that loss of the Tim8-13 complex had on import of Tim23 was tested under two different conditions: first, when the membrane potential was high and second when it was lowered by treatment with antimycinA and oligomycin (AAO). These compounds inhibit the function of complex III and IV respectively, resulting in the loss of movement of hydrogen ions across the inner membrane. The *tim13*^{RIP} strain was chosen over the *tim8*^{RIP} strain for this analysis as it has the lowest levels of both proteins (Figure 10). Loss of the Tim8-13 complex had no effect on the efficiency of import of Tim23 when the membrane potential was high (Figure 13A) but was decreased when the membrane potential was lowered (Figure 13B). To ensure that reduction of membrane potential was effective, the import efficiency of $F_1\beta$ under both conditions was tested. Import of proteins to the mitochondrial matrix is strictly dependent on high membrane potential. Import of $F_1\beta$ is undetectable when mitochondria are treated with AAO, showing that membrane potential is reduced by this treatment (Figure 13C).

To test the hypothesis that the Tim8-13 complex might be involved in the import of porin, I performed *in vitro* import experiments with mitochondria isolated from the *tim13*^{RIP} strain. Import of porin was reduced significantly in mitochondria isolated from the *tim13*^{RIP} strain (Figure 14A). Porin is a β-barrel protein that forms a pore in the MOM through which small molecules can pass. Tom40, the pore forming component of the TOM complex, is also a β-barrel protein. To investigate the possibility that Tim8-13 was involved in import of another outer membrane, β-barrel protein, the import efficiency of Tom40 precursor was investigated in mitochondria isolated from the *tim13*^{RIP} strain. Import of Tom40 was also impaired in the absence of Tim8-13 (Figure 14B). The treatment of mitochondria with proteinase K (PK) following import of Tom40 results in the generation of fragments characteristic of the assembled protein with apparent molecular weights of 26 and 12 kDa (Figure 14B). Since it has been previously reported that import of porin is decreased in mitochondria with damaged MOM (Krimmer *et al.*, 2001), it was necessary to show that the observed import defect was not due to a damaged MOM. Thus, the level of CCHL in whole mitochondria treated with PK was assayed by western analysis. CCHL is a soluble protein localized to the IMS. If the outer membrane was broken, the PK treatment would result in degradation of CCHL. The levels of CCHL were not altered in the mitochondria lacking the Tim8-13 complex (Figure 14C). The same samples were also immunoblotted for Tom22 with an antibody to the C-terminus of the protein which is exposed on the surface of the MOM. Loss of all Tom22 signal indicates that the PK treatment was complete (Figure 14C). This demonstrates that mitochondria lacking the Tim8-13 complex are not sensitive to damage of the MOM. To determine if *N. crassa* mitochondria lacking the Tim8-13 complex had more general import defects, import of other mitochondrial precursors representing different classes of proteins was performed. Import of $F_1\beta$ to the matrix, AAC to the inner membrane, CCHL to the intermembrane space and Tom22 to the outer membrane was unaffected by the absence of Tim8-13 (Figure 15). Thus, only the import of the β-barrel proteins and Tim23 appear to be affected by the loss of the Tim8-13 complex.

3.1.4.4 *Assembly of Tom40 and Porin*

The assembly of Tom40 and porin through discrete intermediates and into their functional complexes can be observed by BNGE. In yeast, porin assembles into three complexes with sizes of 440, 400 and 200 kDa (Krimmer *et al.*, 2001). The 200 kDa complex is the only one of the three that is resistant to alkaline extraction and is therefore believed to be the core complex in yeast (Krimmer *et al.*, 2001). It is not known what the two larger complexes represent functionally. To gain further insight into the involvement of the Tim8-13 complex, assembly of porin was examined in *N. crassa* mitochondria lacking Tim8-13. The assembly of porin in *N. crassa* appears to differ from assembly in yeast. I observed assembly of the precursor into three distinct complexes with estimated sizes of 270, 115 and 66 kDa respectively. Loss of Tim8-13 reduced assembly of porin into all three of these complexes (Figure 16A).

More is known about the assembly pathway for the Tom40 precursor into the TOM complex (see section 1.6.3). Impaired assembly of Tom40 was observed in the absence of Tim8-13 when the import was done for either a short time or at a low temperature (Figure 16B). The amount of the first assembly intermediate of 250 kDa was two to three fold lower than controls under these conditions. When import was performed for a longer time at 25°C, there was no apparent difference in levels of the assembly intermediates at 250 kDa or 100 kDa or in the amount of precursor assembled into the 400 kDa complex.

3.1.4.5 *Crosslinking of Tim8-13 to Precursor Proteins*

To establish a direct interaction between Tim8-13 and the incoming Tom40 molecule, import experiments were performed followed by the addition of the crosslinking reagent DSG to the reaction (see section 2.13). The mitochondria in such reactions were then reisolated, lysed in buffer containing 1% Triton-X-100, and subjected to immunoprecipitation with either Tim8 or Tim13 specific antibodies. A crosslinking adduct between each component of the Tim8-13 complex and Tom40 was observed when import was done for 15 min at 0°C or 1 min at 25°C (Figure 17A). The crosslinking adduct was about 50 kDa in size, in agreement with the predicted combined sizes of either Tim8 or Tim13 and Tom40. These adducts were absent if the experiment was performed in mitochondria lacking the Tim8-13 complex, ruling out the possibility of observing an interaction with another small molecule and Tom40. Also, the adduct was not seen if immunoprecipitations were performed with pre-immune serum or unbound beads, suggesting that the immunoprecipitations are specific for Tim8 and Tim13 (Figure 17B). The adduct was also absent if immunoprecipitations were done in the absence of crosslinking reagent (Figure 17B). Interestingly, there was no crosslink between Tim8-13 and Tom40 if import was done for 15 min at 25°C (Figure 17C).

The loss of an interaction between the precursor and the complex when import is done for 15 min at 25°C suggests that the interaction occurs at an early stage in the assembly process. To test this hypothesis further, I made use of a Tom40 mutant precursor (Tom40ΔKLG). This precursor lacks residues 321-323 and accumulates at the 250 kDa assembly intermediate so that most of the precursor is in this form even after import at 25°C for 15 min (Taylor *et al.*, 2003). I reasoned that if Tim8-13 is in contact with the Tom40 precursor during the early stages of assembly, an interaction with the mutant precursor Tom40ΔKLG should be longer lived than with the wild type precursor. Crosslinked adducts were detected between Tim8-13 and Tom40ΔKLG even after import for 15 min at 25°C (Figure 18). Thus, the mutant precursor has a prolonged interaction with Tim8-13.

It has been shown previously that the Tom40 precursor in the first assembly intermediate of 250 kDa is resistant to treatment with externally added PK (Model *et al.*, 2001). To determine if the Tom40 precursor was interacting with Tim8-13 before or after reaching a PK resistant site, the sensitivity of the crosslinked adduct to PK was examined. Addition of PK did not degrade the crosslinked adduct suggesting that the adduct is in a location that is protected from external proteases (Figure 19).

If contact with the Tim8-13 complex was critical for efficient Tom40 import, it would not be unreasonable to expect a growth phenotype when the complex is absent. However, since this was not observed (section 3.1.4.1) it seemed reasonable to assume that the Tim9-10 complex might have a similar function which compensates for loss of the Tim8-13 complex. Therefore, I performed crosslinking and immunoprecipitations with a Tim9 specific antibody. Although the band representing the adduct is faint, there is a crosslinking product formed between the Tom40 precursor and Tim9. As with Tim8 and Tim13, the adduct is seen when import is performed for 1 min at 25°C but not after 15 min of import (Figure 20).

As the efficiency of Tim23 import was affected by loss of the Tim8-13 complex (section 3.1.4.3), I attempted to establish the existence of a physical interaction by crosslinking analysis. This analysis was performed when import was done after mitochondria were treated with AAO, a condition that lowers the membrane potential, causing the Tim23 precursor protein to be imported more slowly. This analysis revealed an interaction between the Tim8-13 complex and the Tim23 precursor protein (Figure 21). To determine if there was also contact with the Tim9-10 complex, as had been reported by some groups in yeast (Leuenberger *et al.*, 1999; Davis *et al.*, 2000), the equivalent experiment was performed in *N. crassa*. There is also a crosslinking adduct formed between Tim23 and Tim9 when membrane potential is reduced (Figure 21). Thus, *N. crassa* Tim23 precursor appears to interact with both Tim8-13 and Tim9-10 during its import to the inner membrane.

3.2 *Investigation of the Structure and Function of Tim23 in N. crassa*

Tim23 is a major component of the TIM23 complex (see section 1.9.1) and forms a pore in the inner membrane of mitochondria. The protein is predicted to have four membrane spanning domains and both its C-terminus and the N-terminus are predicted to extend into the IMS. The N-terminus has been shown to mediate dimerization of the protein (Bauer *et al.*, 1996). In yeast, Tim23 has been shown to have a unique topology where a portion of the N-terminus spans the MOM and exposes the extreme N-terminus of the protein to the cytosol (Donzeau *et al.*, 2000).

My goal was to characterize the equivalent domain in *N. crassa* Tim23 and investigate the mechanism responsible for targeting and integration into the outer membrane. My work suggests that the *N. crassa* Tim23 N-terminus does not span the MOM. On the other hand, the first 50 amino acids at the N-terminus of the protein do contribute to its function.

3.2.1 *Identification of the Gene*

The *N. crassa tim23* gene was originally identified by PCR of *N. crassa* genomic DNA using degenerate primers by collaborators at the University of Munich. The same primers were used to probe a *N. crassa* cosmid library to identify cosmids containing the *tim23* gene. The gene was initially cloned by the same collaborators at the University of Munich with an N-terminal octa-histidine tag. The gene encodes a 238 amino acid protein with four predicted transmembrane domains (Figure 22).

3.2.2 *Construction of Fusion Proteins for in vitro Import*

If the N-terminal domain of *N. crassa* Tim23 is inserted into the MOM, targeting information should exist within the region to ensure that it acquires the correct topology. It was previously observed in yeast that the first 62 amino acids of Tim23 were sufficient to target a fusion protein to the MOM *in vivo* (Donzeau *et al.*, 2000). To study the properties of the extreme N-terminus in *N. crassa* Tim23, I created constructs containing a portion of the N-terminus of *N. crassa* Tim23 and tested for the ability of such proteins to target and insert into the MOM.

The N-terminus of Tim23 is not highly conserved outside of the dimerization domain and there is no predicted transmembrane domain in this region (Figure 22). However, it was reasonable to assume that a domain spanning the outer membrane would be found closer to the N-terminus than the dimerization domain. The high degree of similarity between *S. cerevisiae* and *N. crassa* in the predicted dimerization domain begins at residue 68 and extends to the C-terminus in *N. crassa*. For this reason, I generated fusion constructs containing the first 67 amino acids of Tim23 fused to the N-terminus of mouse DHFR to be used for *in vitro* import assays. Most proteins targeted to the MOM show receptor dependent import and this was also true for the Tim23 N-terminal fusion constructs tested in yeast (Donzeau *et al.*, 2000). However, the *N. crassa* T23(1-67)-DHFR construct associated with mitochondria with the same properties as DHFR alone showing no dependence on the presence of receptors (Figure 23A). Furthermore, following *in vitro* import into mitochondria, no portion of the protein was resistant to alkaline extraction (Figure 23A). These data suggested that this protein is not inserted into the outer membrane. Unlike the fusion construct, the bona fide MOM protein Tom40 is imported in a receptor dependent manner and is resistant to alkaline extraction (Figure 23B top panel). To ensure that the full length Tim23 preprotein has the characteristic *in vitro* import properties predicted, this precursor was also analyzed. Full length Tim23 shows receptor dependent import in this assay and is resistant to alkaline extraction, as predicted for this protein (Figure 23B bottom panel).

While the first 62 residues of yeast Tim23 was sufficient for targeting DHFR to the MOM *in vivo*, the construct used for *in vitro* targeting studies by this group included the first 73 amino acids with the CH2-CH3 domains of human IgG (Donzeau *et al.*, 2000). For this reason, I constructed another fusion protein containing the first 83 amino acids of the N-terminus of the *N. crassa* Tim23 fused to the CH2-CH3 domains of human IgG (T23(1-83)-IgG) and tested the properties of this protein. Association of this fusion protein with mitochondria did not increase in a receptor dependent fashion (Figure 24A). Although some protein appears to be resistant to alkaline extraction following import, the protein incubated in the absence of mitochondria shows a similar amount in the pellet fraction (Figure 24A and 24B). This could be due to some amount of the protein forming an aggregate which is removed from solution by centrifugation with the membrane fraction of alkaline extraction. Together, these data suggest that the amino terminal domain of Tim23 is not sufficient to direct the import of a protein to the mitochondrial outer membrane. These results are in contrast to those obtained with yeast Tim23 using similar approaches (Donzeau *et al.*, 2000).

3.2.3 *Generation of a Sheltered RIP Mutant Strain*

Since I was unable to demonstrate that the amino terminal region of *N. crassa* Tim23 was capable of insertion into the MOM, it was not obvious what the role of the Tim23 N-terminal region might be. To address this, the mitochondrial function of strains expressing shortened versions of Tim23 was assessed. Generation of a strain expressing only a mutant allele of *tim23* first required the creation of a strain containing a null allele of *tim23* so that the null strain could be rescued with a mutant version of the gene. At the time, Tim23 was known to be an essential component of the import machinery in yeast. To generate a RIP strain of an essential gene, the procedure of sheltered RIP was utilized. The procedure is described in detail in the Material and Methods (see section 2.4) and is shown diagrammatically in Figure 3. Sheltered RIP requires knowledge of the chromosome where the target gene resides. Before the appearance of the *N. crassa* genome sequence, I mapped the *tim23* gene to chromosome III by RFLP analysis (Metzenberg, 1984) with a *tim23* containing cosmid (not shown). To generate a strain with a second exogenous copy of the *tim23* gene, as is required for the process of RIP, the strain H III was transformed with a plasmid (pTIM23, see Table 3) containing the cloned gene with a octa-histidine tag at the N-terminus and a hygromycin resistance marker. Hygromycin resistant colonies were isolated and purified. The presence of a duplication of the *tim23* gene was detected by Southern analysis (Figure 25). The isolate TI23-4 was chosen to be the female in a sheltered RIP cross with the strain M III. Ascospore progeny were screened for slow growth compared to controls on medium containing acriflavin, tryptophan and inositol. These conditions force the predominance of the RIPed nucleus and if the target gene is essential, strains will grow slowly as a result. Slow growing isolates were chosen for sequence analysis of the *tim23* gene in the RIP nucleus. Analysis of the gene in the strain T23R4-12 revealed several mutations consistent with RIP, including one that created a stop codon at amino acid 126 (Figure 26). Southern analysis of this strain indicates that only the endogenous copy of the *tim23* gene is present in the strain (Figure 27). These data demonstrate that the endogenous *tim23* gene was inactivated by RIP in the H III parent nucleus in the strain T23R4-12.

3.2.3.1 *Nutritional Testing of T23R4-12*

To determine if Tim23 is essential in *N. crassa*, nutritional testing of individual conidial isolates from the sheltered RIP heterokaryon was performed. Conidiaspores are multinucleate, containing between one and five nuclei. Therefore, conidiaspores produced by the T23R4-12 heterokaryon could have one of three genotypes, depending on which of the two nuclei comprising the heterokaryon were present (Figure 28A). If Tim23 is essential for function, spores containing only the *tim23*^{RIP} nucleus would be inviable and therefore tryptophan auxotrophs would not be present in the population of conidiaspores produced from the heterokaryon. Conidia collected from T23R4-12 were spread for single colonies on medium containing tryptophan, adenine and inositol. This fulfills the auxotrophic requirements of each nucleus from the heterokaryon. Of 100 single colonies isolated from the strain T23R4-12, all were able to grow on minimal media, demonstrating that all were heterokaryons. This suggested that neither nucleus was viable as a homokaryon, probably because there is a random lethal mutation present in the sheltering nucleus. To generate a strain with a viable nucleus sheltering the *tim23*^{RIP} nucleus, the mate nucleus was swapped out of the *tim23*^{RIP} heterokaryon (see section 2.5). The new *tim23*^{RIP} sheltered heterokaryon was called Hel23R-1 (Figure 28B). Of 100 single colony isolates tested for this strain, 50 were heterokaryons as they grew on minimal media and 50 were histidine and pantothenate auxotrophs. The absence of tryptophan auxotrophs suggests that Tim23 is essential in *N. crassa*. However, to exclude the possibility that a random mutation in another essential gene in the *tim23*^{RIP} nucleus was rendering the nucleus inviable, it was necessary to demonstrate that a functional *tim23* allele could rescue the tryptophan auxotrophic nucleus. This was shown by D. Mokranjac (University of Munich) using a plasmid containing an octa-histidine tagged version of *tim23* (pTIM23).

3.2.4 *Creation of Strains Expressing N-terminal Deletions of Tim23*

In an attempt to define a region of the amino terminus of *N. crassa* Tim23 that is important for function *in vivo*, I chose to create two N-terminal deletions of the gene: the first lacking residues 1-10 and the second lacking residues 1-50. In yeast, it is predicted that 20 amino acids of Tim23 are exposed on the cytosolic surface of the MOM (Donzeau *et al.*, 2000). Therefore, if this domain is also present in a similar region in *N. crassa*, removal of 10 amino acids would not be predicted to affect function (Figure 29A). On the other hand, we would predict that removal of the first 50 amino acids would remove the MOM spanning domain based on analysis in yeast (Figure 29A). For both of these constructs, the organization of the gene was maintained with respect to the promotor and introns. The region encoding the first ten amino acids of Tim23 was removed by site directed mutagenesis. A version of *tim23* lacking the region encoding the first 50 amino acids was generated by ligation of two fragments generated by PCR. The first contained the promotor region including the ATG codon and 1041 bp of upstream sequence. The second contained the region from amino acid 50 to the stop codon plus an additional 386 bp of downstream sequence. To generate strains expressing these constructs, bleomycin resistant plasmids containing the altered versions of *tim23*, pBrT23Δ10 and pBrT23Δ50 (see Table 3), were transformed into the *tim23*^{RIP} sheltered heterokaryotic strain (T23R4-12) and transformants were plated on medium containing bleomycin, acriflavin, tryptophan and inositol to select for integration into the RIPed nucleus. If the shortened Tim23 proteins were functional, the constructs should have rescued the lethal RIP phenotype and given rise to tryptophan auxotrophs. Transformants were tested for nutritional requirements and those that were tryptophan auxotrophs were evaluated by western analysis for the presence of Tim23 protein (Figure 30). Strains T23Δ10-14 and T23Δ50-50 were chosen for further analysis.

3.2.5 *Characterization of Truncated Tim23 Strains*

3.2.5.1 *Growth Rates*

The growth rates of the truncated strains were compared to the growth of controls by race tube analysis (see section 2.1). There was no significant difference in the rate of growth of T23Δ10 and controls (Figure 29B). Growth of T23Δ50 was slower than that of control strains at suggesting that there are residues between amino acid 10 and amino acid 50 that are important for Tim23 function (Figure 29B).

3.2.5.2 *Mitochondrial Protein Import*

Tim23 is a component of the TIM23 translocase that imports precursors with N-terminal targeting signals to the mitochondrial matrix. To test the function of the shortened Tim23 proteins, I examined the import efficiency of matrix targeted precursor proteins into mitochondria containing the altered versions of Tim23. Under standard import conditions, there was no significant difference in the rate of import between mitochondria from strain T23Δ10-14 and wild type controls (Figure 31A). Very minor differences were observed with mitochondria from strain T23Δ50-50 and controls. It is difficult to reconcile the seemingly contradictory phenotypes of the T23Δ50-50 strain which displays a growth phenotype but very minor import deficiency. The *in vitro* import experiments used above contain only small radiolabeled amounts of precursor made during *in vitro* transcription and translation. The translocase complexes *in vivo* are required to process larger amounts of precursors than are present in this assay. To better reflect the *in vivo* situation, I purified chemical amounts of Su9-DHFR, a fusion protein containing the mitochondrial targeting signal from subunit 9 of the ATPase fused to mouse DHFR, and included 0.1μg of this precursor in import reactions. In this assay mitochondria isolated from strain T23Δ50-50 imported precursors targeted to the mitochondrial matrix less efficiently than wild type controls (Figure 32). The import of AAC under the same conditions was not altered in the T23Δ50 mitochondria, showing that the defect is specific for matrix targeted precursors that utilize the TIM23 translocase machinery (Figure 32). These data indicate that the first 50 amino acids of Tim23 are important for the function of the protein.

3.2.5.3 *Mitochondrial Morphology in T23Δ50 Mitochondria*

In filamentous fungi such as *N. crassa*, mitochondria are thread like organelles that are oriented along the hyphal length (Westermann and Prokisch, 2002). Aberrant mitochondrial morphology has been observed by electron microscopy of strains of *N. crassa* that were expressing decreased levels of Tom20, Tom22, Tom70 and Tom40 (Harkness *et al.*, 1994; Nargang *et al.*, 1995; Grad *et al.*, 1999; Taylor *et al.*, 2003). I examined the mitochondrial morphology in the strain expressing T23Δ50 and wild type controls to determine if removal of the first 50 amino acids of Tim23 affects morphology *in vivo*. Wild type cells contained several large mitochondria with many long cristae throughout the organelle (Figure 33, top panel). Mitochondria were plentiful in the mutant but had fewer cristae than controls, some lacking cristae all together, appearing as doughnut-shaped structures (Figure 33, bottom panel). Given that mitochondrial morphology defects coincide with import defects of other translocase mutants, this further confirms that the first 50 amino acids of Tim23 have a role in the function of the protein *in vivo*.

3.2.6 *Treatment of Mitochondria with Proteinase K*

The treatment of intact yeast mitochondria with PK results in the clipping of Tim23, reducing the mass of the protein by about 2 kDa (Donzeau *et al.*, 2000). Clipping of yeast Tim23 was observed when mitochondria were treated at 0°C with PK at a concentration of 50 μg/ml. To determine if the N-terminus of *N. crassa* Tim23 is accessible to externally added PK, freshly isolated mitochondria were treated with 300 μg/ml PK at either 0° or 25°C. Samples were subjected to SDS-PAGE and examined by western blot analysis using a Tim23 specific antibody. Antibodies directed against CCHL and mtHsp70 were also used as controls for the quality of the mitochondria isolated. CCHL is found in the IMS and acts as a control for intactness of the MOM. mtHsp70 a soluble protein in the matrix and acts as a control for the state of the inner mitochondrial membrane. Mitochondria isolated from the T23Δ10-14 and T23Δ50-50 strains are also included as a size reference of Tim23. A small amount of a proteolysis product with a size between the full length precursor and the Tim23(51-238) protein is produced in the presence of 300 μg/ml PK at 0°C (Figure 34). The amount of this product is increased when the treatment is performed at 25°C (Figure 34). However, under these conditions, CCHL is also degraded significantly suggesting that there is PK present in the IMS which would allow full access to the N-terminal domain of Tim23. The degradation observed at this concentration of PK is sensitive to 80 mM KCl, the concentration of salt typically used in an *in vitro* import experiment. This could explain why degradation of Tim23 is not observed in such experiments. These data suggest that Tim23 does not contain a protease sensitive domain exposed on the surface of mitochondria in *N. crassa*.

3.2.7 *Mapping the Topology of the Tim23 N-terminus*

While the *in vitro* import data suggested that the N-terminus of Tim23 does not function to tether Tim23 to the MOM, it is clear that these residues are important for the function of the protein. In an attempt to characterize the topology of the N-terminal region of Tim23 in *N. crassa*, I chose to map the location of the region using SCAM (substituted cysteine accessibility mapping). The basic principle of SCAM is that sulfhydryl labeling reagents such as biotin maleimide will bind covalently to cysteine residues that are in a hydrophilic environment but will not react with cysteine residues that are located in a hydrophobic environment, such as within a lipid bilayer. By changing single amino acids in the N-terminus of Tim23 to cysteine, this analysis can be used to determine the topology of the domain. Regions in the IMS will also be exposed to the compound as its size of 523.6 Da is small enough to cross through the MOM via porin and the TOM complex.

3.2.7.1 *Creation of Single Substituted Cysteine Tim23 Variants*

By analogy to the structure of yeast Tim23, I predicted that if there was a domain in the N-terminus of *N. crassa* Tim23 embedded in the outer membrane, it would be found N-terminal to the dimerization domain. I chose to change approximately every fourth amino acid from residue 5 to 62 to a cysteine as it seemed highly unlikely that a four residue domain could span the MOM (Figure 35). It is conceivable that the topology differs in *N. crassa* such that the N-terminal domain of Tim23 integrates into the inner leaflet of the outer membrane, rather than spanning it entirely. Even in this hypothetical situation, it is unlikely that a region of less than four amino acids could form this structure in a stable integration. Wild type *N. crassa* Tim23 contains two cysteine residues. I chose to remove them to ensure that detection of a label was due solely to the test residue in the N-terminus. To generate an allele of *tim23* with no endogenous cysteine residues, a plasmid containing a genomic copy of the *tim23* gene, complete with its upstream (1041 bp) and downstream (386 bp) regions, was used for site directed mutagenesis. The change of both endogenous cysteines to alanine residues was confirmed by sequence analysis. This cysteine-less *tim23* gene was then used to generate alleles that contained the target residues changed to cysteine by site directed mutagenesis. The resulting bleomycin resistant plasmids containing single-cysteine *tim23* genes were used to transform the *tim23*^{RIP} strain (section 2.9). This approach generated several strains, each expressing a different single cysteine allele of *tim23* (Table 1). The exogenous *tim23* genes in isolates that were auxotrophic for tryptophan were amplified by PCR and examined by sequence analysis for confirmation of the presence of the mutant version of Tim23.

3.2.7.2 *Substituted Cysteine Accessibility Mapping*

The procedure used for SCAM is outlined in detail in section 2.25. Briefly, mitochondria isolated from the single cysteine strains were subjected to treatment with biotin maleimide followed by lysis and immunoprecipitation with a Tim23 specific antibody. Immunoprecipitated proteins were subjected to SDS-PAGE, transferred to nitrocellulose and assayed for labeling of the cysteine residues in the N-terminus using streptavidin-conjugated HRP. Tim23 in mitochondria isolated from a strain expressing a version of Tim23 with the endogenous cysteine residues changed to alanine (T23-cys) does not label in the SCAM analysis (Figure 36). SCAM analysis of the first half of the targeted region (residues W5, T9, K13, E17, P21, A23, S27, P29) shows that all singly replaced residues tested are found in a hydrophilic environment as they are labeled with biotin maleimide (Figure 36). Confirmation that biotin maleimide does not label cysteine residues in a hydrophobic environment was obtained by inclusion of a wild type sample (H III). The two endogenous cysteine residues in wild type *N. crassa* Tim23 are both predicted to fall within membrane spanning domains. Absence of labeling in wild type mitochondria confirms that cysteines located within transmembrane domains were not accessible to labeling with biotin maleimide. This suggests that a domain that stably spans the MOM is not present in *N. crassa* Tim23 N-terminal to amino acid 29. Completion of the SCAM analysis of the second half of the targeted domain (residues T33, S37, Y41, F45, Q49, V53, L57, S61) will determine if such a domain exists at all within the N-terminus of *N. crassa* Tim23.

3.3 *Investigation of the Structure and Function of Tob55 in N. crassa*

Tob55/Sam50 was identified in yeast as an essential protein involved in the assembly of β-barrel proteins into the MOM (Figure 2)(Kozjak *et al.*, 2003; Paschen *et al.*, 2003; Gentle *et al.*, 2004). It is a component of a complex that includes three other proteins identified in yeast, Tob38, Sam37 and Mdm10p. It has been suggested that the pores of yeast Tob55 observed by electron microscopy could act as an Anfinsen-type cage for the assembly of β-barrel proteins, promoting folding by preventing aggregation (Paschen *et al.*, 2003). Purification of the TOB complex could provide further insight into the mechanism involved in folding and insertion of β-barrel proteins to the outer mitochondrial membrane. *N. crassa* is a good organism for purification of whole mitochondrial complexes because large quantities of mitochondria can be obtained cheaply and with relative ease. To study the TOB complex in *N. crassa*, I chose to generate strains expressing affinity tagged versions of the gene to aid purification. To ensure conservation of function, I have also analyzed the effects of reduced expression of Tob55 in *N. crassa*.

3.3.1 *Identification and Cloning of the Gene*

The *N. crassa* homologue of Tob55 was identified by searching the *N. crassa* genome with the yeast protein sequence. *N. crassa* Tob55 is 23% identical to its yeast counterpart and 29% identical to the human protein (Figure 37). The cosmid containing the gene was mapped to chromosome VI during assembly of the genome sequence. The protein is 438 amino acids in size with a predicted molecular weight of 53.8 kDa and is predicted to form a β-barrel structure.

3.3.2 *Creation of a Tob55 Knockout Strain*

A protocol recently developed by Colot *et al.* that depends on homologous recombination of a split marker to replace the endogenous gene with a resistance cassette was used to disrupt the *tob55* gene (Colot, in preparation). A complete description of the protocol is given in Materials and Methods (section 2.6) and is diagrammed in Figure 4. Briefly, a knockout plasmid construct containing a hygromycin resistance cassette flanked by the upstream and downstream genomic regions of the target gene, in this case *tob55,* is made by homologous recombination in yeast. Given that homologous recombination is a relatively rare event in *N. crassa*, the occurrence of transformants that are the result of ectopic insertion events is significantly decreased by splitting the hygromycin resistance cassette for transformation. Thus, hygromycin resistant colonies arise only if the two portions of the resistance marker have undergone homologous recombination to unite the two portions of the resistance cassette.

Since Tob55 is predicted to be an essential protein, the above procedure was carried out using the technique of sheltered disruption (Nargang *et al.*, 1995). The DNA was transformed into a heterokaryon so that when the disruption destroyed the *tob55* gene in one nucleus, the other nucleus would still supply Tob55 function (usually only one nucleus of a heterokaryon takes up DNA during transformation of *N. crassa* (Grotelueschen and Metzenberg, 1995)). The heterokaryotic strain HP1 was chosen for this strategy as the two nuclei each carry different resistance markers to facilitate manipulation of nuclear ratios in the final product (Figure 38). Transformants were screened by Southern analysis for the replacement event (Figure 39). The isolates Tob55KO-1 and Tob55KO-3 were chosen for further analysis.

3.3.3 *Characterization of Tob55KO-3*

3.3.3.1 *Growth Rate*

The growth rates of the *tob55* knockout strains were tested by spotting conidia on sorbose-containing plates containing the appropriate nutrients and inhibitors to determine which nucleus underwent the knockout event (Figure 40)(see section 2.1). Growth of the parental strain HP1 in the presence of histidine and fpa results in the predominance of nucleus 1 while growth in pantothenate and benomyl increases the proportion of nucleus 2 (Figure 38). It was predicted that reduction of an essential gene product resulting from growth in the inhibitor that favours the nucleus carrying the disruption would result in slow growth as has been observed with Tom22 and Tom40 in *N. crassa* (Nargang *et al.*, 1995; Taylor *et al.*, 2003). Growth of the isolates Tob55KO-1 and Tob55KO-3 was tested under these conditions and compared to HP1 (Figure 40A). The growth of all three strains was indistinguishable on minimal medium and on plates containing benomyl and pantothenate. However, the *tob55* knockout strains both grew significantly slower than the control on plates containing fpa and histidine. This indicates that the knockout event occurred in the nucleus bearing fpa resistance and the his-3 mutation (nucleus 1 in Figure 40B). The Tob55KO-3 strain was chosen for further work.

3.3.3.2 *Nutritional Testing*

To determine if *tob55* is an essential gene, conidia from the TOB55KO-3 heterokaryotic strain were plated onto medium containing all nutritional requirements of both nuclei and single colonies were picked. Nutritional testing of 200 isolates revealed that 125 were heterokaryons and 75 were pantothenate requiring auxotrophs. The lack of histidine auxotrophs indicates that loss of Tob55 is lethal. Later, it was shown that this nucleus could be rescued by expression of a his-tagged version of *tob55*, demonstrating that loss of Tob55 was responsible for the observed lethality (section 3.3.4).

3.3.3.3 *Mitochondrial Protein Levels*

The levels of various mitochondrial proteins were examined in the *tob55* knockout strain when grown under two conditions. Protein levels were assessed under conditions which did not change the nuclear ratios and then in the presence of fpa and histidine, which forces the knockout bearing nucleus to become numerically superior (see Figure 40B). Under normal growth conditions there was no detectable difference in the levels of any mitochondrial proteins tested between the parental control strain and the *tob55* knockout strain (Figure 41). However, when the strains were grown in the presence of histidine and fpa, Tob55 was virtually absent from the *tob55* knockout strain mitochondria. In addition, the steady state levels of the two outer membrane β-barrel proteins, Tom40 and porin, were also reduced in the mutant. Tom22 is a component of the core TOM complex and its levels are also reduced in the mutant, probably because there are not enough Tom40 molecules to provide a stable interaction. Similarly, Tom22 was reduced in a Tom40 mutant of *N. crassa* (Taylor *et al.*, 2003). The levels of other mitochondrial proteins examined were unchanged by the reduction in Tob55.

3.3.3.4 *Mitochondrial Protein Import*

To assess the function of Tob55 in the import of precursor proteins, mitochondria were isolated from the *tob55* knockout and HP1 strains grown in the presence of fpa and histidine. The concentration of fpa was reduced from the 400 μM used in Figure 41 to 250 μM since the lower concentration still resulted in significant reduction of Tob55 and gave higher quality mitochondria for performing import assays. Import of all β-barrel proteins (Tom40, porin and Tob55) tested was reduced in the knockout strain compared to the control (Figure 42 B, C & D). As mentioned in Section 3.1, a broken MOM results in decreased import of β-barrel proteins. To ensure that the observed reduction in import was not a reflection of broken outer membranes, the levels of CCHL were examined after

PK treatment by western analysis. There is no difference in the levels of CCHL between the controls or Tob55↓ mitochondria so the membrane can be considered intact (Figure 42E). It might be argued that the reduction in levels of Tom40 and Tom22 are the cause of the reduced import. However, import of proteins (CCHL, AAC and $F_1\beta$) to other mitochondrial compartments was not reduced in Tob55↓ mitochondria (Figure 43). Together, these data indicate that Tob55 is involved in import of outer membrane β-barrel proteins.

3.3.3.5 *Tob55 is Involved in Tom40 and Porin Assembly*

The assembly of Tom40 and porin in Tob55↓ mitochondria was also assessed using BNGE. As discussed in Section 3.1.4.4, porin assembles into three distinct complexes of 270, 115 and 66 kDa in *N. crassa*. The assembly of porin into each of these complexes was reduced in Tob55↓ mitochondria (Figure 44A). Analysis of Tom40 assembly by BNGE reveals two assembly intermediates of 250 kDa and 100 kDa (see Section 3.1.4.4). The level of these intermediates was reduced in Tob55↓ mitochondria (Figure 44B).

Supershift assays were used to obtain direct evidence that Tob55 is a component of an assembly intermediate of Tom40 and porin. Tob55 antibody was added to the import/assembly reactions of Tom40 and porin prior to BNGE. The antibody should bind Tob55, even when it is part of a complex, resulting in a significant change of the size of any Tob55-containing complex. For Tom40, this resulted in a supershift of the 250 kDa assembly intermediate (Figure 45A). This confirms that Tob55 is a component of the 250 kDa Tom40 assembly intermediate. For porin, addition of Tob55 antibody resulted in a shift in the 270 kDa complex (Figure 45B). This is the first evidence that this complex of the porin assembly pathway in *N. crassa* represents an assembly intermediate for porin containing Tob55.

3.3.4 *Creation of Strains Expressing Tagged Versions of Tob55*

To aid the purification of Tob55 from *N. crassa*, I generated alleles of *tob55* that encode affinity purification tags on the N-terminus of the protein. I chose to construct two different tags. An N-terminal tag of six histidine residues is a small tag that should not interfere with Tob55 function and allows the use of Ni-NTA chromatography for purification. A three part tag was also constructed (HI tag). The first component is six histidine residues at the amino terminus. This is followed by a portion of protein A and then a TEV protease cleavage site. This tag permits the use of two chromatography steps which could simplify purification. The tag could then be removed using the TEV protease.

Once constructed, the tagged genes were transformed into the *tob55* knockout heterokaryotic strain, Tob55KO-3, as shown in Figure 46A. Histidine auxotrophs were selected for further screening by western blot analysis for the presence of a tagged Tob55 protein with penta-his specific antibodies. For the histidine tagged protein, Tob55 was detected with both the penta-his and Tob55 antibodies indicating that these strains were expressing the tagged protein (Figure 46B, left panel). Isolates T55his6-1 and T55his6-3 were chosen for use in purification experiments. For the HI tag protein, the construct will be completed and the same procedure described for generation of the his tag strain will be utilized to gerate the HI tag strain.

Given the time constraints of my program, the tagged strains have been sent to our collaborator, Doron Rapaport, the University of Munich for purification.

Figure 5 Alignment of the Tim8 and Tim13 proteins. The Tim8 (A) and Tim13 (B) proteins of *Neurospora crassa* (N.c.), *Saccharomyces cerevisiae* (S.c.) and *Homo sapiens* (H.s.) are shown. While the *H. sapiens* genome contains two *tim8* genes designated DDP1 and DDP2, only DDP1, the gene associated with MTS, is shown. The number of residues is indicated at the right and black shading indicates amino acid identity between at least two species. Arrows indicate the location of introns in the *N. crassa* genes. The conserved CX_3C motif is highlighted by black bars above the sequence.

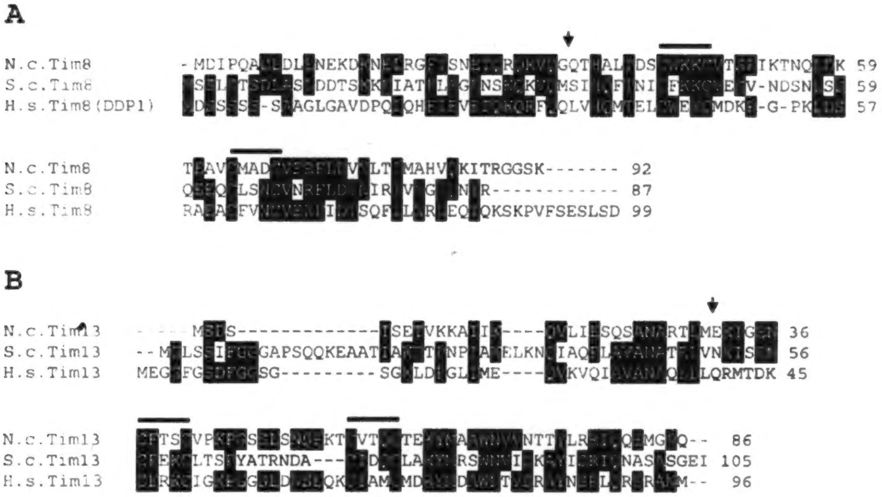
A
N.c.Tim8
S.c.Tim8
H.s.Tim8(DDP1)
59
59
57
N.c.Tim8
S.c.Tim8
H.s.Tim8
92
87
99
B
N.c.Tim13
S.c.Tim13
H.s.Tim13
36
56
45
N.c.Tim13
S.c.Tim13
H.s.Tim13
86
105
96

Figure 6 Determination of the size of the Tim8-13 complex in *N. crassa.* (A) BNGE analysis of the Tim8-Tim13 complex. Mitochondria isolated from a control strain (NCN 251), the strains containing the *tim8* and *tim13* duplications (*tim8* dupl and *tim13* dupl), and the *tim8*^{RIP} and *tim13*^{RIP} strains were solubilized in 1% DDM, loaded in two sets of lanes for immunodetection with either Tim8 or Tim13 antisera and separated by BNGE on the same gel. The proteins were transferred to nitrocellulose membrane (it was determined that the proteins do not bind to PVDF membrane) which was then cut in half for immunodecoration with the two antibodies. The Tim8-13 complex (indicated by an arrowhead) was detected in an identical position corresponding to an apparent molecular mass of 80 kDa with both antisera. The position of standards apoferritin (440 kDa), β-amylase (200 kDa), and bovine serum albumin (66 kDa) are indicated on the left. (B) Gel filtration analysis of *N. crassa* Tim8-Tim13. Mitochondria isolated from a wild type strain (NCN 251) were solubilized in 1% DDM and analysed on a Sephacryl S200 column. Fractions were analyzed by SDS-PAGE and western analysis with either the Tim8 or Tim13 antisera (shown in the inset). Tim8 and Tim13 co-elute in fractions corresponding to a molecular mass of 80 kDa.

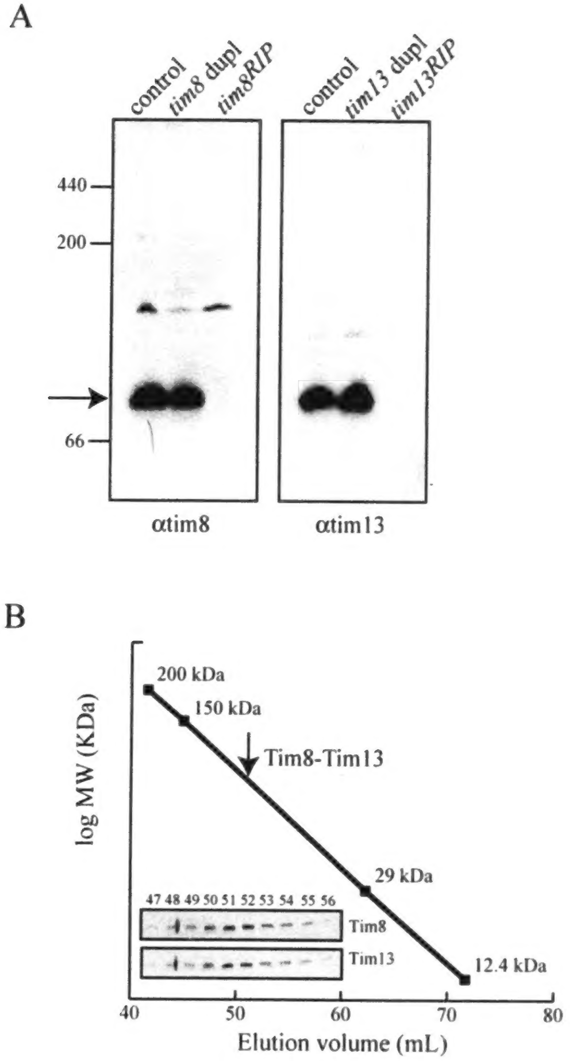
A
control
tim8 dupl
tim8RIP
control
tim13 dupl
tim13RIP
440
200
66
αtim8
αtim13
B
log MW (KDa)
200 kDa
150 kDa
Tim8-Tim13
29 kDa
12.4 kDa
47 48 49 50 51 52 53 54 55 56
Tim8
Tim13
40
50
60
70
80
Elution volume (mL)

Figure 7 Association of Tim8 and Tim13. Wild type mitochondria were solubilized with 1% Triton-X-100 and incubated with antibodies against Tim8 (αTim8) or Tim13 (αTim13) or preimmune serum (PIS) bound to protein A sepharose beads. The beads were collected by centrifugation, washed and bound proteins were eluted with Laemmli cracking buffer. Samples were subjected to SDS-PAGE, transferred to nitrocellulose and immunodecorated with the indicated antibodies. "Total" represents 100% of the material presents in the immunoprecipitation reactions.

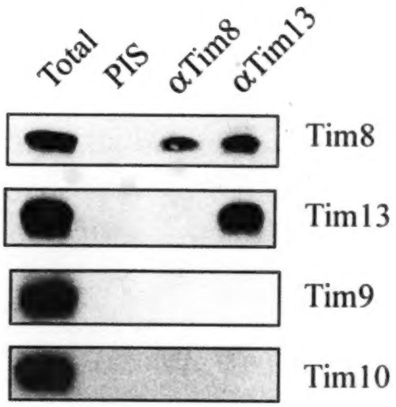
Total
PIS
αTim8
αTim13
Tim8
Tim13
Tim9
Tim10

Figure 8 Localization of Tim8-13 in mitochondria. (A) Alkaline extraction of *N. crassa* Tim8 and Tim13. Wild type mitochondria (NCN 251) were treated with 0.1 M sodium carbonate, pH 11.5 for 30 min on ice. The membrane fraction was collected by centrifugation and soluble proteins in the supernatant were precipitated with 11 % TCA. Samples were analyzed by SDS-PAGE, transferred to nitrocellulose and immunodecorated with the indicated antisera. (B) Submitochondrial localization of Tim8-13. Wild type mitochondria (NCN 251) were isolated and suspended in swelling buffer followed by incubation on ice for 1 hr. Mitoplasts were pelleted by centrifugation and the supernatant was collected as a fraction enriched for IMS proteins. Proteins from the intermembrane space fraction were precipitated with trichloroacetic acid. Samples (5 μg) were subjected to SDS-PAGE and immunodecoration with the indicated antigens.

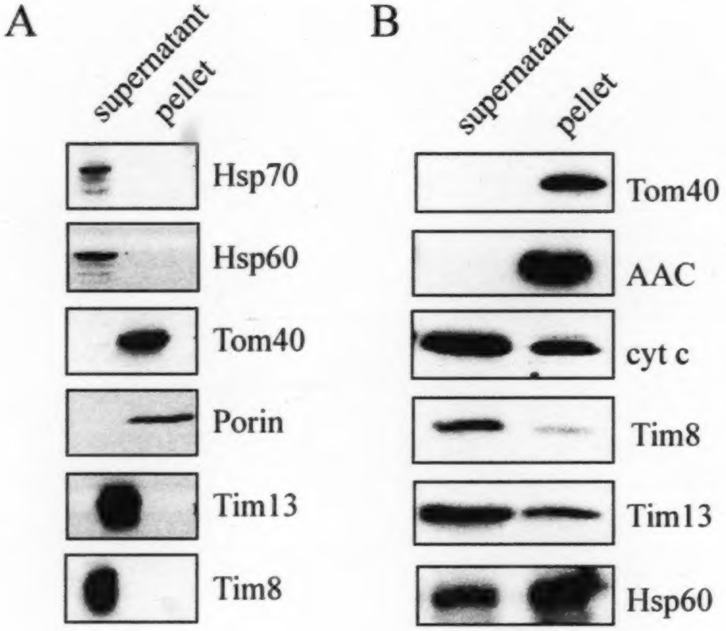
A
supernatant
pellet
Hsp70
Hsp60
Tom40
Porin
Tim13
Tim8
B
supernatant
pellet
Tom40
AAC
cyt c
Tim8
Tim13
Hsp60

Figure 9 Southern blots of candidate *tim8* duplication-containing isolates. Genomic DNA (15 µg) from the parental strain 76-26 (control) and three isolates (T8HL-5,6,7) from the transformation of 76-26 with the plasmid pT8HL7 were digested with *Sst*II. Following electrophoresis on a 0.7% agarose gel, DNA was blotted to a nylon membrane and probed with a ^{32}P-labeled *tim8* probe representing the 2 kbp *Not*I fragment from the plasmid pT8HL7. There is an *Sst*II cleavage site in the center of the *tim8* gene, so the probe should detect two bands per copy of the *tim8* gene. A schematic is shown below the blot with the 2 kbp region in the *N. crassa* genome present in plasmid pT8HL7 represented by a black box. The black line represents *N. crassa* genomic DNA. The double lines through the genomic DNA indicate that an unknown distance separates the *Sst*II site within the *tim8* gene and a *Sst*II site in the surrounding genomic DNA at both the endogenous *tim8* gene and the ectopic insertion site. The probe used is represented by a grey line. The position of the molecular weight markers and their sizes, in number of base pairs, is shown on the left. The bands corresponding to the endogenous copy of *tim8* are indicated with arrowheads on the right. The bands corresponding to the ectopic copy of *tim8* in T8HL-7 are indicated with double arrowheads on the right.

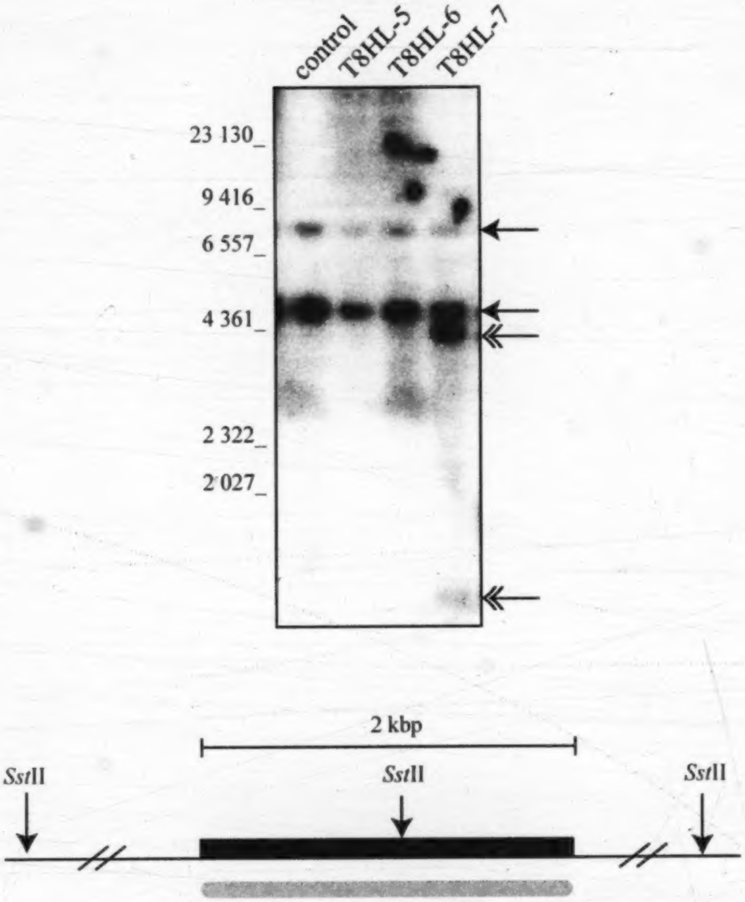
control
T8HL-5
T8HL-6
T8HL-7
23 130
9 416
6 557
4 361
2 322
2 027
2 kbp
SstII
SstII
SstII

Figure 10 Steady state levels of mitochondrial proteins in the *tim8*^{RIP} and *tim13*^{RIP} strains. (A) Mitochondria were isolated from wild type strain (NCN 251), the strains containing the *tim8* and *tim13* duplications (T8HL-7, *tim8* dupl and T13-16, *tim13* dupl respectively) as controls, as well as the *tim8*^{RIP} (T8HL7-7) and *tim13*^{RIP} (T13R16-45) strains. Mitochondrial proteins (20 μg) were separated by SDS-PAGE, blotted to nitrocellulose and immunodecorated with antisera against the proteins indicated on the right. (B) Overexposure of the bottom two panels from (A).

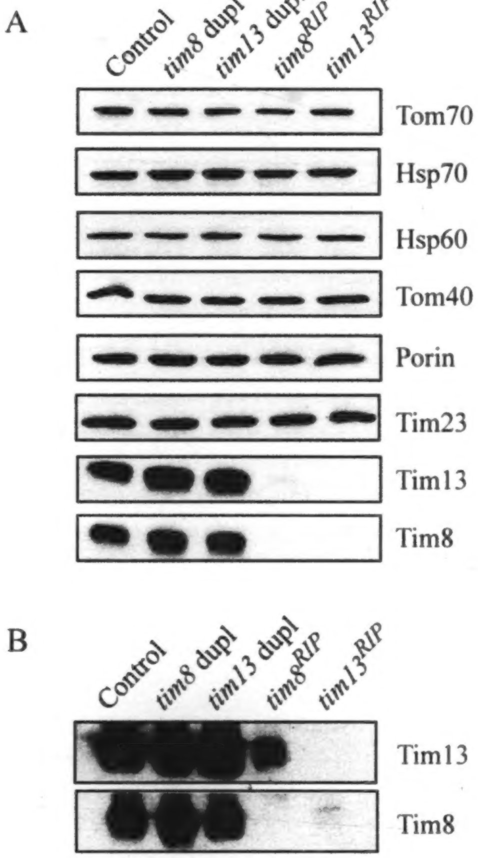
A
Control
tim8 dupl
tim13 dupl
tim8RIP
tim13RIP
Tom70
Hsp70
Hsp60
Tom40
Porin
Tim23
Tim13
Tim8
B
Control
tim8 dupl
tim13 dupl
tim8RIP
tim13RIP
Tim13
Tim8

Figure 11 Sequence analysis of the *tim8*^{RIP} allele. The wild type genomic sequence of *tim8* is shown (*tim8*^{WT}) with amino acid sequence of the protein below. The changes identified in the *tim8*^{RIP} allele in strain T8HL7-7 are shown above the wild type sequence. RIP mutations resulting in premature stop codons are indicated by boxes. The position of the intron splice sites are indicated with arrows below the sequence.

```
tim8^RIP     --------------------------------T-----------T---------
tim8^WT      ATGGATATTCCTCAGGCCGACCTCGATCTCCTCAACGAGAAGGACAAGAACGAG
              M  D  I  P  Q  A  D  L  D  L  L  N  E  K  D  K  N  E

tim8^RIP  -----------T-----T--T------T-----T--------T--------------T--
tim8^WT   CTTCGCGGTTTCATTTCCAACGAGACGCAGCGCCAGAGGGTGCAACGAC GTATGTACCAT
            L  R  G  F  I  S  N  E  T  Q  R  Q  R  V  Q  G ↑

tim8^RIP  -------T--------------------------------T----------------T-
tim8^WT   CTACAACCTTCTAGATCTCCGGCTCCGTCCTGCAGTGCTTCATTCATATCCTCGTCCCT

tim8^RIP  ----T--------------------------------------------T----------
tim8^WT   CTACCATGCCCAAATACAGCTTATTGCCCCTCGCTAAGCCTACCTACCACTTCCCTCTTT

tim8^RIP  ---------T-----T-----------T--------------------------------
tim8^WT   CCCCCCTCCCATAACCATAACCAAAACCATACCCTCTCTCTGTCCCCTCCCCCTTCCATA

tim8^RIP  -------------------------------------------T-----------T----
tim8^WT   TGCTTCTTCCCACATTACTCTACCTCCCAGTGGTTATGTACAACAGATAAACTAACATGC

tim8^RIP  ---------------------T----------T------------------------T---
tim8^WT   TACCTCCCACGTGTAG AGACCCACGCCCTTACCGATTCCTGCTGGAAGAAATGCGTCACC
                          ↑E  T  H  A  L  T  D  S  C  W  K  K  C  V  T

tim8^RIP  -----T--T-----------------T-----------------T---------------
tim8^WT   TCCCCCATCAAGACCAACCAGCTCGACAAGACCGAGGCCGTCTGCATGGCGGACTGCGTT
           S  P  I  K  T  N  Q  L  D  K  T  E  A  V  C  M  A  D  C  V

tim8^RIP  -----------------T-------T----------T-----T-----------------
tim8^WT   GAGCGCTTCCTGGACGTCAACCTGACCATCATGGCCCACGTGCAAAAGATCACCAGGGGT
           E  R  F  L  D  V  N  L  T  I  M  A  H  V  Q  K  I  T  R  G

tim8^RIP  --T--T------------T---------------T-------------------------
tim8^WT   GGCAGCAAGTAGGTCTCGCGCGCCGATAGGAAGGCGTGGGAGGATGCTTATCAGGAGGAG
           G  S  K  *
```

Figure 12 Southern blots of candidate *tim13* duplication containing isolates. Genomic DNA (15 μg) from the parental strain 76-26 (control) and eight isolates from the transformation of 76-26 with the plasmid pCST13 (T13-x) were digested with *Cla*I. Following electrophoresis on a 0.7% agarose gel, DNA was blotted to a nylon membrane and probed with a ^{32}P-labeled *tim13* probe representing the 2.2 kbp *Not*I fragment from the plasmid pCST13. There is a *Cla*I cleavage site in the middle of the *tim13* gene, so the probe should detect two bands per copy of the *tim13* gene. A schematic is shown below the blot with the 2.2 kbp region in the *N. crassa* genome present in plasmid pCST13 represented by a black box. The black line represents *N. crassa* genomic DNA. The double lines through the genomic DNA indicate that an unknown distance separates the *Cla*I site within the *tim13* gene and a *Cla*I site in the surrounding genomic DNA at both the endogenous *tim13* gene and the ectopic insertion site. The position of molecular weight markers and their sizes in number of base pairs is shown on the left. The bands corresponding to the endogenous copy of *tim13* are indicated with arrowheads on the right. The bands corresponding to the ectopic copy of *tim13* in T13-16 are indicated with double arrowheads on the right.

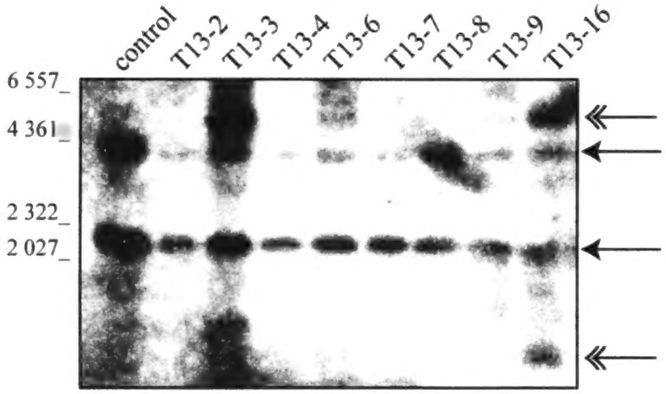
control
T13-2
T13-3
T13-4
T13-6
T13-7
T13-8
T13-9
T13-16
6 557
4 361
2 322
2 027

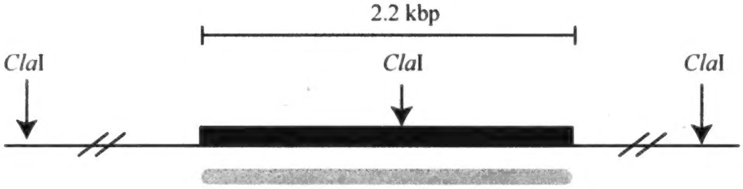
2.2 kbp
*Cla*I
*Cla*I
*Cla*I

Figure 13 Tim8-13 deficient mitochondria are defective in import of Tim23 when $\Delta\Psi$ is reduced. Radiolabeled Tim23 precursor protein was incubated with mitochondria isolated from either the control strain T13-10 (Dupl) or the *tim13*^{RIP} strain at 10°C for the indicated times in the absence (A) or presence (B) of AAO (20 µM antimycin A, 8 µM oligomycin and 2.5 mM ATP). Following a post-import PK treatment, mitochondria were reisolated and subjected to SDS-PAGE. The gels were transferred to nitrocellulose and exposed to x-ray film (insets) and then a PhosphorImager screen for quantitation. One sample from each strain was treated with trypsin prior to import (pre trp) to demonstrate receptor dependent import. (C) The reduction in $\Delta\Psi$ caused by AAO treatment results in decreased import of $F_1\beta$. *In vitro* import was performed as in (A) and (B) with radiolabeled $F_1\beta$ precursor in the presence (bottom) and absence (top) of AAO. "Lys" represents 33% of the total radioactivity added to each reaction.

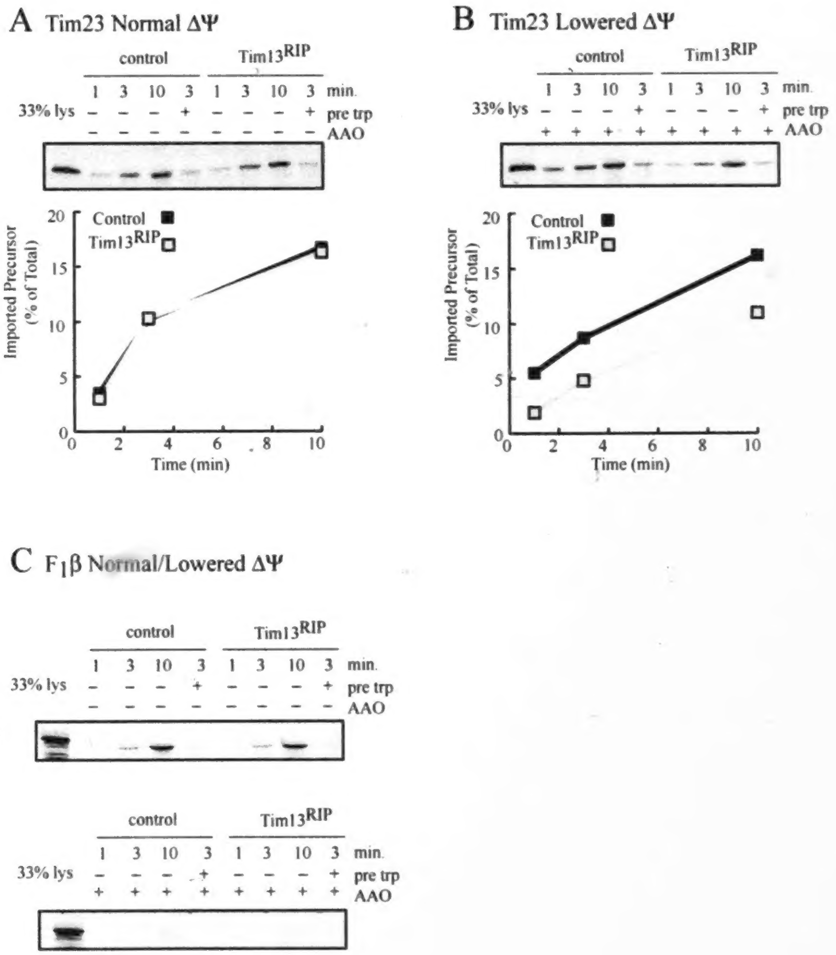
A Tim23 Normal ΔΨ
control
Tim13RIP
1 3 10 3 1 3 10 3 min.
33% lys – – – + – – – + pre trp
– – – – – – – – AAO
20
15
10
5
0
Imported Precursor (% of Total)
Control ■
Tim13RIP □
0 2 4 6 8 10
Time (min)
B Tim23 Lowered ΔΨ
control
Tim13RIP
1 3 10 3 1 3 10 3 min.
33% lys – – – + – – – + pre trp
+ + + + + + + + AAO
20
15
10
5
0
Imported Precursor (% of Total)
Control ■
Tim13RIP □
0 2 4 6 8 10
Time (min)
C F1β Normal/Lowered ΔΨ
control
Tim13RIP
1 3 10 3 1 3 10 3 min.
33% lys – – – + – – – + pre trp
– – – – – – – – AAO
control
Tim13RIP
1 3 10 3 1 3 10 3 min.
33% lys – – – + – – – + pre trp
+ + + + + + + + AAO

Figure 14 Tim8-13 deficient mitochondria are defective in import of porin and Tom40. *In vitro* import was performed as in Figure 13 at 10°C for the indicated times with radiolabeled mitochondrial precursor proteins porin (A) or Tom40 (B). For quantitation, the 26 kDa band of Tom40 was used. (C) Tim8-13 deficient mitochondria are not sensitive to MOM damage during isolation. Mitochondria (50 µg) isolated from the wild type strain NCN 251 (control), the *tim8*^{RIP} strain (T8HL7-7) or the *tim13*^{RIP} strain (T13R16-45) were either treated with 0.1 mg/ml proteinase K at 0°C for 15 min or mock treated for the same time period. The protease was inactivated by the addition of 1 mM PMSF, mitochondria were reisolated, proteins were analyzed by SDS-PAGE, transferred to nitrocellulose and immunodecorated with antisera against the proteins indicated.

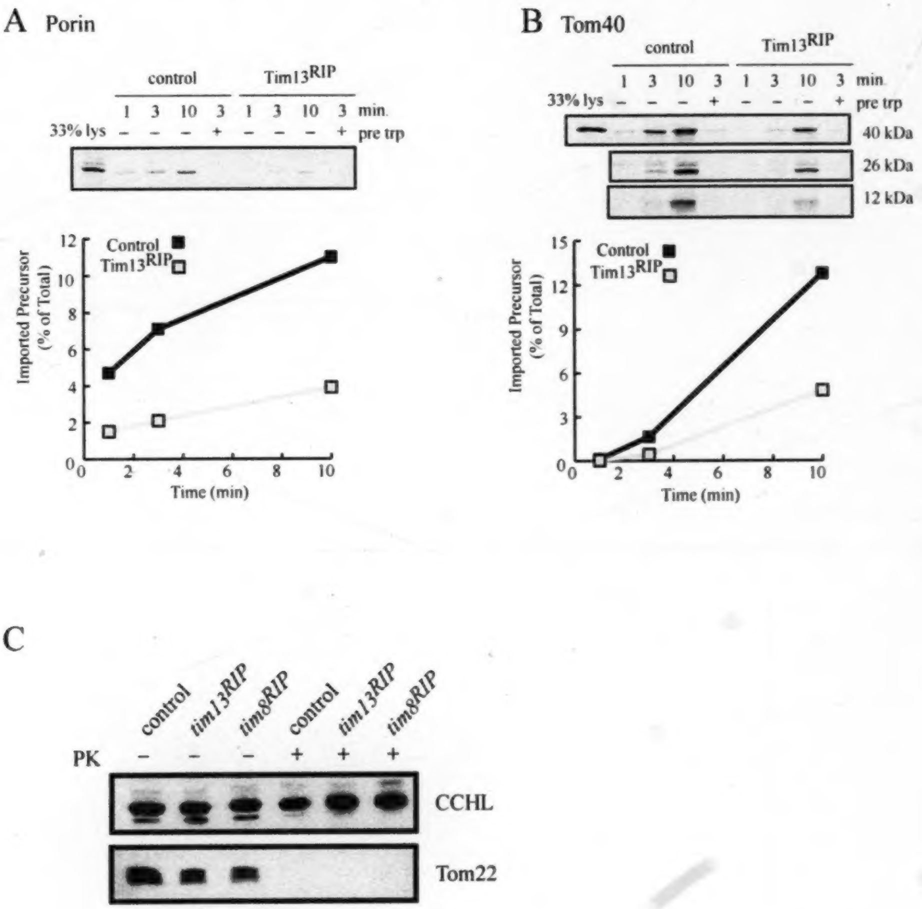
A Porin
control
Tim13RIP
1 3 10 3 1 3 10 3 min.
33% lys – – – + – – – + pre trp
Control
Tim13RIP
Imported Precursor (% of Total)
0 2 4 6 8 10 12
Time (min)
0 2 4 6 8 10
B Tom40
control
Tim13RIP
1 3 10 3 1 3 10 3 min.
33% lys – – – + – – – + pre trp
40 kDa
26 kDa
12 kDa
Control
Tim13RIP
Imported Precursor (% of Total)
0 3 6 9 12 15
Time (min)
0 2 4 6 8 10
C
control
tim13RIP
tim8RIP
control
tim13RIP
tim8RIP
PK – – – + + +
CCHL
Tom22

Figure 15 Tim8-13 deficient mitochondria are not defective in import of all mitochondrial proteins. *In vitro* import was performed as in Figure 13 at 25°C for the indicated times with indicated radiolabeled mitochondrial precursor proteins. The import of the matrix targeted β-subunit of the F_1 ATPase ($F_1\beta$)(A), IMS targeted cytochrome *c* heme lyase (CCHL)(B), MIM targeted ADP-ATP carrier (AAC)(C) and the tail-anchored MOM protein Tom22 (D) are not affected by loss of the Tim8-13 complex.

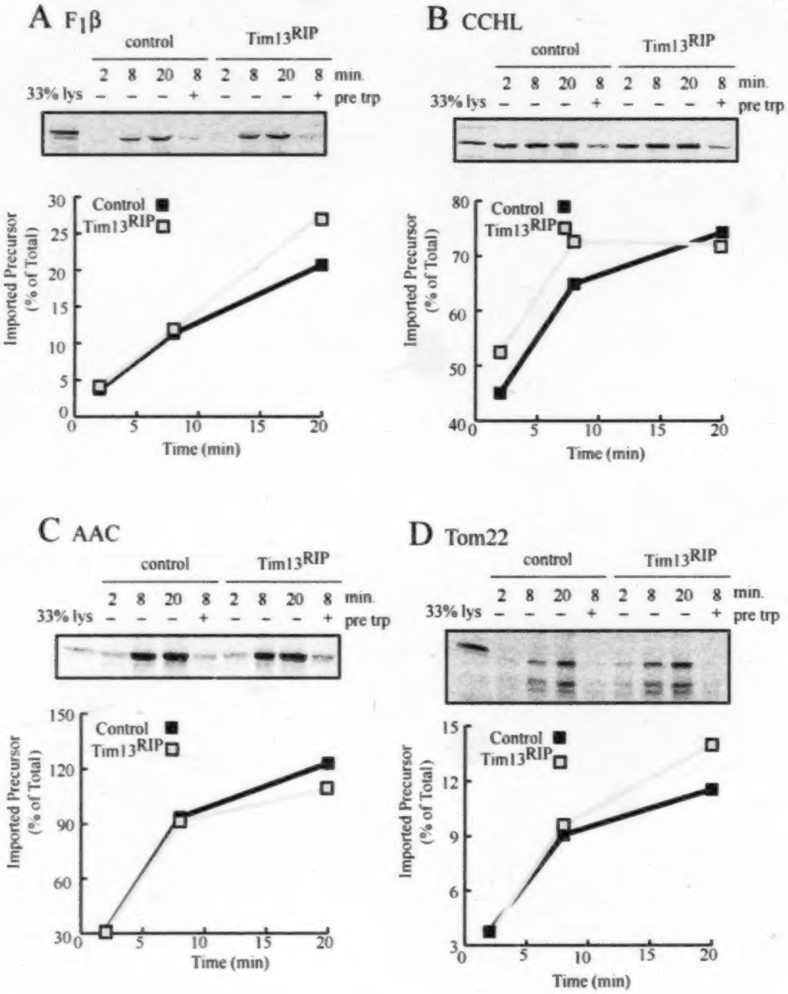
A F1β
control
Tim13RIP
2 8 20 8 2 8 20 8 min.
33% lys
– – – + – – – + pre trp
Control ■
Tim13RIP □
Imported Precursor (% of Total)
0 5 10 15 20 25 30
Time (min)
0 5 10 15 20
B CCHL
control
Tim13RIP
2 8 20 8 2 8 20 8 min.
33% lys
– – – + – – – + pre trp
Control ■
Tim13RIP □
Imported Precursor (% of Total)
40 50 60 70 80
Time (min)
0 5 10 15 20
C AAC
control
Tim13RIP
2 8 20 8 2 8 20 8 min.
33% lys
– – – + – – – + pre trp
Control ■
Tim13RIP □
Imported Precursor (% of Total)
30 60 90 120 150
Time (min)
0 5 10 15 20
D Tom22
control
Tim13RIP
2 8 20 8 2 8 20 8 min.
33% lys
– – – + – – – + pre trp
Control ■
Tim13RIP □
Imported Precursor (% of Total)
3 6 9 12 15
Time (min)
0 5 10 15 20

Figure 16 Import and assembly of porin and Tom40 into Tim8-13 deficient mitochondria. Radiolabeled porin (A) or Tom40 (B) precursor was incubated with mitochondria isolated from the control strain (Ct, T13-16) or the *tim13*^{RIP} strain (RIP, T13R16-45) for the indicated times at the indicated temperature. Mitochondria were washed with 80 mM KCl, reisolated and lysed in blue gel sample buffer containing 1% DIG. The samples were subjected to BNGE, blotted to PVDF membrane and analyzed by autoradiography. Standards used were apoferritin (440 kDa), β-amylase (200 kDa) and BSA (66 kDa) and their positions following electrophoresis are shown on the left. Apparent sizes of the porin species and the known Tom40 assembly intermediates are shown on the right. Quantitation was performed with a phosphorimaging system.

A Porin

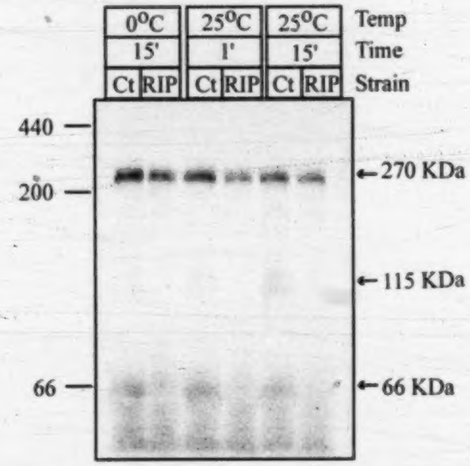

B Tom 40

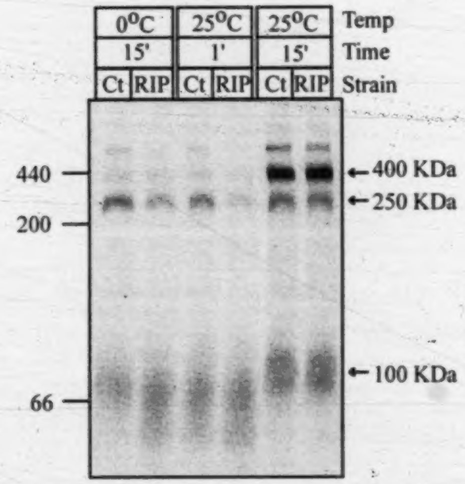

Figure 17 Tom40 precursor contacts the Tim8-13 complex. (A) Radiolabeled Tom40 precursor was incubated with mitochondria isolated from a wild type strain NCN 251 (cont), the *tim13*^{RIP} strain (T13R16-45, 13RIP), or the *tim8*^{RIP} strain (T8HL7-7, 8RIP) for the indicated times at either 0°C or 25°C in several individual reactions containing 40 μg of mitochondrial protein. The import reactions were subjected to crosslinking with 300 μM DSG for 30 min on ice. The excess crosslinker was quenched and the mitochondria were reisolated. In one reaction, the mitochondria were resuspended in cracking buffer at this point, to provide a control for the total content of each reaction (Total). In other reactions, reisolated mitochondria were lysed in 1% Triton-X-100 and subjected to immunoprecipitation (IP) with either Tim8 (α8) or Tim13 (α13) antiserum. Proteins were separated by SDS-PAGE, transferred to nitrocellulose and visualized by PhosphorImaging. (B) Control experiments for crosslinking. Radiolabeled Tom40 precursor was incubated with isolated mitochondria from a wild type strain (cont) at 0°C for 15 min and then processed as in (A). Immunoprecipitation reactions were carried out with either pre-immune serum from rabbits subsequently injected with Tim8 (8PIS) or Tim13 (13PIS), unbound protein A sepharose beads, or Tim8 (α8) or Tim13 (α13) antisera. The presence or absence of DSG in a reaction is indicated. Samples were analyzed as in (A). (C) Radiolabeled Tom40 precursor was incubated with isolated mitochondria as described for panel A, except that the import was done for 15 min at 25°C. Crosslinking and immunoprecipitations were performed as in (A). For all panels, the arrow indicates the expected position of the crosslinked adducts and the asterisk indicates the position of the Tom40 precursor.

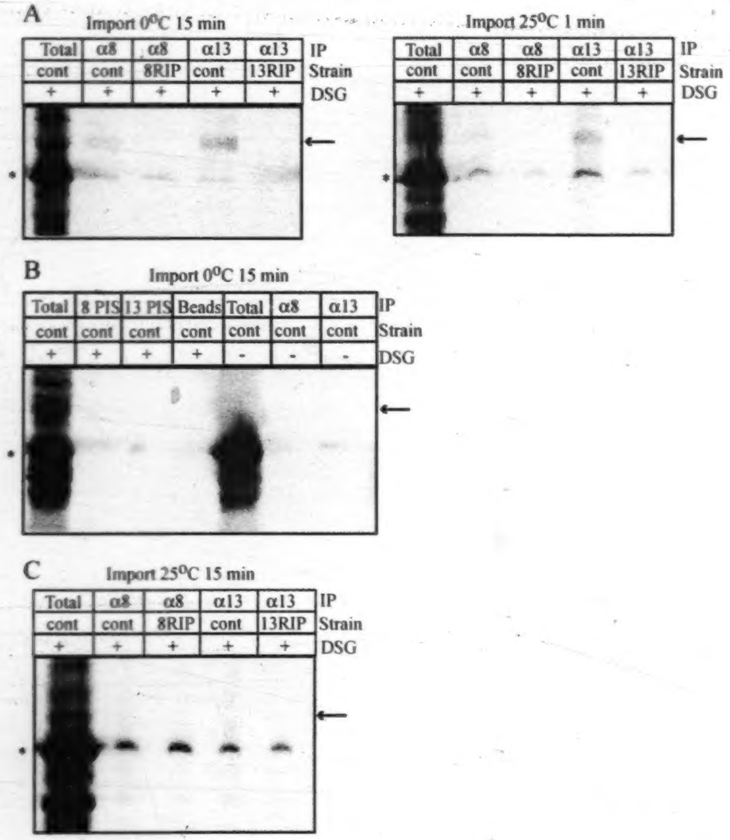
A
Import 0°C 15 min
Total | α8 | α8 | α13 | α13 | IP
cont | cont | 8RIP | cont | 13RIP | Strain
+ | + | + | + | + | DSG
Import 25°C 1 min
Total | α8 | α8 | α13 | α13 | IP
cont | cont | 8RIP | cont | 13RIP | Strain
+ | + | + | + | + | DSG
B
Import 0°C 15 min
Total | 8 PIS | 13 PIS | Beads | Total | α8 | α13 | IP
cont | cont | cont | cont | cont | cont | cont | Strain
+ | + | + | + | - | - | - | DSG
C
Import 25°C 15 min
Total | α8 | α8 | α13 | α13 | IP
cont | cont | 8RIP | cont | 13RIP | Strain
+ | + | + | + | + | DSG
*

Figure 18 A Tom40 mutant precursor stalls at a position where contact with the Tim8-13 complex occurs. Radiolabeled Tom40ΔKLG precursor, which lacks amino acids 321-323, was incubated with mitochondria isolated from a wild type strain (NCN 251, WT) or the *tim13*^{RIP} strain (T13R16-45, 13RIP) or the *tim8*^{RIP} strain (T8HL7-7, 8RIP) for the indicated times at 25°C in individual reactions containing 40 μg of mitochondrial protein. Samples were then processed as in Figure 17A. The arrow indicates the expected position of the crosslinked adducts. The asterisk indicates the position of the Tom40 precursor.

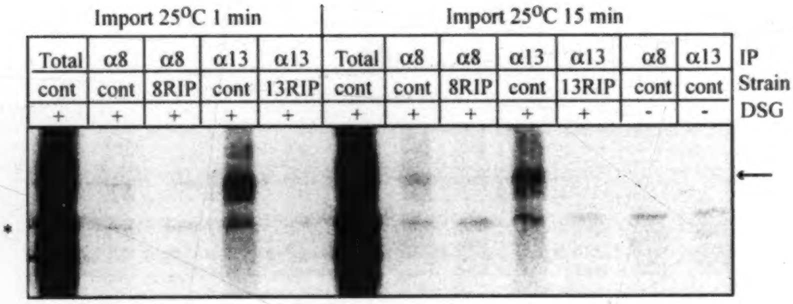
Import 25°C 1 min
Import 25°C 15 min
Total α8 α8 α13 α13 Total α8 α8 α13 α13 α8 α13 IP
cont cont 8RIP cont 13RIP cont cont 8RIP cont 13RIP cont cont Strain
+ + + + + + + + + + - - DSG
*
←

Figure 19 Crosslinked adducts of Tom40 are not accessible to externally added protease. Radiolabeled Tom40 precursor was incubated at 0°C for 15 min with mitochondria isolated from a wild type strain (NCN 251) and import reactions were subjected to crosslinking with 300 μM DSG for 30 min on ice as in Figure 17. Samples were either untreated (-PK) or treated with 0.1 mg/ml proteinase K (+PK) for 15 min on ice before centrifugation to reisolate the mitochondria. One sample was loaded directly to represent the total sample (Total) while a second sample was used for immunoprecipitation (as in Figure 16) with the Tim13 antibody (α13). Samples were subjected to SDS-PAGE, the proteins were transferred to nitrocellulose and the position of labeled bands was detected by PhosphorImaging. The asterisk indicates the position of the Tom40 precursor.

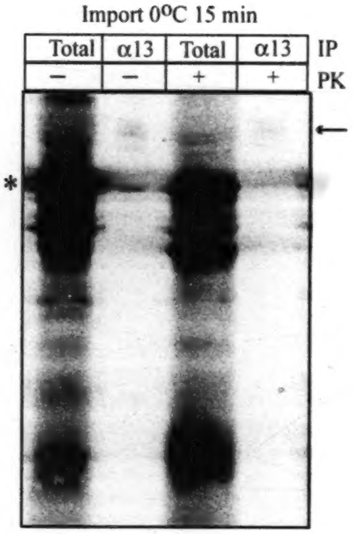
Import 0°C 15 min
Total
α13
Total
α13
IP
−
−
+
+
PK
*
←

Figure 20 Tom40 precursor contacts Tim9. Radiolabeled Tom40 precursor was incubated at 25°C with mitochondria isolated from a wild type strain (NCN 251) and import was performed for the indicated times whereupon the reactions were subjected to crosslinking with 300 μM DSG for 30 min on ice. The samples were processed as in Figure 17 except that immunoprecipitation was performed with Tim9 antiserum. Samples were subjected to SDS-PAGE, the proteins were transferred to nitrocellulose and the position of labeled bands was detected by PhosphorImaging.

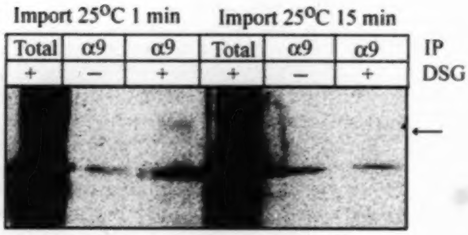
Import 25°C 1 min
Import 25°C 15 min
Total
α9
α9
Total
α9
α9
IP
+
−
+
+
−
+
DSG

Figure 21 Tim8-13 and Tim9-10 contact the Tim23 precursor during import. Radiolabeled Tim23 precursor was incubated with mitochondria isolated from the wild type strain NCN 251 (cont) or the *tim13*^{RIP} strain (T13R16-45, 13RIP) or the *tim8*^{RIP} strain (T8HL7-7, 8RIP) for the indicated times at 25°C in individual reactions containing 40 μg of mitochondrial protein. In each case, the membrane potential was dissipated with FCCP (carbonyl cyanide p-trifluoromethoxyphenylhydrazone) and valinomycin to stall the import of Tim23 as a translocation intermediate. Samples were processed as in Figure 17. Immunoprecipitations (IP) were done with either pre-immune serum (13PIS), or antiserum to Tim8 (α8), Tim13 (α13) or Tim9 (α9). Specific crosslinked adducts of the Tim23 precursor with Tim8 or Tim13 are indicated with arrows. The asterisk indicates the position of the Tim23 precursor.

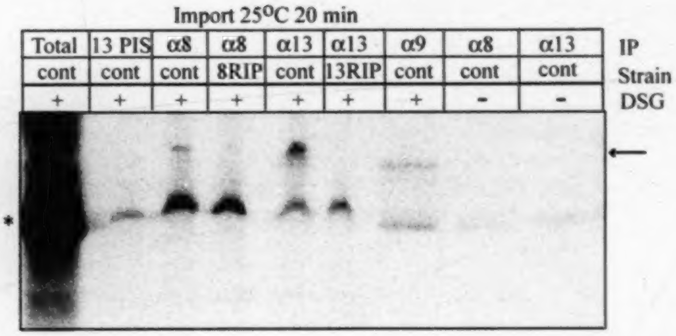
Import 25°C 20 min
Total
13 PIS
α8
α8
α13
α13
α9
α8
α13
IP
cont
cont
cont
8RIP
cont
13RIP
cont
cont
cont
Strain
+
+
+
+
+
+
+
-
-
DSG
*

Figure 22 Sequence alignment of Tim23 protein. The Tim23 proteins of *Neurospora crassa* (N.c.), *Saccharomyces cerevisiae* (S.c.), *Schizosaccharomyces pombe* (S.p.), *Mus musculus* (M.m.) and *Homo sapiens* (H.s.) are shown. The number of residues is indicated at the right and black shading indicates amino acid identity between three or more species. The predicted transmembrane domains are highlighted by black bars above the sequence. The predicted dimerization domain is highlighted by the grey bar above the sequence.

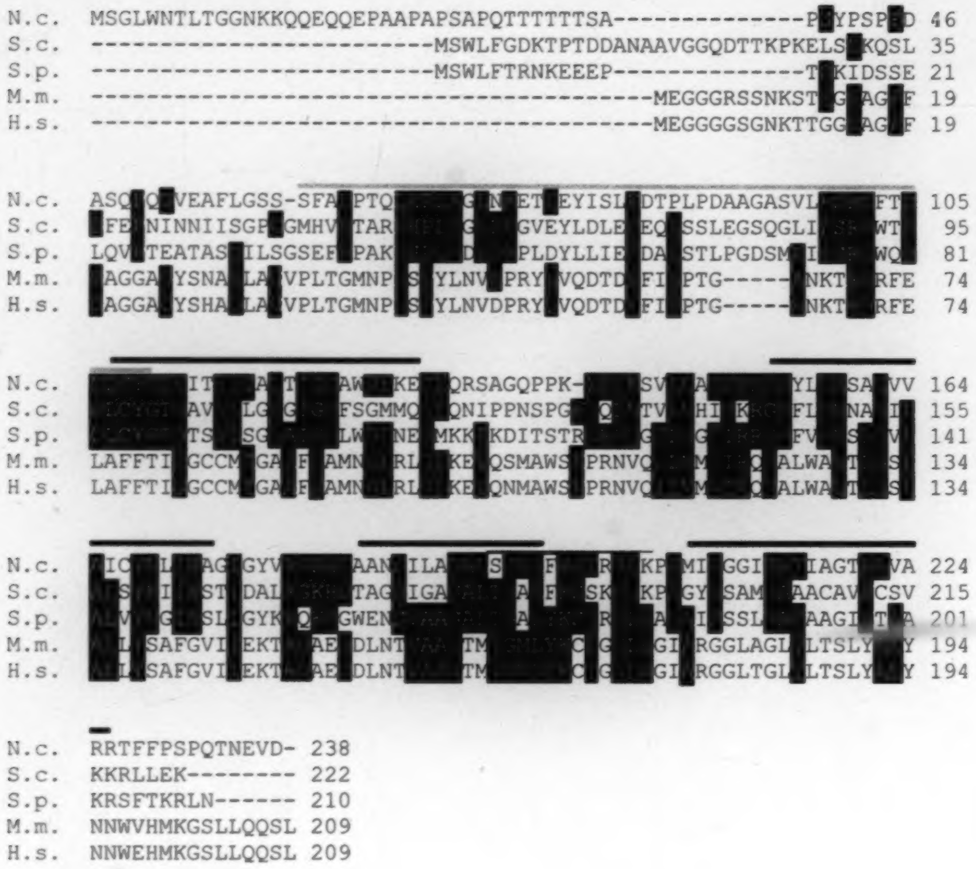
N.c.
S.c.
S.p.
M.m.
H.s.

Figure 23 Import of Tim23(1-67)-DHFR fusion protein. (A) Radiolabeled fusion protein containing the first 67 amino acids of *N. crassa* Tim23 fused to mouse DHFR (A top panel) or radiolabeled DHFR was incubated for 20 min at 25°C with mitochondria isolated from a wild type strain (NCN 251) that were either untreated (-trypsin) or pre-treated with trypsin (+trypsin). Mitochondria were reisolated. One sample was suspended in cracking buffer to represent the total radioactivity associated with the mitochondria. The second sample was subjected to alkaline extraction by treatment with 0.1M $NaCO_3$. The membrane embedded proteins (top) were separated from soluble proteins (bottom) on a two step sucrose gradient. The fractions were subjected to TCA precipitation and the pellets were suspended in running buffer. The samples were subjected to SDS-PAGE. The proteins were transferred to nitrocellulose and exposed to x-ray film. (B) Radiolabeled fusion protein T23(1-67)-DHFR and Tom40 (top panel) or radiolabeled full length Tim23 and Tom40 (bottom panel) were incubated for 20 min at 25°C with mitochondria isolated from a wild type strain (NCN 251) that were either untreated (-trypsin) or pre-treated with trypsin (+trypsin). Mitochondria were reisolated and treated as in (A). "Lys" represents 33% of the total radioactivity added to each reaction.

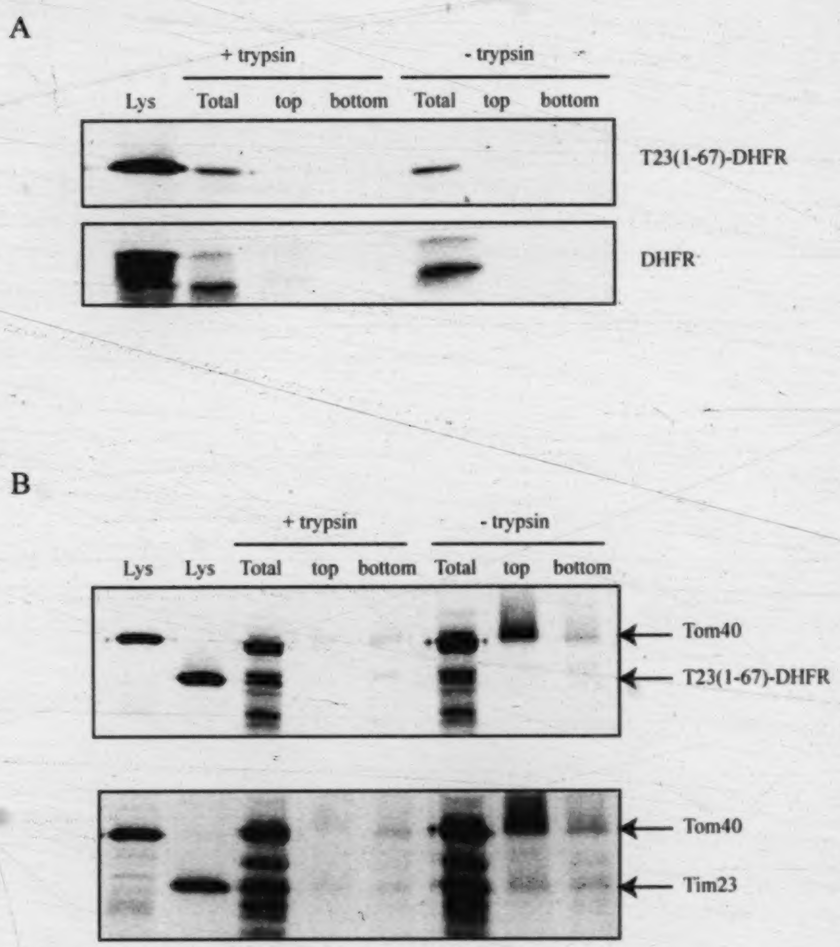
A
+ trypsin
- trypsin
Lys
Total
top
bottom
Total
top
bottom
T23(1-67)-DHFR
DHFR
B
+ trypsin
- trypsin
Lys
Lys
Total
top
bottom
Total
top
bottom
Tom40
T23(1-67)-DHFR
Tom40
Tim23

Figure 24 Import of Tim23(1-83)-IgG fusion protein. (A) Radiolabeled fusion protein containing the first 83 amino acids of *N. crassa* Tim23 fused to the CH2CH3 domains of human IgG (Tim23(1-83)-IgG) was incubated for 20 min at 25°C with mitochondria isolated from a wild type strain (NCN 251) that were either untreated (-trypsin) or pre-treated with trypsin (+trypsin). Following a post-import trypsin treatment, mitochondria were reisolated. One sample was suspended in running buffer to represent the total (T). The second sample was subjected to alkaline extraction by treatment with 0.1M $NaCO_3$. The membrane embedded proteins were pelleted (P) and the proteins in the supernatant were precipitated by treatment with TCA (S). The pellets were suspended in cracking buffer and proteins were separated by SDS-PAGE. Proteins were transferred to nitrocellulose and exposed to x-ray film. (B) Radiolabeled fusion protein T23(1-83)-Ig in solution without mitochondria was subjected to alkaline extraction and then TCA precipitation and treated as in (A).

A

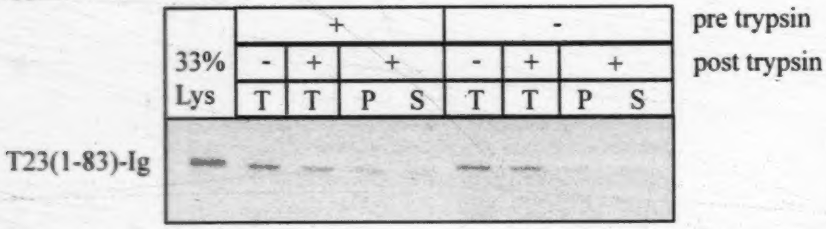
+
-
pre trypsin
33%
Lys
-
+
+
-
+
+
post trypsin
T
T
P
S
T
T
P
S
T23(1-83)-Ig

B

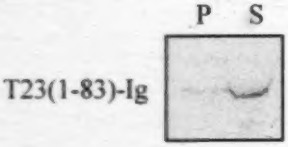
P
S
T23(1-83)-Ig

Figure 25 Southern blots of candidate *tim23* duplication-containing isolates. Genomic DNAs (15 μg) from the parental strain H III (control) and five isolates from the transformation of H III with the plasmid pTIM23 (TI23-x) were digested with *Age*I. Following electrophoresis on a 0.7% agarose gel, DNA was blotted to a nylon membrane and probed with a ^{32}P-labeled *tim23* probe representing the 2.2 kbp fragment from the plasmid pTim23. There is an *Age*I cleavage site in the middle of the *tim23* containing 2.2 kbp fragment, so the probe should detect two bands per copy of the *tim23* gene. A schematic is shown below the blot with the 2.2 kbp region in the *N. crassa* genome present in plasmid pTim23 represented by a black box. The black line represents *N. crassa* genomic DNA. The double lines through the genomic DNA indicate that an unknown distance separates the *Age*I site within the *tim23* gene and an *Age*I site in the surrounding genomic DNA at both the endogenous *tim23* gene and the ectopic insertion site. The probe used is represented by a grey line. The bands corresponding to the endogenous copy of *tim23* are indicated with arrowheads on the right. The bands corresponding to the ectopic copy of *tim23* in TI23-4 are indicated with double arrowheads on the right. The position of molecular weight markers and their sizes, in number of base pairs, is shown on the left.

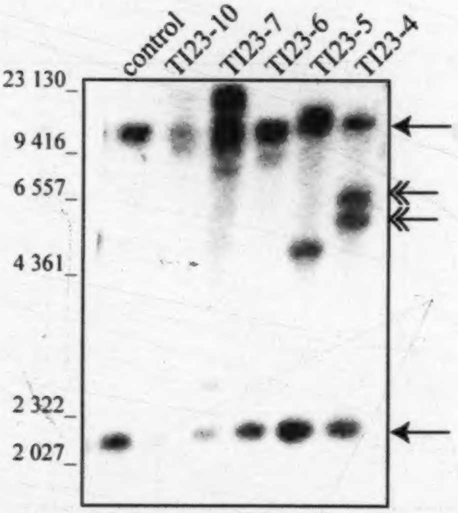
control
TI23-10
TI23-7
TI23-6
TI23-5
TI23-4
23 130
9 416
6 557
4 361
2 322
2 027

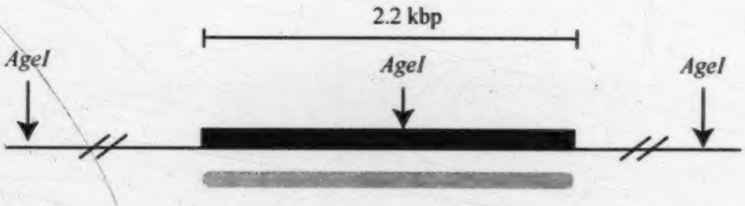
2.2 kbp
AgeI
AgeI
AgeI

Figure 26 Sequence analysis of the *tim23*^{RIP} allele. The wild type sequence of *tim23* is shown with the nucleotide changes generated present in the *tim23*^{RIP} allele of strain T23R4-12 shown above the wild type sequence. The intron splice sites are indicated with arrows. The G to A change resulting in a premature stop codon (TAG) at amino acid 126 is outlined with a box.

```
tim23^WT  CCCTCCACTTCAGTCACAATGTCCGGCCTTTGGAACACCCTCACCGGAGGCAACAAGAAG
                             M  S  G  L  W  N  T  L  T  G  G  N  K  K

tim23^WT  CAGCAAGAGCAGCAAGAGCCCGCCGCACCCGCCCCCAGCGCACCTCAGACAACCACCACC
           Q  Q  E  Q  Q  E  P  A  A  P  A  P  S  A  P  Q  T  T  T  T

tim23^WT  ACCACCTCCGCTCCTTCATATCCCTCGCCCTTCGATGCTAGCCAGCCCCAAGGTGTCGAG
           T  T  S  A  P  S  Y  P  S  P  F  D  A  S  Q  P  Q  G  V  E

tim23^WT  GCCTTTCTCGGTAGCTCTTCCTTCGCCGACCCCACACAACTACACCCTCTTGCCGGCCTC
           A  F  L  G  S  S  S  F  A  D  P  T  Q  L  H  P  L  A  G  L

tim23^RIP -----A------------------------A-------------A------A-----A--
tim23^WT  AACAAGGAAACACTAGAATACATCTCGCTTGAGGATACCCCGCTGCCCGATGCCGCCGGC
           N  K  E  T  L  E  Y  I  S  L  E  D  T  P  L  P  D  A  A  G

tim23^RIP ------A--------------A--------A---------A-------------------
tim23^WT  GCCTCAGTTCTGCCCTCGCGCGGCTTCACTGACGACCTCTGCTACGGAACCGGTATCACC
           A  S  V  L  P  S  R  G  F  T  D  D  L  C  Y  G  T  G  I  T

tim23^RIP --------------T----------------A----------------------------
tim23^WT  TACCTGACGGCCCTCACTATCGGAGGCGCGTGGGGTTTGAAAGAGGGTCTCCAGAGATCG
           Y  L  T  A  L  T  I  G  G  A  W  G  L  K  E  G  L  Q  R  S

tim23^RIP ---------------------------------------------A--------------
tim23^WT  GCCGGCCAGCCGCCCAAGCTGCGCCTCAACTCCGTCCTTAACGCTGTCACCCGTCGCGGT
           A  G  Q  P  P  K  L  R  L  N  S  V  L  N  A  V  T  R  R  G

tim23^RIP ---------------------A--A--A--------------------------------
tim23^WT  CCCTACCTCGGCAACTCGGCTGGTGTTGTCGCCATCTGCTACAACCTAATCAACGCCGGC
           P  Y  L  G  N  S  A  G  V  V  A  I  C  Y  N  L  I  N  A  G

tim23^RIP ---A-------A--------------------T-----------A------A-A----A-
tim23^WT  ATTGGTTACGTGAGGGGCAAGCACGATGCCGCCAACTCAATCCTGGCCGGTGCGCTTAGT
           I  G  Y  V  R  G  K  H  D  A  A  N  S  I  L  A  G  A  L  S

tim23^RIP --------------A--------------A--------A------------------A--
tim23^WT  GGTATGCTCTTCAAGAGCACCAGGGGTCTGAAGCCCATGATGATCTCGGGTGGTATTGTT
           G  M  L  F  K  S  T  R  G  L  K  P  M  M  I  S  G  G  I  V

tim23^RIP -------------------------------------------------------A---A
tim23^WT  GCGACGATAGCCGGTACTTGGGCG GTATGTCACCATTTTTCGTATGGCAGGCGTAGACTG
           A  T  I  A  G  T  W  A ↑

tim23^RIP ------------A-----------A----------------A-------------------
tim23^WT  GAAATACACCTTGCTAACTTTACTGTGTCACTAG GTCGCCAGGAGGACGTTCTTCCCCTCC
                                            ↑ V  A  R  R  T  F  F  P  S

tim23^RIP -------------------------
tim23^WT  CCCCAGACCAACGAGGTTGACTGAAGTGGGGAC
           P  Q  T  N  E  V  D  *
```

Figure 27 Southern blots of the *tim23*^{RIP} strain to determine copy number. Genomic DNA (15 μg) from the parental strain H III (control), the duplication containing strain TI23-4 and the sheltered RIP strain TI23R4-12 were digested with *Age*I and were processed as in Figure 25. The bands corresponding to the endogenous copy of *tim23* are indicated with arrowheads on the right. The bands corresponding to the ectopic copy of *tim23* in the duplication containing strain TI23-4 are indicated with double arrowheads on the right. The position of molecular weight markers and their sizes, in number of base pairs, is shown on the left.

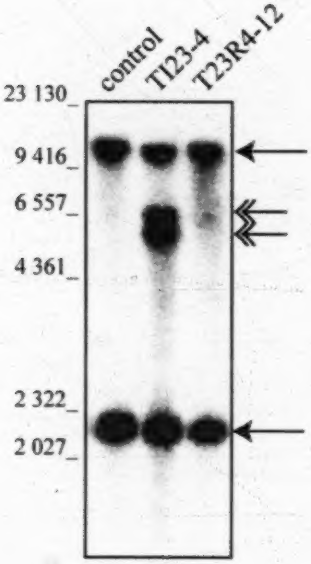
control
TI23-4
T23R4-12
23 130
9 416
6 557
4 361
2 322
2 027

Figure 28 Nucleus swap for *tim23*^{RIP} strain genetic testing. The original *tim23*^{RIP} heterokaryon (T23R4-12) is shown in (A) with the relevant genetic markers important for generation, selection or manipulation of the nuclei in this strain shown. A third nucleus was introduced using the strain Helper 5 (see section 2.5) to form a trikaryon with the existing *tim23*^{RIP} sheltered heterokaryon. The generation of heterokaryons containing the RIP nucleus and the viable nucleus from Helper 5 was done by selection with acriflavin and benomyl. The heterokaryon obtained after the nucleus swapping experiment is shown in (B). Any alleles not shown in common between the two heterokaryons are assumed to be wild type.

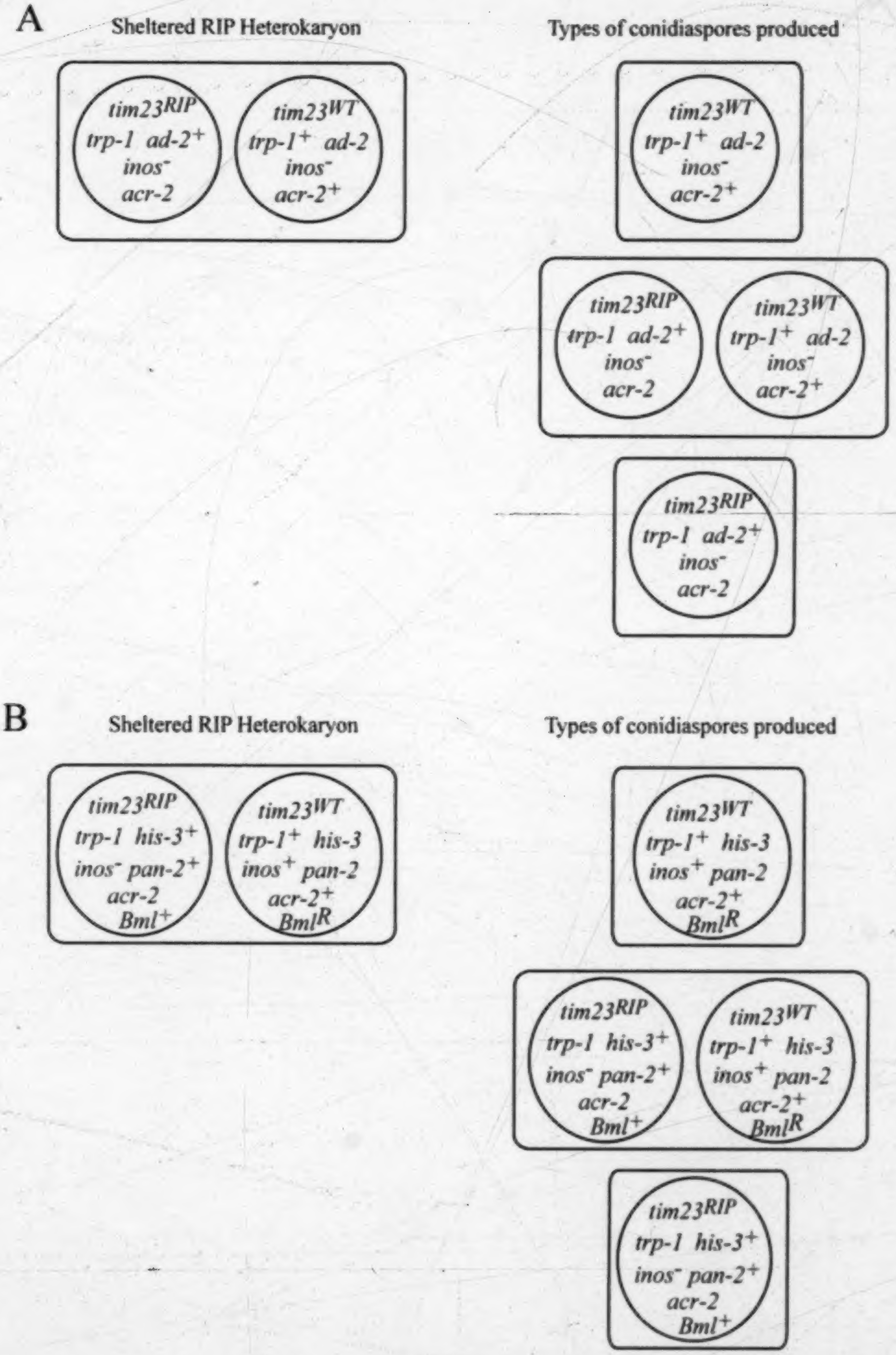
A
Sheltered RIP Heterokaryon
$tim23^{RIP}$ $trp\text{-}1$ $ad\text{-}2^{+}$ $inos^{-}$ $acr\text{-}2$
$tim23^{WT}$ $trp\text{-}1^{+}$ $ad\text{-}2$ $inos^{-}$ $acr\text{-}2^{+}$
Types of conidiaspores produced
$tim23^{WT}$ $trp\text{-}1^{+}$ $ad\text{-}2$ $inos^{-}$ $acr\text{-}2^{+}$
$tim23^{RIP}$ $trp\text{-}1$ $ad\text{-}2^{+}$ $inos^{-}$ $acr\text{-}2$
$tim23^{WT}$ $trp\text{-}1^{+}$ $ad\text{-}2$ $inos^{-}$ $acr\text{-}2^{+}$
$tim23^{RIP}$ $trp\text{-}1$ $ad\text{-}2^{+}$ $inos^{-}$ $acr\text{-}2$
B
Sheltered RIP Heterokaryon
$tim23^{RIP}$ $trp\text{-}1$ $his\text{-}3^{+}$ $inos^{-}$ $pan\text{-}2^{+}$ $acr\text{-}2$ Bml^{+}
$tim23^{WT}$ $trp\text{-}1^{+}$ $his\text{-}3$ $inos^{+}$ $pan\text{-}2$ $acr\text{-}2^{+}$ Bml^{R}
Types of conidiaspores produced
$tim23^{WT}$ $trp\text{-}1^{+}$ $his\text{-}3$ $inos^{+}$ $pan\text{-}2$ $acr\text{-}2^{+}$ Bml^{R}
$tim23^{RIP}$ $trp\text{-}1$ $his\text{-}3^{+}$ $inos^{-}$ $pan\text{-}2^{+}$ $acr\text{-}2$ Bml^{+}
$tim23^{WT}$ $trp\text{-}1^{+}$ $his\text{-}3$ $inos^{+}$ $pan\text{-}2$ $acr\text{-}2^{+}$ Bml^{R}
$tim23^{RIP}$ $trp\text{-}1$ $his\text{-}3^{+}$ $inos^{-}$ $pan\text{-}2^{+}$ $acr\text{-}2$ Bml^{+}

Figure 29 Growth phenotype of the T23Δ10-14 and T23Δ50-50 strains. (A) Schematic of the Tim23 protein showing predicted dimerization domain (grey box) and transmembrane domains (black boxes) which are highly conserved in *S. cerevisiae* and *N. crassa*. The position of the outer membrane spanning domain in *S. cerevisiae* is shown (white box). The removal of the first 10 amino acids in *N. crassa* Tim23 corresponds to a region N-terminal to the predicted outer membrane spanning domain in *S. cerevisiae*. The T23Δ50-50 truncation in *N. crassa* Tim23 removes most of the region N-terminal to the dimerization domain. (B) Growth rates of the sheltered RIP strain (T23R4-12) and the truncated strains were measured in race tubes every 24 hours for 4 days at 22°C.

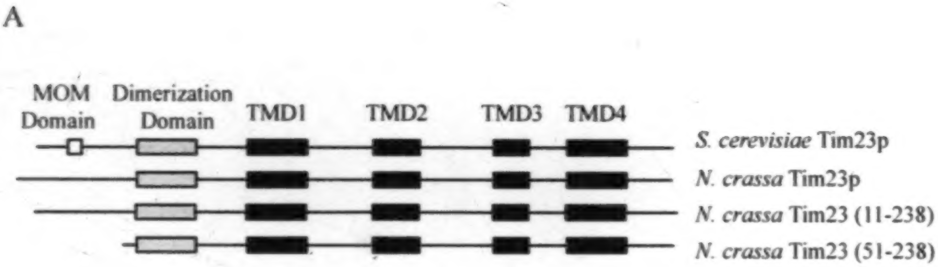
A
MOM Domain
Dimerization Domain
TMD1
TMD2
TMD3
TMD4
S. cerevisiae Tim23p
N. crassa Tim23p
N. crassa Tim23 (11-238)
N. crassa Tim23 (51-238)

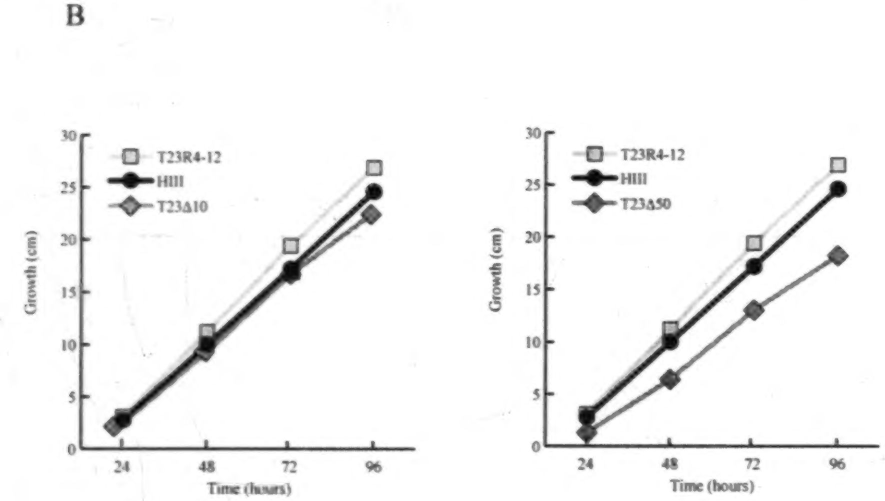
B
T23R4-12
HIII
T23Δ10
Growth (cm)
Time (hours)
0
5
10
15
20
25
30
24
48
72
96
T23R4-12
HIII
T23Δ50
Growth (cm)
Time (hours)
0
5
10
15
20
25
30
24
48
72
96

Figure 30 Rescue of the *tim23*^{RIP} allele with truncated versions of *tim23*. Mitochondria were isolated from a control strain (H III), the strain containing the *tim23* duplication (TI23-4) with one wild type allele (Tim23) and one octa-histidine-tagged allele (his-Tim23), the *tim23*^{RIP} strain (T23R4-12), and the T23Δ10-14 strain (A) and T23Δ50-50 strain (B). Mitochondrial proteins (20 μg) were separated by SDS-PAGE, blotted to nitrocellulose and immunodecorated with antisera against Tim23.

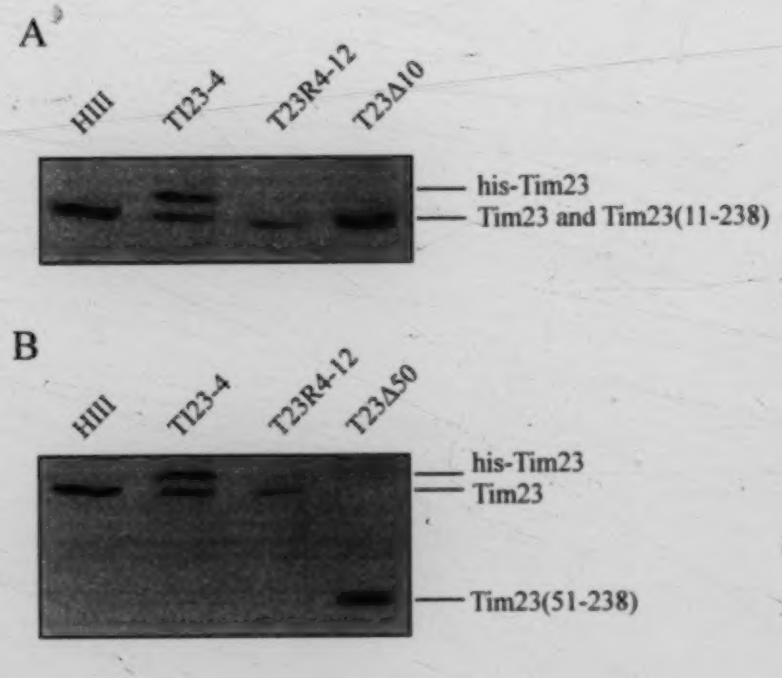
A
HIII
TI23-4
T23R4-12
T23Δ10
his-Tim23
Tim23 and Tim23(11-238)
B
HIII
TI23-4
T23R4-12
T23Δ50
his-Tim23
Tim23
Tim23(51-238)

Figure 31 Truncation of Tim23 does not result in severe deficiency in import of mitochondrial proteins. *In vitro* import was performed as in Figure 13 at 25°C for the indicated times with radiolabeled mitochondrial precursor proteins indicated on the left with mitochondria isolated from the control strain TI23-4 (control), the T23Δ10-14 strain (A) or the T23Δ50-50 strain (B) strain.

A

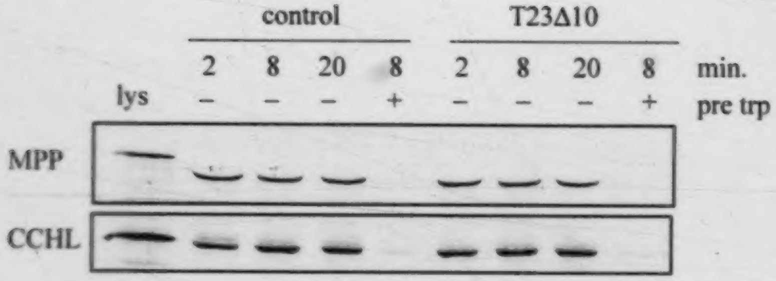
control
T23Δ10
2
8
20
8
2
8
20
8
min.
lys
–
–
–
+
–
–
–
+
pre trp
MPP
CCHL

B

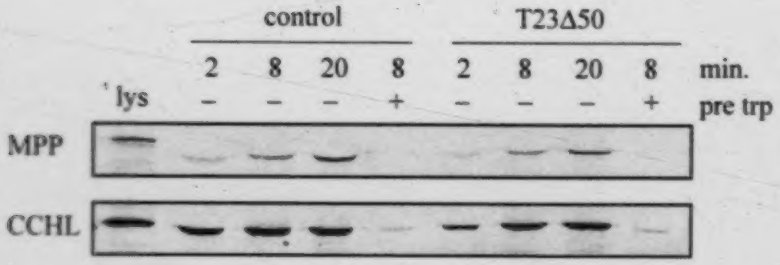
control
T23Δ50
2
8
20
8
2
8
20
8
min.
lys
–
–
–
+
–
–
–
+
pre trp
MPP
CCHL

Figure 32 Deletion of the first 50 amino acids of Tim23 affects the rate of import of mitochondrial matrix proteins. Radiolabeled mitochondrial precursors indicated in each panel and 0.1 μg of purified recombinant Su9-DHFR were incubated at 25°C with mitochondria isolated from either the control strain H III or T23Δ50-50 strain for the indicated times. Following a post-import PK treatment, mitochondria were reisolated and subjected to SDS-PAGE. The gels were transferred to nitrocellulose and exposed to x-ray film (inset) and then a PhosphorImager for quantitation.

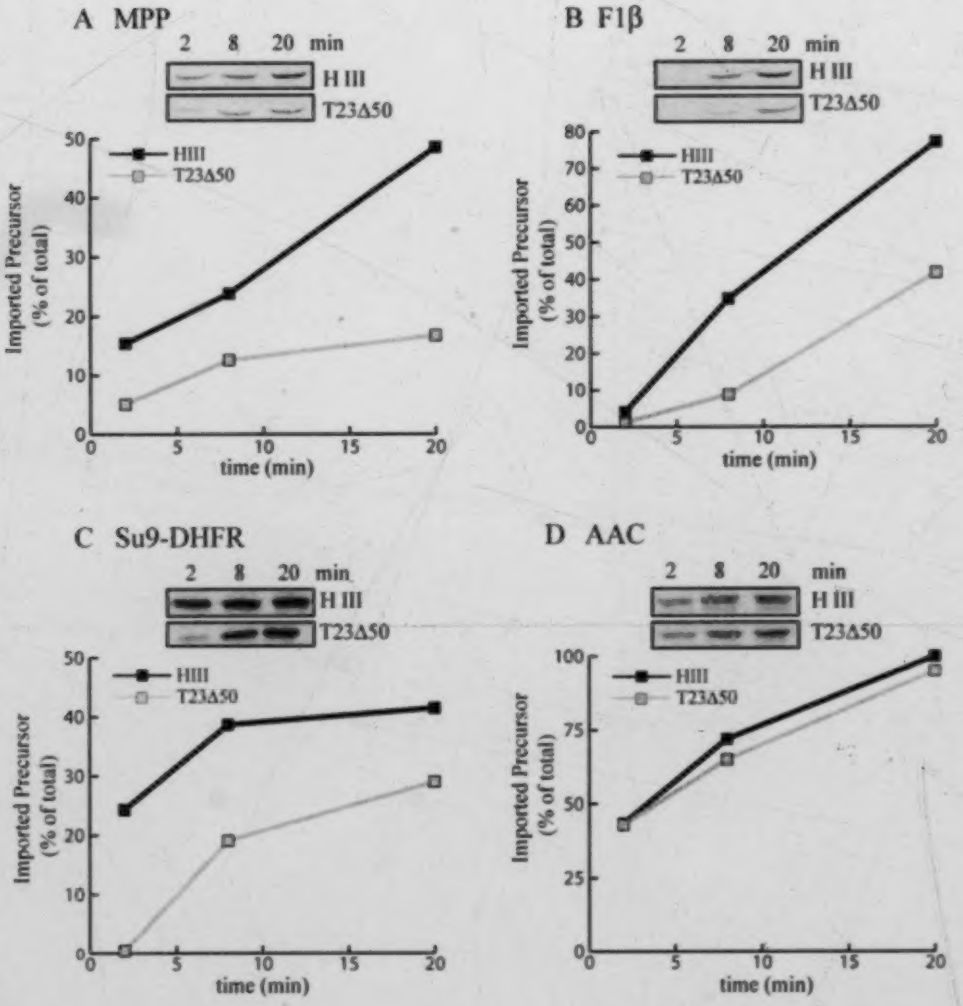
A MPP
2 8 20 min
H III
T23Δ50
Imported Precursor (% of total)
HIII
T23Δ50
0 10 20 30 40 50
0 5 10 15 20
time (min)
B F1β
2 8 20 min
H III
T23Δ50
Imported Precursor (% of total)
HIII
T23Δ50
0 10 20 30 40 50 60 70 80
0 5 10 15 20
time (min)
C Su9-DHFR
2 8 20 min
H III
T23Δ50
Imported Precursor (% of total)
HIII
T23Δ50
0 10 20 30 40 50
0 5 10 15 20
time (min)
D AAC
2 8 20 min
H III
T23Δ50
Imported Precursor (% of total)
HIII
T23Δ50
0 25 50 75 100
0 5 10 15 20
time (min)

Figure 33 Appearance of T23Δ50 mitochondria. Mitochondria were isolated from a control strain (H III) and the strain T23Δ50-50. The mitochondria were processed for analysis by electron microscopy as described in section 2.23.

HIII

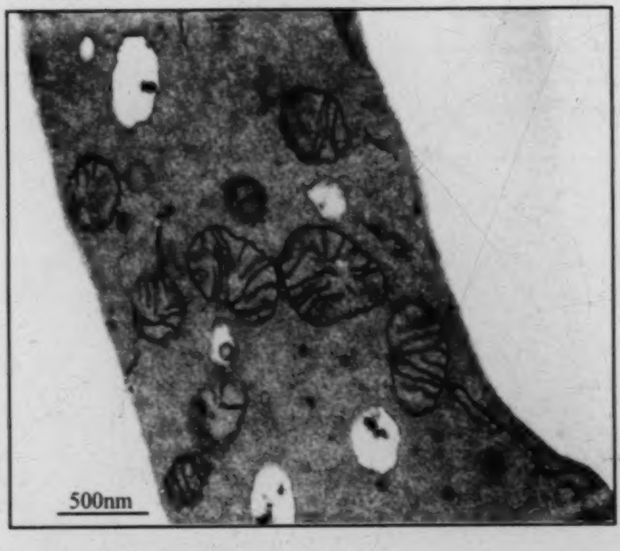

T23Δ50

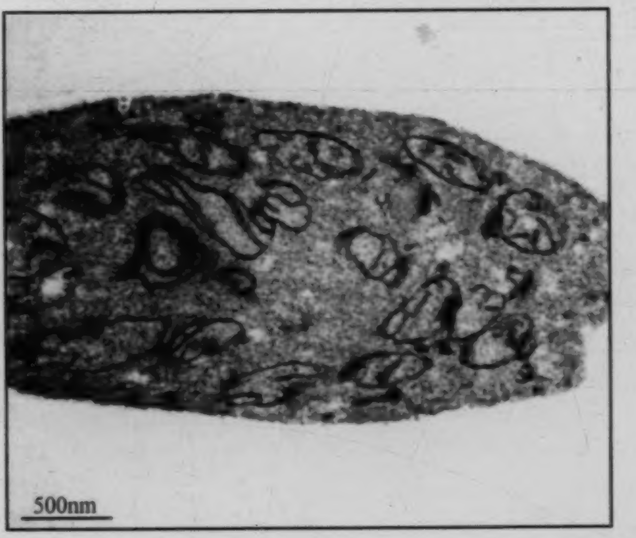

Figure 34 Treatment of mitochondria with Proteinase K. (A) Mitochondria isolated from a wild type strain (NCN 251) were incubated for 20 min on ice with PK at a concentration of 300 μg/ml in the presence or absence of 80 mM KCl. Samples were subjected to SDS-PAGE, transferred to nitrocellulose and immunoblotted with antibodies against the proteins indicated. Mitochondria isolated from the T23Δ50-50 strain are included as a size reference for Tim23.

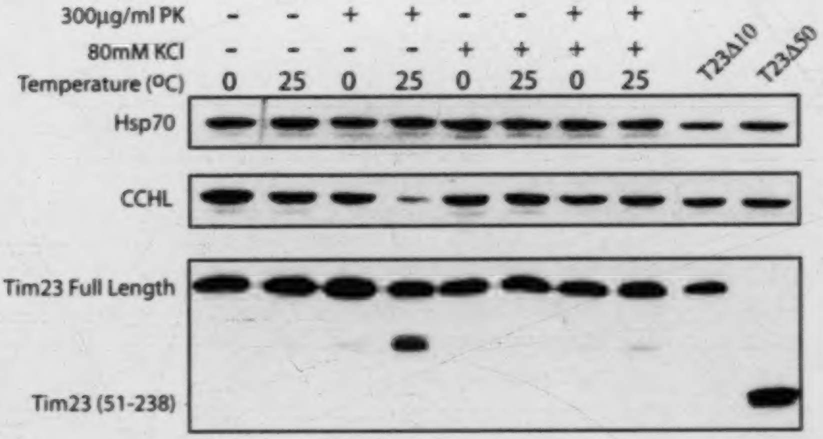
300µg/ml PK - - + + - - + +
80mM KCl - - - - + + + +
Temperature (ºC) 0 25 0 25 0 25 0 25
T23Δ10
T23Δ50
Hsp70
CCHL
Tim23 Full Length
Tim23 (51-238)

Figure 35 Tim23 residues to be mapped by SCAM. The Tim23 proteins of *Neurospora crassa* (N.c.), *Saccharomyces cerevisiae* (S.c.), *Schizosaccharomyces pombe* (S.p.), *Mus musculus* (M.m.) and *Homo sapiens* (H.s.) are shown. The number of residues is indicated at the right and black shading indicates amino acid identity between three or more species. The predicted transmembrane domains are highlighted by black bars above the sequence. The predicted dimerization domain is highlighted by the grey bar above the sequence. Residues of *N. crassa* Tim23 chosen for accessibility mapping are indicated with an arrow above the sequence.

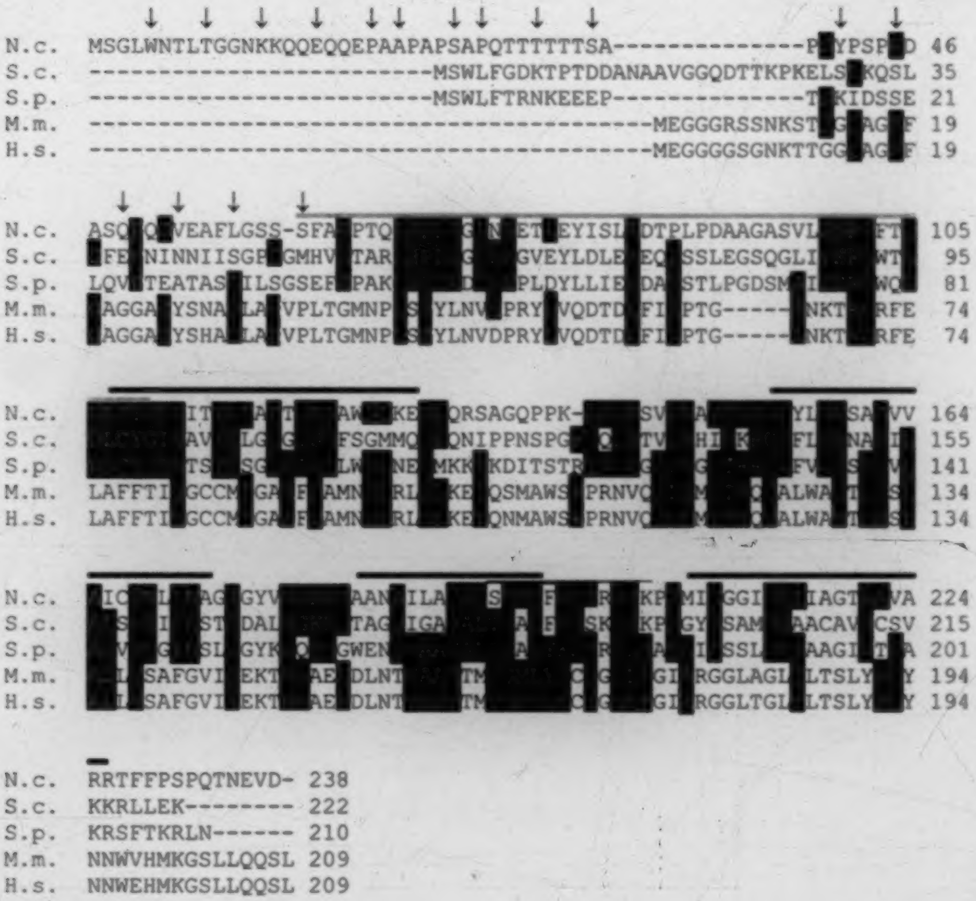
N.c. MSGLWNTLTGGNKKQQEQQEPAAPAPSAPQTTTTTTSA 46
S.c. MSWLFGDKTPTDDANAAVGGQDTTKPKELS KQSL 35
S.p. MSWLFTRNKEEEP KIDSSE 21
M.m. MEGGGRSSNKST 19
H.s. MEGGGGSGNKTTGG 19
N.c. 105
S.c. 95
S.p. 81
M.m. 74
H.s. 74
N.c. 164
S.c. 155
S.p. 141
M.m. 134
H.s. 134
N.c. 224
S.c. 215
S.p. 201
M.m. 194
H.s. 194
N.c. RRTFFPSPQTNEVD- 238
S.c. KKRLLEK-------- 222
S.p. KRSFTKRLN------ 210
M.m. NNWVHMKGSLLQQSL 209
H.s. NNWEHMKGSLLQQSL 209

Figure 36 SCAM analysis of eight positions in the N-terminus of *N. crassa* Tim23. Mitochondria isolated from the indicated strains were incubated for 2 hr at room temperature with biotin maleimide. Mitochondria were reisolated, washed once and then lysed in buffer containing 1% Triton-X-100 and subjected to immunoprecipitation with Tim23 antiserum. Proteins were separated by SDS-PAGE, transferred to nitrocellulose, and decorated with streptavidin conjugated HRP.

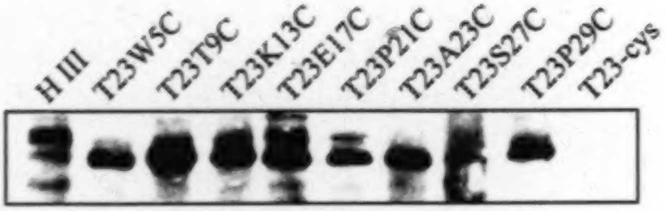
H III
T23W5C
T23T9C
T23K13C
T23E17C
T23P21C
T23A23C
T23S27C
T23P29C
T23-cys

Figure 37 Sequence alignment of Tob55 protein. The Tob55 proteins of *Neurospora crassa* (N.c.), *Saccharomyces cerevisiae* (S.c.), *Schizosaccharomyces pombe* (S.p.), *Mus musculus* (M.m.) and *Homo sapiens* (H.s.) are shown. The number of residues is indicated at the right and black shading indicates amino acid identity between three or more species.

```
N.c. ------MASSPSAPGNPIEDHLLT----------------PA---T█NSIEIH█ANN█RR 35
S.c. -----------MTSSSGVDNEISLDSPMPIFNES-------S---TLKPIRVA█VVTTGT 39
C.e. ---------------------MSEKTFHKAQTIRAKASGVPS---I█EAVQFH█VRI█KN 36
H.s. MGTVHARSLEPLPSSGPDFGGLGEEAEFVEVEPEAKQEILENKDVV█QHVHFD█LGR█KD 60

N.c. GLLD-HVFKPVVEETASPTTT█GEALARIST█TQK█TRF██FKEDGFGV-F█S█ARQQQQ 93
S.c. █HIDPSVLQAYLDDTIMKSIT█GQLVKNADVLNKR█CQHH█ALNAKQSFHFQGNTYISDE 99
C.e. █ALV-KEVSELYR-----SKN█DELVHNSHL█ARH█QEV█LMDN--AVA-L█-█T----- 51
H.s. █III-CEIGDVFK-----AKN█IEVMRKSHE█REK█LRL██FRQ--VDV-L█-█T----- 105

N.c. EQFQSPTDR---TELD█SIR█K█QSRLVFKAG█DF█-█AEGSAYT---NAVLRNIF█GA█ 147
S.c. KETHDVVPL---MEVVSQLDILPPKTF█AKTG█NF█NDNDAEAY█QFEKLIDKKYLKLPT 156
C.e. ----SPSSN---EGYV█NFL█R█PKSF█AGVKAGVST█GDADVS█---NAGKQSVG█RG█ 101
H.s. ----CQGDDALPNGLD█TFE█T█LRRL█GSYN█MV█-█NEGSMV█---GLKLPNLL█RA█ 158

N.c. TLSVNAAA██RTRSAY--█AVFST█VN█-NPDIRLALEALRSSTHK██ASH█EHLT█GN█ 205
S.c. RVNLEILR███IHSSFLF█SYSSLSPQS-ILNLKVFSQF█NWNTNK---GL█IGQR█AR█ 212
C.e. AINTQYTYTV█GDHCF--█ISAIK█FL█WQKYSNVSATL█RSLAHM██NQS█VDENAAV█ 159
H.s. KVTFQFSY███-ETSY--GLSFFK█RR█-NFERNFSVNL█KVTGQF██SSLRETDR█MSA 214

N.c. RLAWS---------TDNG-----DD█ALTYSGV██QLTG------LSAS██PT██AD██D 245
S.c. SLRYEPLFLHKLLHNPHSNESPTLF█EWFLETC██STKICSQGTSAPYMY█GTMLSQ██D 272
C.e. AYNGQ---------LWNQ----KLL█QVKLNAI██TLRA-------TRD█AFS██EQ██H 199
H.s. EYSFP---------IW------KTS█TVKWEGV██ELGC------LSRT██FA██KES█H 253

N.c. S██S█IT█TFTR█R██NPM██QA█Y█VRTAA████WGPLKG█M██H█SEV██SAAQA█PL 305
S.c. Q█RTI█G█TFVL█K██HIMC█TK█SMLKWSN██S-------PGKHL█TQL██NSVKSWMN 325
C.e. T██F██ENAVAV█I██RPI█ASR█I█ARFAQ█Y██V--FG-█I██V█NTLD█QAAAP█PL 256
H.s. S██S██S█AMVI█S█NSSI██RR█A█LKVNQ████Y--TGG█M██I█EDF██QLNKQ█IF 311

N.c. PG-VSVG█G█RA█L█YPLPMGYS█SSTSVA█SR█N███Q████T█████SMGGL██HDGA 364
S.c. DDFITFSTTIKT█Y█K------N█SSQQSL█VH█C█K█QS███S█I███QTFGL██RDLY 379
C.e. GF--ILA█S█QAKH█K------G█---GDREVH█L██CY███QQ█████GLNTI█VKADN 305
H.s. DS--VFS█S█WG█M█V------PI---GDK█SSIA███Y████TS████SMHSI██QSEG 360

N.c. █SV██DVFA██SVNMLL███----RAGPTSPL█FQL█A█G█R█VALQGKKTAEGSVSLDS 420
S.c. █AV██D█FVSYGLSVFSR██WKKV---EKSNF█L█W█F█G█K█V------------NHDN 424
C.e. SCL██G█SL██VVHLYR██IPP-------NMLFA█A█LAS█SVA------------SVH- 345
H.s. █YL██E█YW██GLHLYT███FRPGQGGFGELF█T█F█L█A█N█C------------NLNY 409

N.c. GAVASGM█SAVAE█ANGLPSIAA█F███YA-HPVA█F███FSL█LVVRR█EEARK█L█V█ 479
S.c. ----TSLGNCIGQ█SKE-HST█T█I███LR-HPMA█F███FTL█ITAHENDLIRK█F█F█ 469
C.e. ------S█NLVQQ█QDT-QRV█A█F█A█FVFKSIF█L███YTY█LKYVL█DSLLG█FHI█ 398
H.s. G---EGP█AHIRK█AEC-IRW█Y█A█I█LRLGNIA█L███YCV█MGVQT█DRICD█V█F█ 465

N.c. V█IN██ 485
S.c. L█LA██ 475
C.e. A█VN██ 404
H.s. A█IR██ 471
```

Figure 38 Parent Heterokaryon. The box symbolizes a heterokaryotic cell of strain HP1 with circles representing its component nuclei. The knockout heterokaryotic parent strain (HP1). Genetic markers important for generation, selection or manipulation of the strain are shown.

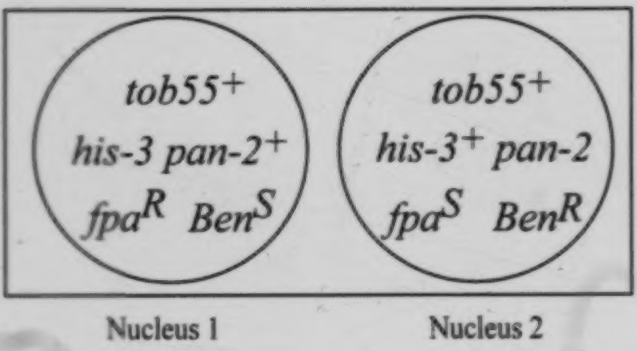
$tob55^+$
$his\text{-}3\ pan\text{-}2^+$
$fpa^R\ Ben^S$
$tob55^+$
$his\text{-}3^+\ pan\text{-}2$
$fpa^S\ Ben^R$
Nucleus 1
Nucleus 2

Figure 39 Southern analysis of *tob55* knockout isolates. (A) Schematic representing genomic DNA in a wild type nucleus (top) and a *tob55* knockout nucleus (bottom). The *tob55* gene is shown as a white box and the hygromycin resistance cassette as a grey box. *Cla*I restriction sites are indicated with arrows. The region used as a probe for Southern analysis is indicated as a black box below the DNA. Predicted sizes of the fragments generated by *Cla*I digestion, which would be identified by the probe, are indicated above the DNA. (B) Southern analysis. *tob55* knockout construct plasmid DNA (KO plasmid, about 5ng) and genomic DNA (15 μg) from the parental strain HP1 and nine isolates from the knockout transformation were digested with *Cla*I. Following electrophoresis on a 0.7% agarose gel, DNA was blotted to a nylon membrane and probed with a ^{32}P-labeled probe representing 3 kbp of *tob55* upstream sequence, as shown in panel A. The band corresponding to the wild type copy of *tob55* is indicated with an arrowhead as 7517 bp and the band corresponding to the homologous replacement event of *tob55* with the resistance marker is shown with an arrowhead as 4500 bp.

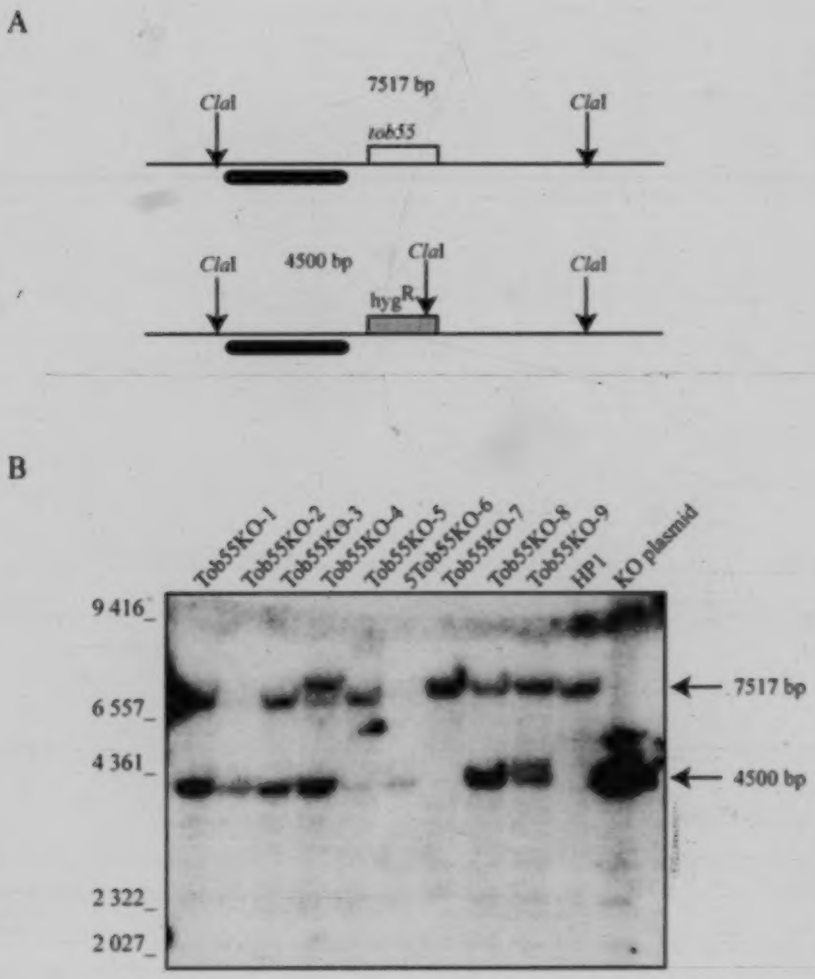
A
7517 bp
ClaI
tob55
ClaI
ClaI
4500 bp
ClaI
hygR
ClaI
ClaI
B
Tob55KO-1
Tob55KO-2
Tob55KO-3
Tob55KO-4
Tob55KO-5
5Tob55KO-6
Tob55KO-7
Tob55KO-8
Tob55KO-9
HP1
KO plasmid
9 416
6 557
4 361
2 322
2 027
7517 bp
4500 bp

Figure 40 Growth of *tob55* knockout isolates.

Serial dilutions of condia from the parent strain HP1 and two *tob55* knockout isolates (Tob55KO-1 and Tob55KO-3) were spotted on plates containing the indicated supplements. Growth on minimal medium (MM) ensures the growth of a heterokaryon, growth on benomyl and pantothenate (ben + pan) causes nucleus 2 to predominate while growth on fpa and histidine (fpa + his) increases the proportion of nucleus 1. Growth was for 3 days at 30°C.

A

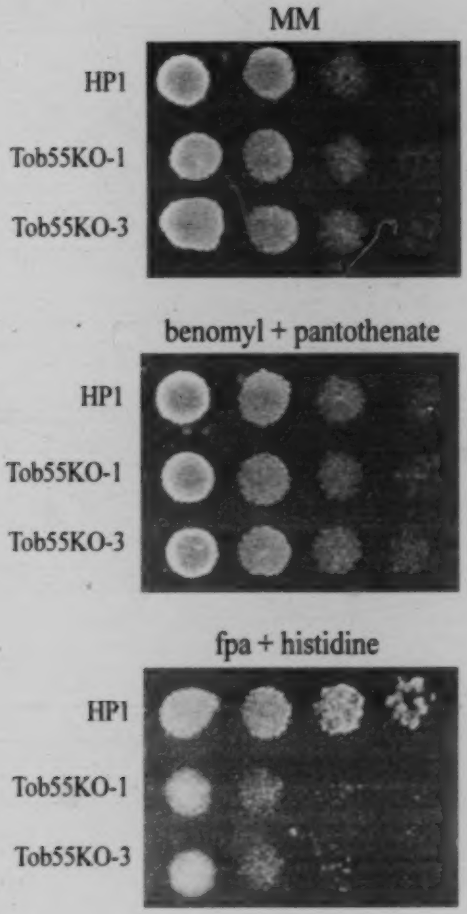
MM
HP1
Tob55KO-1
Tob55KO-3
benomyl + pantothenate
HP1
Tob55KO-1
Tob55KO-3
fpa + histidine
HP1
Tob55KO-1
Tob55KO-3

B

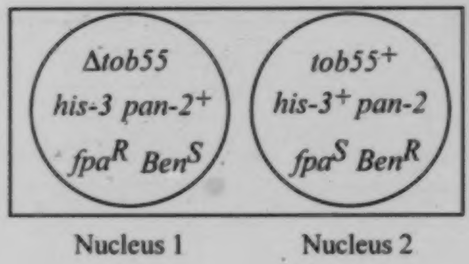
Δtob55
his-3 pan-2⁺
fpa^R Ben^S
tob55⁺
his-3⁺ pan-2
fpa^S Ben^R
Nucleus 1
Nucleus 2

Figure 41 Steady state levels of mitochondrial proteins in the *tob55* knockout strain. Mitochondria were isolated from a control strain (HP1) and the *tob55* knockout heterokaryotic strain following growth in the absence (-) or presence (+) of fpa (400 μM) and histidine. Growth in fpa and histidine results in predominance of nucleus 1 (Figure 40B) and should result in reduction of Tob55 levels in mitochondria due to the deletion of *tob55* in nucleus 1. *N. crassa* Tob55 is present as two bands of 62 and 58 kDa respectively. Mitochondrial proteins (20 μg) were separated by SDS-PAGE, blotted to nitrocellulose and immunodecorated with antisera against the proteins indicated on the right.

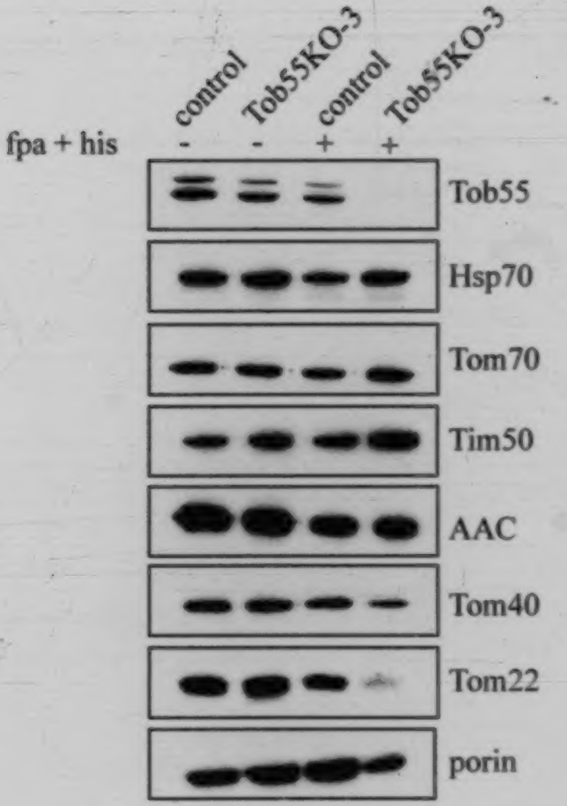
control
Tob55KO-3
control
Tob55KO-3
fpa + his
-
-
+
+
Tob55
Hsp70
Tom70
Tim50
AAC
Tom40
Tom22
porin

Figure 42 Tob55 deficient mitochondria are defective in import of outer membrane β-barrel proteins. (A) Mitochondria were isolated from a control strain (HP1, control) and the *tob55* knockout strain (Tob55KO-3, *Δtob55*) following growth in the absence (-) or presence (+) of fpa (250 μM) + histidine. Mitochondrial proteins (20 μg) were separated by SDS-PAGE, blotted to nitrocellulose and immunodecorated with antisera against the proteins indicated on the right. The reduced level of Tob55 results in decreased efficiency of import of the β-barrel proteins Tom40 (B), porin (C) and Tob55 itself (D). For import assays, radiolabeled mitochondrial precursors were incubated at 15°C for the indicated times with mitochondria isolated from either the control strain HP1 (control) or the $tob55^{KO}$ strain both grown in the presence of fpa (250 μM) and histidine. Following a post-import PK treatment, mitochondria were reisolated and subjected to SDS-PAGE. The gels were transferred to nitrocellulose and exposed to x-ray film and then a PhosphorImager screen for quantitation. One sample from each strain was treated with trypsin prior to import (pre trp) to demonstrate receptor dependent import. "Lys" represents 33% of the total radioactivity added to each reaction.

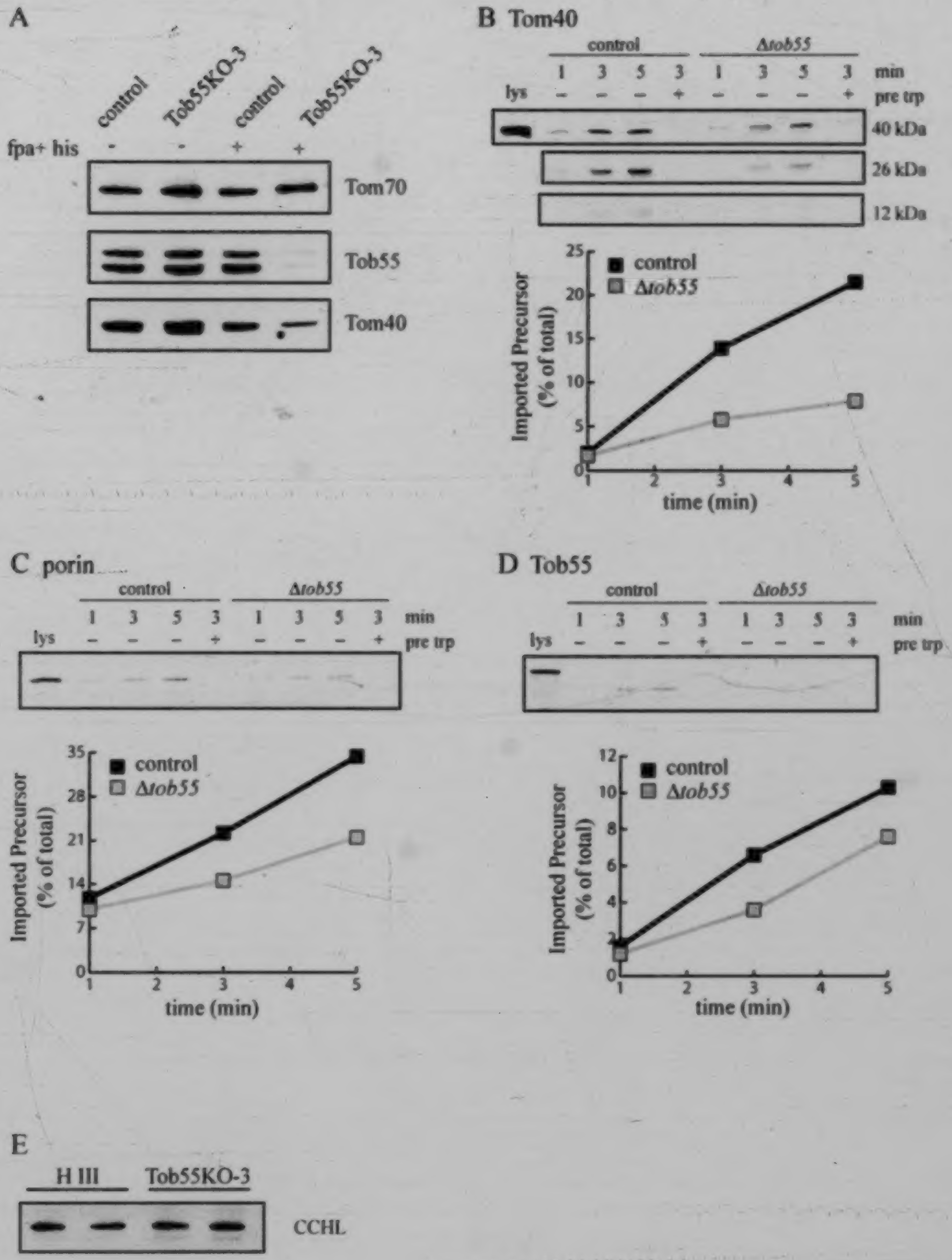
A
control
Tob55KO-3
control
Tob55KO-3
fpa+ his
-
-
+
+
Tom70
Tob55
Tom40
B Tom40
control
Δtob55
1 3 5 3 1 3 5 3 min
lys – – – + – – – + pre trp
40 kDa
26 kDa
12 kDa
control
Δtob55
Imported Precursor (% of total)
0 5 10 15 20 25
1 2 3 4 5
time (min)
C porin
control
Δtob55
1 3 5 3 1 3 5 3 min
lys – – – + – – – + pre trp
control
Δtob55
Imported Precursor (% of total)
0 7 14 21 28 35
1 2 3 4 5
time (min)
D Tob55
control
Δtob55
1 3 5 3 1 3 5 3 min
lys – – – + – – – + pre trp
control
Δtob55
Imported Precursor (% of total)
0 2 4 6 8 10 12
1 2 3 4 5
time (min)
E
H III
Tob55KO-3
CCHL

Figure 43 Tob55 deficient mitochondria are not defective in import of non β-barrel mitochondrial proteins. The reduction of Tob55 does not decrease the efficiency of import of the intermembrane space protein CCHL (A), the inner membrane protein AAC (B) or the mitochondrial matrix protein $F_1\beta$ (C). Radiolabeled mitochondrial precursors were incubated at 15°C for the indicated times with mitochondria isolated from either the control strain HP1 (control) or the *tob55* strain (Tob55KO-3, KO), both grown in the presence of fpa (250 μM) and histidine. Following a post-import PK treatment, mitochondria were reisolated and subjected to SDS-PAGE. The gels were transferred to nitrocellulose and exposed to x-ray film and then a PhosphorImager screen for quantitation. One sample from each strain was treated with trypsin prior to import (pre trp) to demonstrate receptor dependent import. "Lys" represents 33% of the total radioactivity added to each reaction.

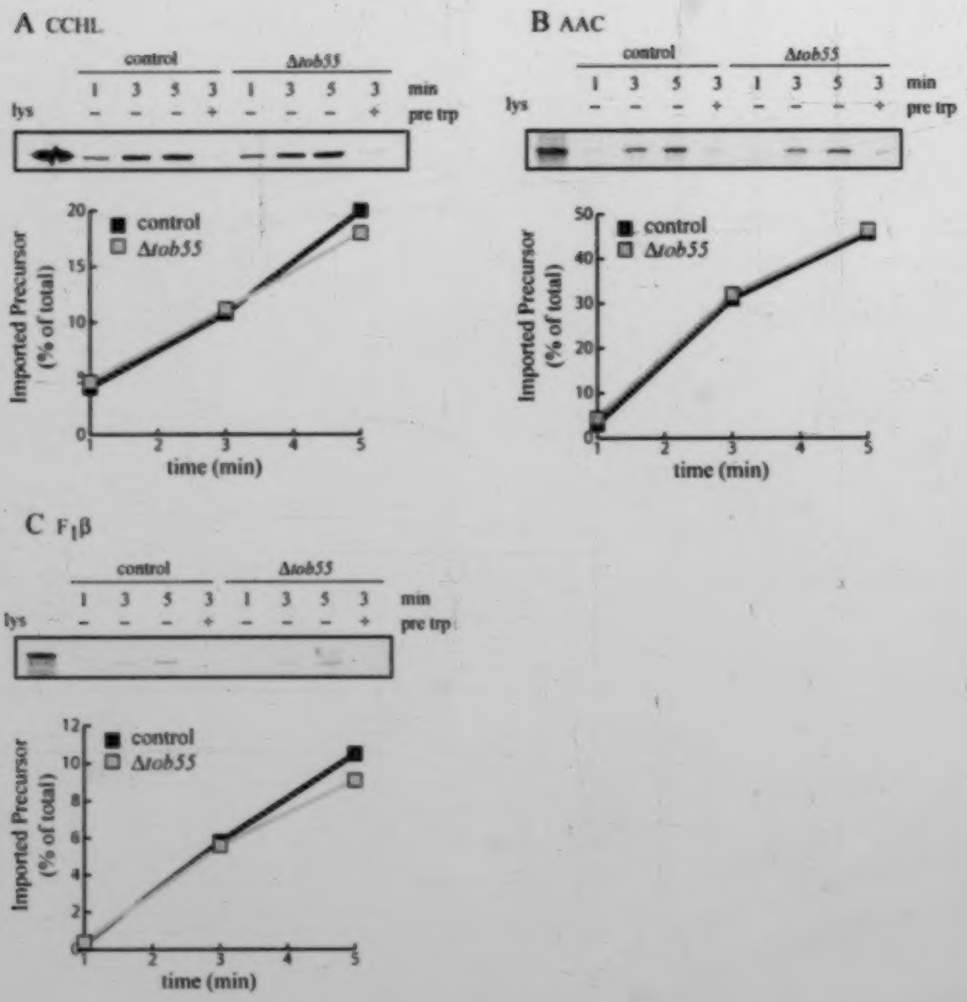
A CCHL
control
Δtob55
1 3 5 3 1 3 5 3 min
lys – – – + – – – + pre trp
Imported Precursor (% of total)
20
15
10
5
0
■ control
□ Δtob55
time (min)
1 2 3 4 5
B AAC
control
Δtob55
1 3 5 3 1 3 5 3 min
lys – – – + – – – + pre trp
Imported Precursor (% of total)
50
40
30
20
10
0
■ control
□ Δtob55
time (min)
1 2 3 4 5
C F$_1$β
control
Δtob55
1 3 5 3 1 3 5 3 min
lys – – – + – – – + pre trp
Imported Precursor (% of total)
12
10
8
6
4
2
0
■ control
□ Δtob55
time (min)
1 2 3 4 5

Figure 44 Assembly of Tom40 and Porin in Tob55↓ mitochondria. Radiolabeled Tom40 (A) or porin (B) precursor were incubated for the indicated times at the indicated temperature with mitochondria isolated from the control strain HP1 (cont) or the *tob55* knockout strain (Tob55KO-3, KO), both grown in the presence of fpa (250 μM) and histidine. Mitochondria were washed with 80 mM KCl, reisolated and lysed in blue gel sample buffer containing 1% DIG. The samples were subjected to BN-PAGE, blotted to PVDF membrane and analyzed by autoradiography. Apparent sizes of the porin species and the known Tom40 assembly intermediates are shown on the right.

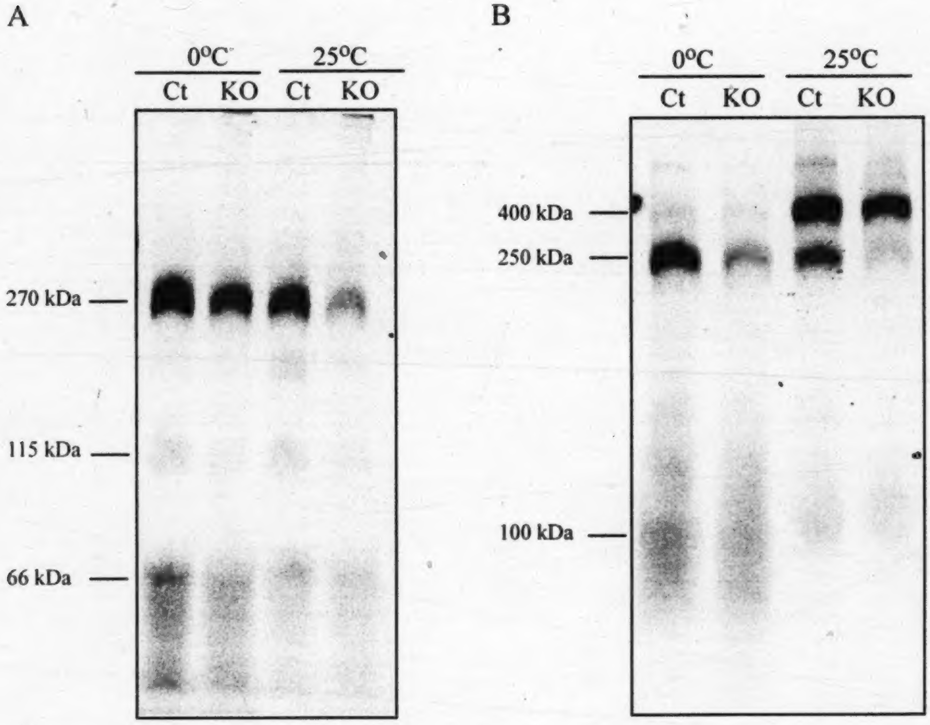
A
0°C
25°C
Ct
KO
Ct
KO
270 kDa
115 kDa
66 kDa
B
0°C
25°C
Ct
KO
Ct
KO
400 kDa
250 kDa
100 kDa

Figure 45 Antibody supershift of Tom40 and porin assembly intermediates. Import was performed as in Figure 44 using mitochondria isolated from a wild type strain (NCN 251) and Tom40 (A) and porin (B) precursor proteins. Following lysis of samples in 1% DIG, 20 µl of affinity purified Tob55 antibody was either added (+) or not (-). Samples were incubated for 2 hours at 4°C and then subjected to BNGE and processing as in Figure 44. Apparent sizes of the porin species and the known Tom40 assembly intermediates are shown on the left. The position of the supershifted product is shown with an arrow on the right.

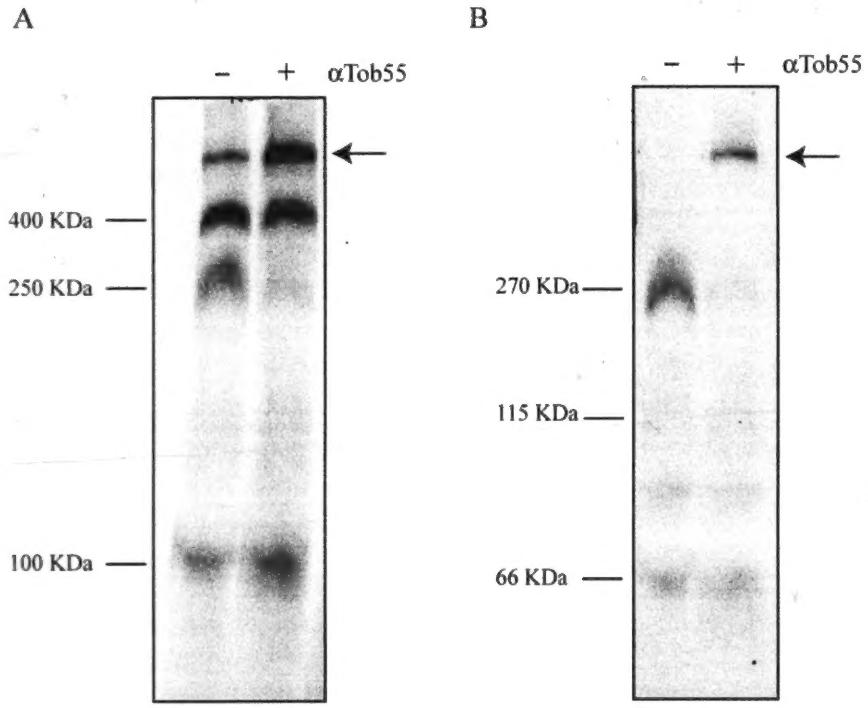
A
-
+
αTob55
400 KDa
250 KDa
100 KDa
B
-
+
αTob55
270 KDa
115 KDa
66 KDa

Figure 46 Generation of Tob55 protein tag strains. (A) Transformation of Tob55KO-3 with tagged alleles of *tob55*, carried on a bleomycin resistant plasmid. To select for homokaryons expressing the tagged alleles of *tob55*, transformants were plated on medium containing histidine, fpa (400 μM) and bleomycin (3.7 μg/ml). Caffeine (0.5 mg/ml) was added to enhance the bleomycin selection. (B) Mitochondria were isolated from control strain (HP1) and *his6-tob55* transformation isolates T55his6-1 and T55his6-3. The mitochondria were examined for expression of the N-terminally tagged protein. Mitochondrial proteins (50 μg) were separated by SDS-PAGE, blotted to nitrocellulose and immunodecorated with either Tob55 antiserum or penta-his antiserum.

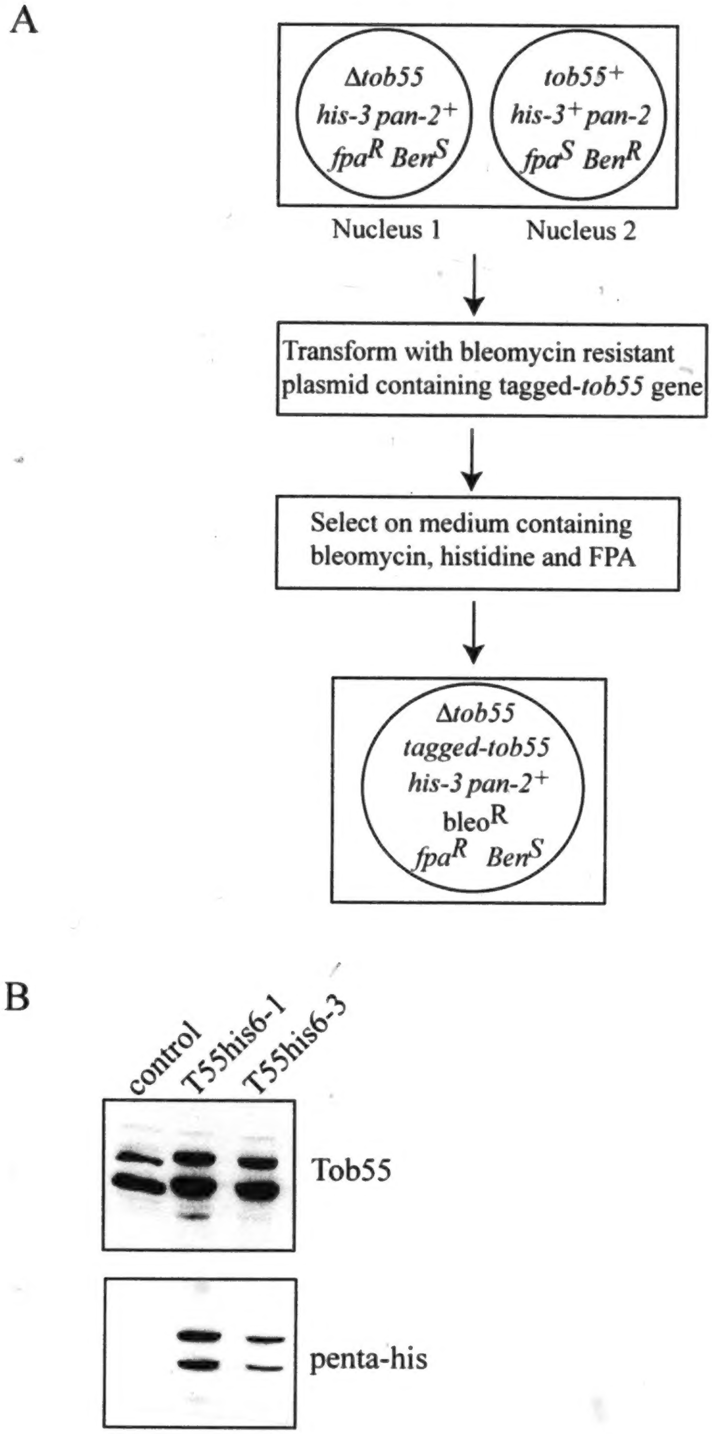
A
Δtob55
his-3 pan-2+
fpaR BenS
tob55+
his-3+ pan-2
fpaS BenR
Nucleus 1
Nucleus 2
Transform with bleomycin resistant plasmid containing tagged-tob55 gene
Select on medium containing bleomycin, histidine and FPA
Δtob55
tagged-tob55
his-3 pan-2+
bleoR
fpaR BenS
B
control
T55his6-1
T55his6-3
Tob55
penta-his

4 DISCUSSION

4.1 *N. crassa Tim8-13 Complex*

The components of the Tim8-13 complex were originally characterized as non-essential proteins in yeast. Tim8 was identified as the homologue of DDP1, the gene responsible for Mohr-Tranebjaerg Syndrome in humans, and Tim13 as a homologue of Tim8 (Koehler *et al.*, 1999). I have identified the homologues in *N. crassa* and have demonstrated that the complex is not essential for viability in this organism either. As in yeast, the Tim8-13 complex is a soluble, hetero-oligomeric complex localized to the IMS. The complex has an apparent molecular weight that is slightly larger in *N. crassa* than in yeast (80 kDa vs 70 kDa)(Koehler *et al.*, 1999).

The technique of RIP was used to inactivate both the *tim8* and *tim13* genes. Western blot analysis revealed that loss of Tim8 results in the degradation of most of Tim13 and conversely, loss of Tim13 results in a dramatic reduction in the amount of Tim8. This suggests that the formation of the complex is necessary to stabilize the individual proteins. The loss of the complex did not affect the steady state levels of any other mitochondrial proteins examined and did not affect growth of the $tim8^{RIP}$ strain.

The Tim8-13 complex in yeast was originally implicated in the import of Tim23 (Leuenberger *et al.*, 1999; Davis *et al.*, 2000; Paschen *et al.*, 2000) which requires the TIM22 complex for insertion into the MIM (Kaldi *et al.*, 1998). The Tim9-10 complex has been characterized to perform a chaperone-like function in escorting hydrophobic membrane proteins across the IMS to the TIM22 complex (see section 1.8.1). I have shown that loss of the Tim8-13 complex only impairs the import of Tim23 if membrane potential is reduced. Since a high membrane potential across the MIM is strictly required for TIM22-dependent insertion of proteins (Rehling *et al.*, 2003), it is apparent that Tim8-13 is important for Tim23 import only under sub-optimal import conditions. The detection of crosslinking adducts between Tim8-13 and Tim23 under conditions of low membrane potential demonstrates that contact between the precursor and the complex occurs. The presence of a crosslinking adduct between Tim9 and Tim23 supports the idea that the import of Tim23 under these conditions is not solely dependent on the Tim8-13 complex. An interaction between the *N. crassa* Tim9-10 complex with Tim23 has also been demonstrated using peptide scanning analysis and the purified Tim9-10 complex (Vasiljev *et al.*, 2004). A physical interaction between a stalled Tim23 precursor and both the Tim8-13 and Tim9-10 complexes in the IMS has also been demonstrated in yeast (Davis *et al.*, 2000).

My analysis also revealed a function for the Tim8-13 complex in the import of β-barrel proteins to the MOM. I observed a reduction in the import of the precursors for Tom40 and porin into mitochondria lacking the Tim8-13 complex. More direct evidence was obtained through crosslinking analysis, which revealed a direct interaction between the Tom40 precursor and components of the Tim8-13 complex. The fact that I could not detect an interaction if import was done for longer times suggested that the interaction occurred transiently at an early point in the import and assembly process. It has also been observed that crosslinks between Sam37 and Tom40 precursor protein are lost after longer import times (Wiedemann *et al.*, 2003). The Tim8-13 complex is not a component of the 250 kDa assembly intermediate because this intermediate is still formed in the absence of the Tim8-13 complex. Thus, it appears that the interaction between the Tom40 precursor and Tim8-13 occurs before the formation of the 250 kDa complex. This conclusion is supported by the observation that Tim8-13 interacts with the mutant Tom40 precursor, Tom40ΔKLG, even after 15 min of import at 25°C. It has been shown that the 250 kDa intermediate is resistant to degradation by externally added PK. I have shown that the crosslinked adduct between the Tom40 precursor and Tim8-13 is also resistant to external PK. Together, these data indicate that the Tom40 precursor interacts with the Tim8-13 complex before the formation of the 250 kDa complex, most likely as the precursor emerges in the IMS from the TOM complex. It has recently been demonstrated in yeast that impaired function of the Tim9-10 complex also impedes the import and assembly of Tom40 (Wiedemann *et al.*, 2004).

It seems unusual that Tim8-13 is involved in the import of the essential proteins Tom40 and Tim23 and yet the growth of the $tim8^{RIP}$ and $tim13^{RIP}$ strains are not altered nor are the levels of Tom40 and Tim23. While the import defects are clear *in vitro*, there is no growth defect associated with the loss of the Tim8-13 complex. This suggests that *in vivo*, the rate of import and assembly of the affected proteins must not be below a threshold that would limit the rate of growth. This could be a result of the redundancy of the system as the Tim9-10 complex is able to largely compensate for loss of Tim8-13.

Assembly of β-barrel proteins in *E. coli* is analogous in some respects. The periplasmic space protein Skp acts as a chaperone for the assembly of β-barrel proteins into the bacterial outer membrane (Chen and Henning, 1996; De Cock *et al.*, 1999). Deletion of the gene encoding Skp does not affect the growth rate of *E. coli* (Schafer *et al.*, 1999), although it does result in a reduction in the steady state levels of affected proteins (Chen and Henning, 1996). Characterization of a synthetic lethal phenotype in strains harboring deletions for the genes of both Skp and another periplasmic chaperone protein suggests that this system also relies on redundant components (Rizzitello *et al.*, 2001).

A correlation between this new function for Tim8-13 and Mohr-Tranebjaerg syndrome is difficult to draw. Patients suffering from the syndrome show no clear affects on mitochondrial morphology or oxidative phosphorylation (Binder *et al.*, 2003). The problem is also complicated by the presence of a second Tim8 protein in humans, DDP2 (Koehler *et al.*, 1999) which could compensate somewhat for the loss of DDP1. It is conceivable that import defects of Tim23 and Tom40 due to loss of the Tim8-13 complex contribute to overall mitochondrial dysfunction.

4.2 *N. crassa Tim23*

Tim23 is an essential component of the mitochondrial import machinery, forming a pore in the MIM through which proteins pass to enter the mitochondrial matrix. The protein has two distinct domains: a C-terminal domain containing four predicted transmembrane segments and an N-terminal domain predicted to be hydrophilic in nature. The C-terminal domain is responsible for forming the pore and for interaction with Tim17 (Ryan *et al.*, 1998; Truscott *et al.*, 2001). A region of about 50 amino acids in the N-terminal region mediates the dimerization of Tim23, which is essential for function (Bauer *et al.*, 1996). In yeast, the finding that the extreme N-terminus of Tim23 is accessible to externally added protease led to the conclusion that this region of the protein actually crossed the MOM (Donzeau *et al.*, 2000). In support of this conclusion it was further shown that the first 62 amino acids of yeast Tim23 are able to mediate the targeting and insertion of a fusion protein into the MOM.

It was proposed that this topology could function to tether the TIM23 complex of the inner membrane to the outer membrane. Thus the TIM23 complex would be excluded from the folds of the MIM that form cristae and therefore localized solely to the inner membrane boundary (Donzeau *et al.*, 2000). The mechanism responsible for the insertion of this domain into the MOM has not been examined. It is conceivable that a signal exists in this region that acts in a similar fashion to stop-transfer signals in proteins that insert into the MIM through the TIM23 complex. This is an attractive model as the region appears to be capable of insertion into the membrane independently of the rest of the protein (Donzeau *et al.*, 2000). Given that the Tim23 precursor is thought to cross the TOM complex as two loops, each containing two transmembrane domains, the extreme N-terminus could cross the membrane after the rest of the protein (Curran *et al.*, 2002). The targeting sequences responsible for localization of outer membrane proteins are not highly conserved so it is difficult to predict these sequences. It would be of interest to determine what amino acids in the extreme N-terminus of Tim23 are responsible for targeting and insertion into the MOM. In addition, determining what components of the TOM complex, if any, are necessary for insertion of the Tim23 N-terminus into the MOM would also aid in our understanding of the process.

I investigated the structure and function of the N-terminus of Tim23 in *N. crassa*. The region of Tim23 preceding the dimerization domain is not highly conserved among Tim23 proteins from various organisms and there is no predicted membrane spanning domain. Results discussed here suggest that Tim23 does not span both mitochondrial membranes in *N. crassa*.

Donzeau *et al.*, were able to target the CH2-CH3 domain of human IgG to the outer membrane of isolated yeast mitochondria by fusing the first 62 amino acids of yeast Tim23 to this domain (Donzeau *et al.*, 2000). The import of this fusion construct was dependent on receptors and independent of membrane potential, similar to other outer membrane proteins (Donzeau *et al.*, 2000). The first 67 or 83 amino acids of *N. crassa* Tim23 did not confer the same targeting properties in fusions to DHFR or the CH2-CH3 domain. These data suggest that the N-terminus of Tim23 is not capable of targeting a protein to the MOM.

It is conceivable that the mechanism of insertion of Tim23 into the outer membrane is different in yeast and *N. crassa*. Although the *N. crassa* N-terminal region is not capable of acting as an outer membrane targeting signal, the interaction of this region with the TOM complex during translocation of the Tim23 precursor protein could stimulate insertion. Another possibility is that, in *N. crassa*, insertion of the domain occurs following insertion of Tim23 into the MIM.

To determine if the extreme N-terminal domain of Tim23 was important for function in *N. crassa*, I generated strains expressing only truncated versions of the protein. Removal of the first 10 amino acids is not detrimental to the function of Tim23 as these strains exhibited no growth or import defects. While the removal of the first 50 amino acids of yeast Tim23 is lethal at elevated temperatures (Donzeau *et al.*, 2000), removal of the first 50 amino acids of the *N. crassa* protein resulted in only a slight growth defect at 22°C. Use of mitochondria isolated from this strain for *in vitro* import assays demonstrates an import defect of several precursors targeted to the mitochondrial matrix when the translocase machinery is saturated with a high concentration of precursor proteins. This suggests that this region of the protein is important for full function of the TIM23 translocase. It has been observed previously that mutations in components of the mitochondrial translocase complexes results in abnormal mitochondrial morphology (Harkness *et al.*, 1994; Nargang *et al.*, 1995; Grad *et al.*, 1999; Taylor *et al.*, 2003). In addition to the growth and import defects, mitochondria containing only the shortened version of Tim23 have aberrant morphology as revealed in electron micrographs. Thus the first 50 residues of the *N. crassa* protein are important for the function of Tim23. The possibility that the domain is required for insertion into the MOM cannot be ruled out. Other functions such as association with Tim50, or a role in precursor protein recognition are also possible.

Donzeau *et al.* observed a reduction in the size of yeast Tim23 when whole mitochondria were treated with PK in a low salt buffer, suggesting that a region crossed the MOM and exposed its extreme N-terminus to the cytosol (Donzeau *et al.*, 2000). I was unable to detect a similar effect with *N. crassa* Tim23. PK is a serine protease that cleaves amino acid chains at hydrophobic aliphatic and aromatic residues. There are several sites in the first 50 amino acids of Tim23 at which PK should cleave. This suggests that if a portion of this region were exposed on the surface of the mitochondria, it should be digested readily. However, it is conceivable that the N-terminus of *N. crassa* Tim23 does cross the outer membrane with only a few residues exposed on the surface.

In this situation, it is unlikely that a change in the mobility of the protein due to removal of less than ten residues would be observed as removal of the first 10 amino acids does not change the electrophoretic mobility of the protein (Figure 30). It is also possible that some form of steric interference prevents a cytosolic domain of Tim23 from being digested with PK in *N. crassa*.

I chose to use SCAM to determine the localization of the N-terminal domain of Tim23 in *N. crassa*. The replacement of single amino acids with cysteine should not alter the gross structure of the protein or the possible insertion of the N-terminal domain into the MOM. The accessibility of 15 amino acids spaced throughout the first 62 residues of the protein were chosen to be mapped. The largest gap between these positions was three residues which should not be large enough to span a lipid bilayer. If a domain spanning the MOM exists, at least one of the residues tested should be protected by its location in the bilayer and should not label. On the other hand, if no residues are found in the membrane, every position tested should be accessible to the biotin label. SCAM analysis has been performed to examine the accessibility of amino acids at positions W5, T9, K13, E17, P21, A23, S27, and P29 to biotin maleimide. I have shown that all of these residues are found in a hydrophilic environment as they all label with biotin maleimide when the residue at that position is changed to cysteine.

The topology of the TIM23 complex in *N. crassa* appears to be different than the topology that has been reported in other organisms. The yeast Tim23 protein tethers the complex to the MOM through an outer membrane spanning domain in the N-terminus of the protein (Donzeau *et al.*, 2000). The Tim17 protein in *Arabidopsis* has been shown to contain an outer membrane spanning domain in its C-terminus which results in the same tethering of the TIM23 complex to the MOM (Murcha *et al.*, 2005). Thus, it seems that localization of the TIM23 complex to regions of the inner membrane that are near the outer membrane is functionally important. My analysis suggests that tethering of the *N. crassa* TIM23 complex does not occur through a mechanism similar to yeast. It seems unlikely that Tim17 is responsible as the C-terminal extension that exists in the *Arabidopsis* protein is not found in fungal proteins (Murcha *et al.*, 2005). Studies using a GFP-fusion construct revealed that Tim23 in human cells is excluded from the regions of the MIM that form cristae (John *et al.*, 2005), yet there have been no reports suggesting that human Tim23 contains an N-terminal MOM domain. It is possible that a different mechanism exists in *N. crassa* and humans to limit the distribution of the TIM23 complex in the MIM.

4.3 *N. crassa Tob55*

Tob55 was found to be the major component of the TOB complex in yeast. The complex is responsible for insertion of β-barrel proteins into the MOM (Kozjak *et al.*, 2003; Paschen *et al.*, 2003; Gentle *et al.*, 2004). The conservation of this protein from bacteria to humans highlights the importance of its function (Paschen *et al.*, 2003). Proteins that form β-barrel structures in membranes are unique to mitochondria, chloroplasts and Gram negative bacteria. To gain insight into the mechanistic aspects of β-barrel assembly, it would be advantageous to determine the structure of the Tob55 complex. *N. crassa* is a useful organism for such studies as large quantities of mitochondria can be isolated with relative ease. The use of affinity protein tags can simplify the purification process without interfering with the native structure of the tagged protein. I developed strains of *N. crassa* expressing only tagged versions of the Tob55 protein to facilitate the purification of this complex.

To generate such a strain, I first had to inactivate the wild type allele of *tob55*. I generated a heterokaryotic strain composed of one nucleus with a wild type *tob55* gene and a second where the *tob55* gene was replaced by a resistance marker cassette. The levels of Tob55 can be substantially reduced by manipulation of the heterokaryon forcing the numerical superiority of the knockout nucleus. I have demonstrated that reduced levels of Tob55 result in slow growth and reduced import efficiency of the β-barrel proteins Tom40, porin and Tob55. An observed reduction of Tom22 is probably a secondary effect resulting from reduced levels of Tom40, either a result of decreased import of the Tom40 precursor or decreased assembly to the TOM complex. A similar reduction in the levels of Tom22 was observed in mitochondria containing reduced levels of Tom40 (Taylor *et al.*, 2003) and in mitochondria lacking both Tom6 and Tom7 (Sherman, 2005). The slow growth is likely a result of the inability of this strain to accumulate essential mitochondrial factors *in vivo*. The reduction in Tom40 and the TOM complex probably reduces the import capacity of the mitochondrion to a point that limits growth of the organism. Import of mitochondrial precursors targeted to other compartments including the matrix, MIM and IMS, is not affected by reduced levels of Tob55 *in vitro*. This suggests that Tob55 is involved specifically in the import of proteins to the MOM.

Mitochondria with reduced levels of Tob55 are impaired in the assembly of Tom40. The formation of the first assembly intermediate at 250 kDa is reduced and assembly to the 400 kDa TOM complex is delayed. I also demonstrate that the 250 kDa complex in the Tom40 assembly pathway contains Tob55 as antibodies against the N-terminus of Tob55 supershift the size of that complex. Together, these data confirm that Tob55 is a component of the first assembly intermediate in the Tom40 assembly pathway.

Little is known about the assembly pathway of porin, particularly the *N. crassa* porin. It is not known what each of the complexes observed by BNGE represents. Assembly of porin into all three complexes is impaired when Tob55 levels are reduced. This implies that Tob55 is the first intermediate in the assembly of porin and that the formation of the other complexes is slowed when levels of Tob55 are reduced. I have found that Tob55 is a component of the 270 kDa complex. Antibodies against Tob55 increase the size of this complex on native gels, directly demonstrating that it is a component of this complex. This is the first characterization of the porin assembly pathway that results in the identification of one of the complexes observed by BNGE. From this I conclude that porin interacts with Tob55 during its assembly in a complex of 270 kDa in *N. crassa*.

Identification of the components of the TOB complex in yeast has revealed unique machinery essential for the assembly of β-barrel proteins into the MOM. The mechanism of insertion is not understood, although it seems to be conserved from bacteria to mitochondria in all eukaryotes. In bacteria, outer membrane proteins are inserted from the periplasmic side using Omp85, the bacterial homologue of Tob55 (Gentle *et al.*, 2004). In mitochondria, the IMS is equivalent to the bacterial periplasm and it appears that the β-barrel proteins must be presented from this side of the outer membrane for assembly.

Purification of the TOB complex from *N. crassa* would allow direct identification of proteins associated with Tob55. In addition, further structural analysis could provide insight into the mechanistic aspects of β-barrel insertion into membranes. To facilitate the purification process, I have generated strains of *N. crassa* expressing versions of Tob55 with N-terminal affinity tags. The first is a small tag of six histidine residues that permits the utilization of Ni-NTA chromatography. The second is a larger tag containing six histidine residues, a portion of protein A and a TEV cleavage site that can be used for removal of the tag. Both versions of Tob55 rescue the lethal phenotype of the knockout, suggesting that the protein is functional. The strains I have generated are being used by collaborators for purification of the complex.

REFERENCES

Abe, Y., Shodai, T., Muto, T., Mihara, K., Torii, H., Nishikawa, S., Endo, T., and Kohda, D. (2000). Structural basis of presequence recognition by the mitochondrial protein import receptor Tom20. Cell *100*, 551-560.

Adam, A., Endres, M., Sirrenberg, C., Lottspeich, F., Neupert, W., and Brunner, M. (1999). Tim9, a new component of the TIM22.54 translocase in mitochondria. EMBO J *18*, 313-319.

Ahting, U., Thun, C., Hegerl, R., Typke, D., Nargang, F.E., Neupert, W., and Nussberger, S. (1999). The TOM core complex: the general protein import pore of the outer membrane of mitochondria. J Cell Biol *147*, 959-968.

Ahting, U., Waizenegger, T., Neupert, W., and Rapaport, D. (2005). Signal-anchored Proteins Follow a Unique Insertion Pathway into the Outer Membrane of Mitochondria. J Biol Chem *280*, 48-53.

Alconada, A., Kubrich, M., Moczko, M., Honlinger, A., and Pfanner, N. (1995). The mitochondrial receptor complex: the small subunit Mom8b/Isp6 supports association of receptors with the general insertion pore and transfer of preproteins. Mol Cell Biol *15*, 6196-6205.

Ali, V., Shigeta, Y., Tokumoto, U., Takahashi, Y., and Nozaki, T. (2004). An intestinal parasitic protist, *Entamoeba histolytica*, possesses a non-redundant nitrogen fixation-like system for iron-sulfur cluster assembly under anaerobic conditions. J Biol Chem *279*, 16863-16874.

Allen, J.F. (2003). The function of genomes in bioenergetic organelles. Philos Trans R Soc Lond B Biol Sci *358*, 19-37; discussion 37-18.

Allen, R., Egan, B., Gabriel, K., Beilharz, T., and Lithgow, T. (2002). A conserved proline residue is present in the transmembrane-spanning domain of Tom7 and other tail-anchored protein subunits of the TOM translocase. FEBS Lett *514*, 347-350.

Allen, S., Lu, H., Thornton, D., and Tokatlidis, K. (2003). Juxtaposition of the two distal CX3C motifs via intrachain disulfide bonding is essential for the folding of Tim10. J Biol Chem *278*, 38505-38513.

Altamura, N., Capitanio, N., Bonnefoy, N., Papa, S., and Dujardin, G. (1996). The *Saccharomyces cerevisiae* OXA1 gene is required for the correct assembly of cytochrome *c* oxidase and oligomycin-sensitive ATP synthase. FEBS Lett *382*, 111-115.

Andersson, S.G., and Kurland, C.G. (1999). Origins of mitochondria and hydrogenosomes. Curr Opin Microbiol *2*, 535-541.

Armstrong, L.C., Komiya, T., Bergman, B.E., Mihara, K., and Bornstein, P. (1997). Metaxin is a component of a preprotein import complex in the outer membrane of the mammalian mitochondrion. J Biol Chem *272*, 6510-6518.

Armstrong, L.C., Saenz, A.J., and Bornstein, P. (1999). Metaxin 1 interacts with metaxin 2, a novel related protein associated with the mammalian mitochondrial outer membrane. J Cell Biochem *74*, 11-22.

Arretz, M., Schneider, H., Guiard, B., Brunner, M., and Neupert, W. (1994). Characterization of the mitochondrial processing peptidase of *Neurospora crassa*. J Biol Chem *269*, 4959-4967.

Asai, T., Takahashi, T., Esaki, M., Nishikawa, S., Ohtsuka, K., Nakai, M., and Endo, T. (2004). Reinvestigation of the requirement of cytosolic ATP for mitochondrial protein import. J Biol Chem *279*, 19464-19470.

Atencio, D.P., and Yaffe, M.P. (1992). MAS5, a yeast homolog of DnaJ involved in mitochondrial protein import. Mol Cell Biol *12*, 283-291.

Baker, K.P., Schaniel, A., Vestweber, D., and Schatz, G. (1990). A yeast mitochondrial outer membrane protein essential for protein import and cell viability. Nature *348*, 605-609.

Bartlett, K., and Eaton, S. (2004). Mitochondrial beta-oxidation. Eur J Biochem *271*, 462-469.

Bauer, M., Behrens, M., Esser, K., Michaelis, G., and Pratje, E. (1994). PET1402, a nuclear gene required for proteolytic processing of cytochrome oxidase subunit 2 in yeast. Mol Gen Genet *245*, 272-278.

Bauer, M.F., Gempel, K., Reichert, A.S., Rappold, G.A., Lichtner, P., Gerbitz, K.D., Neupert, W., Brunner, M., and Hofmann, S. (1999). Genetic and structural characterization of the human mitochondrial inner membrane translocase. J Mol Biol *289*, 69-82.

Bauer, M.F., Hofmann, S., Neupert, W., and Brunner, M. (2000). Protein translocation into mitochondria: the role of TIM complexes. Trends Cell Biol *10*, 25-31.

Bauer, M.F., Sirrenberg, C., Neupert, W., and Brunner, M. (1996). Role of Tim23 as voltage sensor and presequence receptor in protein import into mitochondria. Cell *87*, 33-41.

Beasley, E.M., Muller, S., and Schatz, G. (1993). The signal that sorts yeast cytochrome b2 to the mitochondrial intermembrane space contains three distinct functional regions. EMBO J *12*, 2303-2311.

Beddoe, T., and Lithgow, T. (2002). Delivery of nascent polypeptides to the mitochondrial surface. Biochim Biophys Acta *1592*, 35-39.

Berthold, J., Bauer, M.F., Schneider, H.C., Klaus, C., Dietmeier, K., Neupert, W., and Brunner, M. (1995). The MIM complex mediates preprotein translocation across the mitochondrial inner membrane and couples it to the mt-Hsp70/ATP driving system. Cell *81*, 1085-1093.

Binder, J., Hofmann, S., Kreisel, S., Wohrle, J.C., Bazner, H., Krauss, J.K., Hennerici, M.G., and Bauer, M.F. (2003). Clinical and molecular findings in a patient with a novel mutation in the deafness-dystonia peptide (DDP1) gene. Brain *126*, 1814-1820.

Blackstone, C., Roberts, R.G., Seeburg, D.P., and Sheng, M. (2003). Interaction of the deafness-dystonia protein DDP/TIMM8a with the signal transduction adaptor molecule STAM1. Biochem Biophys Res Commun *305*, 345-352.

Blanchard, J.L., and Lynch, M. (2000). Organellar genes: why do they end up in the nucleus? Trends Genet *16*, 315-320.

Blatch, G.L., and Lassle, M. (1999). The tetratricopeptide repeat: a structural motif mediating protein-protein interactions. Bioessays *21*, 932-939.

Blom, J., Kubrich, M., Rassow, J., Voos, W., Dekker, P.J., Maarse, A.C., Meijer, M., and Pfanner, N. (1993). The essential yeast protein MIM44 (encoded by MPI1) is involved in an early step of preprotein translocation across the mitochondrial inner membrane. Mol Cell Biol *13*, 7364-7371.

Bolliger, L., Deloche, O., Glick, B.S., Georgopoulos, C., Jeno, P., Kronidou, N., Horst, M., Morishima, N., and Schatz, G. (1994). A mitochondrial homolog of bacterial GrpE interacts with mitochondrial hsp70 and is essential for viability. EMBO J *13*, 1998-2006.

Bomer, U., Maarse, A.C., Martin, F., Geissler, A., Merlin, A., Schonfisch, B., Meijer, M., Pfanner, N., and Rassow, J. (1998). Separation of structural and dynamic functions of the mitochondrial translocase: Tim44 is crucial for the inner membrane import sites in translocation of tightly folded domains, but not of loosely folded preproteins. EMBO J *17*, 4226-4237.

Bonnefoy, N., Chalvet, F., Hamel, P., Slonimski, P.P., and Dujardin, G. (1994). OXA1, a *Saccharomyces cerevisiae* nuclear gene whose sequence is conserved from prokaryotes to eukaryotes controls cytochrome oxidase biogenesis. J Mol Biol *239*, 201-212.

Bradley, P.J., Lahti, C.J., Plumper, E., and Johnson, P.J. (1997). Targeting and translocation of proteins into the hydrogenosome of the protist Trichomonas: similarities with mitochondrial protein import. EMBO J *16*, 3484-3493.

Brix, J., Dietmeier, K., and Pfanner, N. (1997). Differential recognition of preproteins by the purified cytosolic domains of the mitochondrial import receptors Tom20, Tom22, and Tom70. J Biol Chem *272*, 20730-20735.

Brix, J., Ziegler, G.A., Dietmeier, K., Schneider-Mergener, J., Schulz, G.E., and Pfanner, N. (2000). The mitochondrial import receptor Tom70: identification of a 25 kDa core domain with a specific binding site for preproteins. J Mol Biol *303*, 479-488.

Broadley, S.A., Demlow, C.M., and Fox, T.D. (2001). Peripheral mitochondrial inner membrane protein, Mss2p, required for export of the mitochondrially coded Cox2p C tail in *Saccharomyces cerevisiae*. Mol Cell Biol *21*, 7663-7672.

Bukau, B., and Horwich, A.L. (1998). The Hsp70 and Hsp60 chaperone machines. Cell *92*, 351-366.

Burri, L., Vascotto, K., Fredersdorf, S., Tiedt, R., Hall, M.N., and Lithgow, T. (2004). Zim17, a novel zinc finger protein essential for protein import into mitochondria. J Biol Chem *279*, 50243-50249.

Capaldi, R.A. (2000). The changing face of mitochondrial research. Trends Biochem Sci *25*, 212-214.

Catlett, N.L., and Weisman, L.S. (2000). Divide and multiply: organelle partitioning in yeast. Curr Opin Cell Biol *12*, 509-516.

Cavero, S., Vozza, A., del Arco, A., Palmieri, L., Villa, A., Blanco, E., Runswick, M.J., Walker, J.E., Cerdan, S., Palmieri, F., and Satrustegui, J. (2003). Identification and metabolic role of the mitochondrial aspartate-glutamate transporter in *Saccharomyces cerevisiae*. Mol Microbiol *50*, 1257-1269.

Chacinska, A., Pfannschmidt, S., Wiedemann, N., Kozjak, V., Sanjuan Szklarz, L.K., Schulze-Specking, A., Truscott, K.N., Guiard, B., Meisinger, C., and Pfanner, N. (2004). Essential role of Mia40 in import and assembly of mitochondrial intermembrane space proteins. EMBO J *23*, 3735-3746.

Chacinska, A., Rehling, P., Guiard, B., Frazier, A.E., Schulze-Specking, A., Pfanner, N., Voos, W., and Meisinger, C. (2003). Mitochondrial translocation contact sites: separation of dynamic and stabilizing elements in formation of a TOM-TIM-preprotein supercomplex. EMBO J *22*, 5370-5381.

Chen, R., and Henning, U. (1996). A periplasmic protein (Skp) of *Escherichia coli* selectively binds a class of outer membrane proteins. Mol Microbiol *19*, 1287-1294.

Colot, H.V., Park, G., Ringelberg, C., Curilla, S., Crew, C., Borkovich, KA., and Dunlap, J. C. In preparation.

Corral-Debrinski, M., Blugeon, C., and Jacq, C. (2000). In yeast, the 3' untranslated region or the presequence of ATM1 is required for the exclusive localization of its mRNA to the vicinity of mitochondria. Mol Cell Biol *20*, 7881-7892.

Court, D.A., Kleene, R., Neupert, W., and Lill, R. (1996). Role of the N- and C-termini of porin in import into the outer membrane of *Neurospora* mitochondria. FEBS Lett *390*, 73-77.

Court, D.A., Nargang, F.E., Steiner, H., Hodges, R.S., Neupert, W., and Lill, R. (1996). Role of the intermembrane-space domain of the preprotein receptor Tom22 in protein import into mitochondria. Mol Cell Biol *16*, 4035-4042.

Craig, E.A., Kramer, J., and Kosic-Smithers, J. (1987). SSC1, a member of the 70-kDa heat shock protein multigene family of *Saccharomyces cerevisiae*, is essential for growth. Proc Natl Acad Sci U S A *84*, 4156-4160.

Craig, E.A., Kramer, J., Shilling, J., Werner-Washburne, M., Holmes, S., Kosic-Smithers, J., and Nicolet, C.M. (1989). SSC1, an essential member of the yeast HSP70 multigene family, encodes a mitochondrial protein. Mol Cell Biol *9*, 3000-3008.

Crowley, K.S., and Payne, R.M. (1998). Ribosome binding to mitochondria is regulated by GTP and the transit peptide. J Biol Chem *273*, 17278-17285.

Curran, S.P., Leuenberger, D., Leverich, E.P., Hwang, D.K., Beverly, K.N., and Koehler, C.M. (2004). The role of Hot13p and redox chemistry in the mitochondrial TIM22 import pathway. J Biol Chem *279*, 43744-43751.

Curran, S.P., Leuenberger, D., Oppliger, W., and Koehler, C.M. (2002a). The Tim9p-Tim10p complex binds to the transmembrane domains of the ADP/ATP carrier. EMBO J *21*, 942-953.

Curran, S.P., Leuenberger, D., Schmidt, E., and Koehler, C.M. (2002b). The role of the Tim8p-Tim13p complex in a conserved import pathway for mitochondrial polytopic inner membrane proteins. J Cell Biol *158*, 1017-1027.

D'Agostino, D.M., Ranzato, L., Arrigoni, G., Cavallari, I., Belleudi, F., Torrisi, M.R., Silic-Benussi, M., Ferro, T., Petronilli, V., Marin, O., Chieco-Bianchi, L., Bernardi, P., and Ciminale, V. (2002). Mitochondrial alterations induced by the p13II protein of human T-cell leukemia virus type 1. Critical role of arginine residues. J Biol Chem *277*, 34424-34433.

D'Silva, P., Liu, Q., Walter, W., and Craig, E.A. (2004). Regulated interactions of mtHsp70 with Tim44 at the translocon in the mitochondrial inner membrane. Nat Struct Mol Biol *11*, 1084-1091.

D'Silva, P.D., Schilke, B., Walter, W., Andrew, A., and Craig, E.A. (2003). J protein cochaperone of the mitochondrial inner membrane required for protein import into the mitochondrial matrix. Proc Natl Acad Sci U S A *100*, 13839-13844.

Davis, A.J., Sepuri, N.B., Holder, J., Johnson, A.E., and Jensen, R.E. (2000). Two intermembrane space TIM complexes interact with different domains of Tim23p during its import into mitochondria. J Cell Biol *150*, 1271-1282.

Davis, A.J.a.D.S., F.J. (1970). Genetic and microbiological research techniques for *Neurospora crassa*. Methods Enzymol *17*, 79-143.

De Cock, H., Schafer, U., Potgeter, M., Demel, R., Muller, M., and Tommassen, J. (1999). Affinity of the periplasmic chaperone Skp of Escherichia coli for phospholipids, lipopolysaccharides and non-native outer membrane proteins. Role of Skp in the biogenesis of outer membrane protein. Eur J Biochem *259*, 96-103.

Dekker, P.J., Keil, P., Rassow, J., Maarse, A.C., Pfanner, N., and Meijer, M. (1993). Identification of MIM23, a putative component of the protein import machinery of the mitochondrial inner membrane. FEBS Lett *330*, 66-70.

Dekker, P.J., Martin, F., Maarse, A.C., Bomer, U., Muller, H., Guiard, B., Meijer, M., Rassow, J., and Pfanner, N. (1997). The Tim core complex defines the number of mitochondrial translocation contact sites and can hold arrested preproteins in the absence of matrix Hsp70-Tim44. EMBO J *16*, 5408-5419.

Dekker, P.J., Ryan, M.T., Brix, J., Muller, H., Honlinger, A., and Pfanner, N. (1998). Preprotein translocase of the outer mitochondrial membrane: molecular dissection and assembly of the general import pore complex. Mol Cell Biol *18*, 6515-6524.

DEMBOwski, M., Kunkele, K.P., Nargang, F.E., Neupert, W., and Rapaport, D. (2001). Assembly of Tom6 and Tom7 into the TOM core complex of *Neurospora crassa*. J Biol Chem *276*, 17679-17685.

Deshaies, R.J., Koch, B.D., Werner-Washburne, M., Craig, E.A., and Schekman, R. (1988). A subfamily of stress proteins facilitates translocation of secretory and mitochondrial precursor polypeptides. Nature *332*, 800-805.

Dietmeier, K., Honlinger, A., Bomer, U., Dekker, P.J., Eckerskorn, C., Lottspeich, F., Kubrich, M., and Pfanner, N. (1997). Tom5 functionally links mitochondrial preprotein receptors to the general import pore. Nature *388*, 195-200.

DiMauro, S. (2001). Lessons from mitochondrial DNA mutations. Semin Cell Dev Biol *12*, 397-405.

Donzeau, M., Kaldi, K., Adam, A., Paschen, S., Wanner, G., Guiard, B., Bauer, M.F., Neupert, W., and Brunner, M. (2000). Tim23 links the inner and outer mitochondrial membranes. Cell *101*, 401-412.

Dyall, S.D., Koehler, C.M., Delgadillo-Correa, M.G., Bradley, P.J., Plumper, E., Leuenberger, D., Turck, C.W., and Johnson, P.J. (2000). Presence of a member of the mitochondrial carrier family in hydrogenosomes: conservation of membrane-targeting pathways between hydrogenosomes and mitochondria. Mol Cell Biol *20*, 2488-2497.

Egea, G., Izquierdo, J.M., Ricart, J., San Martin, C., and Cuezva, J.M. (1997). mRNA encoding the beta-subunit of the mitochondrial F1-ATPase complex is a localized mRNA in rat hepatocytes. Biochem J *322 (Pt 2)*, 557-565.

Eilers, M., and Schatz, G. (1986). Binding of a specific ligand inhibits import of a purified precursor protein into mitochondria. Nature *322*, 228-232.

Embley, T.M., van der Giezen, M., Horner, D.S., Dyal, P.L., Bell, S., and Foster, P.G. (2003). Hydrogenosomes, mitochondria and early eukaryotic evolution. IUBMB Life *55*, 387-395.

Emtage, J.L., and Jensen, R.E. (1993). MAS6 encodes an essential inner membrane component of the yeast mitochondrial protein import pathway. J Cell Biol *122*, 1003-1012.

Endo, T., Yamamoto, H., and Esaki, M. (2003). Functional cooperation and separation of translocators in protein import into mitochondria, the double-membrane bounded organelles. J Cell Sci *116*, 3259-3267.

Enns, G.M. (2003). The contribution of mitochondria to common disorders. Mol Genet Metab *80*, 11-26.

Esaki, M., Kanamori, T., Nishikawa, S., and Endo, T. (1999). Two distinct mechanisms drive protein translocation across the mitochondrial outer membrane in the late step of the cytochrome b(2) import pathway. Proc Natl Acad Sci U S A *96*, 11770-11775.

Esaki, M., Shimizu, H., Ono, T., Yamamoto, H., Kanamori, T., Nishikawa, S., and Endo, T. (2004). Mitochondrial protein import. Requirement of presequence elements and tom components for precursor binding to the TOM complex. J Biol Chem *279*, 45701-45707.

Frazier, A.E., Dudek, J., Guiard, B., Voos, W., Li, Y., Lind, M., Meisinger, C., Geissler, A., Sickmann, A., Meyer, H.E., Bilanchone, V., Cumsky, M.G., Truscott, K.N., Pfanner, N., and Rehling, P. (2004). Pam16 has an essential role in the mitochondrial protein import motor. Nat Struct Mol Biol *11*, 226-233.

Frey, T.G., and Mannella, C.A. (2000). The internal structure of mitochondria. Trends Biochem Sci *25*, 319-324.

Fujiki, M., and Verner, K. (1991). Coupling of protein synthesis and mitochondrial import in a homologous yeast in vitro system. J Biol Chem *266*, 6841-6847.

Fujiki, M., and Verner, K. (1993). Coupling of cytosolic protein synthesis and mitochondrial protein import in yeast. Evidence for cotranslational import in vivo. J Biol Chem *268*, 1914-1920.

Funes, S., Nargang, F.E., Neupert, W., and Herrmann, J.M. (2004). The Oxa2 protein of Neurospora crassa plays a critical role in the biogenesis of cytochrome oxidase and defines a ubiquitous subbranch of the Oxa1/YidC/Alb3 protein family. Mol Biol Cell *15*, 1853-1861.

Funfschilling, U., and Rospert, S. (1999). Nascent polypeptide-associated complex stimulates protein import into yeast mitochondria. Mol Biol Cell *10*, 3289-3299.

Gakh, O., Cavadini, P., and Isaya, G. (2002). Mitochondrial processing peptidases. Biochim Biophys Acta *1592*, 63-77.

Galagan, J.E., and Selker, E.U. (2004). RIP: the evolutionary cost of genome defense. Trends Genet *20*, 417-423.

Gautschi, M., Lilie, H., Funfschilling, U., Mun, A., Ross, S., Lithgow, T., Rucknagel, P., and Rospert, S. (2001). RAC, a stable ribosome-associated complex in yeast formed by the DnaK-DnaJ homologs Ssz1p and zuotin. Proc Natl Acad Sci U S A *98*, 3762-3767.

Geissler, A., Chacinska, A., Truscott, K.N., Wiedemann, N., Brandner, K., Sickmann, A., Meyer, H.E., Meisinger, C., Pfanner, N., and Rehling, P. (2002). The mitochondrial presequence translocase: an essential role of Tim50 in directing preproteins to the import channel. Cell *111*, 507-518.

Gentle, I., Gabriel, K., Beech, P., Waller, R., and Lithgow, T. (2004). The Omp85 family of proteins is essential for outer membrane biogenesis in mitochondria and bacteria. J Cell Biol *164*, 19-24.

George, R., Beddoe, T., Landl, K., and Lithgow, T. (1998). The yeast nascent polypeptide-associated complex initiates protein targeting to mitochondria in vivo. Proc Natl Acad Sci U S A *95*, 2296-2301.

Good, A.G., Crosby, W. L. (1989). Anaerobic induction of alanine aminotransferase in barley root tissue. Plant Physiol *90*, 1305-1309.

Grad, L.I., Descheneau, A.T., Neupert, W., Lill, R., and Nargang, F.E. (1999). Inactivation of the *Neurospora crassa* mitochondrial outer membrane protein TOM70 by repeat-induced point mutation (RIP) causes defects in mitochondrial protein import and morphology. Curr Genet *36*, 137-146.

Gratzer, S., Lithgow, T., Bauer, R.E., Lamping, E., Paltauf, F., Kohlwein, S.D., Haucke, V., Junne, T., Schatz, G., and Horst, M. (1995). Mas37p, a novel receptor subunit for protein import into mitochondria. J Cell Biol *129*, 25-34.

Gray, M.W., Burger, G., and Lang, B.F. (2001). The origin and early evolution of mitochondria. Genome Biol *2*, REVIEWS1018.

Grotelueschen, J., and Metzenberg, R.L. (1995). Some property of the nucleus determines the competence of *Neurospora crassa* for transformation. Genetics *139*, 1545-1551.

Hachiya, N., Alam, R., Sakasegawa, Y., Sakaguchi, M., Mihara, K., and Omura, T. (1993). A mitochondrial import factor purified from rat liver cytosol is an ATP-dependent conformational modulator for precursor proteins. EMBO J *12*, 1579-1586.

Hachiya, N., Komiya, T., Alam, R., Iwahashi, J., Sakaguchi, M., Omura, T., and Mihara, K. (1994). MSF, a novel cytoplasmic chaperone which functions in precursor targeting to mitochondria. EMBO J *13*, 5146-5154.

Hachiya, N., Mihara, K., Suda, K., Horst, M., Schatz, G., and Lithgow, T. (1995). Reconstitution of the initial steps of mitochondrial protein import. Nature *376*, 705-709.

Hallermayer, G., Zimmermann, R., and Neupert, W. (1977). Kinetic studies on the transport of cytoplasmically synthesized proteins into the mitochondria in intact cells of Neurospora crassa. Eur J Biochem *81*, 523-532.

Hamajima, S., Sakaguchi, M., Mihara, K., Ono, S., and Sato, R. (1988). Both amino- and carboxy-terminal portions are required for insertion of yeast porin into the outer mitochondrial membrane. J Biochem (Tokyo) *104*, 362-367.

Hammen, P.K., and Weiner, H. (1998). Mitochondrial leader sequences: structural similarities and sequence differences. J Exp Zool *282*, 280-283.

Harkness, T.A., Metzenberg, R.L., Schneider, H., Lill, R., Neupert, W., and Nargang, F.E. (1994). Inactivation of the *Neurospora crassa* gene encoding the mitochondrial protein import receptor MOM19 by the technique of "sheltered RIP". Genetics *136*, 107-118.

Harkness, T.A., Nargang, F.E., van der Klei, I., Neupert, W., and Lill, R. (1994). A crucial role of the mitochondrial protein import receptor MOM19 for the biogenesis of mitochondria. J Cell Biol *124*, 637-648.

Harmey, M.A., Hallermayer, G., Korb, H., and Neupert, W. (1977). Transport of cytoplasmically synthesized proteins into the mitochondria in a cell free system from Neurospora crassa. Eur J Biochem *81*, 533-544.

Hartl, F.U. (1996). Molecular chaperones in cellular protein folding. Nature *381*, 571-579.

Haucke, V., and Schatz, G. (1997). Reconstitution of the protein insertion machinery of the mitochondrial inner membrane. EMBO J *16*, 4560-4567.

Hawlitschek, G., Schneider, H., Schmidt, B., Tropschug, M., Hartl, F.U., and Neupert, W. (1988). Mitochondrial protein import: identification of processing peptidase and of PEP, a processing enhancing protein. Cell *53*, 795-806.

He, S., and Fox, T.D. (1999). Mutations affecting a yeast mitochondrial inner membrane protein, pnt1p, block export of a mitochondrially synthesized fusion protein from the matrix. Mol Cell Biol *19*, 6598-6607.

Hell, K., Herrmann, J., Pratje, E., Neupert, W., and Stuart, R.A. (1997). Oxa1p mediates the export of the N- and C-termini of pCoxII from the mitochondrial matrix to the intermembrane space. FEBS Lett *418*, 367-370.

Herrmann, J.M., and Hell, K. (2005). Chopped, trapped or tacked - protein translocation into the IMS of mitochondria. Trends Biochem Sci *30*, 205-212.

Herrmann, J.M., and Neupert, W. (2003). Protein insertion into the inner membrane of mitochondria. IUBMB Life *55*, 219-225.

Herrmann, J.M., Neupert, W., and Stuart, R.A. (1997). Insertion into the mitochondrial inner membrane of a polytopic protein, the nuclear-encoded Oxa1p. EMBO J *16*, 2217-2226.

Hill, K., Model, K., Ryan, M.T., Dietmeier, K., Martin, F., Wagner, R., and Pfanner, N. (1998). Tom40 forms the hydrophilic channel of the mitochondrial import pore for preproteins [see comment]. Nature *395*, 516-521.

Hines, V., Brandt, A., Griffiths, G., Horstmann, H., Brutsch, H., and Schatz, G. (1990). Protein import into yeast mitochondria is accelerated by the outer membrane protein MAS70. EMBO J *9*, 3191-3200.

Hofmann, S., Rothbauer, U., Muhlenbein, N., Neupert, W., Gerbitz, K.D., Brunner, M., and Bauer, M.F. (2002). The C66W mutation in the deafness dystonia peptide 1 (DDP1) affects the formation of functional DDP1.TIM13 complexes in the mitochondrial intermembrane space. J Biol Chem *277*, 23287-23293.

Hofmann, S.a.B., M.F. (2004). Protein translocation into mammalian mitochondria and its role in development of human mitochondrial disorders. Topics in Current Genetics *8*, 201-225.

Honlinger, A., Bomer, U., Alconada, A., Eckerskorn, C., Lottspeich, F., Dietmeier, K., and Pfanner, N. (1996). Tom7 modulates the dynamics of the mitochondrial outer membrane translocase and plays a pathway-related role in protein import. EMBO J *15*, 2125-2137.

Honlinger, A., Kubrich, M., Moczko, M., Gartner, F., Mallet, L., Bussereau, F., Eckerskorn, C., Lottspeich, F., Dietmeier, K., Jacquet, M., and et al. (1995). The mitochondrial receptor complex: Mom22 is essential for cell viability and directly interacts with preproteins. Mol Cell Biol *15*, 3382-3389.

Hoppins, S.C., and Nargang, F.E. (2004). The Tim8-Tim13 complex of *Neurospora crassa* functions in the assembly of proteins into both mitochondrial membranes. J Biol Chem *279*, 12396-12405.

Hoppins, S.C., Taylor, R.D., Nargang, F.E. (2004). Import of Proteins into Mitochondria. In: The Mycota III Biochemistry and Molecular Biology, ed. R.B.G.A. Marzluf, Berlin-Heidelberg: Springer, 33-44.

Horie, C., Suzuki, H., Sakaguchi, M., and Mihara, K. (2003). Targeting and assembly of mitochondrial tail-anchored protein Tom5 to the TOM complex depend on a signal distinct from that of tail-anchored proteins dispersed in the membrane. J Biol Chem *278*, 41462-41471.

Horst, M., Hilfiker-Rothenfluh, S., Oppliger, W., and Schatz, G. (1995). Dynamic interaction of the protein translocation systems in the inner and outer membranes of yeast mitochondria. EMBO J *14*, 2293-2297.

Horst, M., Oppliger, W., Rospert, S., Schonfeld, H.J., Schatz, G., and Azem, A. (1997). Sequential action of two hsp70 complexes during protein import into mitochondria. EMBO J *16*, 1842-1849.

Horwich, A.L., Kalousek, F., Fenton, W.A., Furtak, K., Pollock, R.A., and Rosenberg, L.E. (1987). The ornithine transcarbamylase leader peptide directs mitochondrial import through both its midportion structure and net positive charge. J Cell Biol *105*, 669-677.

Huang, S., Ratliff, K.S., Schwartz, M.P., Spenner, J.M., and Matouschek, A. (1999). Mitochondria unfold precursor proteins by unraveling them from their N-termini. Nat Struct Biol *6*, 1132-1138.

Humphries, A.D., Streimann, I.C., Stojanovski, D., Johnston, A.J., Yano, M., Hoogenraad, N.J., and Ryan, M.T. (2005). Dissection of the mitochondrial import and assembly pathway for human TOM40. J Biol Chem.

Ikeda, E., Yoshida, S., Mitsuzawa, H., Uno, I., and Toh-e, A. (1994). YGE1 is a yeast homologue of *Escherichia coli* grpE and is required for maintenance of mitochondrial functions. FEBS Lett *339*, 265-268.

Irelan, J.T., and Selker, E.U. (1997). Cytosine methylation associated with repeat-induced point mutation causes epigenetic gene silencing in *Neurospora crassa*. Genetics *146*, 509-523.

Isaya, G., Miklos, D., and Rollins, R.A. (1994). MIP1, a new yeast gene homologous to the rat mitochondrial intermediate peptidase gene, is required for oxidative metabolism in *Saccharomyces cerevisiae*. Mol Cell Biol *14*, 5603-5616.

Ishikawa, D., Yamamoto, H., Tamura, Y., Moritoh, K., and Endo, T. (2004). Two novel proteins in the mitochondrial outer membrane mediate beta-barrel protein assembly. J Cell Biol *166*, 621-627.

Jarosch, E., Rodel, G., and Schweyen, R.J. (1997). A soluble 12-kDa protein of the mitochondrial intermembrane space, Mrs11p, is essential for mitochondrial biogenesis and viability of yeast cells. Mol Gen Genet *255*, 157-165.

Jarosch, E., Tuller, G., Daum, G., Waldherr, M., Voskova, A., and Schweyen, R.J. (1996). Mrs5p, an essential protein of the mitochondrial intermembrane space, affects protein import into yeast mitochondria. J Biol Chem *271*, 17219-17225.

Jia, L., Dienhart, M., Schramp, M., McCauley, M., Hell, K., and Stuart, R.A. (2003). Yeast Oxa1 interacts with mitochondrial ribosomes: the importance of the C-terminal region of Oxa1. EMBO J *22*, 6438-6447.

John, G.B., Shang, Y., Li, L., Renken, C., Mannella, C.A., Selker, J.M., Rangell, L., Bennett, M.J., and Zha, J. (2005). The mitochondrial inner membrane protein mitofilin controls cristae morphology. Mol Biol Cell *16*, 1543-1554.

Johnston, A.J., Hoogenraad, J., Dougan, D.A., Truscott, K.N., Yano, M., Mori, M., Hoogenraad, N.J., and Ryan, M.T. (2002). Insertion and assembly of human tom7 into the preprotein translocase complex of the outer mitochondrial membrane. J Biol Chem *277*, 42197-42204.

Joseph-Horne, T., Hollomon, D.W., and Wood, P.M. (2001). Fungal respiration: a fusion of standard and alternative components. Biochim Biophys Acta *1504*, 179-195.

Kaldi, K., Bauer, M.F., Sirrenberg, C., Neupert, W., and Brunner, M. (1998). Biogenesis of Tim23 and Tim17, integral components of the TIM machinery for matrix-targeted preproteins. EMBO J *17*, 1569-1576.

Kanaji, S., Iwahashi, J., Kida, Y., Sakaguchi, M., and Mihara, K. (2000). Characterization of the signal that directs Tom20 to the mitochondrial outer membrane. J Cell Biol *151*, 277-288.

Kang, P.J., Ostermann, J., Shilling, J., Neupert, W., Craig, E.A., and Pfanner, N. (1990). Requirement for hsp70 in the mitochondrial matrix for translocation and folding of precursor proteins. Nature *348*, 137-143.

Karlberg, O., Canback, B., Kurland, C.G., and Andersson, S.G. (2000). The dual origin of the yeast mitochondrial proteome. Yeast *17*, 170-187.

Kassenbrock, C.K., Cao, W., and Douglas, M.G. (1993). Genetic and biochemical characterization of ISP6, a small mitochondrial outer membrane protein associated with the protein translocation complex. EMBO J *12*, 3023-3034.

Kaufmann, T., Schlipf, S., Sanz, J., Neubert, K., Stein, R., and Borner, C. (2003). Characterization of the signal that directs Bcl-x(L), but not Bcl-2, to the mitochondrial outer membrane. J Cell Biol *160*, 53-64.

Keil, P., Weinzierl, A., Kiebler, M., Dietmeier, K., Sollner, T., and Pfanner, N. (1993). Biogenesis of the mitochondrial receptor complex. Two receptors are required for binding of MOM38 to the outer membrane surface. J Biol Chem *268*, 19177-19180.

Kellems, R.E., Allison, V.F., and Butow, R.A. (1975). Cytoplasmic type 80S ribosomes associated with yeast mitochondria. IV. Attachment of ribosomes to the outer membrane of isolated mitochondria. J Cell Biol *65*, 1-14.

Kelley, W.L. (1998). The J-domain family and the recruitment of chaperone power. Trends Biochem Sci *23*, 222-227.

Kennell, J.C., Collins, R.A., Griffiths, A.J.F., Nargang, F.E. (2004). Mitochondrial Genetics of *Neurospora*. The Mycota, Vol. 2: Genetics and Biotechnology. 2nd Edition. 95-112.

Kerscher, O., Holder, J., Srinivasan, M., Leung, R.S., and Jensen, R.E. (1997). The Tim54p-Tim22p complex mediates insertion of proteins into the mitochondrial inner membrane. J Cell Biol *139*, 1663-1675.

Kerscher, O., Sepuri, N.B., and Jensen, R.E. (2000). Tim18p is a new component of the Tim54p-Tim22p translocon in the mitochondrial inner membrane. Mol Biol Cell *11*, 103-116.

Kiebler, M., Keil, P., Schneider, H., van der Klei, I.J., Pfanner, N., and Neupert, W. (1993). The mitochondrial receptor complex: a central role of MOM22 in mediating preprotein transfer from receptors to the general insertion pore. Cell *74*, 483-492.

Kiebler, M., Pfaller, R., Sollner, T., Griffiths, G., Horstmann, H., Pfanner, N., and Neupert, W. (1990). Identification of a mitochondrial receptor complex required for recognition and membrane insertion of precursor proteins. Nature *348*, 610-616.

Kispal, G., Csere, P., Prohl, C., and Lill, R. (1999). The mitochondrial proteins Atm1p and Nfs1p are essential for biogenesis of cytosolic Fe/S proteins. EMBO J *18*, 3981-3989.

Knight, S.A., Kim, R., Pain, D., and Dancis, A. (1999). The yeast connection to Friedreich ataxia. Am J Hum Genet *64*, 365-371.

Knox, C., Sass, E., Neupert, W., and Pines, O. (1998). Import into mitochondria, folding and retrograde movement of fumarase in yeast. J Biol Chem *273*, 25587-25593.

Koehler, C.M. (2004). New developments in mitochondrial assembly. Annu Rev Cell Dev Biol *20*, 309-335.

Koehler, C.M. (2004). The small Tim proteins and the twin Cx3C motif. Trends Biochem Sci *29*, 1-4.

Koehler, C.M., Jarosch, E., Tokatlidis, K., Schmid, K., Schweyen, R.J., and Schatz, G. (1998). Import of mitochondrial carriers mediated by essential proteins of the intermembrane space. Science *279*, 369-373.

Koehler, C.M., Leuenberger, D., Merchant, S., Renold, A., Junne, T., and Schatz, G. (1999). Human deafness dystonia syndrome is a mitochondrial disease. Proc Natl Acad Sci U S A *96*, 2141-2146.

Koehler, C.M., Merchant, S., Oppliger, W., Schmid, K., Jarosch, E., Dolfini, L., Junne, T., Schatz, G., and Tokatlidis, K. (1998). Tim9p, an essential partner subunit of Tim10p for the import of mitochondrial carrier proteins. EMBO J *17*, 6477-6486.

Koehler, C.M., Murphy, M.P., Bally, N.A., Leuenberger, D., Oppliger, W., Dolfini, L., Junne, T., Schatz, G., and Or, E. (2000). Tim18p, a new subunit of the TIM22 complex that mediates insertion of imported proteins into the yeast mitochondrial inner membrane. Mol Cell Biol *20*, 1187-1193.

Komiya, T., Hachiya, N., Sakaguchi, M., Omura, T., and Mihara, K. (1994). Recognition of mitochondria-targeting signals by a cytosolic import stimulation factor, MSF. J Biol Chem *269*, 30893-30897.

Komiya, T., Rospert, S., Schatz, G., and Mihara, K. (1997). Binding of mitochondrial precursor proteins to the cytoplasmic domains of the import receptors Tom70 and Tom20 is determined by cytoplasmic chaperones. EMBO J *16*, 4267-4275.

Komiya, T., Sakaguchi, M., and Mihara, K. (1996). Cytoplasmic chaperones determine the targeting pathway of precursor proteins to mitochondria. EMBO J *15*, 399-407.

Kovermann, P., Truscott, K.N., Guiard, B., Rehling, P., Sepuri, N.B., Muller, H., Jensen, R.E., Wagner, R., and Pfanner, N. (2002). Tim22, the essential core of the mitochondrial protein insertion complex, forms a voltage-activated and signal-gated channel. Mol Cell *9*, 363-373.

Kozany, C., Mokranjac, D., Sichting, M., Neupert, W., and Hell, K. (2004). The J domain-related cochaperone Tim16 is a constituent of the mitochondrial TIM23 preprotein translocase. Nat Struct Mol Biol *11*, 234-241.

Kozjak, V., Wiedemann, N., Milenkovic, D., Lohaus, C., Meyer, H.E., Guiard, B., Meisinger, C., and Pfanner, N. (2003). An essential role of Sam50 in the protein sorting and assembly machinery of the mitochondrial outer membrane. J Biol Chem *278*, 48520-48523.

Krimmer, T., Rapaport, D., Ryan, M.T., Meisinger, C., Kassenbrock, C.K., Blachly-Dyson, E., Forte, M., Douglas, M.G., Neupert, W., Nargang, F.E., and Pfanner, N. (2001). Biogenesis of porin of the outer mitochondrial membrane involves an import pathway via receptors and the general import pore of the TOM complex. J Cell Biol *152*, 289-300.

Kubrich, M., Keil, P., Rassow, J., Dekker, P.J., Blom, J., Meijer, M., and Pfanner, N. (1994). The polytopic mitochondrial inner membrane proteins MIM17 and MIM23 operate at the same preprotein import site. FEBS Lett *349*, 222-228.

Kunkele, K.P., Heins, S., DEMBOwski, M., Nargang, F.E., Benz, R., Thieffry, M., Walz, J., Lill, R., Nussberger, S., and Neupert, W. (1998). The preprotein translocation channel of the outer membrane of mitochondria. Cell *93*, 1009-1019.

Kunkele, K.P., Juin, P., Pompa, C., Nargang, F.E., Henry, J.P., Neupert, W., Lill, R., and Thieffry, M. (1998). The isolated complex of the translocase of the outer membrane of mitochondria. Characterization of the cation-selective and voltage-gated preprotein-conducting pore. J Biol Chem *273*, 31032-31039.

Kuroda, R., Ikenoue, T., Honsho, M., Tsujimoto, S., Mitoma, J.Y., and Ito, A. (1998). Charged amino acids at the carboxyl-terminal portions determine the intracellular locations of two isoforms of cytochrome b5. J Biol Chem *273*, 31097-31102.

Kurz, M., Martin, H., Rassow, J., Pfanner, N., and Ryan, M.T. (1999). Biogenesis of Tim proteins of the mitochondrial carrier import pathway: differential targeting mechanisms and crossing over with the main import pathway. Mol Biol Cell *10*, 2461-2474.

Laemmli, U.K. (1970). Cleavage of structural proteins during the assembly of the head of bacteriophage T4. Nature *227*, 680-685.

Laloraya, S., Gambill, B.D., and Craig, E.A. (1994). A role for a eukaryotic GrpE-related protein, Mge1p, in protein translocation. Proc Natl Acad Sci U S A *91*, 6481-6485.

Lee, C.M., Sedman, J., Neupert, W., and Stuart, R.A. (1999). The DNA helicase, Hmi1p, is transported into mitochondria by a C-terminal cleavable targeting signal. J Biol Chem *274*, 20937-20942.

Leon-Avila, G., and Tovar, J. (2004). Mitosomes of *Entamoeba histolytica* are abundant mitochondrion-related remnant organelles that lack a detectable organellar genome. Microbiology *150*, 1245-1250.

Leuenberger, D., Bally, N.A., Schatz, G., and Koehler, C.M. (1999). Different import pathways through the mitochondrial intermembrane space for inner membrane proteins. EMBO J *18*, 4816-4822.

Lightowlers, R.N., Chinnery, P.F., Turnbull, D.M., and Howell, N. (1997). Mammalian mitochondrial genetics: heredity, heteroplasmy and disease. Trends Genet *13*, 450-455.

Lill, R., and Kispal, G. (2000). Maturation of cellular Fe-S proteins: an essential function of mitochondria. Trends Biochem Sci *25*, 352-356.

Lithgow, T., Junne, T., Suda, K., Gratzer, S., and Schatz, G. (1994). The mitochondrial outer membrane protein Mas22p is essential for protein import and viability of yeast. Proc Natl Acad Sci U S A *91*, 11973-11977.

Lithgow, T., Junne, T., Wachter, C., and Schatz, G. (1994). Yeast mitochondria lacking the two import receptors Mas20p and Mas70p can efficiently and specifically import precursor proteins. J Biol Chem *269*, 15325-15330.

Liu, Q., D'Silva, P., Walter, W., Marszalek, J., and Craig, E.A. (2003). Regulated cycling of mitochondrial Hsp70 at the protein import channel. Science *300*, 139-141.

Lohret, T.A., Jensen, R.E., and Kinnally, K.W. (1997). Tim23, a protein import component of the mitochondrial inner membrane, is required for normal activity of the multiple conductance channel, MCC. J Cell Biol *137*, 377-386.

Lu, H., Allen, S., Wardleworth, L., Savory, P., and Tokatlidis, K. (2004). Functional TIM10 chaperone assembly is redox-regulated in vivo. J Biol Chem *279*, 18952-18958.

Lu, H., Golovanov, A.P., Alcock, F., Grossmann, J.G., Allen, S., Lian, L.Y., and Tokatlidis, K. (2004). The structural basis of the TIM10 chaperone assembly. J Biol Chem *279*, 18959-18966.

Lutz, T., Neupert, W., and Herrmann, J.M. (2003). Import of small Tim proteins into the mitochondrial intermembrane space. EMBO J *22*, 4400-4408.

Maarse, A.C., Blom, J., Grivell, L.A., and Meijer, M. (1992). MPI1, an essential gene encoding a mitochondrial membrane protein, is possibly involved in protein import into yeast mitochondria. EMBO J *11*, 3619-3628.

Maarse, A.C., Blom, J., Keil, P., Pfanner, N., and Meijer, M. (1994). Identification of the essential yeast protein MIM17, an integral mitochondrial inner membrane protein involved in protein import. FEBS Lett *349*, 215-221.

Maccecchini, M.L., Rudin, Y., Blobel, G., and Schatz, G. (1979). Import of proteins into mitochondria: precursor forms of the extramitochondrially made F1-ATPase subunits in yeast. Proc Natl Acad Sci U S A *76*, 343-347.

MacKenzie, J.A., and Payne, R.M. (2004). Ribosomes specifically bind to mammalian mitochondria via protease-sensitive proteins on the outer membrane. J Biol Chem *279*, 9803-9810.

Mannella, C.A. (1996). Mitochondrial channels revisited. J Bioenerg Biomembr *28*, 89-91.

Mansy, S.S., and Cowan, J.A. (2004). Iron-sulfur cluster biosynthesis: toward an understanding of cellular machinery and molecular mechanism. Acc Chem Res *37*, 719-725.

Marc, P., Margeot, A., Devaux, F., Blugeon, C., Corral-Debrinski, M., and Jacq, C. (2002). Genome-wide analysis of mRNAs targeted to yeast mitochondria. EMBO Rep *3*, 159-164.

Margolin, B.S., Freitag, M., Selker, E.U. (1997). Improved plasmids for gene targeting at the his-3 locus of *Neurospora crassa* by electroporation. Fungal Genet Newslett. *44*, 34-36.

Margolin, B.S., Freitag, M., Selker, E.U. (2000). Improved plasmids for gene targeting at the his-3 locus of *Neurospora crassa* by electoporation:correction. fungal Genet Newslett. *47*, 112.

Martin, W., Hoffmeister, M., Rotte, C., and Henze, K. (2001). An overview of endosymbiotic models for the origins of eukaryotes, their ATP-producing organelles (mitochondria and hydrogenosomes), and their heterotrophic lifestyle. Biol Chem *382*, 1521-1539.

Martin, W., and Muller, M. (1998). The hydrogen hypothesis for the first eukaryote. Nature *392*, 37-41.

Mayer, A., Lill, R., and Neupert, W. (1993). Translocation and insertion of precursor proteins into isolated outer membranes of mitochondria. J Cell Biol *121*, 1233-1243.

Mayer, A., Nargang, F.E., Neupert, W., and Lill, R. (1995). MOM22 is a receptor for mitochondrial targeting sequences and cooperates with MOM19. EMBO J *14*, 4204-4211.

Mayer, A., Neupert, W., and Lill, R. (1995). Mitochondrial protein import: reversible binding of the presequence at the trans side of the outer membrane drives partial translocation and unfolding. Cell *80*, 127-137.

McBride, H.M., Millar, D.G., Li, J.M., and Shore, G.C. (1992). A signal-anchor sequence selective for the mitochondrial outer membrane. J Cell Biol *119*, 1451-1457.

Meisinger, C., Rissler, M., Chacinska, A., Szklarz, L.K., Milenkovic, D., Kozjak, V., Schonfisch, B., Lohaus, C., Meyer, H.E., Yaffe, M.P., Guiard, B., Wiedemann, N., and Pfanner, N. (2004). The mitochondrial morphology protein Mdm10 functions in assembly of the preprotein translocase of the outer membrane. Dev Cell *7*, 61-71.

Meisinger, C., Ryan, M.T., Hill, K., Model, K., Lim, J.H., Sickmann, A., Muller, H., Meyer, H.E., Wagner, R., and Pfanner, N. (2001). Protein import channel of the outer mitochondrial membrane: a highly stable Tom40-Tom22 core structure differentially interacts with preproteins, small tom proteins, and import receptors. Mol Cell Biol *21*, 2337-2348.

Merlin, A., Voos, W., Maarse, A.C., Meijer, M., Pfanner, N., and Rassow, J. (1999). The J-related segment of tim44 is essential for cell viability: a mutant Tim44 remains in the mitochondrial import site, but inefficiently recruits mtHsp70 and impairs protein translocation. J Cell Biol *145*, 961-972.

Metzenberg, R.L., Stevens, J.N., Selker, E.U., and Morzycka-Wroblewska, E. (1985). Identification and chromosomal distribution of 5S rRNA genes in *Neurospora crassa*. Proc Natl Acad Sci U S A *82*, 2067-2071.

Metzenberg, R.L., Stevens, J., Selker, E., Morzycka-Wroblewska, E. (1984). A method for finding the genetic map position of cloned DNA fragments. Neurospora Newsl *31*, 35-39.

Metzenberg, R.L.a.G., J.S. (1992). Disruption of essential genes in *Neurospora* by RIP. Fungal Genet Newslett. *39*, 37-49.

Milenkovic, D., Kozjak, V., Wiedemann, N., Lohaus, C., Meyer, H.E., Guiard, B., Pfanner, N., and Meisinger, C. (2004). Sam35 of the mitochondrial protein sorting and assembly machinery is a peripheral outer membrane protein essential for cell viability. J Biol Chem *279*, 22781-22785.

Milisav, I., Moro, F., Neupert, W., and Brunner, M. (2001). Modular structure of the TIM23 preprotein translocase of mitochondria. J Biol Chem *276*, 25856-25861.

Moczko, M., Bomer, U., Kubrich, M., Zufall, N., Honlinger, A., and Pfanner, N. (1997). The intermembrane space domain of mitochondrial Tom22 functions as a trans binding site for preproteins with N-terminal targeting sequences. Mol Cell Biol *17*, 6574-6584.

Moczko, M., Dietmeier, K., Sollner, T., Segui, B., Steger, H.F., Neupert, W., and Pfanner, N. (1992). Identification of the mitochondrial receptor complex in Saccharomyces cerevisiae. FEBS Lett *310*, 265-268.

Moczko, M., Ehmann, B., Gartner, F., Honlinger, A., Schafer, E., and Pfanner, N. (1994). Deletion of the receptor MOM19 strongly impairs import of cleavable preproteins into Saccharomyces cerevisiae mitochondria. J Biol Chem *269*, 9045-9051.

Model, K., Meisinger, C., Prinz, T., Wiedemann, N., Truscott, K.N., Pfanner, N., and Ryan, M.T. (2001). Multistep assembly of the protein import channel of the mitochondrial outer membrane. Nat Struct Biol *8*, 361-370.

Model, K., Prinz, T., Ruiz, T., Radermacher, M., Krimmer, T., Kuhlbrandt, W., Pfanner, N., and Meisinger, C. (2002). Protein translocase of the outer mitochondrial membrane: role of import receptors in the structural organization of the TOM complex. J Mol Biol *316*, 657-666.

Mohr, J., and Mageroy, K. (1960). Sex-linked deafness of a possibly new type. Acta Genet Stat Med *10*, 54-62.

Mokranjac, D., Paschen, S.A., Kozany, C., Prokisch, H., Hoppins, S.C., Nargang, F.E., Neupert, W., and Hell, K. (2003). Tim50, a novel component of the TIM23 preprotein translocase of mitochondria. EMBO J *22*, 816-825.

Mokranjac, D., Sichting, M., Neupert, W., and Hell, K. (2003). Tim14, a novel key component of the import motor of the TIM23 protein translocase of mitochondria. EMBO J *22*, 4945-4956.

Moro, F., Okamoto, K., Donzeau, M., Neupert, W., and Brunner, M. (2002). Mitochondrial protein import: molecular basis of the ATP-dependent interaction of MtHsp70 with Tim44. J Biol Chem *277*, 6874-6880.

Moro, F., Sirrenberg, C., Schneider, H.C., Neupert, W., and Brunner, M. (1999). The TIM17.23 preprotein translocase of mitochondria: composition and function in protein transport into the matrix. EMBO J *18*, 3667-3675.

Muhlenbein, N., Hofmann, S., Rothbauer, U., and Bauer, M.F. (2004). Organization and function of the small Tim complexes acting along the import pathway of metabolite carriers into mammalian mitochondria. J Biol Chem *279*, 13540-13546.

Muhlenhoff, U., and Lill, R. (2000). Biogenesis of iron-sulfur proteins in eukaryotes: a novel task of mitochondria that is inherited from bacteria. Biochim Biophys Acta *1459*, 370-382.

Mukhopadhyay, A., Heard, T.S., Wen, X., Hammen, P.K., and Weiner, H. (2003). Location of the actual signal in the negatively charged leader sequence involved in the import into the mitochondrial matrix space. J Biol Chem *278*, 13712-13718.

Mukhopadhyay, A., Ni, L., and Weiner, H. (2004). A co-translational model to explain the in vivo import of proteins into HeLa cell mitochondria. Biochem J *382*, 385-392.

Murakami, H., Pain, D., and Blobel, G. (1988). 70-kD heat shock-related protein is one of at least two distinct cytosolic factors stimulating protein import into mitochondria. J Cell Biol *107*, 2051-2057.

Murcha, M.W., Elhafez, D., Millar, A.H., and Whelan, J. (2005). The C-terminal region of TIM 17 links the outer and inner mitochondrial membranes in arabidopsis and is essential for protein import. J Biol Chem.

Murphy, M.P., Leuenberger, D., Curran, S.P., Oppliger, W., and Koehler, C.M. (2001). The essential function of the small Tim proteins in the TIM22 import pathway does not depend on formation of the soluble 70-kilodalton complex. Mol Cell Biol *21*, 6132-6138.

Muto, T., Obita, T., Abe, Y., Shodai, T., Endo, T., and Kohda, D. (2001). NMR identification of the Tom20 binding segment in mitochondrial presequences. J Mol Biol *306*, 137-143.

Nakai, M., and Endo, T. (1995). Identification of yeast MAS17 encoding the functional counterpart of the mitochondrial receptor complex protein MOM22 of Neurospora crassa. FEBS Lett *357*, 202-206.

Nakai, M., Kato, Y., Ikeda, E., Toh-e, A., and Endo, T. (1994). Yge1p, a eukaryotic GrpE homolog, is localized in the mitochondrial matrix and interacts with mitochondrial Hsp70. Biochem Biophys Res Commun *200*, 435-442.

Naoe, M., Ohwa, Y., Ishikawa, D., Ohshima, C., Nishikawa, S., Yamamoto, H., and Endo, T. (2004). Identification of Tim40 that mediates protein sorting to the mitochondrial intermembrane space. J Biol Chem *279*, 47815-47821.

Nargang, F.E., Kunkele, K.P., Mayer, A., Ritzel, R.G., Neupert, W., and Lill, R. (1995). 'Sheltered disruption' of *Neurospora crassa* MOM22, an essential component of the mitochondrial protein import complex. EMBO J *14*, 1099-1108.

Nargang, F.E., Preuss, M., Neupert, W., and Herrmann, J.M. (2002). The Oxa1 protein forms a homooligomeric complex and is an essential part of the mitochondrial export translocase in *Neurospora crassa*. J Biol Chem *277*, 12846-12853.

Nargang, F.E., Rapaport, D., Ritzel, R.G., Neupert, W., and Lill, R. (1998). Role of the negative charges in the cytosolic domain of TOM22 in the import of precursor proteins into mitochondria. Mol Cell Biol *18*, 3173-3181.

Neupert, W., and Brunner, M. (2002). The protein import motor of mitochondria. Nat Rev Mol Cell Biol *3*, 555-565.

Ni, L., Heard, T.S., and Weiner, H. (1999). In vivo mitochondrial import. A comparison of leader sequence charge and structural relationships with the in vitro model resulting in evidence for co-translational import. J Biol Chem *274*, 12685-12691.

Okamoto, K., Brinker, A., Paschen, S.A., Moarefi, I., Hayer-Hartl, M., Neupert, W., and Brunner, M. (2002). The protein import motor of mitochondria: a targeted molecular ratchet driving unfolding and translocation. EMBO J *21*, 3659-3671.

Palmieri, L., Pardo, B., Lasorsa, F.M., del Arco, A., Kobayashi, K., Iijima, M., Runswick, M.J., Walker, J.E., Saheki, T., Satrustegui, J., and Palmieri, F. (2001). Citrin and aralar1 are Ca(2+)-stimulated aspartate/glutamate transporters in mitochondria. EMBO J *20*, 5060-5069.

Paschen, S.A., and Neupert, W. (2001). Protein import into mitochondria. IUBMB Life *52*, 101-112.

Paschen, S.A., Rothbauer, U., Kaldi, K., Bauer, M.F., Neupert, W., and Brunner, M. (2000). The role of the TIM8-13 complex in the import of Tim23 into mitochondria. EMBO J *19*, 6392-6400.

Paschen, S.A., Waizenegger, T., Stan, T., Preuss, M., Cyrklaff, M., Hell, K., Rapaport, D., and Neupert, W. (2003). Evolutionary conservation of biogenesis of beta-barrel membrane proteins. Nature *426*, 862-866.

Pfanner, N., Hoeben, P., Tropschug, M., and Neupert, W. (1987). The carboxyl-terminal two-thirds of the ADP/ATP carrier polypeptide contains sufficient information to direct translocation into mitochondria. J Biol Chem *262*, 14851-14854.

Pfanner, N., and Neupert, W. (1990). The mitochondrial protein import apparatus. Annu Rev Biochem *59*, 331-353.

Pfanner, N., Wiedemann, N., Meisinger, C., and Lithgow, T. (2004). Assembling the mitochondrial outer membrane. Nat Struct Mol Biol *11*, 1044-1048.

Preuss, M., Leonhard, K., Hell, K., Stuart, R.A., Neupert, W., and Herrmann, J.M. (2001). Mba1, a novel component of the mitochondrial protein export machinery of the yeast Saccharomyces cerevisiae. J Cell Biol *153*, 1085-1096.

Prokisch, H., Nussberger, S., and Westermann, B. (2002). Protein import into mitochondria of *Neurospora crassa*. Fungal Genet Biol *36*, 85-90.

Ramage, L., Junne, T., Hahne, K., Lithgow, T., and Schatz, G. (1993). Functional cooperation of mitochondrial protein import receptors in yeast. EMBO J *12*, 4115-4123.

Rapaport, D. (2003). Finding the right organelle. Targeting signals in mitochondrial outer-membrane proteins. EMBO Rep *4*, 948-952.

Rapaport, D., Kunkele, K.P., DEMBOwski, M., Ahting, U., Nargang, F.E., Neupert, W., and Lill, R. (1998). Dynamics of the TOM complex of mitochondria during binding and translocation of preproteins. Mol Cell Biol *18*, 5256-5262.

Rapaport, D., Mayer, A., Neupert, W., and Lill, R. (1998). cis and trans sites of the TOM complex of mitochondria in unfolding and initial translocation of preproteins. J Biol Chem *273*, 8806-8813.

Rapaport, D., and Neupert, W. (1999). Biogenesis of Tom40, core component of the TOM complex of mitochondria. J Cell Biol *146*, 321-331.

Rapaport, D., Neupert, W., and Lill, R. (1997). Mitochondrial protein import. Tom40 plays a major role in targeting and translocation of preproteins by forming a specific binding site for the presequence. J Biol Chem *272*, 18725-18731.

Rapaport, D., Taylor, R.D., Kaser, M., Langer, T., Neupert, W., and Nargang, F.E. (2001). Structural requirements of Tom40 for assembly into preexisting TOM complexes of mitochondria. Mol Biol Cell *12*, 1189-1198.

Rassow, J., Guiard, B., Wienhues, U., Herzog, V., Hartl, F.U., and Neupert, W. (1989). Translocation arrest by reversible folding of a precursor protein imported into mitochondria. A means to quantitate translocation contact sites. J Cell Biol *109*, 1421-1428.

Rassow, J., Maarse, A.C., Krainer, E., Kubrich, M., Muller, H., Meijer, M., Craig, E.A., and Pfanner, N. (1994). Mitochondrial protein import: biochemical and genetic evidence for interaction of matrix hsp70 and the inner membrane protein MIM44. J Cell Biol *127*, 1547-1556.

Rassow, J., Voos, W., and Pfanner, N. (1995). Partner proteins determine multiple functions of Hsp70. Trends Cell Biol *5*, 207-212.

Rehling, P., Brandner, K., and Pfanner, N. (2004). Mitochondrial import and the twin-pore translocase. Nat Rev Mol Cell Biol *5*, 519-530.

Rehling, P., Model, K., Brandner, K., Kovermann, P., Sickmann, A., Meyer, H.E., Kuhlbrandt, W., Wagner, R., Truscott, K.N., and Pfanner, N. (2003). Protein insertion into the mitochondrial inner membrane by a twin-pore translocase. Science *299*, 1747-1751.

Rehling, P., Pfanner, N., and Meisinger, C. (2003). Insertion of hydrophobic membrane proteins into the inner mitochondrial membrane--a guided tour. J Mol Biol *326*, 639-657.

Rizzitello, A.E., Harper, J.R., and Silhavy, T.J. (2001). Genetic evidence for parallel pathways of chaperone activity in the periplasm of Escherichia coli. J Bacteriol *183*, 6794-6800.

Roesch, K., Curran, S.P., Tranebjaerg, L., and Koehler, C.M. (2002). Human deafness dystonia syndrome is caused by a defect in assembly of the DDP1/TIMM8a-TIMM13 complex. Hum Mol Genet *11*, 477-486.

Roesch, K., Hynds, P.J., Varga, R., Tranebjaerg, L., and Koehler, C.M. (2004). The calcium-binding aspartate/glutamate carriers, citrin and aralar1, are new substrates for the DDP1/TIMM8a-TIMM13 complex. Hum Mol Genet *13*, 2101-2111.

Roise, D., Theiler, F., Horvath, S.J., Tomich, J.M., Richards, J.H., Allison, D.S., and Schatz, G. (1988). Amphiphilicity is essential for mitochondrial presequence function. EMBO J *7*, 649-653.

Rothbauer, U., Hofmann, S., Muhlenbein, N., Paschen, S.A., Gerbitz, K.D., Neupert, W., Brunner, M., and Bauer, M.F. (2001). Role of the deafness dystonia peptide 1 (DDP1) in import of human Tim23 into the inner membrane of mitochondria. J Biol Chem *276*, 37327-37334.

Ryan, K.R., Leung, R.S., and Jensen, R.E. (1998). Characterization of the mitochondrial inner membrane translocase complex: the Tim23p hydrophobic domain interacts with Tim17p but not with other Tim23p molecules. Mol Cell Biol *18*, 178-187.

Saracco, S.A., and Fox, T.D. (2002). Cox18p is required for export of the mitochondrially encoded *Saccharomyces cerevisiae* Cox2p C-tail and interacts with Pnt1p and Mss2p in the inner membrane. Mol Biol Cell *13*, 1122-1131.

Saraste, M. (1999). Oxidative phosphorylation at the fin de siecle. Science *283*, 1488-1493.

Schafer, U., Beck, K., and Muller, M. (1999). Skp, a molecular chaperone of gram-negative bacteria, is required for the formation of soluble periplasmic intermediates of outer membrane proteins. J Biol Chem *274*, 24567-24574.

Schagger, H., Cramer, W.A., and von Jagow, G. (1994). Analysis of molecular masses and oligomeric states of protein complexes by blue native electrophoresis and isolation of membrane protein complexes by two-dimensional native electrophoresis. Anal Biochem *217*, 220-230.

Schagger, H., and von Jagow, G. (1991). Blue native electrophoresis for isolation of membrane protein complexes in enzymatically active form. Anal Biochem *199*, 223-231.

Scherer, P.E., Manning-Krieg, U.C., Jeno, P., Schatz, G., and Horst, M. (1992). Identification of a 45-kDa protein at the protein import site of the yeast mitochondrial inner membrane. Proc Natl Acad Sci U S A *89*, 11930-11934.

Schilke, B., Voisine, C., Beinert, H., and Craig, E. (1999). Evidence for a conserved system for iron metabolism in the mitochondria of *Saccharomyces cerevisiae*. Proc Natl Acad Sci U S A *96*, 10206-10211.

Schlossmann, J., Dietmeier, K., Pfanner, N., and Neupert, W. (1994). Specific recognition of mitochondrial preproteins by the cytosolic domain of the import receptor MOM72. J Biol Chem *269*, 11893-11901.

Schmitt, S., Ahting, U., Eichacker, L., Granvogl, B., Go, N.E., Nargang, F.E., Neupert, W., and Nussberger, S. (2005). Role of TOM5 in maintaining the structural stability of the TOM complex of mitochondria. J Biol Chem.

Schneider, A., Behrens, M., Scherer, P., Pratje, E., Michaelis, G., and Schatz, G. (1991). Inner membrane protease I, an enzyme mediating intramitochondrial protein sorting in yeast. EMBO J *10*, 247-254.

Schneider, H.C., Westermann, B., Neupert, W., and Brunner, M. (1996). The nucleotide exchange factor MGE exerts a key function in the ATP-dependent cycle of mt-Hsp70-Tim44 interaction driving mitochondrial protein import. EMBO J *15*, 5796-5803.

Schulke, N., Sepuri, N.B., Gordon, D.M., Saxena, S., Dancis, A., and Pain, D. (1999). A multisubunit complex of outer and inner mitochondrial membrane protein translocases stabilized in vivo by translocation intermediates. J Biol Chem *274*, 22847-22854.

Schwartz, M.P., Huang, S., and Matouschek, A. (1999). The structure of precursor proteins during import into mitochondria. J Biol Chem *274*, 12759-12764.

Schwartz, M.P., and Matouschek, A. (1999). The dimensions of the protein import channels in the outer and inner mitochondrial membranes. Proc Natl Acad Sci U S A *96*, 13086-13090.

Scott, S.V., Cassidy-Stone, A., Meeusen, S.L., and Nunnari, J. (2003). Staying in aerobic shape: how the structural integrity of mitochondria and mitochondrial DNA is maintained. Curr Opin Cell Biol *15*, 482-488.

Scotti, P.A., Urbanus, M.L., Brunner, J., de Gier, J.W., von Heijne, G., van der Does, C., Driessen, A.J., Oudega, B., and Luirink, J. (2000). YidC, the *Escherichia coli* homologue of mitochondrial Oxa1p, is a component of the Sec translocase. EMBO J *19*, 542-549.

Selker, E.U. (1990). Premeiotic instability of repeated sequences in *Neurospora crassa.* Annu Rev Genet *24*, 579-613.

Shaw, J.M., and Nunnari, J. (2002). Mitochondrial dynamics and division in budding yeast. Trends Cell Biol *12*, 178-184.

Sherman, E.L. (2005). Characterization of the TOM complex in *Neurospora crassa.* Thesis.

Shoubridge, E.A. (2001). Nuclear genetic defects of oxidative phosphorylation. Hum Mol Genet *10*, 2277-2284.

Simon, D.K., and Johns, D.R. (1999). Mitochondrial disorders: clinical and genetic features. Annu Rev Med *50*, 111-127.

Singer, M.J., Marcotte, B.A., and Selker, E.U. (1995). DNA methylation associated with repeat-induced point mutation in *Neurospora crassa.* Mol Cell Biol *15*, 5586-5597.

Sirrenberg, C., Bauer, M.F., Guiard, B., Neupert, W., and Brunner, M. (1996). Import of carrier proteins into the mitochondrial inner membrane mediated by Tim22. Nature *384*, 582-585.

Sirrenberg, C., Endres, M., Becker, K., Bauer, M.F., Walther, E., Neupert, W., and Brunner, M. (1997). Functional cooperation and stoichiometry of protein translocases of the outer and inner membranes of mitochondria. J Biol Chem *272*, 29963-29966.

Sirrenberg, C., Endres, M., Folsch, H., Stuart, R.A., Neupert, W., and Brunner, M. (1998). Carrier protein import into mitochondria mediated by the intermembrane proteins Tim10/Mrs11 and Tim12/Mrs5. Nature *391*, 912-915.

Smagula, C., and Douglas, M.G. (1988). Mitochondrial import of the ADP/ATP carrier protein in *Saccharomyces cerevisiae*. Sequences required for receptor binding and membrane translocation. J Biol Chem *263*, 6783-6790.

Smagula, C.S., and Douglas, M.G. (1988). ADP-ATP carrier of Saccharomyces cerevisiae contains a mitochondrial import signal between amino acids 72 and 111. J Cell Biochem *36*, 323-327.

Sogo, L.F., and Yaffe, M.P. (1994). Regulation of mitochondrial morphology and inheritance by Mdm10p, a protein of the mitochondrial outer membrane. J Cell Biol *126*, 1361-1373.

Sollner, T., Griffiths, G., Pfaller, R., Pfanner, N., and Neupert, W. (1989). MOM19, an import receptor for mitochondrial precursor proteins. Cell *59*, 1061-1070.

Sollner, T., Pfaller, R., Griffiths, G., Pfanner, N., and Neupert, W. (1990). A mitochondrial import receptor for the ADP/ATP carrier. Cell *62*, 107-115.

Sollner, T., Rassow, J., Wiedmann, M., Schlossmann, J., Keil, P., Neupert, W., and Pfanner, N. (1992). Mapping of the protein import machinery in the mitochondrial outer membrane by crosslinking of translocation intermediates. Nature *355*, 84-87.

Stan, T., Ahting, U., DEMBOwski, M., Kunkele, K.P., Nussberger, S., Neupert, W., and Rapaport, D. (2000). Recognition of preproteins by the isolated TOM complex of mitochondria. EMBO J *19*, 4895-4902.

Steger, H.F., Sollner, T., Kiebler, M., Dietmeier, K.A., Pfaller, R., Trulzsch, K.S., Tropschug, M., Neupert, W., and Pfanner, N. (1990). Import of ADP/ATP carrier into mitochondria: two receptors act in parallel. J Cell Biol *111*, 2353-2363.

Stehling, O., Elsasser, H.P., Bruckel, B., Muhlenhoff, U., and Lill, R. (2004). Iron-sulfur protein maturation in human cells: evidence for a function of frataxin. Hum Mol Genet *13*, 3007-3015.

Strub, A., Rottgers, K., and Voos, W. (2002). The Hsp70 peptide-binding domain determines the interaction of the ATPase domain with Tim44 in mitochondria. EMBO J *21*, 2626-2635.

Sutak, R., Dolezal, P., Fiumera, H.L., Hrdy, I., Dancis, A., Delgadillo-Correa, M., Johnson, P.J., Muller, M., and Tachezy, J. (2004). Mitochondrial-type assembly of FeS centers in the hydrogenosomes of the amitochondriate eukaryote *Trichomonas vaginalis*. Proc Natl Acad Sci U S A *101*, 10368-10373.

Suzuki, H., Kadowaki, T., Maeda, M., Sasaki, H., Nabekura, J., Sakaguchi, M., and Mihara, K. (2004). Membrane-embedded C-terminal segment of rat mitochondrial TOM40 constitutes protein-conducting pore with enriched beta-structure. J Biol Chem *279*, 50619-50629.

Suzuki, H., Maeda, M., and Mihara, K. (2002). Characterization of rat TOM70 as a receptor of the preprotein translocase of the mitochondrial outer membrane. J Cell Sci *115*, 1895-1905.

Suzuki, H., Okazawa, Y., Komiya, T., Saeki, K., Mekada, E., Kitada, S., Ito, A., and Mihara, K. (2000). Characterization of rat TOM40, a central component of the preprotein translocase of the mitochondrial outer membrane. J Biol Chem *275*, 37930-37936.

Szyrach, G., Ott, M., Bonnefoy, N., Neupert, W., and Herrmann, J.M. (2003). Ribosome binding to the Oxa1 complex facilitates co-translational protein insertion in mitochondria. EMBO J *22*, 6448-6457.

Tachezy, J., Sanchez, L.B., and Muller, M. (2001). Mitochondrial type iron-sulfur cluster assembly in the amitochondriate eukaryotes *Trichomonas vaginalis* and *Giardia intestinalis*, as indicated by the phylogeny of IscS. Mol Biol Evol *18*, 1919-1928.

Taylor, A.B., Smith, B.S., Kitada, S., Kojima, K., Miyaura, H., Otwinowski, Z., Ito, A., and Deisenhofer, J. (2001). Crystal structures of mitochondrial processing peptidase reveal the mode for specific cleavage of import signal sequences. Structure (Camb) *9*, 615-625.

Taylor, R.D., McHale, B.J., and Nargang, F.E. (2003). Characterization of *Neurospora crassa* Tom40-deficient mutants and effect of specific mutations on Tom40 assembly. J Biol Chem *278*, 765-775.

Thorsness, P.E., and Fox, T.D. (1990). Escape of DNA from mitochondria to the nucleus in Saccharomyces cerevisiae. Nature *346*, 376-379.

Tovar, J., Fischer, A., and Clark, C.G. (1999). The mitosome, a novel organelle related to mitochondria in the amitochondrial parasite *Entamoeba histolytica*. Mol Microbiol *32*, 1013-1021.

Tranebjaerg, L., Schwartz, C., Eriksen, H., Andreasson, S., Ponjavic, V., Dahl, A., Stevenson, R.E., May, M., Arena, F., Barker, D., and et al. (1995). A new X linked recessive deafness syndrome with blindness, dystonia, fractures, and mental deficiency is linked to Xq22. J Med Genet *32*, 257-263.

Trifunovic, A., Wredenberg, A., Falkenberg, M., Spelbrink, J.N., Rovio, A.T., Bruder, C.E., Bohlooly, Y.M., Gidlof, S., Oldfors, A., Wibom, R., Tornell, J., Jacobs, H.T., and Larsson, N.G. (2004). Premature ageing in mice expressing defective mitochondrial DNA polymerase. Nature *429*, 417-423.

Truscott, K.N., Kovermann, P., Geissler, A., Merlin, A., Meijer, M., Driessen, A.J., Rassow, J., Pfanner, N., and Wagner, R. (2001). A presequence- and voltage-sensitive channel of the mitochondrial preprotein translocase formed by Tim23. Nat Struct Biol *8*, 1074-1082.

Truscott, K.N., Voos, W., Frazier, A.E., Lind, M., Li, Y., Geissler, A., Dudek, J., Muller, H., Sickmann, A., Meyer, H.E., Meisinger, C., Guiard, B., Rehling, P., and Pfanner, N. (2003). A J-protein is an essential subunit of the presequence translocase associated protein import motor of mitochondria. J Cell Biol *163*, 707-713.

Truscott, K.N., Wiedemann, N., Rehling, P., Muller, H., Meisinger, C., Pfanner, N., and Guiard, B. (2002). Mitochondrial import of the ADP/ATP carrier: the essential TIM complex of the intermembrane space is required for precursor release from the TOM complex. Mol Cell Biol *22*, 7780-7789.

Ungermann, C., Neupert, W., and Cyr, D.M. (1994). The role of Hsp70 in conferring unidirectionality on protein translocation into mitochondria. Science *266*, 1250-1253.

van Wilpe, S., Ryan, M.T., Hill, K., Maarse, A.C., Meisinger, C., Brix, J., Dekker, P.J., Moczko, M., Wagner, R., Meijer, M., Guiard, B., Honlinger, A., and Pfanner, N. (1999). Tom22 is a multifunctional organizer of the mitochondrial preprotein translocase. Nature *401*, 485-489.

Vasiljev, A., Ahting, U., Nargang, F.E., Go, N.E., Habib, S.J., Kozany, C., Panneels, V., Sinning, I., Prokisch, H., Neupert, W., Nussberger, S., and Rapaport, D. (2004). Reconstituted TOM core complex and Tim9/Tim10 complex of mitochondria are sufficient for translocation of the ADP/ATP carrier across membranes. Mol Biol Cell *15*, 1445-1458.

Vestweber, D., Brunner, J., Baker, A., and Schatz, G. (1989). A 42K outer-membrane protein is a component of the yeast mitochondrial protein import site. Nature *341*, 205-209.

Voisine, C., Craig, E.A., Zufall, N., von Ahsen, O., Pfanner, N., and Voos, W. (1999). The protein import motor of mitochondria: unfolding and trapping of preproteins are distinct and separable functions of matrix Hsp70. Cell *97*, 565-574.

von Heijne, G. (1986). Mitochondrial targeting sequences may form amphiphilic helices. EMBO J *5*, 1335-1342.

Voos, W., Gambill, B.D., Laloraya, S., Ang, D., Craig, E.A., and Pfanner, N. (1994). Mitochondrial GrpE is present in a complex with hsp70 and preproteins in transit across membranes. Mol Cell Biol *14*, 6627-6634.

Voos, W., and Rottgers, K. (2002). Molecular chaperones as essential mediators of mitochondrial biogenesis. Biochim Biophys Acta *1592*, 51-62.

Voos, W., von Ahsen, O., Muller, H., Guiard, B., Rassow, J., and Pfanner, N. (1996). Differential requirement for the mitochondrial Hsp70-Tim44 complex in unfolding and translocation of preproteins. EMBO J *15*, 2668-2677.

Waizenegger, T., Habib, S.J., Lech, M., Mokranjac, D., Paschen, S.A., Hell, K., Neupert, W., and Rapaport, D. (2004). Tob38, a novel essential component in the biogenesis of beta-barrel proteins of mitochondria. EMBO Rep *5*, 704-709.

Waizenegger, T., Schmitt, S., Zivkovic, J., Neupert, W., and Rapaport, D. (2005). Mim1, a protein required for the assembly of the TOM complex of mitochondria. EMBO Rep *6*, 57-62.

Waizenegger, T., Stan, T., Neupert, W., and Rapaport, D. (2003). Signal-anchor domains of proteins of the outer membrane of mitochondria: structural and functional characteristics. J Biol Chem *278*, 42064-42071.

Wallace, D.C. (1999). Mitochondrial diseases in man and mouse. Science *283*, 1482-1488.

Weiss, C., Oppliger, W., Vergeres, G., Demel, R., Jeno, P., Horst, M., de Kruijff, B., Schatz, G., and Azem, A. (1999). Domain structure and lipid interaction of recombinant yeast Tim44. Proc Natl Acad Sci U S A *96*, 8890-8894.

Wendland, J., Lengeler, K., Kothe, E. (1996). An instant preparation method for nucleic acis of filamentous fungi. Fungal Genet Newslett. *43*, 54-55.

Westermann, B. (2002). Merging mitochondria matters: cellular role and molecular machinery of mitochondrial fusion. EMBO Rep *3*, 527-531.

Westermann, B., and Prokisch, H. (2002). Mitochondrial dynamics in filamentous fungi. Fungal Genet Biol *36*, 91-97.

White, B.a.W., D. (1995). A simple method for making disposable race tubes. Fungal Genetics Newslett *42*, 79.

Wiedemann, N., Kozjak, V., Chacinska, A., Schonfisch, B., Rospert, S., Ryan, M.T., Pfanner, N., and Meisinger, C. (2003). Machinery for protein sorting and assembly in the mitochondrial outer membrane. Nature *424*, 565-571.

Wiedemann, N., Pfanner, N., and Ryan, M.T. (2001). The three modules of ADP/ATP carrier cooperate in receptor recruitment and translocation into mitochondria. EMBO J *20*, 951-960.

Wiedemann, N., Truscott, K.N., Pfannschmidt, S., Guiard, B., Meisinger, C., and Pfanner, N. (2004). Biogenesis of the protein import channel Tom40 of the mitochondrial outer membrane: intermembrane space components are involved in an early stage of the assembly pathway. J Biol Chem *279*, 18188-18194.

Yaffe, M.P. (1999). Dynamic mitochondria. Nat Cell Biol *1*, E149-150.

Yamamoto, H., Esaki, M., Kanamori, T., Tamura, Y., Nishikawa, S., and Endo, T. (2002). Tim50 is a subunit of the TIM23 complex that links protein translocation across the outer and inner mitochondrial membranes. Cell *111*, 519-528.

Yamamoto, H., Momose, T., Yatsukawa, Y., Ohshima, C., Ishikawa, D., Sato, T., Tamura, Y., Ohwa, Y., and Endo, T. (2005). Identification of a novel member of yeast mitochondrial Hsp70-associated motor and chaperone proteins that facilitates protein translocation across the inner membrane. FEBS Lett *579*, 507-511.

Yang, D., Oyaizu, Y., Oyaizu, H., Olsen, G.J., and Woese, C.R. (1985). Mitochondrial origins. Proc Natl Acad Sci U S A *82*, 4443-4447.

Yang, M., Jensen, R.E., Yaffe, M.P., Oppliger, W., and Schatz, G. (1988). Import of proteins into yeast mitochondria: the purified matrix processing protease contains two subunits which are encoded by the nuclear MAS1 and MAS2 genes. EMBO J 7, 3857-3862.

Young, J.C., Hoogenraad, N.J., and Hartl, F.U. (2003). Molecular chaperones Hsp90 and Hsp70 deliver preproteins to the mitochondrial import receptor Tom70. Cell *112*, 41-50.

Zeviani, M. (2001). The expanding spectrum of nuclear gene mutations in mitochondrial disorders. Semin Cell Dev Biol *12*, 407-416.